

# **Reactivity of Strained Systems in Alkyne Cycloaddition Reactions – Synthesis of Substituted Cycloparaphenylenes**

**Inauguraldissertation**

zur Erlangung der Würde eines

**Doktors der Philosophie**

vorgelegt der

**Philosophisch-Naturwissenschaftlichen Fakultät der Universität Basel**

Von

**Anne-Florence Stoessel Tran-Van**

aus Kembs

France

Basel, 2015

Originaldokument gespeichert auf dem Dokumentenserver der Universität Basel

**edoc.unibas.ch**



This work is licenced under the agreement  
„Attribution Non-Commercial No Derivatives – 3.0 Switzerland“ (CC BY-NC-ND 3.0 CH).

The complete text may be reviewed here:  
[creativecommons.org/licenses/by-nc-nd/3.0/ch/deed.en](https://creativecommons.org/licenses/by-nc-nd/3.0/ch/deed.en)

Genehmigt von der Philosophisch-Naturwissenschaftlichen Fakultät  
auf Antrag von

Prof. Dr. Andreas Pfaltz  
Prof. Dr. Hermann Wegner  
Prof. Dr. Dennis Gillingham

Basel, den 10.12.2013

Prof. Dr. Jörg Schibler  
Dekan



Namensnennung-Keine kommerzielle Nutzung-Keine Bearbeitung 3.0 Schweiz  
(CC BY-NC-ND 3.0 CH)

Sie dürfen: Teilen — den Inhalt kopieren, verbreiten und zugänglich machen

Unter den folgenden Bedingungen:



Namensnennung — Sie müssen den Namen des Autors/Rechteinhabers in der von ihm festgelegten Weise nennen.



Keine kommerzielle Nutzung — Sie dürfen diesen Inhalt nicht für kommerzielle Zwecke nutzen.



Keine Bearbeitung erlaubt — Sie dürfen diesen Inhalt nicht bearbeiten, abwandeln oder in anderer Weise verändern.

Wobei gilt:

- Verzichtserklärung — Jede der vorgenannten Bedingungen kann aufgehoben werden, sofern Sie die ausdrückliche Einwilligung des Rechteinhabers dazu erhalten.
- Public Domain (gemeinfreie oder nicht-schützbares Inhalte) — Soweit das Werk, der Inhalt oder irgendein Teil davon zur Public Domain der jeweiligen Rechtsordnung gehört, wird dieser Status von der Lizenz in keiner Weise berührt.
- Sonstige Rechte — Die Lizenz hat keinerlei Einfluss auf die folgenden Rechte:
  - Die Rechte, die jedermann wegen der Schranken des Urheberrechts oder aufgrund gesetzlicher Erlaubnisse zustehen (in einigen Ländern als grundsätzliche Doktrin des fair use bekannt);
  - Die Persönlichkeitsrechte des Urhebers;
  - Rechte anderer Personen, entweder am Lizenzgegenstand selber oder bezüglich seiner Verwendung, zum Beispiel für Werbung oder Privatsphärenschutz.
- Hinweis — Bei jeder Nutzung oder Verbreitung müssen Sie anderen alle Lizenzbedingungen mitteilen, die für diesen Inhalt gelten. Am einfachsten ist es, an entsprechender Stelle einen Link auf diese Seite einzubinden.

*A straight line may be the shortest distance between two points,  
but it is by no means the most interesting.*

-The Doctor-



## Aknowledgments

---

First of all, I would like to thank my supervisor Prof. Dr. Hermann A. Wegner who not only gave me the chance to come back to organic chemistry and provided me with his constant support and interesting projects, but also shared his enthusiasm for nanomolecules and introduced me to this fascinating field.

I am grateful to Prof. Dr. Andreas Pfaltz for being the advisor and examiner of this thesis. I also thank Prof. Dr. Denis Gillingham for co-examining the thesis and Prof. Dr. Marcel Mayor for chairing the defense.

Many thanks to all the past and present member of the Wegner group for the nice working atmosphere, especially Jonathan Basler, Matthieu Auzias, Raphael Reuter, Simon Kessler, Silvia Bellotto, Luca Schweighauser and Sebastian Ales.

I would also like to extend my thanks to Daniel Hausinger and his group for their kindness their help with NMR investigations.

A special thank to my lab mates Luca and Heiko: thank you for the nice time we had together in the cellar-labs.

I am thankful to the students who contributed to my projects during their internship: Elena Huxol and Silas Goetz.

I express my gratitude to Daniel Häussinger, Heiko Gsellinger and Kaspar Zimmermann for performing NMR experiments, Dr. Markus Neuburger for the solid state structure determinations, Dr. Heinz Nadig for mass spectrometric analyses, Werner Kirsch and Sylvie Mittelhauser for elemental analyses. I also thank the technical and administrative staff of the chemistry department.

I would like to thank all the colleagues from the chemistry department especially Dr. Michael Parmentier (merci pour tes conseils et encouragements), Dr. Adrian Von der Hö (thanks for the nice coffee breaks and lunch breaks), Dr. Maurizio Bernasconi (merci de m'avoir accueillie dans le Pfaltz group après le déménagement).

I thank Adrian and Jonathan for taking the time to proofread this thesis

I also want to thank Christian Ragot who taught me all the organic chemistry laboratory techniques back in my internship at Novartis in 2005.

Je remercie ma famille qui a toujours été là pour me soutenir, vous avez fait de moi ce que je suis aujourd'hui. J'aimerais tout spécialement remercier mes parents qui m'ont soutenue et encouragée et qui ont toujours cru en moi tout au long de mes études, sans vous rien n'aurait été possible.

Enfin je remercie mon mari, Julien, de m'avoir supportée (dans tous les sens du terme), merci pour ta patience, ta compréhension et ton soutien.



## **Table of content**

Chapter 1: Reactivity of Strained Systems in Alkyne Cycloaddition Reactions .....	1
1.1 Introduction .....	1
1.1.1 [2+2+2] Cycloaddition reactions .....	1
1.1.2 Mechanism of the [2+2+2] cycloaddition.....	6
1.1.3 Macrocycles .....	9
1.2 Project and strategy .....	17
1.2.1 Synthesis of cycloparaphenylene via [2+2+2] cycloaddition reaction .....	17
1.2.2 Initial investigation on strained model.....	17
1.3 Results and Discussion .....	19
1.3.1 Terphenyl synthesis via [2+2+2] cycloaddition reaction.....	19
1.3.2 Synthetic strategies toward the macrocyclic precursor.....	25
1.3.3 Cycloaddition reaction of strained systems .....	34
1.4 Conclusion.....	47
1.5 References .....	49
Chapter 2: Synthesis of Substituted Cycloparaphenylenes .....	53
2.1 Introduction .....	55
2.1.1 Carbon.....	55
2.1.2 Carbon Nanotubes.....	56
2.1.3 Nanobelts .....	58
2.1.4 From nanobelts to nanotubes .....	59
2.1.5 Cycloparaphenylene syntheses .....	60
2.1.6 Properties of Cycloparaphenylenes.....	65
2.2 Project and strategy .....	71
2.2.1 Initial strategy .....	71
2.2.2 Combined strategy .....	72
2.3 Results and Discussion .....	73



2.3.1	Macrocyclic synthesis .....	73
2.3.2	[2+2+2] Cycloaddition reaction .....	84
2.3.3	Aromatisation Reaction .....	85
2.3.4	Properties of substituted CPPs .....	91
2.3.5	Toward the Nanobelt.....	96
2.4	Conclusion .....	104
2.5	References .....	106
Chapter 3: Experimental part .....		109
3.1	General information:.....	111
3.2	Experimental procedures .....	113
3.2.1	Diyne synthesis .....	113
3.2.2	Linear precursor synthesis .....	116
3.2.3	[2+2+2] cycloaddition reaction on linear molecules .....	118
3.2.4	Macrocyclic synthesis via Sonogashira .....	126
3.2.5	Synthesis of Macrocyclic by Ring closure metathesis.....	128
3.2.6	Synthesis of macrocyclic by ether formation.....	129
3.2.7	Cycloaddition reaction on macrocyclic 66.....	135
3.2.8	Synthesis of substituted CPP Jasti strategy.....	144
3.2.9	Synthesis of Substituted CPP Itami strategy.....	147
3.2.10	Nanobelt synthesis : diphenylphenanthrene strategy.....	181
3.3	Crystallographic data:.....	185
3.1	References .....	195
Appendix .....		197
Abbreviations.....		199
Curriculum vitae .....		201

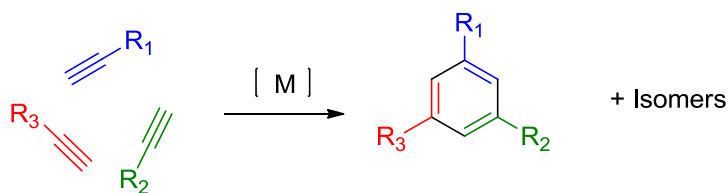
**Chapter 1:**  
**Reactivity of Strained Systems in Alkyne  
Cycloaddition Reactions**



## 1.1 INTRODUCTION

### 1.1.1 [2+2+2] Cycloaddition reactions

The [2+2+2] cycloaddition reaction of alkynes is one of the most elegant and powerful methods to synthesize multi-substituted benzene derivatives and polycyclic molecules in one step. Such a strategy is interesting from an atom-economical point of view, and it allows for the construction of complex molecules in a modular and versatile fashion. The reaction involves 6  $\pi$ -electrons in the cyclic combination of three alkynes to form an aromatic molecule. A general example is shown in Scheme 1.



**Scheme 1:** Cycloaddition reaction of alkynes

By simply changing the combination of alkynes one can obtain numerous variously substituted benzenes. This reaction adds into the toolbox of the organic chemist alongside the aromatic electrophilic substitution, Friedel-Crafts reaction and other recent cross-coupling reactions. This method completes the picture, introducing several substituents at once, and avoiding substituent effect limitations as well as multi-step reactions. Moreover, the alkyne cycloaddition reaction provides access to a large number of products due to its high functional group tolerance.

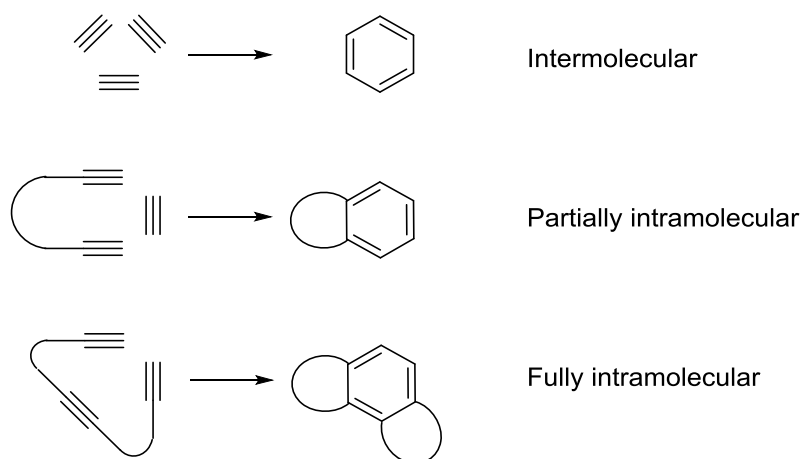
The story of alkyne cyclotrimerization started in 1866, when Bertholet discovered the thermal trimerization of acetylene to form benzene. Despite being exothermic ( $\Delta H = -594$  kJ/mol), this process required high temperatures (400°C) because of entropic and kinetic considerations. The reaction produced a complex mixture of products.<sup>1</sup> The next milestone in the history of alkyne cyclotrimerization was set by Reppe in 1948 with the development of the first transition metal catalyzed alkyne cyclotrimerization.<sup>2</sup> The real potential of this reaction was revealed by transition metal catalysis. Following this pioneering work, Müller in 1974<sup>3</sup> applied the method to tethered diynes, thereby controlling the reaction to achieve chemo- and region-selectivity. Eight years later, in 1982, Grigg further explored the reaction of tethered diynes using Wilkinson's catalyst.<sup>4,5</sup> Since these promising debuts, the evolution of this method has continued over the next three decades. Multiple catalytic systems have been developed and many reviews are covering the field.<sup>6-10</sup>

Among other transition metals, cobalt is one of the most used catalysts for [2+2+2] cycloaddition reactions, and more especially the typical catalyst  $\text{CpCo}(\text{CO})_2$ . The use of rhodium as catalyst for this reaction is also well known, especially Wilkinson's catalyst  $\text{RhCl}(\text{PPh}_3)_3$ , but also

[RhCl(cod)]<sub>2</sub>, and [RhCl(cod)<sub>2</sub>]BF<sub>4</sub>. Nickel complexes (NiBr<sub>2</sub>/L, Ni(cod)<sub>2</sub>) have been used by Reppe in his pioneering work. Catalyst based on other transition metals have also been used for this reaction, most commonly based on iridium ([IrCl(cod)]<sub>2</sub>), ruthenium, palladium and titanium.

Despite the reaction's great potential, it also suffers from several limitations. It is for example often difficult to control the chemoselectivity and the regioselectivity of the reaction. Recent works tend to give solutions and push the limits of the reaction.<sup>11-13</sup> Achieving the selective synthesis of a desired product via hetero-cyclotrimerization of two or three alkynes is difficult. For this to be successful, it would be necessary to control the chemoselectivity of the addition of the first two alkynes in the formation of the metallacyclopentadiene as well as the regioselectivity in the subsequent addition of the third alkyne.

An elegant way to control the regio- and chemo-selectivity is to tether the alkynes together, thereby, performing the reaction intramolecularly or just partially intramolecularly (Scheme 2).<sup>4,14,15</sup> Without tethering the alkynes together, the selectivity in the intermolecular alkyne heterotrimerization reactions remains limited. However, progress in the development of regioselective intermolecular alkyne homo-cyclotrimerization reactions has been made. Sterics and coordination determine which regioisomers is formed preferably.<sup>13</sup> The nature of the ligand on the metal can also influence the selectivity by sterics or electronic effects.<sup>16</sup> Thus, a way of gaining regioselectivity is to introduce regiodirecting groups, inducing regioselectivity either by steric hinderance or by chelation.



**Scheme 2:** Different types of [2+2+2] cycloaddition reactions

The enantioselective synthesis of chiral systems can be achieved using chiral ligands in the [2+2+2] cycloaddition reaction. Reaction with a sterically demanding prochiral substrate such as **5** leads to axially chiral products (Figure 1). Such syntheses have been extensively investigated by Tanaka et al.<sup>7</sup> These products are interesting as they can be used as chiral ligands for asymmetric catalysis. The enantioselective synthesis of the helicene **8** affording planar chiral product can also

be done by [2+2+2] cycloaddition reaction with a chiral catalyst.<sup>17</sup> A more classic type of chirality can be induced by enantioselective desymmetrization of a symmetrical diyne such as **2**.<sup>18</sup>

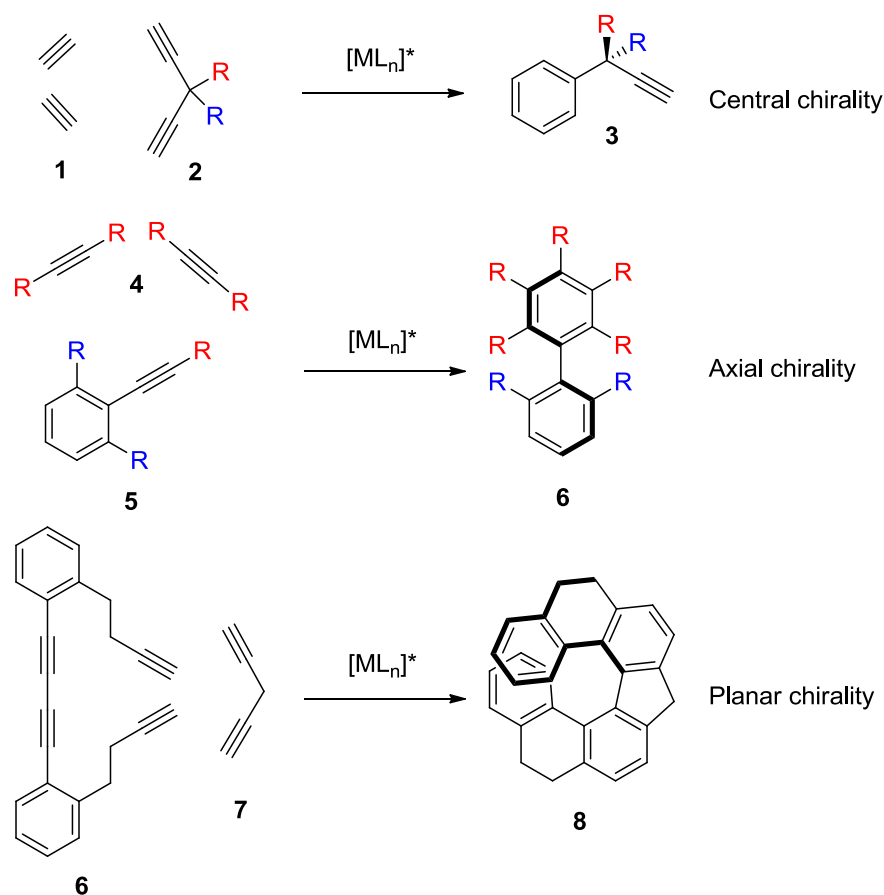
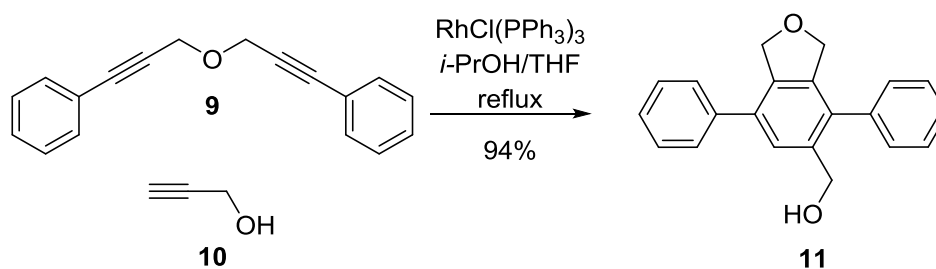


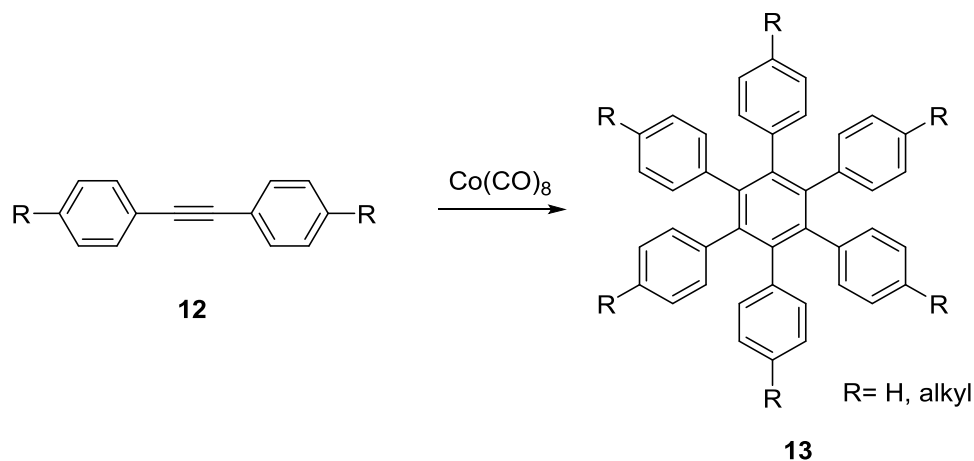
**Figure 1:** Enantioselective synthesis of chiral systems by [2+2+2] cycloaddition reaction

The [2+2+2] cycloaddition reaction has been applied to synthesize a variety of molecules, from simple substituted benzenes,<sup>9</sup> pyridines and biaryls, to more complex structures such as polycyclic aromatic hydrocarbons (PAHs),<sup>15,16</sup> cyclophanes, helicenes or biologically active compounds.<sup>8</sup> Consequently, the reaction is very suitable for the synthesis of organic compound applicable in material sciences. For instance for the synthesis of oligo*para*phenylenes which are electronic conductors and light emitting organic compounds. The [2+2+2] cycloaddition reaction allows the synthesis of polymeric *para*-polyphenyl in a monodispersive way.<sup>19</sup> An example of the synthesis of the terphenyl **11** via [2+2+2] cycloaddition reaction is shown in Scheme 3.



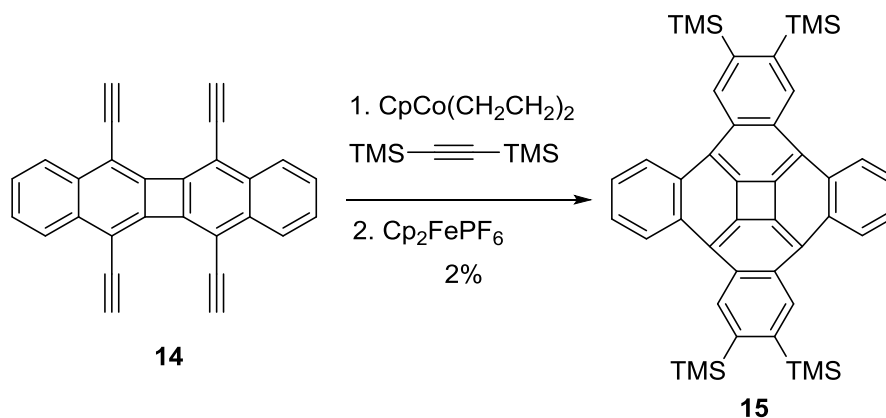
**Scheme 3:** Synthesis of a terphenyl via [2+2+2] cycloaddition reaction

Another application of the [2+2+2] cycloaddition reaction is the cobalt catalyzed reaction of biphenyl acetylene. This is one of the key steps in the strategy used by Müllen et al. for the synthesis of hexaphenylbenzenes **13** which can be converted into the corresponding hexabenzocoronenes (HBCs) (Scheme 4).<sup>20</sup>



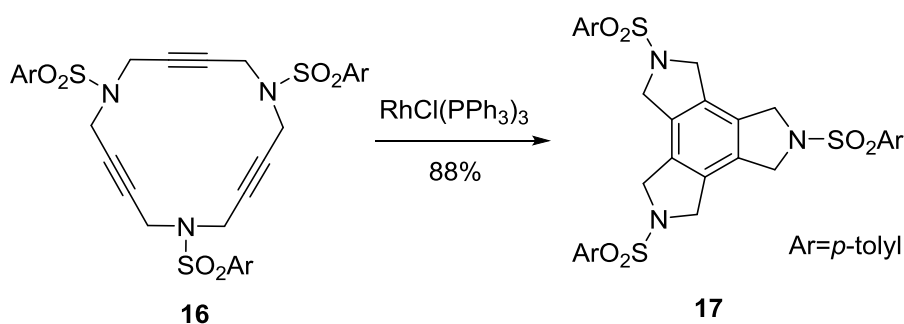
**Scheme 4:** Synthesis of hexaphenylbenzenes via [2+2+2] cyclotrimerization

An important example of the power of this reaction is demonstrated in the synthesis of the strained quadranulene **15** by King et al.,<sup>21</sup> in which the tetra-alkyne **14** reacts with bis-trimethylsilylacetylene to afford the strained quadranulene **15** in 2% yield. The [2+2+2] cycloaddition reaction was used to synthesize this bowl shaped molecule, using the aromaticity gain to overcome the strain energy (Scheme 5).



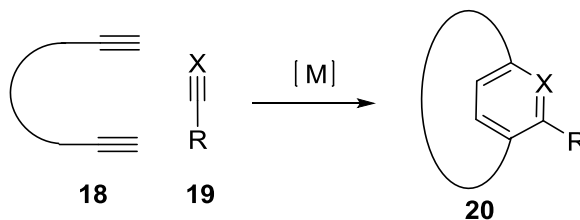
**Scheme 5:** Synthesis of the quadranulene **15** via [2+2+2] cycloaddition reaction

The [2+2+2] cycloaddition reaction can also be applied to macrocyclic systems as demonstrated by the work of Roglans and coworkers (Scheme 6).<sup>22,23</sup> They synthesized aza-macrocycles of different sizes (comprised of 15- 20- and 25-atoms) and observed that the 20-membered macrocycle was not reactive because it would result in the formation of a strained 10-membered ring which is not favorable as confirmed by a computational study. Other examples of [2+2+2] cycloaddition reactions of macrocycles have been reported in the literature.<sup>22,24-26</sup>



**Scheme 6:** [2+2+2] Cycloaddition reaction on [15]-aza-macrocycle<sup>23</sup>

The use of the [2+2+2] cycloaddition reaction as a macrocyclization tool is a particularly challenging application. Maryanoff et al. rose the challenge and developed a cobalt catalyzed cyclotrimerization reaction of long-chain  $\alpha,\omega$ -diynes **18** with nitriles, cyanamides or isocyanates to yield pyridine containing macrocycles **20** (Scheme 7).<sup>24</sup> This method allows the formation of a macrocycle and a pyridine ring in a single step, increasing significantly the molecular complexity.



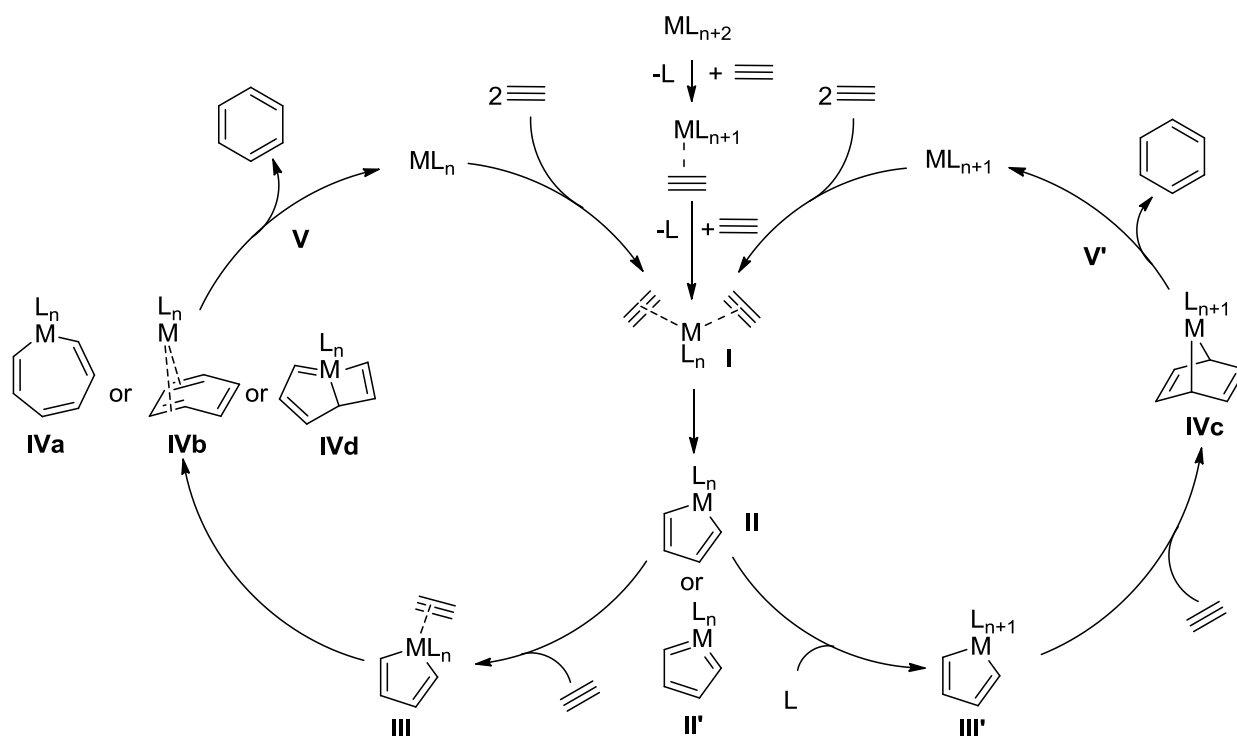
**Scheme 7:** [2+2+2] Cycloaddition mediated macrocyclization



### 1.1.2 Mechanism of the [2+2+2] cycloaddition

The [2+2+2] cycloaddition reaction is a highly exothermic process. The thermodynamic driving force is the formation of three  $\sigma$ -bonds and of an energetically favorable aromatic system.

Several computational studies have been undertaken to elucidate the mechanism of the [2+2+2] cycloaddition reaction.<sup>27-29</sup> Furthermore, kinetic studies<sup>30</sup> were conducted and intermediates were isolated and characterized.<sup>31</sup> As a result of all these studies, a generally accepted mechanism is presented in Scheme 8.



**Scheme 8:** General mechanism of [2+2+2] cycloaddition reaction

In the first step **I**, the ligands are substituted by two alkyne moieties.

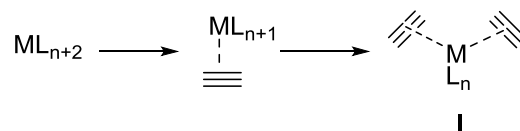


**Figure 2**

The oxidative coupling of the alkynes then leads to formation of a five-membered metallacycle **II** or **II'**. The favored resonance structure is depending of the nature of the catalyst.

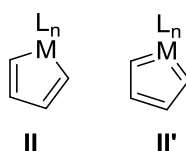


Figure 3

Subsequently, the cyclometallapentadiene complex coordinates to a third alkyne or to a ligand.

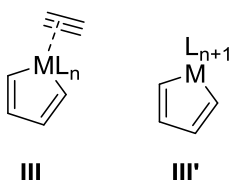


Figure 4

The next step involves the insertion of the third alkyne moiety. This can take place through different mechanisms and intermediates (Figure 5):

- insertion to form the metalla-cycloheptatriene (**IVa**)
  - intramolecular [4+2] cycloaddition leading to a  $\eta^4$ -arene complex (**IVb**)
  - intermolecular [4+2] cycloaddition from **III'** (the alkyne is not coordinated) to form the metalla-norbornadiene derivative (**IVc**)
  - [2+2] cycloaddition reaction to form the bicyclic metalla-[3.2.0]heptatriene derivative (**IVd**).
- The elimination from this intermediate is symmetry forbidden and proceeds through a seven-membered metallacycle.

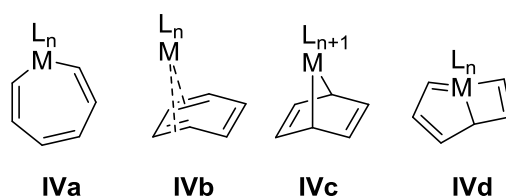


Figure 5

In the last step of the catalytic cycle, reductive elimination occurs giving either directly the product and the catalyst (**V**) or the  $\eta^6$ -coordinated arene (**V'**), which dissociates to give the product and regenerate the catalyst (Figure 6).

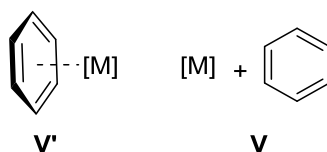
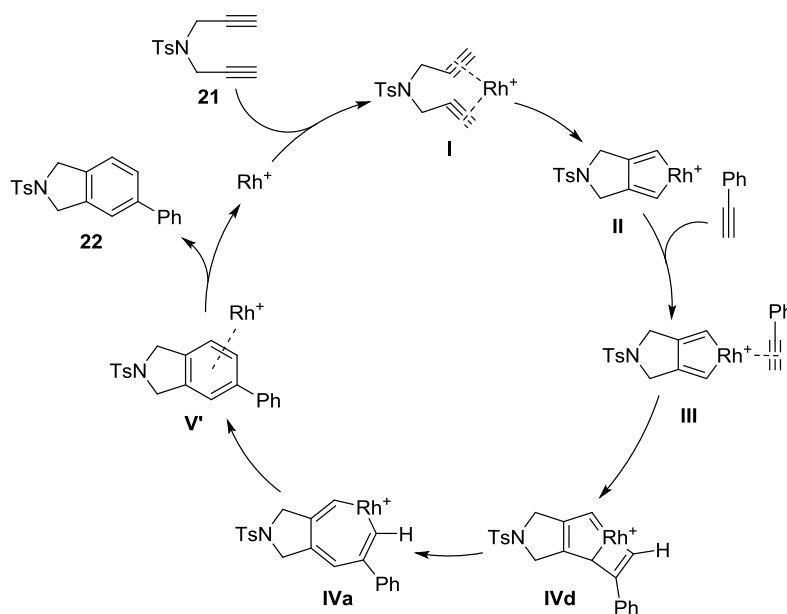


Figure 6

The actual pathway of a specific [2+2+2] cycloaddition reaction is strongly dependent on the metal, ligands, substrate and solvent. It is therefore hard to propose a general mechanism applying to all [2+2+2] cycloaddition reactions. The different possible intermediates are favored in specific cases. In some cases, the metalla-cyclopentadiene intermediate can undergo reductive elimination to give stable  $\eta^4$ -cyclobutadiene complexes. These are thermodynamical trap of the catalytic cycle. Moreover,  $\eta^4$ -cyclobutadiene complexes have already been observed.<sup>24</sup>

Rogland et al. carried out a kinetic study of the [2+2+2] cycloaddition reaction of a diyne and a monoyne catalyzed by Wilkinson catalyst. The two global steps have been followed by cyclic voltametry, <sup>31</sup>P-NMR and ESI mass spectrometry. They found that in the case of bulky substrates, the coordination and oxidative coupling of the alkyne moieties of the diyne (steps **I** to **II**) was the rate determining step. In contrast, when non bulky diynes were employed, the reaction of the metalla-cyclopentadiene with the monoyne was the rate determining step (steps **III** to **V**). These results show that the rate determining step depends on the structure of the substrates.

In a recent study, Roglans et al. used ESI mass spectrometry to detect all intermediates of the reaction between a diyne and a monoyne catalyzed by a cationic rhodium complex. The intermediate resulting from the monoyne insertion **IVa** was detected, and with the help of DFT calculations, its likely structure was determined. The results suggest the formation of the cycloheptatriene (**IVa**) although the other bicyclic [3.2.0]heptatriene (**IVd**) derivative could not be completely ruled out. The catalytic cycle that was proposed on the basis of these findings is shown in Scheme 9. Again, it is important to keep in mind that the mechanism of a precise [2+2+2] cycloaddition reaction is highly depending of the nature of all the reaction components and conditions.



**Scheme 9:** Proposed catalytic cycle of the [2+2+2] cycloaddition reaction of a diyne and a monoyne with a Rhodium/bisphosphine catalyst (ligand omitted for clarity)

### 1.1.3 Macrocycles

#### 1.1.3.1 Application of macrocycles

Macrocycles are defined as containing at least one large ring of twelve or more atoms. Macrocyclic molecules are commonly found as bioactive natural products and pharmaceutical molecules.<sup>32-35</sup> Numerous natural occurring macrocyclic compounds such as erythromycin, rapamycin (**23**), vancomycin, cyclosporine and epothilone proved to be efficient drugs (Figure 7). Their conformationally restricted structures provide the big advantage of a higher target binding and a better ability to interact with shallow surfaces, which are more challenging for linear analogs. Indeed, linear counterparts are usually more flexible and thus have lower binding abilities to the target and an increased sensitivity toward degradation. Macrocycles often have higher solubility and lipophilicity, allowing membrane penetration, as well as a higher biological stability, making them potential drug candidates.

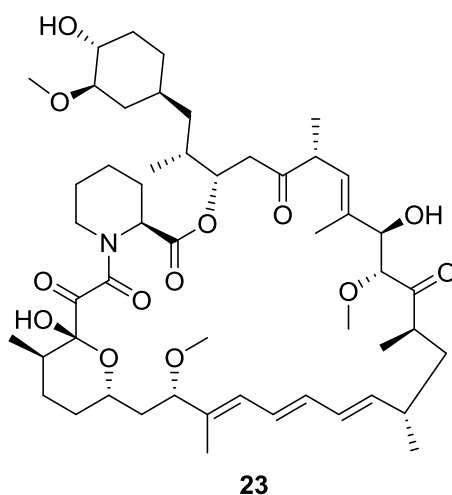


**Figure 7:** Rapamycin (an immunosuppressant) as an example of macrocyclic drug

Also in other domains such as host-guest or in metallo-supramolecular chemistry, macrocycles have gained interest due to the enhanced kinetic and thermodynamic stabilities of their metal complexes (known as macrocyclic effect). Their special structures often afford unique properties such as particular spectral, magnetic, redox and catalytic properties, making them appealing for applications in different domains of supramolecular chemistry.<sup>36</sup> Many examples of macrocyclic host molecules such as crown ethers,<sup>37,38</sup> calixarenes (**24**),<sup>39</sup> benzocrown (**25**),<sup>40,41</sup> terphenylcrown,<sup>42</sup> and crownphane<sup>43</sup> have been studied. (Figure 8)

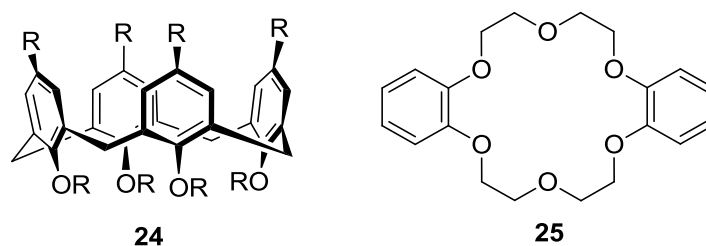


**Figure 8:** Example of calixarene **24** and benzocrown **25**

For material scientists, shape persistent macrocycles<sup>44</sup> and conjugated macrocycles<sup>45-47</sup> are of outmost interest. First, because of their architectural beauty, but also because they can serve as models to explore the nature of less accessible or structurally more complex nanomaterials. The interest in these molecules is not only theoretical, but also from an experimental point of view, because they possess novel properties that could possibly be exploited in nanotechnological applications such as molecular devices or switches. They present a rigid scaffold that can organize into ordered structures and form  $\pi$ -stacked structures, tubular arrangements, or nanoporous solids. Moreover, they possess inner cavities, opening the way to new applications as host molecules. Fully conjugated macrocycles also constitute a model for infinite conjugated systems with special magnetic, optical and electronical properties.

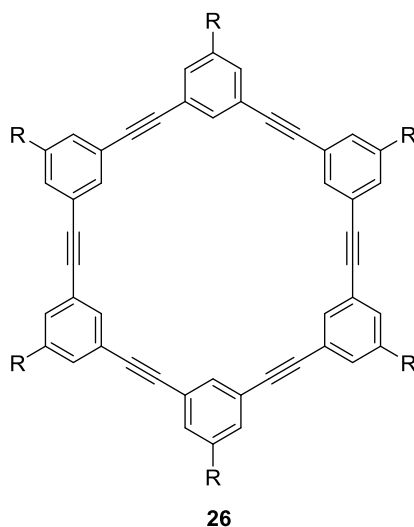


**Figure 9:** Example of shape persistent macrocycle

Other nanodevices relying on macrocycles are catenanes and rotaxanes (Figure 10). These molecules can be seen as molecular machines which produce movement at the molecular level in response to a stimulus.

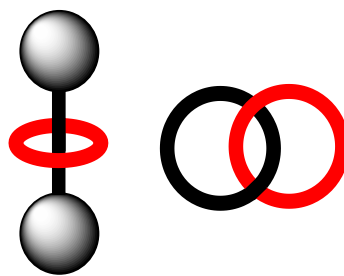


**Figure 10:** Graphical representation of a rotaxane (left) and a catenane (right)

Another impressive example of the beauty of macrocyclic chemistry is demonstrated by the catenane **27** designed by Sauvage et al. which is shown in Figure 11.<sup>48,49</sup> This three-configuration Cu(I) catenane can undergo a sequence of rearrangement reactions with electron transfer steps and ring gliding motions induced by the oxidation of the central metal from Cu(I) to Cu(II) or reduction back to the monovalent state.

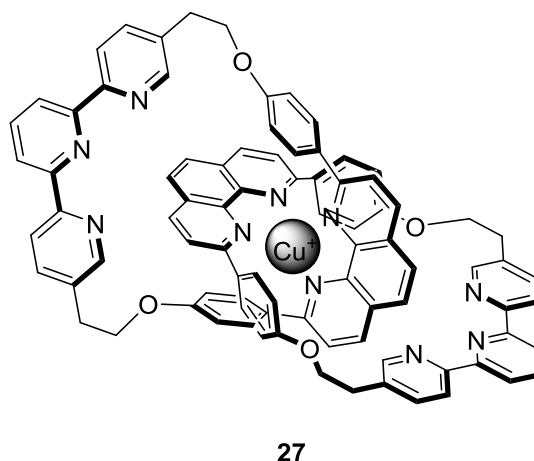


**Figure 11:** Catenane **27** designed and synthesized by Sauvage and coworkers

The study of macrocycles containing aromatic rings such as cyclophanes (Figure 12) could help to explore the effect of strain on aromatic systems. As a matter of fact, macrocycles provide excellent models to study the effects of the distortion on a benzene ring and the resulting properties.<sup>45,46</sup> This field has triggered the curiosity of scientists for a long time, as researchers are trying to answer the question of how bent a benzene ring can be, thus pushing aromaticity to its limits. One of the strategies chosen for the synthesis of cyclophanes is the [2+2+2] cycloaddition reaction.<sup>25,26</sup>

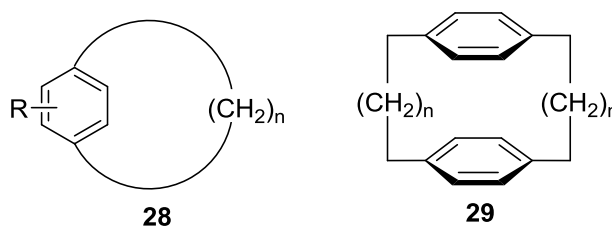


**Figure 12:** Examples of cyclophanes

### 1.1.3.2 General strategies of macrocyclization

As discussed in the previous section, macrocycles represent interesting molecules, but their syntheses remain challenging. In the following section the general strategies used for the synthesis of macrocycles will be presented. Different strategies are illustrated on Figure 13.

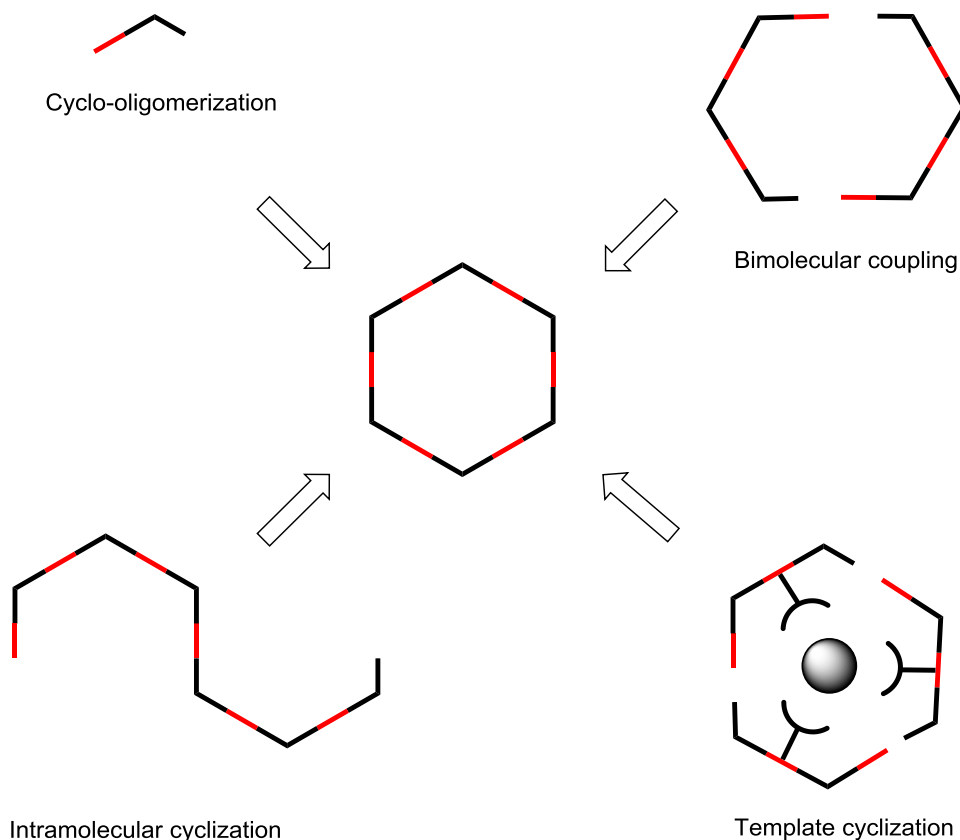


**Figure 13:** General strategies of macrocycle syntheses

#### - Cyclo-oligomerization:

The main advantage of this strategy is that it produces the macrocycle in a single step from readily available building blocks avoiding a long multistep synthesis. In this strategy, a monomeric building block is growing into an open chain oligomer and the cyclization occurs in competition with chain elongation. This method suffers from inevitably low yields because of the tight competition between the formation of the target macrocycle and all other possible linear and cyclic oligomeric products. Thus the statistical distribution of products governs the outcome of the reaction. Furthermore, as the ring size increases, the number of possible undesired products and competing reactions increases. Another big disadvantage of this method is that the isolation and purification of the desired molecule from the complex mixture of products is complicated. All of these drawbacks make this strategy very poorly suitable for the selective synthesis of macrocycles. Therefore, alternative strategies to improve the yield and purification process of macrocyclization were developed.

**- Intramolecular cyclization**

In this strategy the precursor for the macrocyclization is synthesized in a stepwise approach, often relying on a repeated sequence of protection/reaction/deprotection reactions. The macrocyclization proceeds through an intramolecular cyclization of a bifunctional molecule. This method often affords the desired macrocycle in better yield than cyclo-oligomerization method.

High dilution or pseudo-high-dilution techniques can be applied to improve the yield of the cyclization reaction. In the high dilution technique, the reaction mixture is diluted to favor the intramolecular reaction over the intermolecular oligomerization. A different technique called pseudo-high-dilution offers a more practical method by slow addition of the precursor to a solution of the catalyst. The unimolecular reaction is usually kinetically favored over intermolecular reactions. In addition to the higher yield of this process, it makes it possible to selectively introduce functional groups in specific positions, thus reaching full control over the design.

Although this method permits the synthesis of macrocycles in higher yield than the cyclo-oligomerization reaction, the multistep process and the large number of intermediate purification steps necessary limit the efficiency of the method in large scale applications. Alternative strategies have to be designed incorporating the advantages of the previously described methods and offering solutions for their drawbacks to improve the strategy toward macrocyclization.

**- Bimolecular coupling (dimerization)**

In the bimolecular coupling strategy, two oligomeric precursors with appropriate terminal functionalities are coupled intermolecularly followed by an intramolecular cyclization step in one pot. Although this step might result in lower yield than in the previously described intramolecular cyclization strategy, the overall yield is usually higher because of the shorter synthesis of the building block, making this approach cost and time economic.

The process is improved by the preformation of oligomers, but the macrocyclization step remains a weak point in the synthesis of macrocycles.

**- Template synthesis**

Another approach to perform the macrocyclization efficiently uses a template to arrange the building blocks together thus promoting the intramolecular coupling. Covalent linkage does, however, imply the introduction of specific functional groups and additional synthetic steps for the attachment and cleavage of the template. A way to circumvent this is to use non covalent templates.

A perfect example of such a method is provided by the work of Anderson et al. (Figure 14 and Figure 15). They used a Vernier complex for the synthesis of a 12-porphyrin nanoring.<sup>50</sup> The



formation of a Vernier complex between components with different numbers of binding sites is the key point of their strategy, giving access to larger macrocycles while using small templates. In their case, one building block consists of four binding units and the template presents six binding units. The least common multiple of four and six is twelve. The building blocks and template combine to give a complex with twelve binding units as shown in Figure 14. Removing the template after covalent coupling gives the twelve porphyrine units macrocycle (Figure 15).

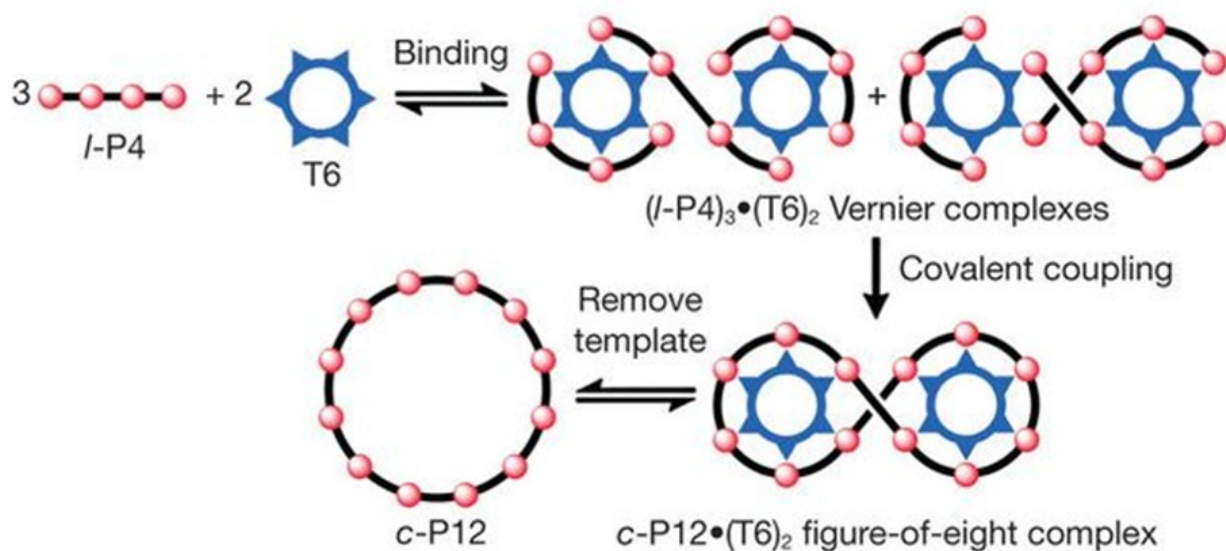


**Figure 14:** Principle of the Vernier template used by Anderson et al (reprinted from literature<sup>50</sup>).

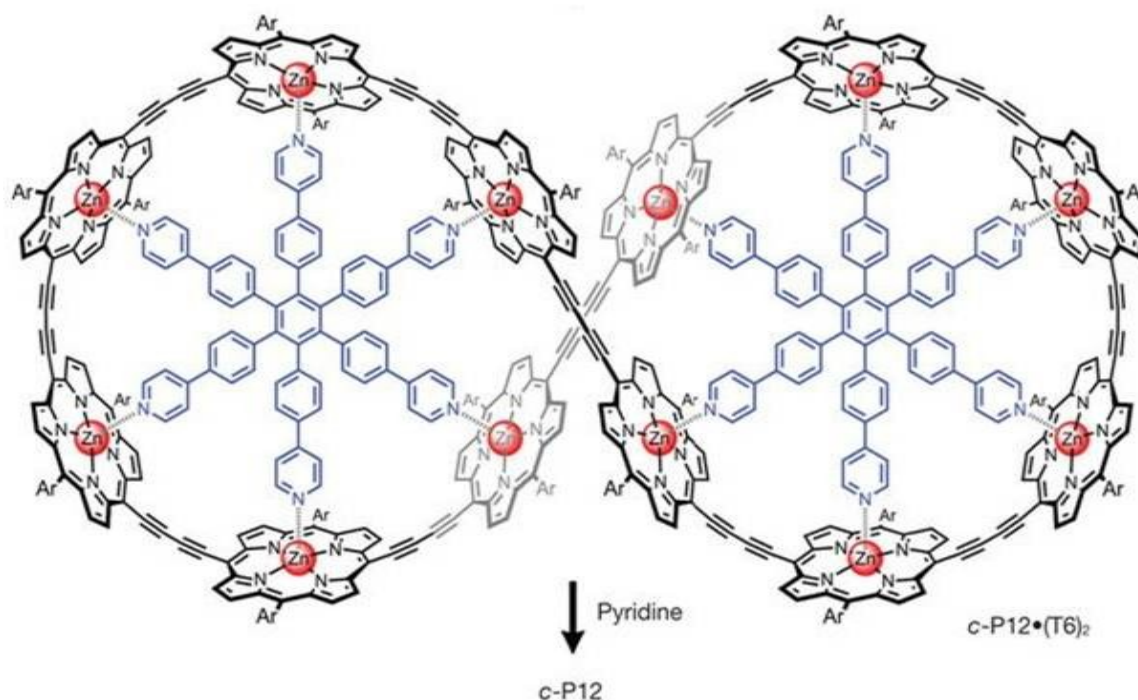


**Figure 15:** Illustration of the application of a Vernier template macrocycle synthesis (reprinted from literature)<sup>50</sup>

### - Thermodynamically driven reactions

The big disadvantages of all the previous macrocyclization strategies are mainly due to the fact that the formation of the product is controlled by kinetics. If, however, the reactions were reversible, then the product formation would be thermodynamically controlled. Thus the resulting product would depend on the relative stability of all the possible products, provided the energy gap between the possible structures is large enough. One such reversible reaction is the metathesis reaction. In the case of flexible macrocycles, the macrocycle formation is entropically driven and in general leads to the formation of macrocycles with the minimum number of monomer unit (eg. ring closing metathesis which gives mainly monomeric cyclic products). This approach is however not suitable for the synthesis of strained macrocycles which are enthalpically disfavored. Another critical point is the sometimes solubility of the product and the intermediates, which can be an issue in the case of large macrocycles.

### - Conformationally driven reactions<sup>51</sup>

The proximity of two reaction centers increases the chance of productive interaction. The activation energy of the macrocyclization can be lowered by bringing the ends into close proximity by preorganization. Several interactions such as covalent bonding, H-bonding, steric interaction,  $\pi$ -interaction, and electronic interactions (electrostatic, repulsive forces, polarization, charge transfer) could help in this purpose.

Many reactions can be used as ring closing method. But among all reactions available, the most efficient and commonly used for macrocyclization are macrolactonizations, macrolactamizations, transition metal-catalyzed cross coupling reactions, ring-closing metathesis reactions, and substitution reactions (Figure 16).

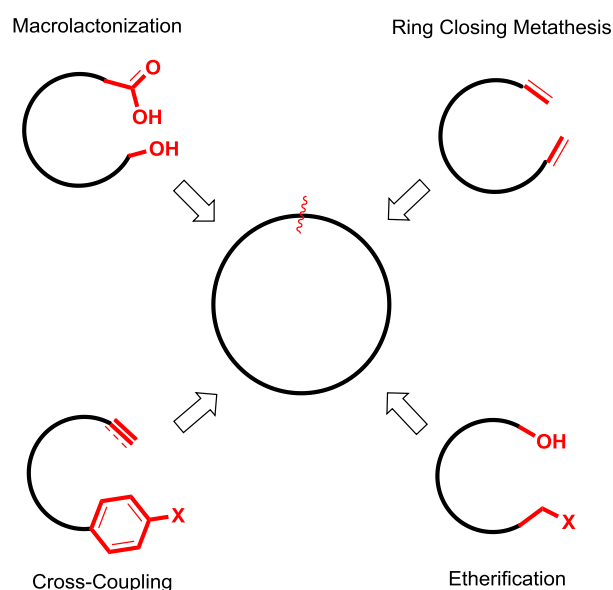


**Figure 16:** Commonly used macrocyclization reactions

In spite of all the strategies described in the present section, the synthesis of macrocycles remains a challenge. Because the cyclization of a linear precursor relies on the same reaction as the intermolecular oligomerization, the classic way of avoiding the side reaction is to dilute the reaction mixture, thus slowing the rate of the intermolecular reaction. Typical high dilution conditions are around 1 mM and less. As a result, the reaction time of a macrocyclization is slow and the reaction requires a large amount of solvent, very often the yield is low and undesired products are formed complicating the purification process. Furthermore, in the case of a catalyzed reaction, the catalyst is diluted as well which results in slow reactions. In the case of strained macrocycles, the situation is even more complicated as the cyclization is even less favored due to torsion and transannular interactions. These conditions are prohibitive for industrial synthesis, considering the amount of solvent and the implication in term of cost, environmental and safety issues. Not even considering the long reaction time and the low yield of these reactions.<sup>52</sup>

## 1.2 PROJECT AND STRATEGY

### 1.2.1 Synthesis of cycloparaphenylene via [2+2+2] cycloaddition reaction

A previous research project in the group of Prof. Dr. Wegner was the synthesis of cycloparaphenylenes (CPPs) via [2+2+2] cycloaddition reaction as a key step to bring strain in the system, taking advantage of the aromaticity gain to overcome the strain energy (Figure 17). This strategy seemed feasible since King et al. used this reaction for the synthesis of strained quadrannulene<sup>21</sup> and Maryanoff et al. used the [2+2+2] cycloaddition as a macrocyclization reaction.<sup>24</sup> The big advantage of this strategy is the introduction of substituent and strain at the same time.

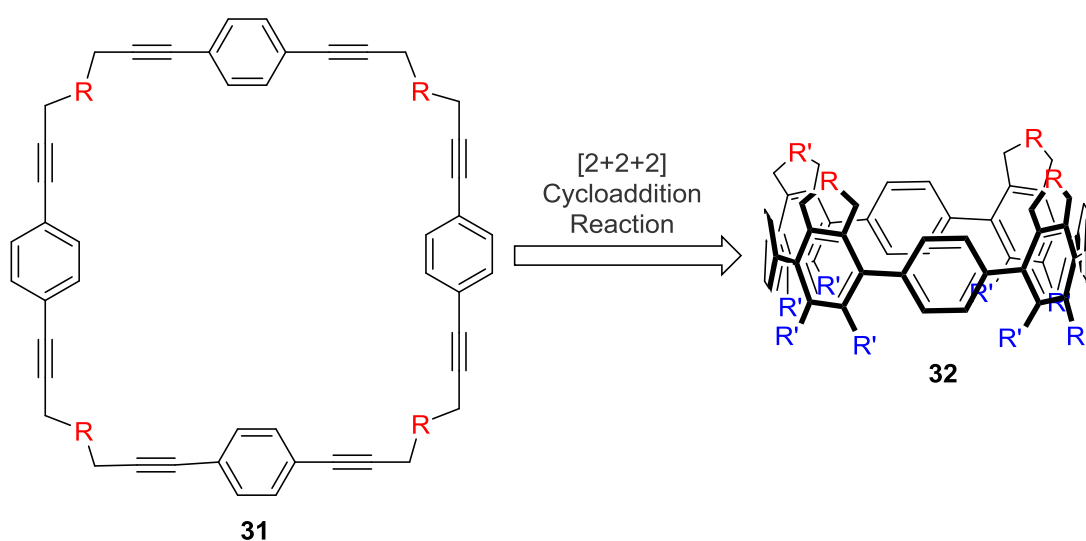
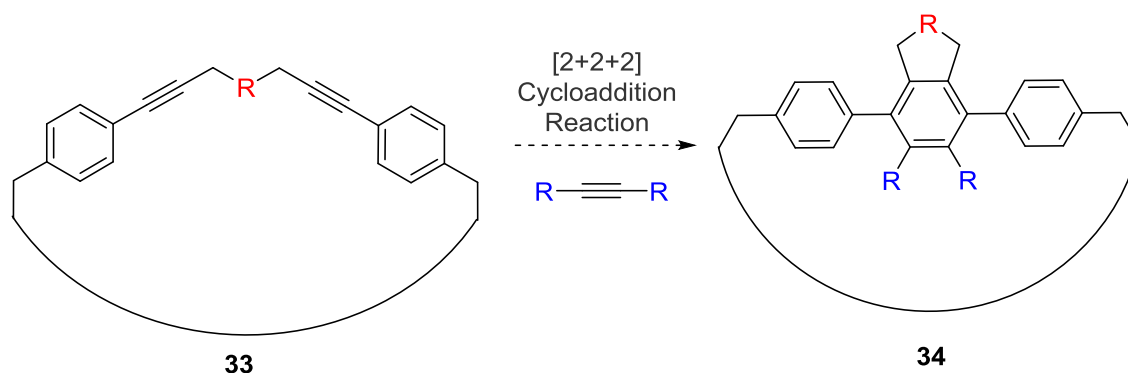


**Figure 17:** [2+2+2] Cycloaddition reaction as key step in the synthesis of cycloparaphenylenes

### 1.2.2 Initial investigation on strained model

During the course of the synthesis of the CPP, difficulties were encountered when attempting to isolate the desired macrocycle.<sup>53</sup> The cycloaddition test reactions performed with the mixture of macrocycles were not conclusive. Therefore, a proof of concept was necessary before performing the reaction with more complex systems. Indeed, this reaction on multialkyne molecule is not straightforward. Roglans et al. already studied the reactivity of aza-macrocycles in the [2+2+2] cycloaddition reaction.<sup>54</sup> In one of their macrocycles, the formation of a strained 10-membered ring prevented the reaction to occur. A similar problem could arise in our case. Hence, it is crucial to synthesize a model system (Scheme 10) to explore the possibility of applying the [2+2+2] cycloaddition reaction on strained systems and probe the applicability of our initial strategy to the synthesis of CPPs.

Consequently, the aim of this project was to develop and optimize reaction conditions for [2+2+2] cycloaddition reaction on strained systems. With a working protocol, the properties of a model strained aromatic system could be compared with those of its linear counterpart.



**Scheme 10:** [2+2+2] Cycloaddition reaction on a strained model

In order to investigate the reactivity of strained systems in the [2+2+2] cycloaddition reaction, a macrocyclic precursor is required. This macrocycle had to contain a diyne system (precursor for the [2+2+2] cycloaddition reaction) between two phenyl rings (for conjugation), linked by a short chain to build strain in the system.

The general strategies in focus are summarized in Figure 18. Approaches using the Sonogashira reaction, ring closing metathesis and etherification reactions for the macrocyclization step were envisioned.

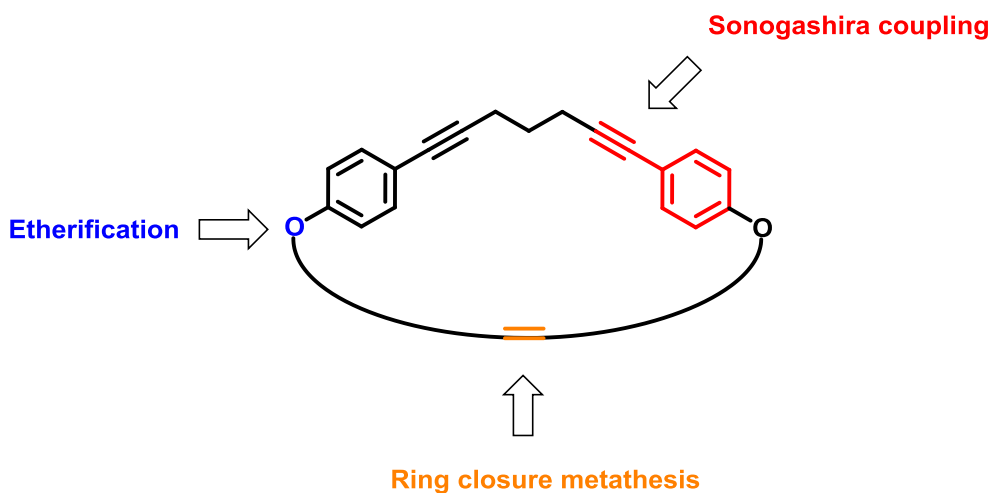


**Figure 18:** Strategies to the macrocycle synthesis

In summary, the aims of the present project are:

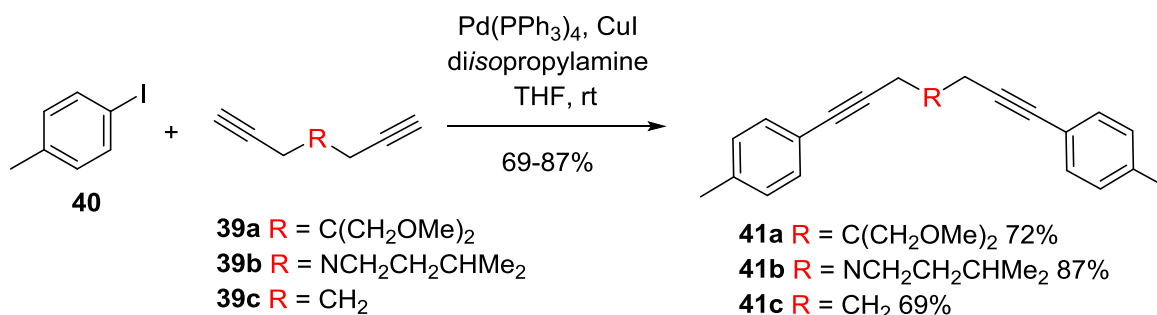
- Develop cycloaddition reaction conditions on a linear precursor
- Synthesize a macrocyclic precursor as model for strained systems
- Investigate the cycloaddition reaction on the macrocyclic precursor.

### 1.3 RESULTS AND DISCUSSION

#### 1.3.1 Terphenyl synthesis via [2+2+2] cycloaddition reaction

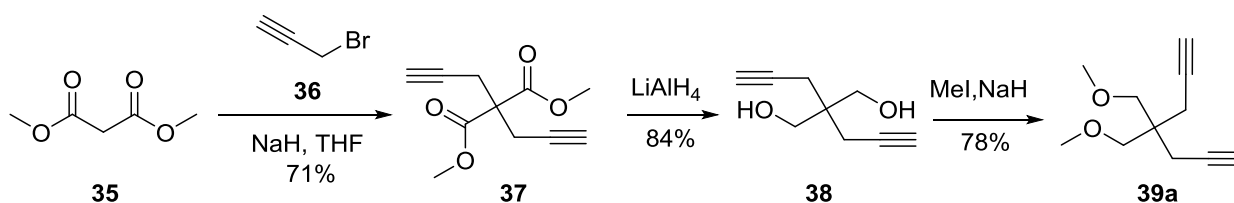
##### 1.3.1.1 Synthesis of the linear precursor

Before performing the reaction with strained systems, we initially investigated the [2+2+2] cycloaddition reaction on linear systems. In this course, linear molecules were synthesized using Sonogashira coupling reactions of a tethered diyne and 4-iodotoluene (Scheme 11).



**Scheme 11:** Synthesis of linear precursor **41a-c**

The diyne **39a** was synthesized in three steps as shown in Scheme 12 from dimethyl malonate **35**. Double addition of propargyl bromide on dimethyl malonate afforded the intermediate **37** which was subsequently reduced by  $\text{LiAlH}_4$  to the diol **38**. The diol **38** was finally methylated to give the desired diyne building block **39a**. The diyne **39b** was synthesized by a previous student in our group.<sup>53</sup>



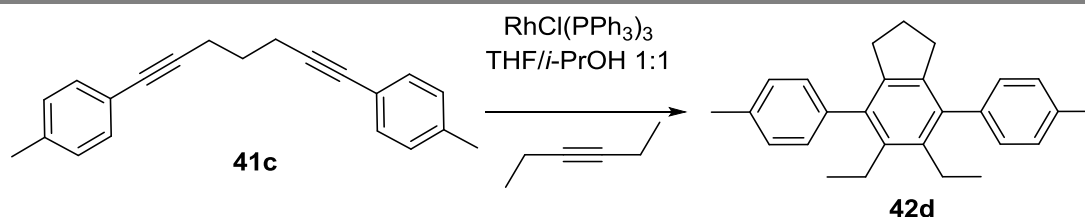
**Scheme 12:** Synthesis of diyne **39a**

Different diynes were coupled with 4-iodotoluene **40** catalyzed by palladium tetrakis(triphenylphosphine) and copper iodide in a Sonogashira reaction. The 4-iodotoluene was chosen for practical reasons because its symmetry facilitates the analysis. The Sonogashira coupling of the diyne building block with 4-iodotoluene provided the expected linear precursors **41a-c** in good to very good yields (Scheme 11).

### 1.3.1.2 Optimization of the [2+2+2] Cycloaddition reaction

With the linear precursors in hand, the [2+2+2] cycloaddition reaction was performed using the conditions reported by Grigg<sup>4</sup> and McDonald<sup>19</sup> for the synthesis of oligo-*paraphenylenes*. First, test reactions of diyne **41c** with but-3-yn-1-ol and but-2-yn-1,4-diol were performed. However, the reaction required two additions of 5 mol% catalyst and 40 hours to reach completion with 64% and 60% yield respectively. These yields were lower than those reported in the literature for similar reactions (94%). However, the lower yield of the reaction can also be attributed to losses during workup and purification procedures which were complicated by the presence of the polar hydroxyl group. Another test reaction with acetylene as monoynone partner was made, but this reaction did not afford the desired product. Analyses indicated that acetylene polymerization had occurred instead. Due to the unsuccessful reaction and safety concerns, acetylene is not a suitable alkyne for the optimization of this reaction. Therefore, the reaction was optimized using the unfunctionalized symmetric hex-3-yne which also presents the advantage to be volatile, facilitating the purification process.

In recent years, the use of microwave irradiation in organic synthesis has increased considerably.<sup>55-57</sup> Reaction rate enhancements are often observed when applying microwave irradiation instead of traditional heating. Shortening the reaction time permits to reduce the amount of side products formed and thereby promotes higher yields. The energy of a microwave photon is too low to induce a chemical reaction itself. The advantage of microwave enhanced reactions is based on efficient internal heating by directly transferring microwave energy to the molecules (solvents, reagents, catalysts). Microwave irradiation results in the alignment of dipoles and ions parallel to the applied electric field. As this field is oscillating, the dipoles and ions tend to realign themselves with the alternating field, losing energy in the process in the form of molecular friction and dielectric loss, generating heat. Thus, the polarity of the implicated molecules plays an important role in microwave enhanced reactions. Among other reactions, several examples of cycloaddition reactions of alkynes enhanced by microwaves can be found in recent literature.<sup>15,58-61</sup> Therefore, we also performed the reaction in a microwave reactor at 100°C for six hours with 10 mol% catalyst without second addition and obtained the product in very good yield (85%, Table 1, Entry 1).

**Table 1:** Optimization of the [2+2+2] cycloaddition reaction on a linear precursor

Entry	Heating	Catalyst Loading	Alkyne	Concentration	Isolated Yield
1	MW 100°C 6 h	10 mol%	30 eq.	20 mM	85%
2	Reflux 2 d	2 x 5 mol% <sup>a</sup>	30 eq.	20 mM	85%
3	MW 100°C 6 h	5 mol%	30 eq.	20 mM	87%
4	MW 100°C 6 h	5 mol%	10 eq.	20 mM	- <sup>b</sup>
5	MW 100°C 6 h	5 mol%	10 eq.	75 mM	80%

<sup>a</sup>second addition of catalyst after 24 hours <sup>b</sup>no conversion was observed

This first result was very encouraging as the reaction time could be dramatically reduced compared to traditional heating conditions. Further optimization showed that it was possible to reduce the catalyst loading to 5 mol% without lowering the yield. The excess of the monoynone could also be lowered from 30 to 10 equivalents provided the concentration was increased (Table 1, Entry 5). Moreover, no workup was necessary in the case of hex-3-yne.

During the exploration of the reaction scope, the reaction of diyne **41a** with hex-3-yne was stopped after one hour due to a sudden raise in pressure. Nevertheless, the reaction was already finished (85% yield), showing that the experiment time could in principle be shortened. However, in order to keep a general procedure, and because the microwave reactor does not allow for reaction control without stopping the reaction, all reactions were set up for six hours to ensure completion.

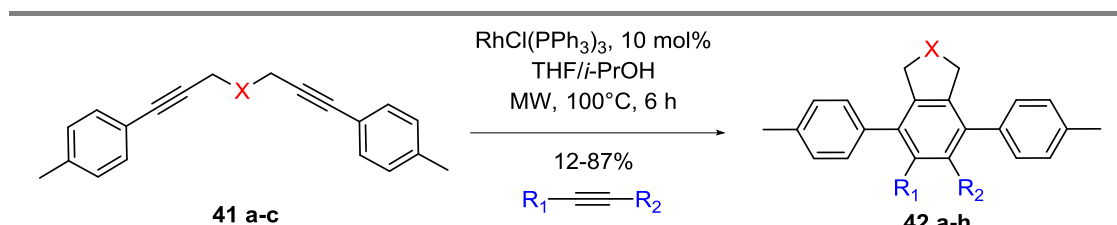
Although the catalyst loading could in principle be reduced, we decided to use 10 mol% for the sake of reproducibility on the reaction scale we used for the study of the scope of the optimized reaction.



## 1.3.1.3 Scope of the microwave mediated [2+2+2] cycloaddition reaction

The scope of the optimized [2+2+2] cycloaddition reaction of tethered diynes with different monoynes was explored. A variety of linear *p*-terphenyls was synthesized from tethered diynes in moderate to very good yields using Wilkinson's catalyst and 10 equivalents of monoynes in a mixture of *i*-PrOH and THF under microwave irradiation. The results of the [2+2+2] cycloaddition reaction with linear precursors are shown in Table 2.

Table 2: Scope of the [2+2+2] cycloaddition on linear precursors



Entry	Alkyne		Diyne X	Product	Isolated Yield
	R <sub>1</sub>	R <sub>2</sub>			
1	Et	Et	C(CH <sub>2</sub> OMe) <sub>2</sub>	42a	85%
2	CH <sub>2</sub> OH	CH <sub>2</sub> OH	C(CH <sub>2</sub> OMe) <sub>2</sub>	42b	48%
3	TMS	TMS	C(CH <sub>2</sub> OMe) <sub>2</sub>	-	<sup>a</sup>
4	H	CH <sub>2</sub> CH <sub>2</sub> OH	CH <sub>2</sub>	42c	64%
5	Et	Et	CH <sub>2</sub>	42d	87%
7	Ph	Ph	CH <sub>2</sub>	42e	76%
8	TMS	H	CH <sub>2</sub>	42f	75%
9		MeCN	CH <sub>2</sub>	42g	12%
10	Et	Et	N(CH <sub>2</sub> CH <sub>2</sub> CH(CH <sub>3</sub> ) <sub>2</sub> )	42h	85%

<sup>a</sup>Starting material was recovered

The substitution on the tethered diyne building block had no influence on the yield of the reaction (Table 2, Entries 1, 5 and 10) and differently substituted diynes reacted with hex-3-yne to afford the respective products in 85–87% yield.

However, some differences were observed when varying the monoynone. Alcohol containing monoynes gave somewhat lower yields (48–64%) presumably because of losses during workup and purification (Table 2, Entries 2 and 4). Terminal alkynes reacted with diynes in good yields (Table 2, Entries 4 and 8). The more hindered phenylacetylene also gave a satisfying yield of 76% (Table 2, Entry 7). Only acetonitrile was not very reactive under those reaction conditions, the product was obtained in only 12% yield (Table 2, Entry 9). Bis(trimethylsilyl)acetylene and dimethyl

acetylenedicarboxylate did not react at all with the diyne **41c**. This shows that the reaction of electron deficient alkynes with diynes is not favored under these reaction conditions.

The structures of several examples of terphenyls were analyzed by X-ray crystallography (Figure 19). The torsion angles between the middle phenyl ring and its neighboring phenyl rings are in the range of 92–110°. The phenyl rings adopt a quasi perpendicular arrangement. The substituent on the middle ring had no influence on the relative orientation of the rings. This is in sharp contrast to the X-ray structure of the unsubstituted *p*-terphenyl for which all benzene ring adopted a planar arrangement.<sup>62-65</sup> The substitution on the middle phenyl ring brings more steric hinderance, thus forcing the ring to adopt a twisted configuration even in the crystal form.

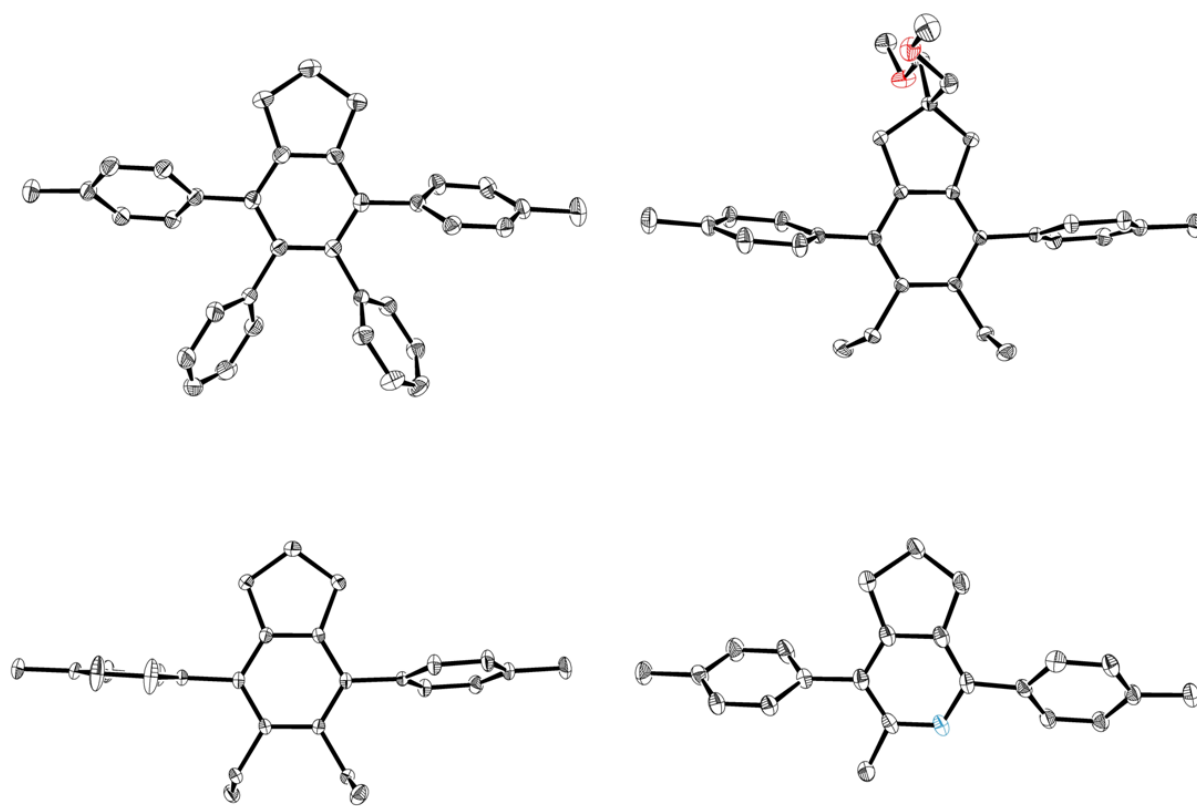


**Figure 19:** Solid state structure of linear substituted terphenyls **42a**, **42d**, **42e** and **42g** (Ortep drawing, hydrogens omitted)

### 1.3.1.4 Optical properties of substituted *p*-terphenyls

The UV absorption and emission spectra were measured in chloroform ( $2.5 \cdot 10^{-5}$  M) for the differently substituted terphenyls (Figure 20). All terphenyls present a maximum of absorption around 230 nm. Terphenyls with only one substituent presented a distinct second absorption maximum at a longer wavelength (260 nm). This can probably be attributed to the better rotation ability of those less hindered terphenyls. On the contrary terphenyl substituted with larger group on both sides of the middle phenyl ring (**42e**, **42a**, and **42b**) only show shoulder peaks around these wavelengths due to a less flexible structure with less possible conformations. Between the two extremes, the molecule **42d** with substituents on both sides of the middle ring but smaller groups on the cyclopentane moiety also presents a second maximum at larger wavelengths. The phenyl-substituted terphenyl **42e** and the pyridine molecule **42g** showed a second maximum peak around 240 nm and several shoulder peaks. This is characteristic for highly conjugated systems which have different conformers and different transitions between vibrational levels.

No identifiable trend could be drawn from the fluorescence spectra. The emission maxima span from 330–350 nm. The shape of the emission spectra of the different terphenyls is similar and all terphenyls present quite large Stokes shifts. This shows that a lot of excitation energy is lost during the relaxation from the excitation state most probably by rotational and vibrational relaxations.

In summary, it is quite difficult to generalize the observations for the different molecules. They present unique features depending on their substitution pattern.

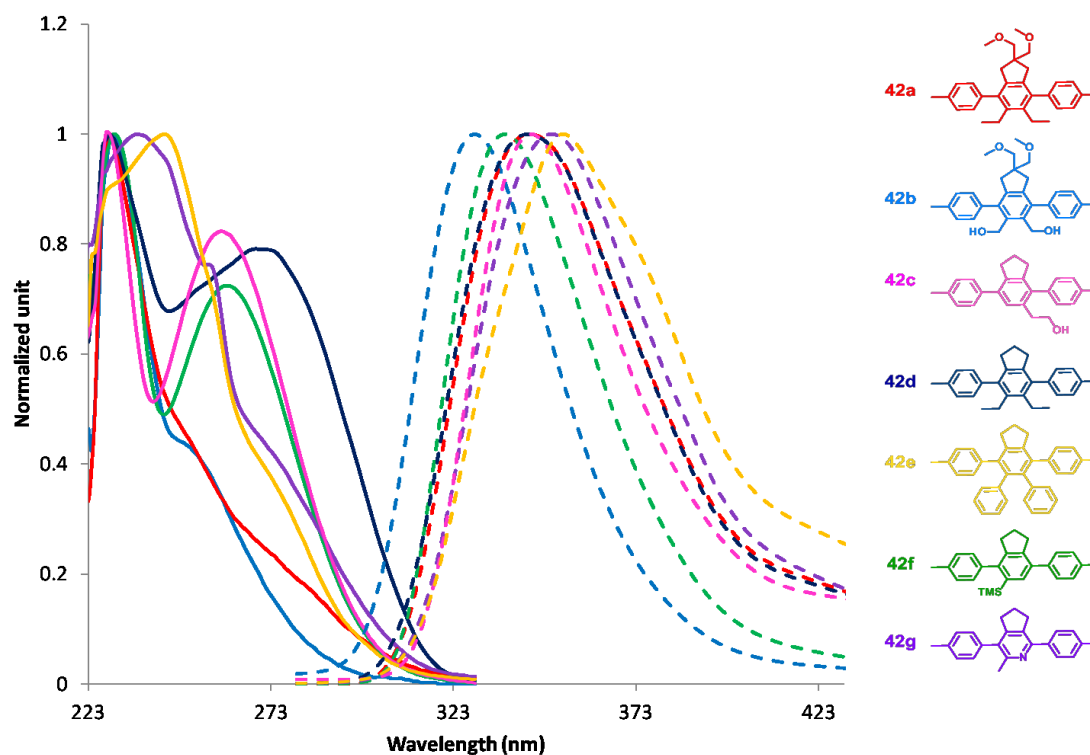


**Figure 20:** UV absorption (solid lines) and fluorescence (dashed lines) spectra of substituted terphenyls

### 1.3.2 Synthetic strategies toward the macrocyclic precursor

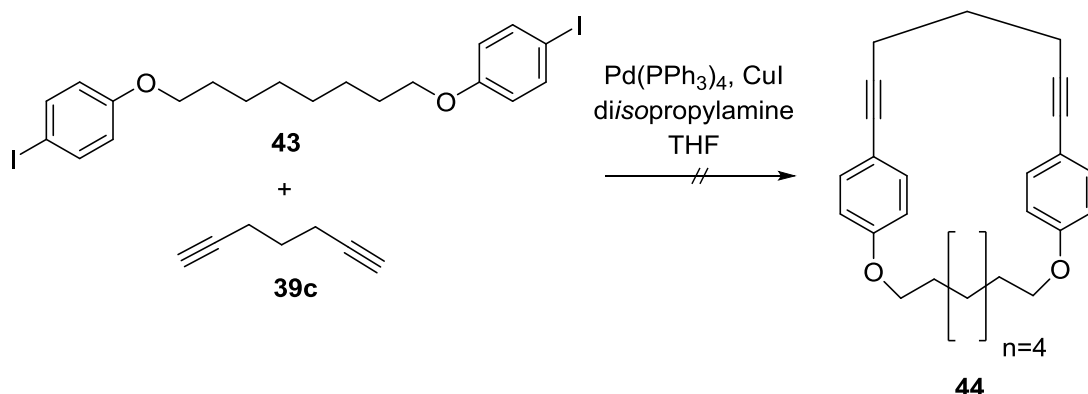
Several strategies have been explored in order to synthesize a macrocyclic precursor for the [2+2+2] cycloaddition reaction. Among the possible macrocyclization reaction available, we choose to probe the Sonogashira coupling, the ring closing metathesis and ether formation reactions. Those methods were investigated in parallel, and efforts were then focused on the most promising strategy.

#### 1.3.2.1 Synthesis of the macrocycle via Sonogashira reaction

The Sonogashira reaction was the strategy investigated initially.<sup>53</sup> It was also the reaction of choice for the synthesis of the linear precursor **41** (section 1.3.1.1). As the principal requirement for our macrocycle is the presence of a tethered diyne building block between two phenyl units, it seems quite natural to choose the Sonogashira coupling as ring closing method.

##### - First strategy

The first strategy we tested is depicted in Scheme 13. The macrocycle should be produced by coupling of hepta-1,6-diyne with the diiodide **43**.

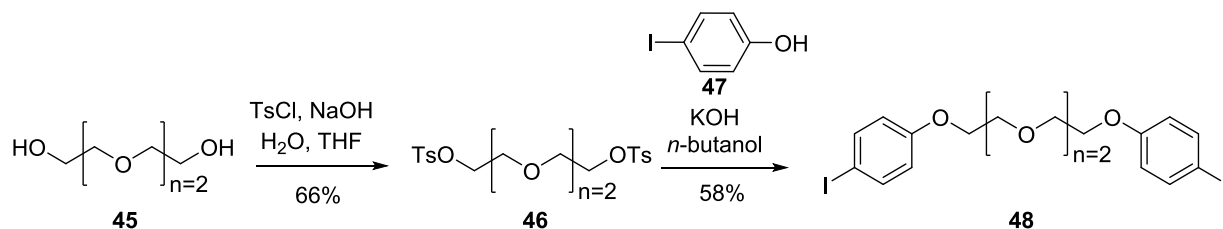


**Scheme 13:** First Sonogashira macrocyclization strategy

Several test reactions were performed also on larger scale in order to facilitate isolation of the product. Starting material was always present even after extended reaction time (48 h) and further addition of catalyst, but only linear oligomeric products were isolated. When pseudo-high dilution was used by slow addition of starting material to a solution of the catalysts, the same result was observed. Many attempts to isolate the desired macrocycle from the complex mixture were performed without success.

- **Second strategy**

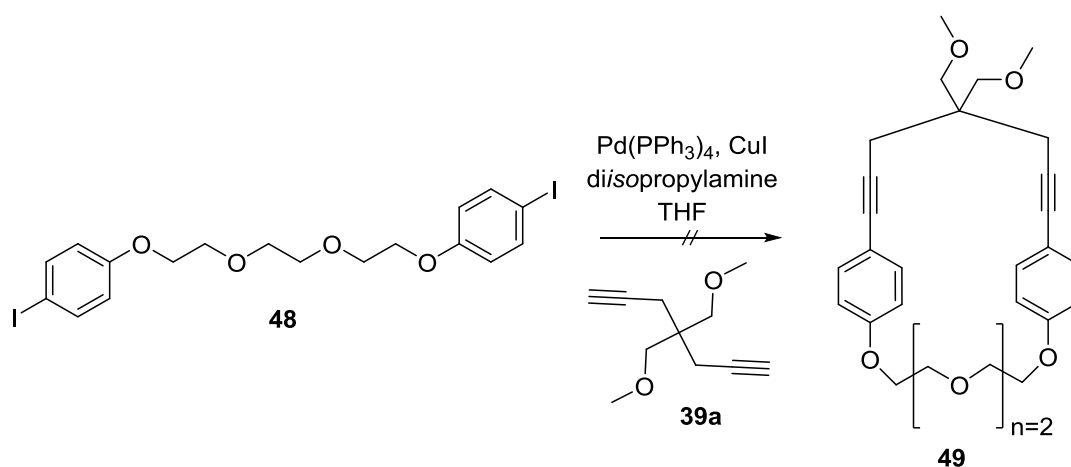
As one of the major problems with the previous strategy might have been that the alkyl chain was not flexible enough to permit the macrocyclization, a more flexible ethylene glycol chain was used instead (Scheme 15).<sup>66-68</sup> Ditosylated triethylene glycol **46** was synthesized in good yield (66%) by tosylation of triethylene glycol according to a literature procedure.<sup>69</sup> Then, substitution of the tosyl groups with 4-iodophenol afforded the building block **48** in 58% yield (Scheme 14).



**Scheme 14:** Synthesis of the diiodide building block

In order to favor the macrocyclization, the diyne **39a** was devised as the ether tail bridge should bring the alkyne moieties in the proper position to favor the macrocyclization through a Thorpe Ingold effect. Indeed, by increasing the size of two substituents on a quaternary carbon, the angle between those substituents is increased, which induces a decrease of the angle between the other two parts of the molecule, bringing them closer together. This effect is commonly employed to enhance cyclization reactions.<sup>70</sup> The synthesis of diyne **39a** was previously discussed in section 1.3.1.1.

When the macrocyclization was attempted under classical conditions (14 mM), a complex mixture of oligomers was obtained. Under high dilution conditions, no reaction was observed. The reaction was also performed under pseudo-high dilution conditions (slow addition during 24 h at 40°C), but here again only oligomers were obtained.

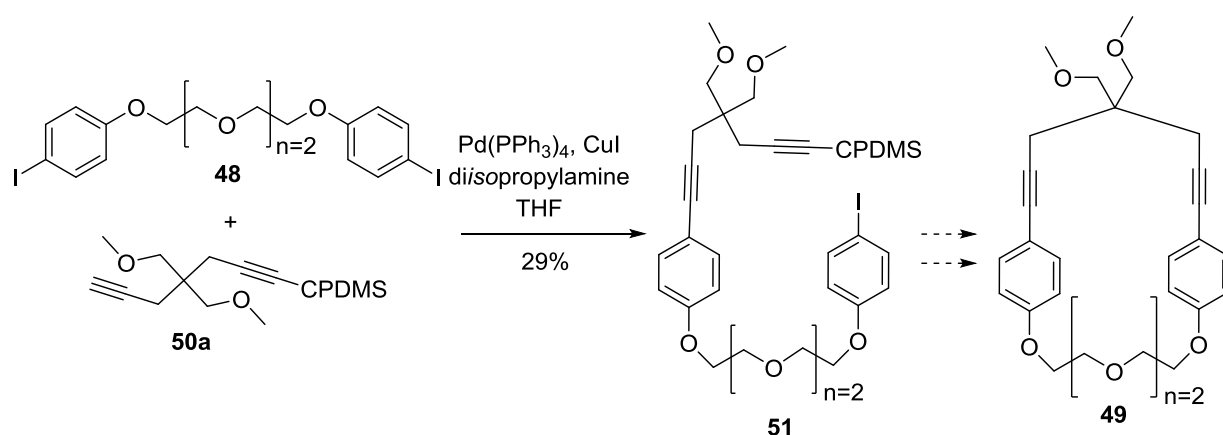


**Scheme 15:** Second Sonogashira macrocyclization strategy

Another possible solution would be to use some sort of template effect. Coordination of a cation to the oxygens of the ethylene glycol chain, for example, would bring the extremities of the molecules closer together. Sodium or potassium cations would be good candidates in this endeavor. A Sonogashira procedure with only copper iodide as the catalyst in water and KOH as base was reported in the literature.<sup>71</sup> These reaction conditions were tried with our substrate. The reaction led only to oligomers, and required high temperature (140°C, 6 h) and high concentration.

### - Third strategy

In order to prevent the formation of oligomers, a stepwise approach was envisioned which involved the Sonogashira coupling of the protected diyne **50a**, followed by the deprotection and subsequent intramolecular macrocyclization reaction (Scheme 16).



**Scheme 16:** Third Sonogashira macrocyclization strategy

The coupling of the (3-cyanopropyl)dimethylsilyl (CPDMS) protected building block **50a** and the diiodide **48** gave the product **51** in only 29% yield. The theoretical yield is limited by the statistical reaction of the bifunctionalized molecule.

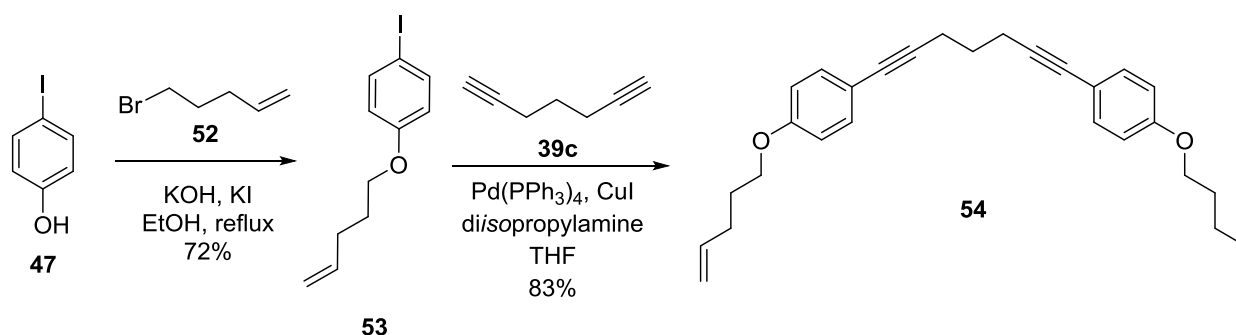
As the protection of the diyne **50a** was already hampered by a low yield (statistical reaction), this strategy is not very efficient as another critical point will be the ring closure step. Therefore the efforts were directed towards other strategies. However, it is worth mentioning that one of the advantages of this strategy would be to help to identify the desired product in the complex mixture obtained with the strategies mentioned above.

In conclusion, the choice of the Sonogashira reaction as ring closing method turned out to be not as successful as originally expected. In general, the successful macrocyclization via Sonogashira coupling involved substrates with well designed persistent shapes which assemble together like puzzle pieces.

### 1.3.2.2 Synthesis of macrocycle via ring closing metathesis

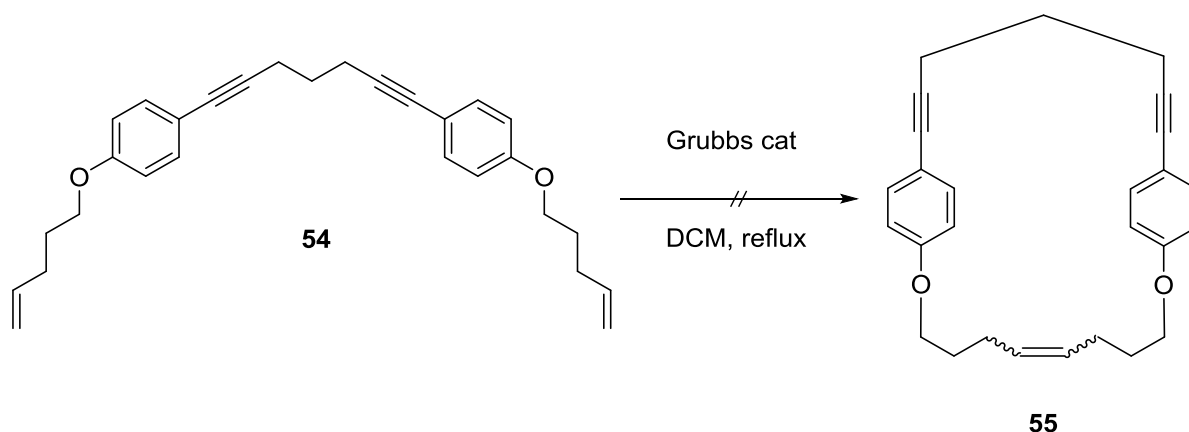
Besides the macrolactamization and macrolactonization strategies, the ring closing metathesis (RCM) reaction is one of the most common methods for macrocyclization. This is due the reversibility of this reaction as discussed in the introduction (section 1.1.3.2). Indeed, under reversible reaction conditions, the formation of the reaction product is thermodynamically controlled. The smallest oligomer is preferably produced and intramolecular reactions are favored over intermolecular reactions. Therefore, this strategy was investigated to achieve the macrocycle synthesis.

The building block was obtained by substitution reaction with the bromide **52** in 72% yield (Scheme 17). The next step was performed by Sonogashira coupling of the iodide **53** with hepta-1,6-diyne, producing the product **54** in 83% yield.



**Scheme 17:** Synthesis of the precursor for the RCM macrocyclization

With the precursor **54** in hand, metathesis with Grubbs II catalyst was attempted (Scheme 18). Unfortunately, no reaction was observed even after extended reaction time and adding additional catalyst.



**Scheme 18:** Attempted RCM mediated macrocyclization

The reaction was tried again with Grubbs I catalyst. This time, the formation of the desired product was observed by mass spectrometry analysis.  $^1\text{H-NMR}$  analysis of the reaction mixture

suggests that a mixture of E and Z isomers was formed. After this first promising result, the reaction was performed again on larger scale in order to isolate the product. However, this time a complex mixture of different products was obtained.

One problem of this catalyst is that it is also known to catalyse other reactions such as enyne metathesis. Moreover, the formation of other oligomers can not be excluded if the macrocycle is too strained to be thermodynamically favorable. Therefore, considering the problem of scaling up as well as the complexity of the mixture, efforts were further focused on another strategy.

### 1.3.2.3 Synthesis of macrocycles via ether formation

In order to circumvent the disadvantages of the previously described methods namely catalysis and side reactions, another strategy was undertaken. The key reaction of this strategy is to close the ring on the oxygen atoms by ether formation. We had already predicted that a flexible polyethylene glycol chain would bring the necessary flexibility to permit the macrocyclization. We were inspired by syntheses of crown ethers and benzocrown from the literature with high yields for macrocyclization reaction.<sup>42</sup> The high yields of such reactions were obtained thanks to the coordination of the oxygens of the polyethylene glycol chains to a cation which brings the two ends of the molecule in close proximity to each other, thereby, providing a templating effect. We developed our strategy in this direction with the two approaches depicted on Figure 21.

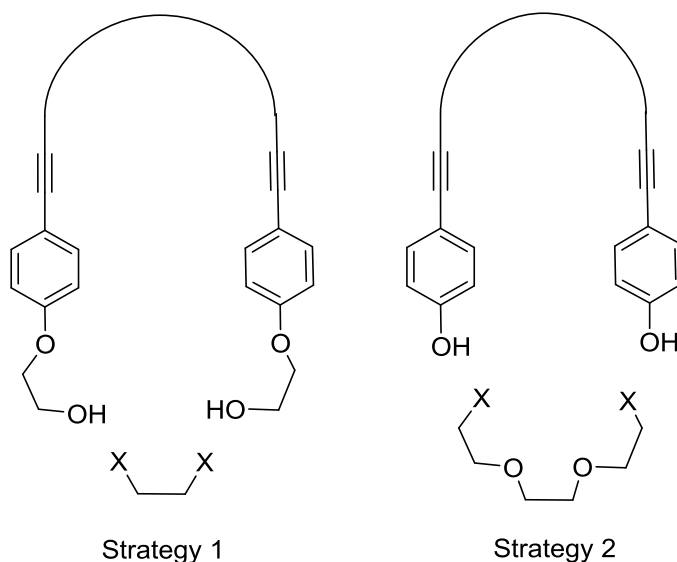
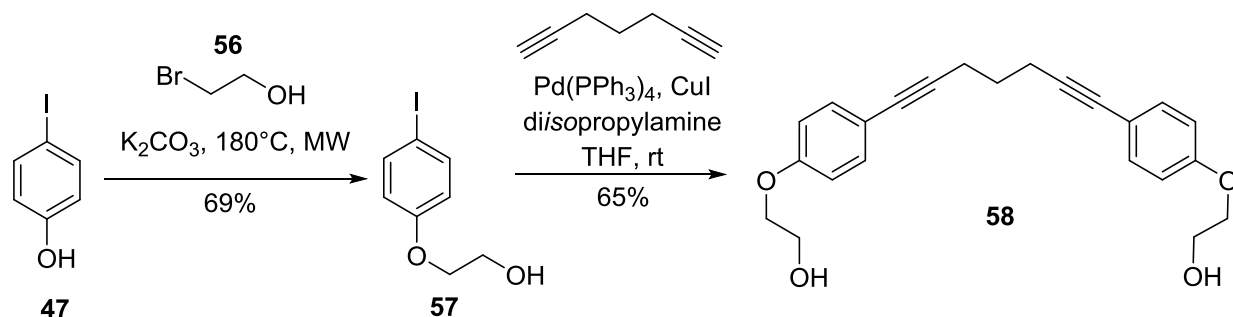


**Figure 21:** Two strategies towards the macrocyclization via ether formation



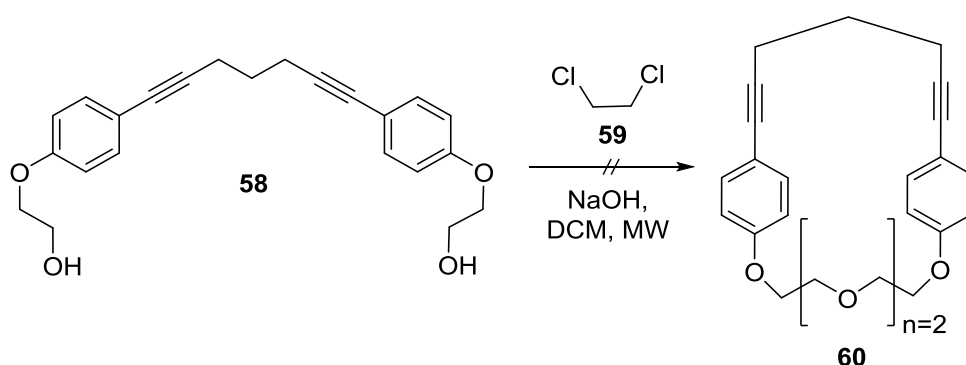
**Strategy 1**

The first approach was to close the ring with a small building block. In principle the coordination of sodium or potassium should hold the hydroxyl termini close together to favor the substitution reaction with the small fragment **59**. Building block **58** was synthesized via cross coupling reaction.



**Scheme 19:** Synthesis of the precursor **58**

Different conditions were tried to get the first step to work. The first reaction with chloroethanol in DMF gave **57** only in 52% yield. A microwave assisted reaction was attempted but high pressure developed in the reaction vessel which made this reaction unfeasible. Finally, the reaction with bromoethanol under microwave irradiation proceeded satisfactory to give the product **57** in 69% yield (Scheme 19). This building block was then combined with hepta-1,6-diyne by Sonogashira coupling to afford the diyne **58** in 65% yield. A test reaction for the next step was performed under microwave reaction conditions with NaOH and dichloroethane **59**, but no reaction was observed (Scheme 20).



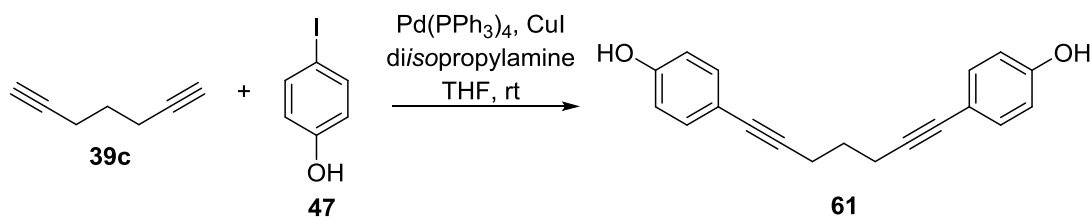
**Scheme 20:** Macrocyclization via ether formation

**Strategy 2:**

In parallel to the first strategy, another strategy was investigated which involved the assembly of the macrocycle from a ethylene glycol ditosylate chain and a diol building block containing the tethered diyne between two phenyl rings.

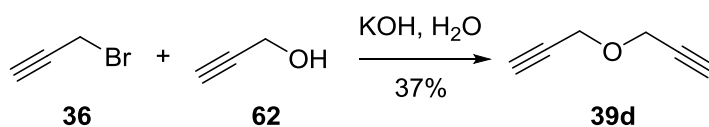
We first envisioned the building block **61** which was synthesized by Sonogashira coupling from iodophenol **47** and hepta-1,6-diyne **39c** (Scheme 21). Unfortunately, the solvent free product **61** was

not stable which will complicate the outcome of the macrocyclization if in parallel to the possible macrocyclization and oligomerization, degradation can occur.



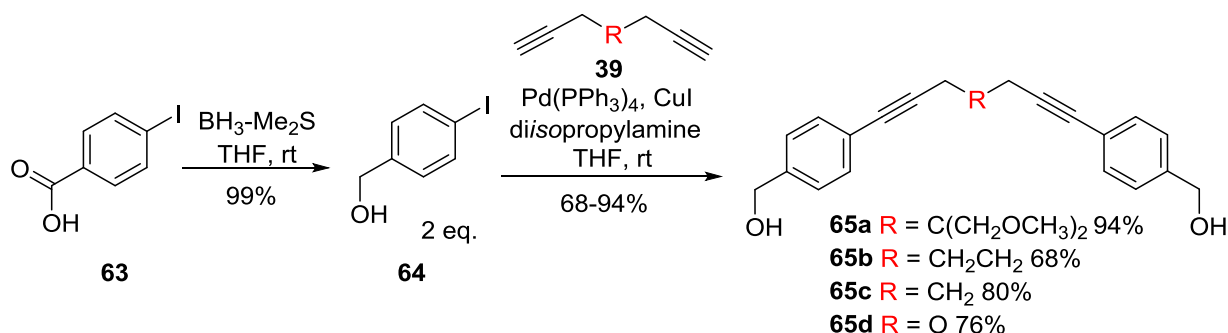
**Scheme 21:** Synthesis of building block **61**

Thus another building block was designed using benzylic alcohol **64**. The benzylic alcohol was synthesized by reduction of the corresponding carboxylic acid with  $\text{BH}_3 \cdot \text{SMe}_2$  in quantitative yield. Different diynes were used for the Sonogashira coupling with benzylic alcohol **64**.



**Scheme 22:** Synthesis of the diyne **39d**

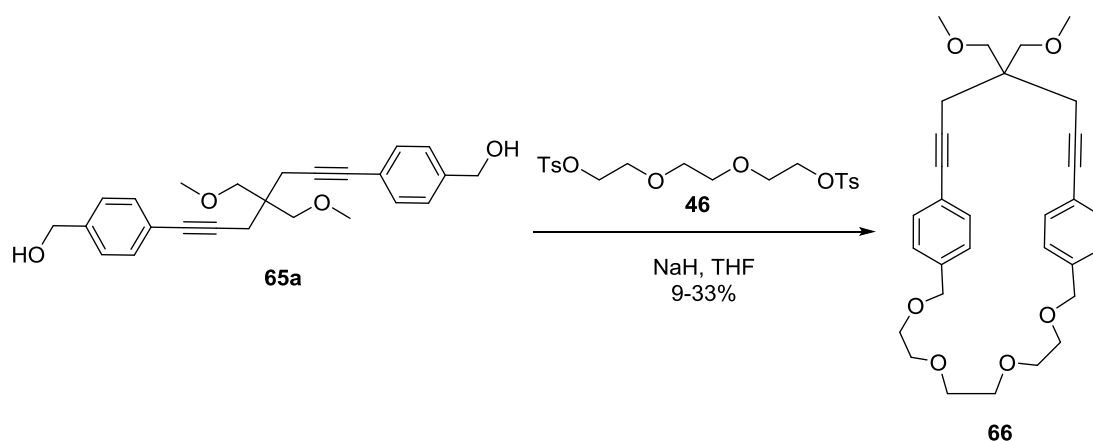
The synthesis of diyne **39a** was discussed in section 1.3.1.1. The diyne **39d** was synthesized by substitution reaction of propargyl bromide with propargyl alcohol in 37% yield (Scheme 22). The building blocks were combined by Sonogashira reaction in good to excellent yields (Scheme 23). The coupling partner for the macrocyclization was the triethylene glycol ditosylate **46** for which the synthesis was described previously (Section 1.3.2.1).



**Scheme 23:** Synthesis of the diyne building blocks

The macrocyclization was attempted according to the work of Rathore et al. who already used the coordination of tetraethylene glycol to potassium for the synthesis of terphenyl crown ethers.<sup>42</sup> They obtained their desired macrocycle in 75% yield using four equivalents of potassium hydride in THF. We decided to use similar conditions for our macrocyclization. However, we chose sodium hydride because we expected sodium to fit better with the smaller triethylene glycol chain, and it is also easier to handle than potassium hydride. Building block **65a** was treated with  $\text{NaH}$  (4 eq.) in THF followed by addition of the triethylene glycol ditosylate **46** and the resulting mixture was

refluxed overnight. Our first attempt at this reaction with 9% isolated yield was not as successful as the macrocyclization of Rathore et al. (Scheme 24).



The macrocyclization reaction was tried with the different building blocks **65a-d**, which differ in the substitution on the diyne moiety. Only the macrocycle **66** resulting from the reaction of the ether tailed building block **65a** with triethylene glycol ditosylate **46** could be isolated in 9% yield. The reaction with other substituent on the bridge only gave complex mixtures. The presence of side chains on the bridge is apparently required for the success of the macrocyclization reaction. This can be rationalized by a positive Thorpe Ingold effect of the substituents on the bridge atom to push the alcohol moieties of the molecule closer together, thereby favoring the shape for the connection with the ditosylated building block **46**. From the  $^1\text{H-NMR}$  spectrum of crude product obtained from the macrocyclization reaction between **65a** and **46** (Figure 22) it is obvious that the desired macrocycle **66** was not the major product formed during the reaction.

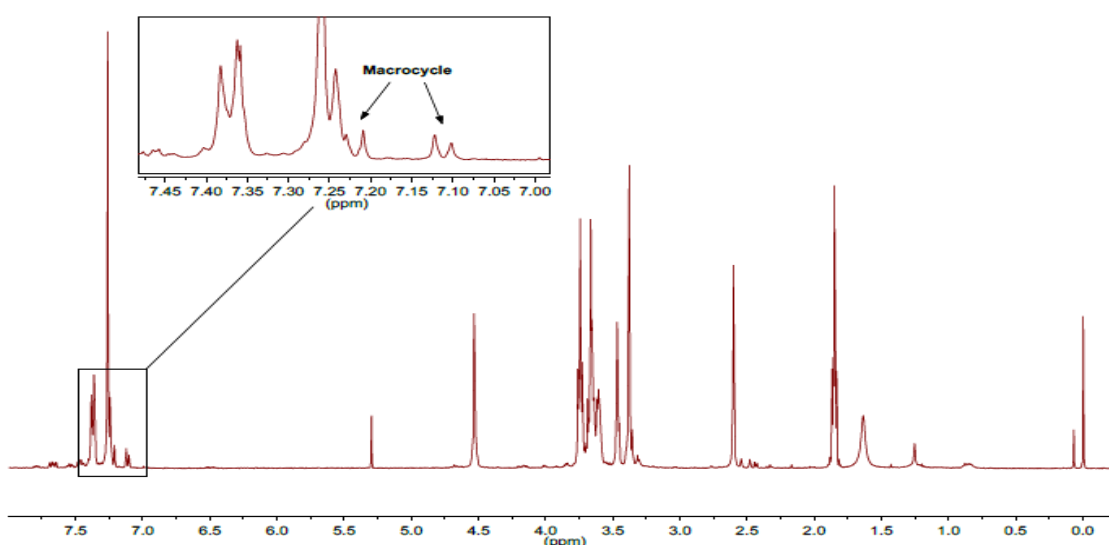


**Figure 22:** Crude  $^1\text{H-NMR}$  spectrum (400MHz,  $\text{CDCl}_3$ ) of the macrocyclization reaction between **45a** and **46**

When controlling the reaction by thin layer chromatography (TLC), the major part of the reaction mixture consisted of very polar products. Several possibilities can be imagined. Most probably, the reaction produces a mixture of several oligomeric products. Macrocyclic and linear oligomers but also interlinked macrocycles can be formed. The formation of complexes between the desired macrocycle **66** and the sodium cation is also possible.

Consequently, we tried to optimize the reaction in order to obtain the macrocycle as major product. The outcome of the test reactions could be qualitatively analyzed by  $^1\text{H-NMR}$  spectroscopy of the crude reaction mixture. The proportion between the aromatic peaks of the baseline products and the aromatic peaks of the desired macrocycle give a good point for the evaluation of the different conditions. Varying, the hydride ( $\text{NaH}$ ,  $\text{KH}$ ,  $\text{CaH}_2$ ), the excess of hydride (2 eq., 4 eq., 10 eq.), the solvent (THF, DCE), the chain length (triethylen-, tetraethylene glycol), the concentration or the reaction duration, no significant improvement could be achieved.

Repetitions of the synthesis at different scale (0.5–1.0 g) gave better isolated yields in the range of 19–33%. This variability can be attributed mainly to improved isolation and purification techniques. Although no major impurities were observed in the recorded  $^1\text{H-NMR}$  spectra, the macrocycle **66** was obtained as yellow oil. Many efforts were dedicated to the crystallization of the product. Indeed, if the macrocycle was isolated as a solid it could be purified by recrystallization. A very pure fraction of macrocycle **66** as a white solid was obtained by trituration and extraction with hexane. The structure in the crystal was determined by X-ray diffraction analysis and confirmed the structure of the desired macrocycle **66** (Figure 23). Although the macrocycle could in some cases, be obtained as a solid after single column chromatographical purification, the solid is in general not homogenous and not crystalline.

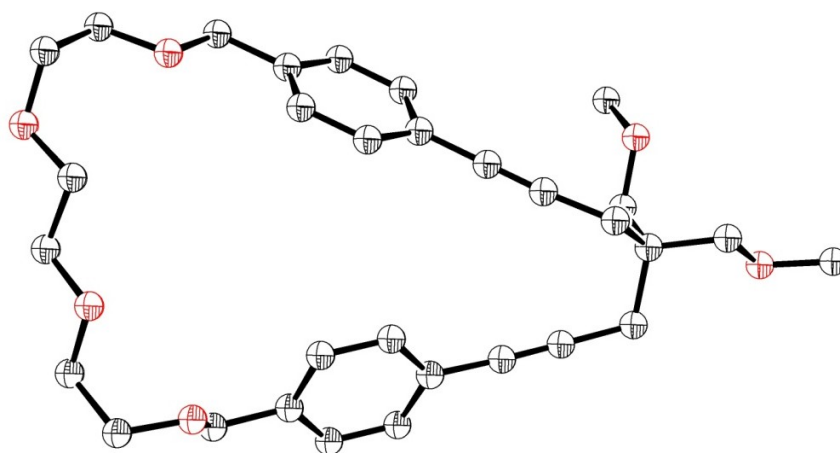


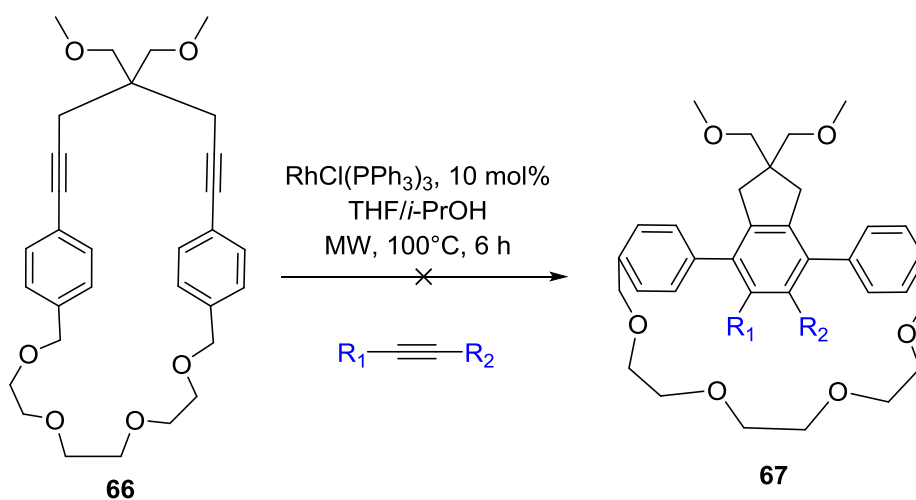
**Figure 23:** X-ray structure of macrocycle **66** (Ortep drawing, hydrogens and solvent omitted)

In conclusion, we explored different strategies in order to achieve the synthesis of a macrocycle containing the diyne precursor for the [2+2+2] cycloaddition. The ether formation strategy was successful, utilizing the Thorpe-Ingold effect of the ether tail on the bridge of the diyne moiety and the template effect of the ethylene glycol chain. The different strategies were explored in parallel in the course of the work. We then focused on the strategy with most promising result. It is thus possible (and even probable) that all other strategies would eventually lead to the synthesis of the desired macrocycle provided the right macrocyclization conditions are found.

### 1.3.3 Cycloaddition reaction of strained systems

#### 1.3.3.1 Investigation of the cycloaddition on strained systems

With the desired macrocycle **66** in hand, we investigated its reactivity in the alkyne cyclotrimerization reaction. Submitting macrocycle **66** to the optimized reaction conditions described in Section 1.3.1.2, we expected the formation of the strained *p*-terphenylene product **67** (Scheme 25).



**Scheme 25:** Expected [2+2+2] cycloaddition reaction

Surprisingly, the formed product was not the desired *p*-terphenyl molecule **67**. Although the mass spectrum corresponded to the mass of the desired product, the <sup>1</sup>H-NMR spectrum was not in agreement with the expected structure **67**. The spectrum of the isolated product contained nearly twice the number of peaks, suggesting that an asymmetric molecule was formed rather than the symmetric product **67**. Initial reactions were performed with the polar but-2-yne-1,4-diol and the apolar hex-3-yne as monoynes components for the [2+2+2] cycloaddition reaction. Unsymmetric products were formed in both cases.

After purification, a sample of the product **68a** was obtained in crystalline form. A picture of the molecular structure in the crystal which was determined by X-ray diffraction analysis is shown in Figure 24.

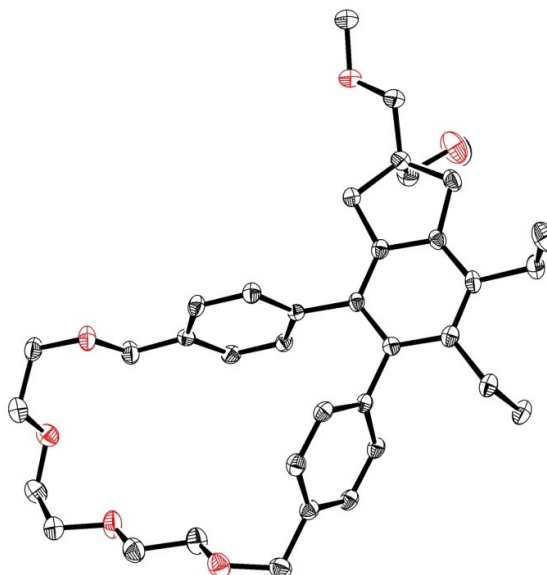


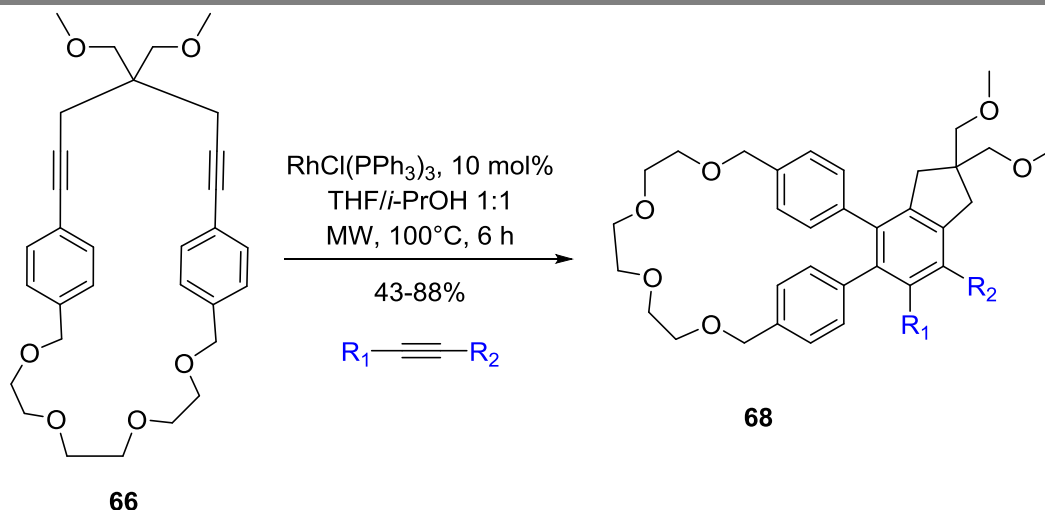
**Figure 24:** X-ray structure of the cycloaddition product of the reaction on strained system **68a**.  
(Ortep drawing, Hydrogen, solvent and disorder omitted)

The crystal presented several disorders, notably on the ether tail on the cyclopentane ring and in the solvent molecules present in the crystal. This crystal structure was the crucial point to understand the unexpected reaction which occurred on the strained molecule. The NMR spectra is in perfect agreement with solid state structure.

## 1.3.3.2 Scope of the cycloaddition reaction

The scope of the reaction was explored using different monoyne for the cycloaddition on the strained precursor **66**. The results are reported in Table 3.

**Table 3:** Scope of the cycloaddition reaction on strained system **66**



Entry	Alkyne		Product	Isolated Yield
	R <sub>1</sub>	R <sub>2</sub>		
1	Et	Et	<b>68a</b>	88%
2	Ph	Ph	<b>68b</b>	64%
3	CH <sub>2</sub> OH	CH <sub>2</sub> OH	<b>68c</b>	59%
4	Ph	H	<b>68d</b>	67%
5	CH(CH <sub>3</sub> ) <sub>2</sub> (OH)	H	<b>68e</b>	62%
6	CH <sub>2</sub> CH <sub>2</sub> CH <sub>3</sub>	H	<b>68f</b>	64%
7	CH <sub>2</sub> CH <sub>2</sub> OH	H	<b>68g</b>	43%
8	Me	CH <sub>2</sub> OH	<b>68h</b>	64%
9	COOMe	COOMe		- <sup>a</sup>
10	TMS	TMS		- <sup>a</sup>
11	TMS	H		- <sup>a</sup>

<sup>a</sup>homotrimerization of the monoyne

The products were obtained in moderate to good yields with different functional groups (alkyl, phenyl, alcohol). Even the more hindered phenyl substituted alkyne reacted with macrocycle **66** in moderate yield (64%) (Table 3, Entry 2). The TMS containing alkynes did, however, not react with the macrocycle (Table 3, Entries 10 and 11), but homotrimerization of the monoyne occurred instead which was accompanied by degradation of the macrocycle. The same result was observed

with the ester substituted monoyne (Table 3, Entry 9). It seems that electrodeficient alkynes are not reactive in the cycloaddition reaction with our strained system under those reaction conditions, just as in the case of the linear diynes.

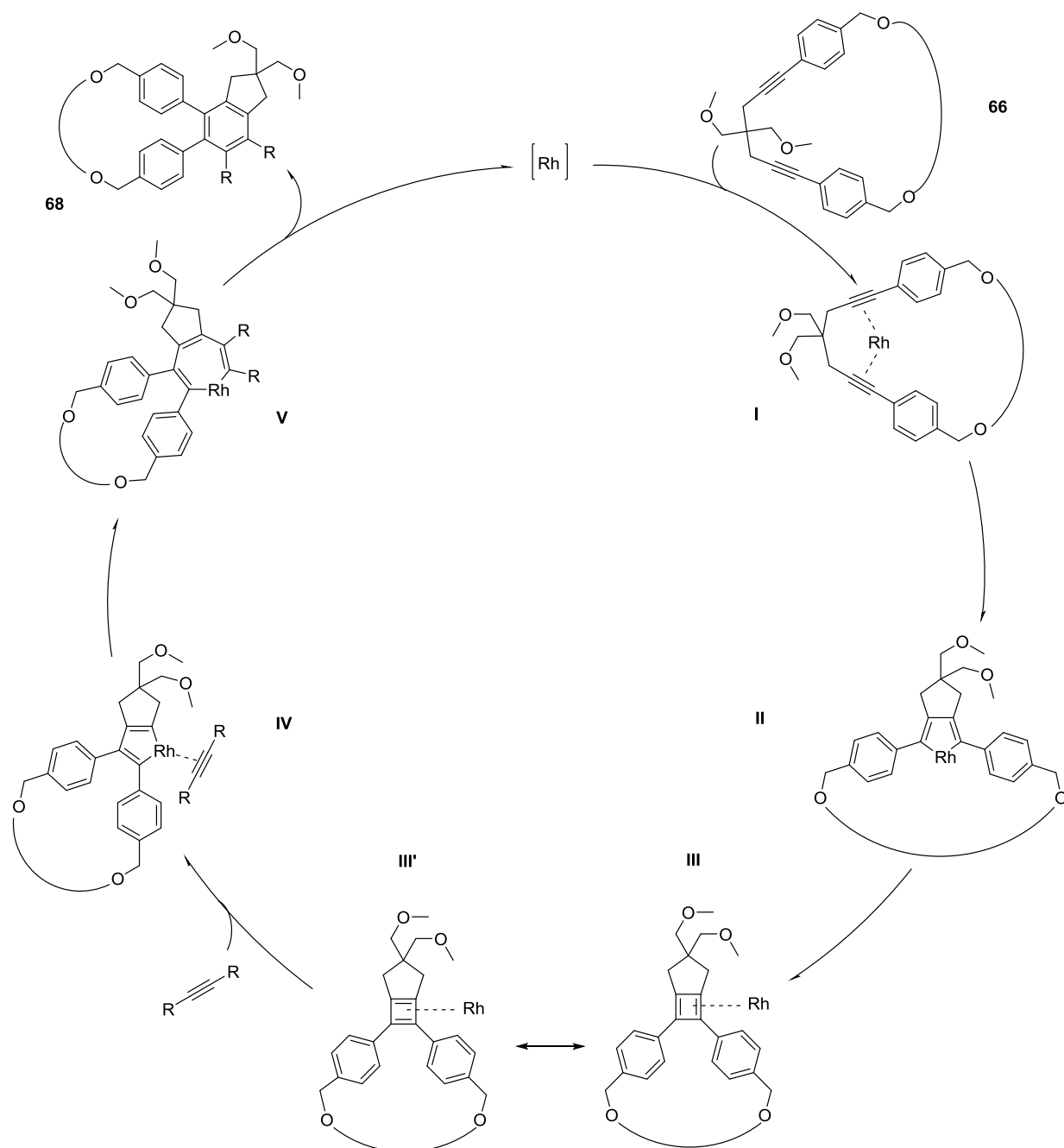
In the case of the terminal alkynes, the cycloaddition products were isolated in moderate yields (43–67%, Table 3, Entries 4–7). Mostly one regio-isomer was obtained, but traces of the other region-isomer were also observed. From these results, it can be concluded that sterically hindered substituents are better accommodated on the phenyl side than on the cyclopentane side. However, for the asymmetric but-2-yn-1-ol, the opposite regioselectivity was observed. This suggests that in case of similar hinderance, other factors like coordination could affect the orientation of the monoyne.

The scope of the reaction proved its general applicability with different substrates. The reaction is therefore not just an exception but occurs with all reactive monoynes.

### 1.3.3.3 Mechanism

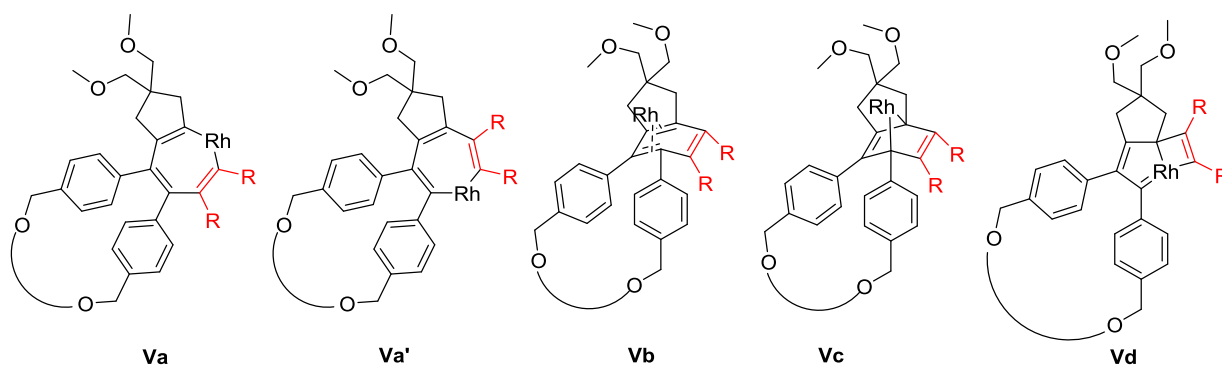
To explain the formation of the unexpected product, we propose a possible mechanism shown in Scheme 26. The first step involves ligand dissociation and coordination of the two alkyne moieties of the macrocycle **66** to the rhodium catalyst (**I**). Oxidative coupling of the alkynes leads to the rhodacyclopentadiene (**II**). Because of the strain in the macrocycle, the complex then undergoes reductive elimination leading to the  $\eta^4$ -cyclobutadiene rhodium complex. This complex presents two resonance structures (**III** and **III'**). Then, the metal reinserts to form the less strained rhodacyclopentadiene (**IV**) which then follows the classical [2+2+2] cycloaddition mechanism discussed in the introduction (Section 1.1.2.): coordination of the mono-alkyne followed by its insertion to form intermediate **V**.





**Scheme 26:** Proposed mechanism for the cycloaddition reaction observed on strained systems

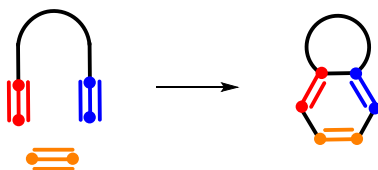
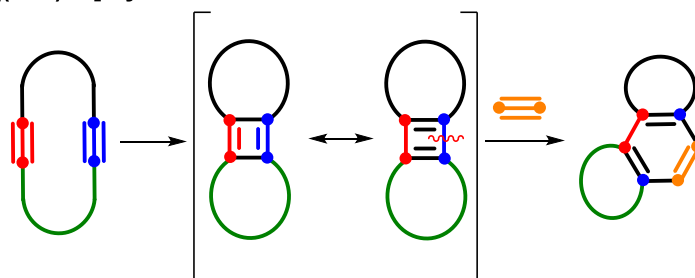
Only one of the possibilities is depicted in the scheme for the sake of clarity. However, the mechanism can also take place via formation of the  $\eta^4$ -arene complex **Vb** by intramolecular [4+2] cycloaddition, or [2+2] cycloaddition to afford a [3.2.0]heptatriene **Vd** or the intermolecular [4+2] pathway leading to a norbornadiene intermediate **Vc**. Furthermore, as the molecule is asymmetric, the insertion of the alkyne can occur at different sides of the metal: next to the phenyl **Va'** or next to the cyclopentadiene **Va** (Figure 25). This could provide possible rationalization for the observed stereoselectivity.


**Figure 25:** Possible intermediates **V**

The mechanism of the [2+2+2] cycloaddition reaction is still an actual topic of investigation.<sup>10,22,27-31</sup> As mentioned in the literature, the exact mechanism for the cycloaddition reaction is strongly depending on the reaction conditions (solvent, catalyst, ligand, substrate etc.). Thus, it could be possible that different monoynes react through different pathways.

The typical mechanism of the [2+2+2] cycloaddition reaction does not involve cyclobutadiene intermediates. However, numerous stable cyclobutadiene complexes of cobalt and rhodium have been isolated in the literature.<sup>72-80</sup> This supports our proposed mechanism.

The reaction product does not correspond to the classical [2+2+2] cycloaddition product (Scheme 27). The reaction is therefore not a formal [2+2+2] cycloaddition reaction, although it still involves six  $\pi$ -electrons and forms a six membered ring. Formally, the proposed mechanism first involves a [2+2] cycloaddition to form the cyclobutadiene complex, and then the insertion of the mono-alkyne (two  $\pi$ -electrons) occurs. Therefore, the reaction is better described as a [(2+2)+2] cycloaddition reaction.

**[2+2+2] cycloaddition**

**[(2+2)+2] cycloaddition**

**Scheme 27:** [2+2+2] cycloaddition vs. [(2+2)+2] cycloaddition reaction

In our case, the change of reactivity is clearly attributable to the strain in the macrocycle. To avoid the buildup of strain, the rhodacyclopentadiene rearranges into the less strained isomer through a cyclobutadiene complex intermediate. This demonstrates that indeed, strain has an effect on the cycloaddition reaction. Strained molecules follow a different mechanism ( $[(2+2)+2]$  cycloaddition) than their unstrained analogs ( $[2+2+2]$  cycloaddition).

### 1.3.3.4 Screening for $[2+2+2]$ cycloaddition reaction

As the product of the reaction using our conditions led to another product than the expected strained *p*-terphenyl molecule, we screened different solvents and catalysts to see whether the desired  $[2+2+2]$  cycloaddition product could be obtained with modified conditions.

Because it has been mentioned through the literature that the reaction mechanism is highly dependent on the choice of solvent, we screened various solvents in the reaction between macrocycle **66** and the monoyne 2-butyne-1,4-diol. The results are summarized in Table 4.

**Table 4:** Screening of solvent for the cycloaddition reaction

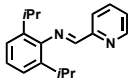
Entry	Solvent	Temperature	Concentration (macrocycle <b>66</b> )	Observed product
1	THF: <i>i</i> PrOH (1:1)	MW 150°C	2 mM	$[(2+2)+2]$ product
2	THF: <i>i</i> PrOH (1:1)	Reflux	6 mM	$[(2+2)+2]$ product
3	THF: <i>i</i> PrOH (1:1)	MW 150°C	27 mM	$[(2+2)+2]$ product
4	THF: <i>i</i> PrOH (1:1)	MW 150°C	47 mM	$[(2+2)+2]$ product
5	Toluene: <i>i</i> PrOH (1:1)	MW 100°C	72 mM <sup>a</sup>	$[(2+2)+2]$ product
6	DMSO	MW 150°C	20 mM	$[(2+2)+2]$ product
7	Toluene	MW 90°C	20 mM	$[(2+2)+2]$ product
8	<i>i</i> PrOH	MW 100°C	47 mM	$[(2+2)+2]$ product
9	DCM	MW 90°C	47 mM	$[(2+2)+2]$ product
10	DMF:H <sub>2</sub> O (1:1)	MW 150°C	47 mM	Degradation
11	THF: <i>i</i> PrOH (1:1)	MW 150°C	47 mM <sup>b</sup>	$[(2+2)+2]$ product

<sup>a</sup> hex-3-yne was used as the monoyne <sup>b</sup> Tetraethyleneglycol macrocycle

Variations of the concentration (Table 4, Entries 1–5), did not have any influence on the product formed. All tested dry solvents afforded the same  $[(2+2)+2]$  cycloaddition product (Table 4, Entries 4–9). Also the use of the tetraethyleneglycol macrocycle produced the  $[(2+2)+2]$  cycloaddition product (Table 4, Entry 11).

We then screened different conditions and catalysts (Table 5) based on those reported in the literature for the [2+2+2] cycloaddition reaction with nickel, ruthenium, palladium and cobalt.  
6,9,12,23,81-84

**Table 5:** Screening of catalysts for the cycloaddition reaction

Entry	Catalyst	Conditions	Results
1	RhCl(PPh <sub>3</sub> ) <sub>3</sub>	MW, 150°C	[(2+2)+2] product
2	RhCl(PPh <sub>3</sub> ) <sub>3</sub> + AgOTf	MW, 150°C	[(2+2)+2] product
3	NiBr <sub>2</sub> Dppe/Zn (20 mol%)	rt, 2 <sup>nd</sup> addition of catalyst, then MW 6h 100°C	No reaction
4	CoCl <sub>2</sub> •6H <sub>2</sub> O (5 mol%) 	rt, then MW 100-150°C, 2 <sup>nd</sup> addition of catalyst	No reaction
5	CoI <sub>2</sub> /Zn	rt, then MW 150°C	No reaction
6	CoCp(Fumarate)	MW 200°C	Monoyne trimerization
7	Pd(PPh <sub>3</sub> ) <sub>4</sub> , 1 eq.	130°C	No reaction
8	Grubbs I (20 mol%)	130°C	No reaction
9	CpCo(CO) <sub>2</sub> , 2 eq.	140°C	Cobalt Complexes with macrocycle <b>10</b>

NiBr<sub>2</sub>Dppe was synthesized following a literature procedure,<sup>85</sup> and was then used as catalyst, using zinc to reduce the catalyst in situ.<sup>86,87</sup> In our case no reaction occurred even after four days at room temperature and the addition of more catalyst or microwave irradiation (6 h at 100°C). A procedure using CoCl<sub>2</sub> and the ligand depicted in Table 5 Entry 4,<sup>88</sup> again, no conversion was observed even after several days and after long microwave irradiation. Using CoI<sub>2</sub> together with zinc,<sup>89</sup> the starting material was still the major compound after seven days and further addition of catalyst and microwave irradiation (6 h, 150°C). A cobalt complex with fumarate ligand was synthesized according to the procedure described in the literature<sup>90</sup> and used under the conditions described therein (microwave, 200°C, 10 min). Only monoyne trimerization occurred. When Pd(PPh<sub>3</sub>)<sub>4</sub> was used in stoichiometric amount,<sup>23</sup> the reaction mixture was refluxed in toluene for seven days, but no reaction occurred. Also the Grubbs I catalyst<sup>23</sup> gave no conversion.

When two equivalents of the cobalt catalyst CpCo(CO)<sub>2</sub> were used full conversion to a cobalt complex was observed within 24 hours. According to analytical data, the isolated product is a complex between cobalt and the molecule **66**. Several possible complex structures are depicted in Figure 26.

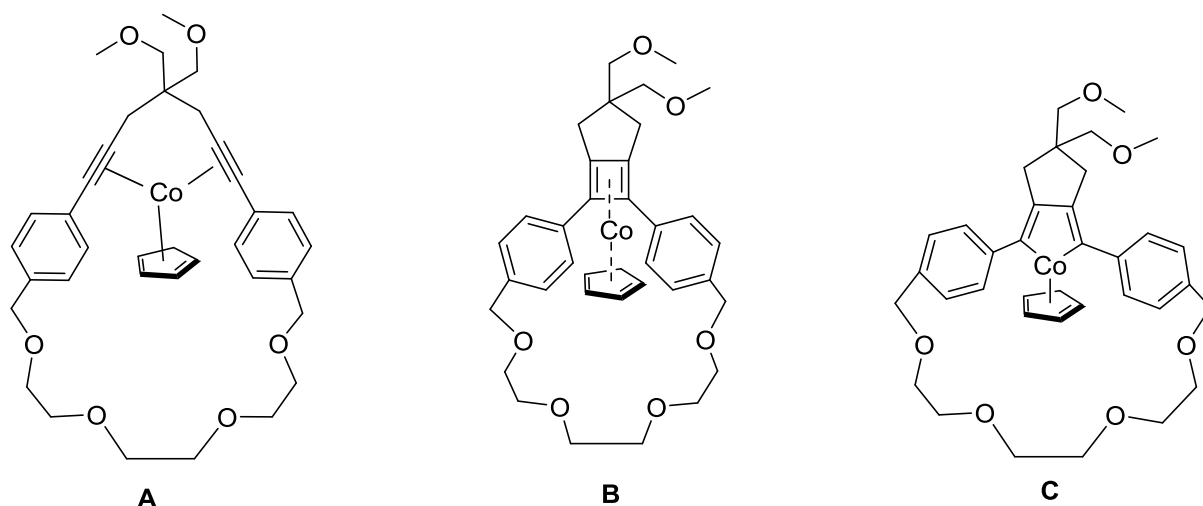


**Figure 26:** Possible structures of the cobalt complex formed by reaction between  $\text{CpCo}(\text{CO})_2$  and **66**

As a conclusion, it seems that only rhodium catalyzed reaction led to the same  $[(2+2)+2]$  cycloaddition product. The other catalysts were mostly unreactive with the strained system and only cyclotrimerization of the monoynes was observed with cobalt catalyst.

### 1.3.3.5 Coordination experiment

Non covalent cation- $\pi$  interactions are playing an important role in stabilizing biological and chemical assemblies. Therefore, polyaromatic systems combined with crown ether cavity could function as electrochemical sensors for sodium or potassium cations. Such molecules hold potential application for functional extractants or conductive electrolytes. Consequently, we were interested in investigating the ability of our molecule to bind cations such as  $\text{Na}^+$  and  $\text{K}^+$ .

The binding of the sodium or potassium cation to macrocycle **68a** was monitored by  $^1\text{H-NMR}$  spectroscopy in deuterated acetone (0.02 M) with the incremental addition of a solution of  $\text{NaPF}_6$  or  $\text{KPF}_6$  (0.008 M in acetone  $\text{d}_6$ ) analogously to the procedure reported by Rathore et al.<sup>42</sup> The addition of potassium resulted in a dramatic shift of the signals of both the aromatic and the ethylene glycol protons (by up to 0.1 ppm), see Figure 27. This indicates a strong coordination of the potassium cation to both the crown ether part of the molecule and the phenyl rings.

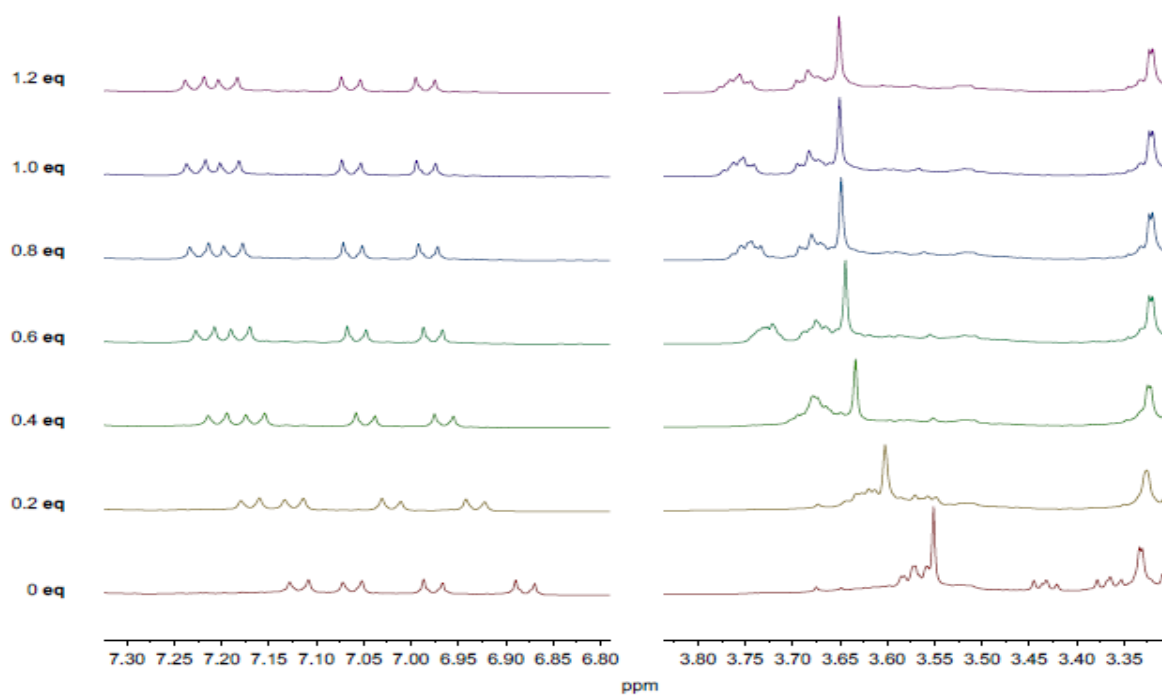


**Figure 27:** Coordination experiment with potassium

The addition of sodium cations led, however, only to a shifting of the ethylene glycol protons signals (0.05 ppm), while the aromatic signals remained unchanged (see Figure 28).

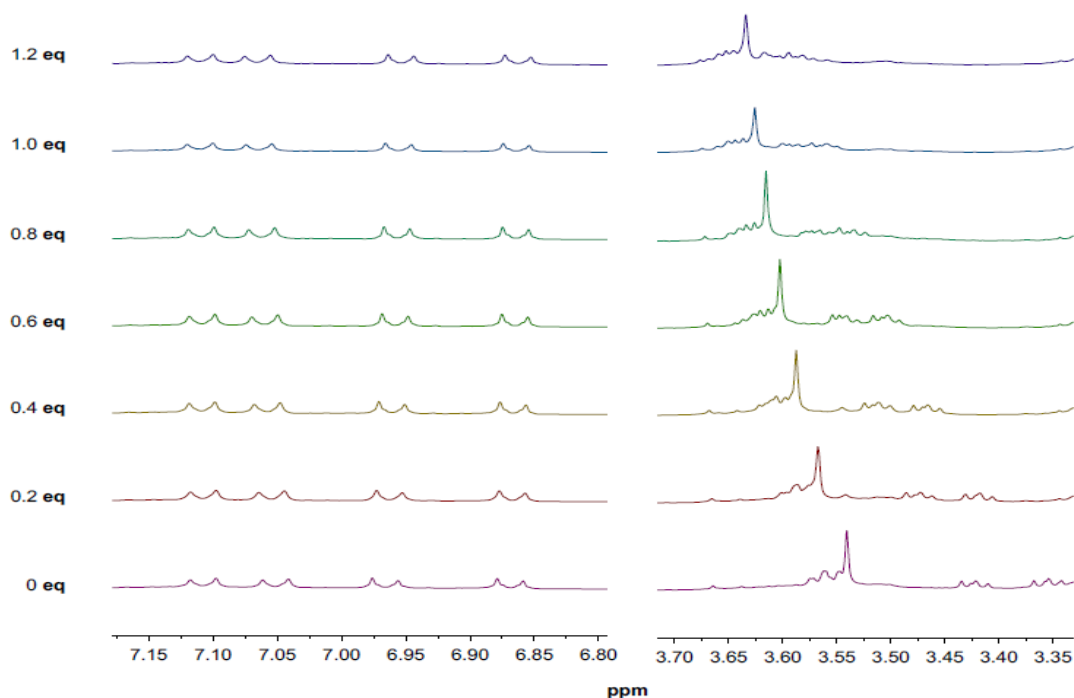


**Figure 28:** Coordination experiment with sodium

The sodium cation is smaller than the potassium cation, and can be fully accommodated by the triethylene glycol crown ether part of the molecule further away from the phenyl moieties as can be seen in modeled structures depicted in Figure 29.

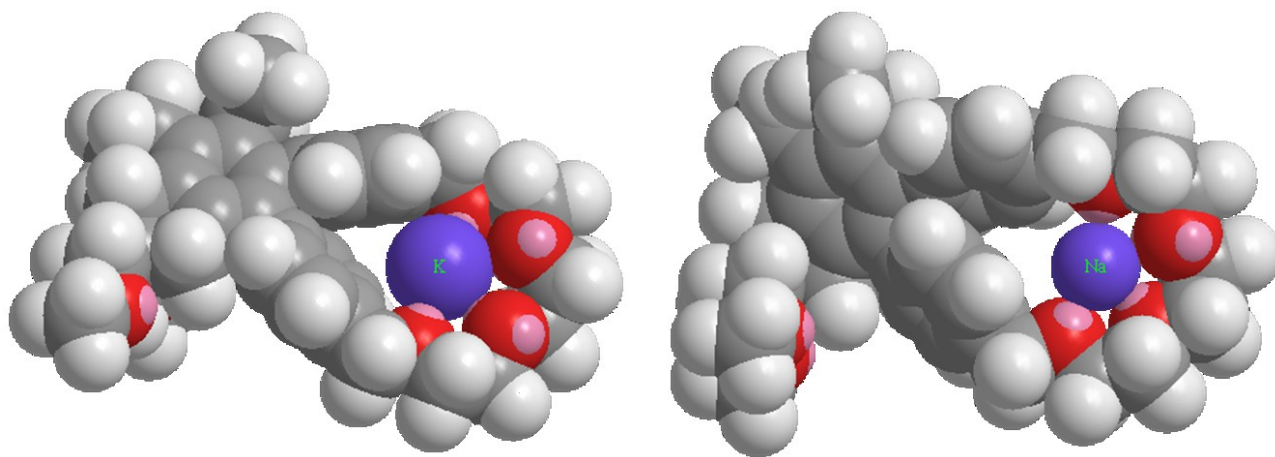


**Figure 29:** Space-filling model (MM2 optimization) of the complex between the macrocycle **68a** and potassium (left) or sodium (right)

The chemical shift evolution of the proton singlet signal belonging to the CH<sub>2</sub> of the triethylene glycol chain upon addition of Na/K is presented on Figure 30.

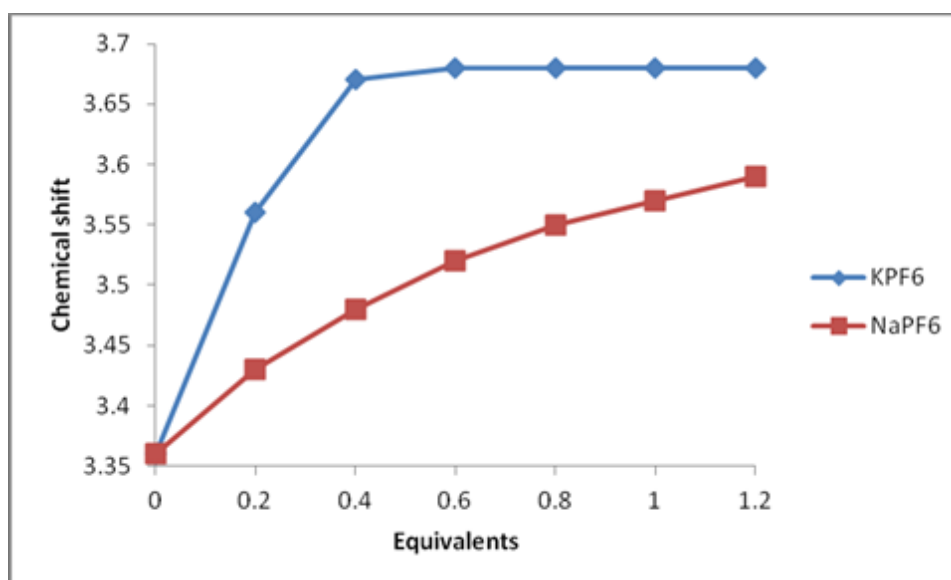


**Figure 30:** Comparison of the effect of sodium and potassium on the chemical shift of the ethylene glycol protons

This graph illustrates the larger effect of the coordination of potassium on the molecule. The sodium cation is smaller than the potassium cation, and can be fully accommodated by the triethylene glycol crown ether part of the molecule further away from the phenyl moieties as can be seen in modeled structures. Similar to Rathore et al<sup>42</sup> the binding constants could not be determined by the NMR titration experiments as the values were too high.

A job plot analysis was performed in order to define the stoichiometry of the sodium and potassium complexes. Equimolar solutions of macrocycle **68a**, NaPF<sub>6</sub> or KPF<sub>6</sub> (18.5 mM in acetone-*d*<sub>6</sub>) were mixed in different proportions, keeping the total concentration constant. The H-NMR spectra of the solutions were recorded and the Job plot was obtained by plotting the product

of the chemical shift ( $\Delta\delta$ ) difference and the molar fraction of **68a** ( $x_{68a}$ ) against the molar fraction of **68a**. The maximum of the curve has been observed for a molar fraction of 0.5 accounting for a 1:1 stoichiometry for both the sodium and the potassium complexes as can be seen on Figure 31.

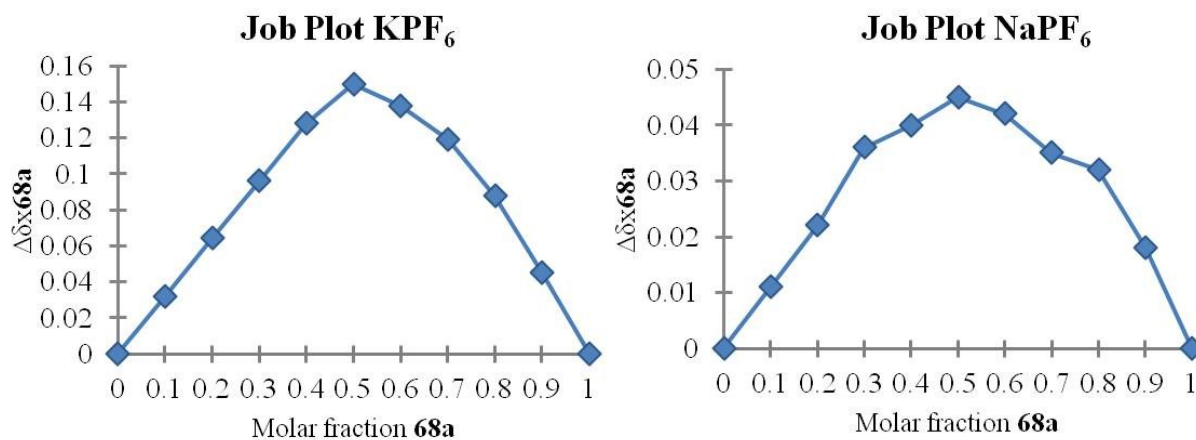


**Figure 31:** Job Plot analysis of the complexes of **68a** with sodium and potassium

The results show that there is an effective coordination between the cations and the macrocyclic terphenylcrown. Therefore, such macrocycles could potentially find application as chemosensors or extractants.



### 1.3.3.6 Optical properties of the macrocyclic molecules

In general, conjugated aromatic systems have enhanced photooptical properties. We were thus interested in analyzing these properties as a function of the different substituents on the *ortho*-terphenyl macrocycle.

The UV absorption spectra (plain lines) and emission spectra (dashed lines) were measured in chloroform ( $10^{-4}$  M) and are presented in Figure 32.

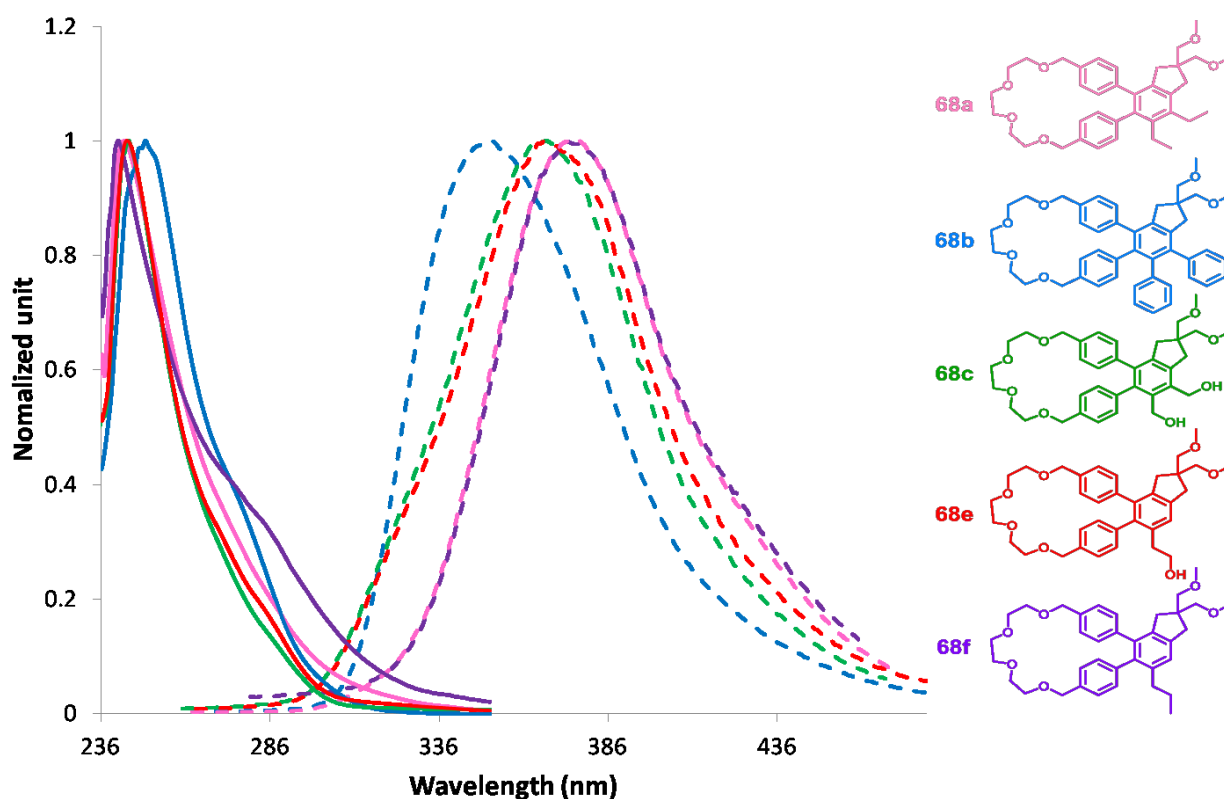


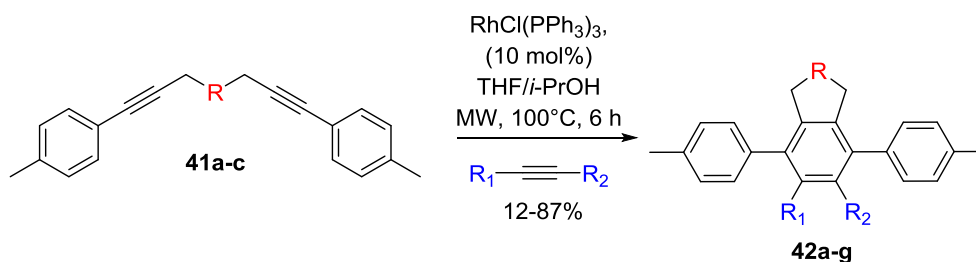
**Figure 32:** UV absorption spectra (plain lines) and emission spectra (dashed lines) of the [(2+2)+2] cycloaddition products

The absorption spectra of all our substituted macrocycles were quite similar and contained maxima at 245 nm for alkyl and alcohol substituted molecules. The absorption maximum of the diphenyl derivative was slightly shifted to a longer wavelength (249 nm).

As for the emission spectra, they can be divided in three different trends. The alcohol substituted molecules show a similar spectrum with maxima at 367 nm (green and red curve). The spectra of alkyl substituted molecules show a common maximum at 375 nm with a very similar curve. Regarding the diphenyl analog, the shape of the curve resembles those of the other macrocycles, but the maximum lies at a shorter wavelength (350 nm). As a result, this molecule presents a much smaller Stokes shift than the others.

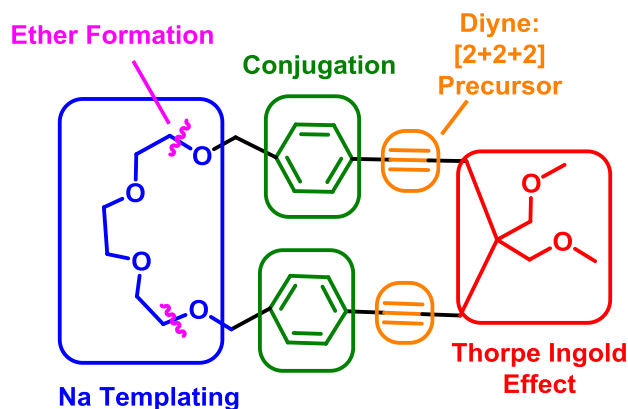
## 1.4 CONCLUSION

In this chapter we presented the synthesis of substituted *p*-terphenyl molecules via [2+2+2] cycloaddition reaction. The reaction involves a tethered diyne molecule and a monoalkyne as reaction partners (Scheme 28). The conditions have been optimized using microwave irradiation, Wilkinson's catalyst and 10–30 equivalents of alkyne. Differently substituted *p*-terphenyls were synthesized with this method.



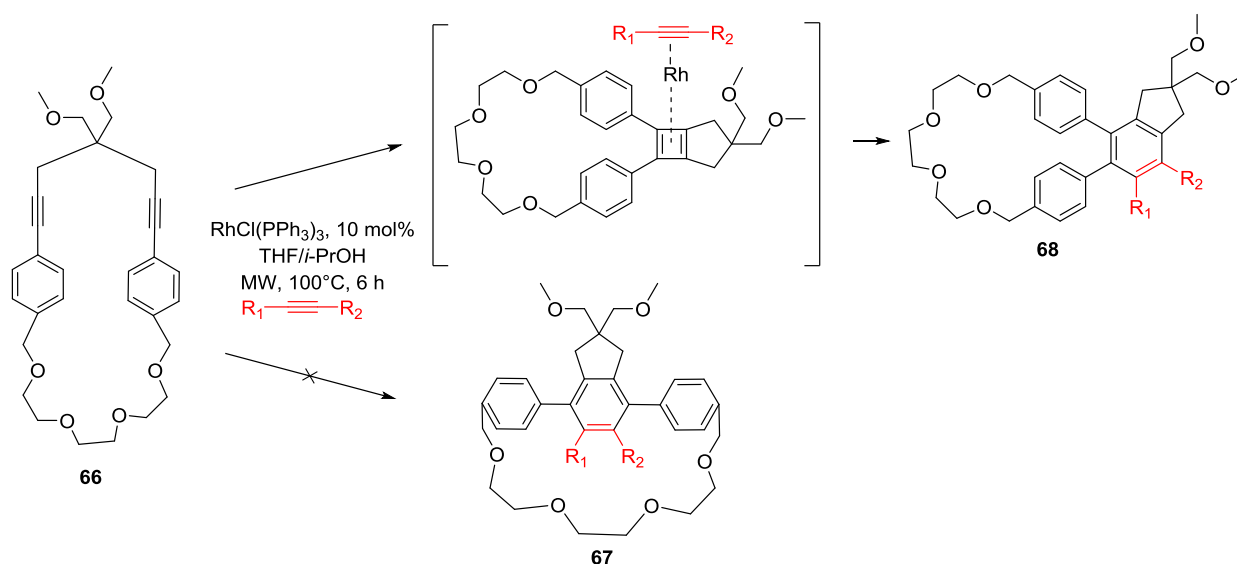
**Scheme 28:** [2+2+2] Cycloaddition reaction of linear precursor

In order to test the reaction on strained systems, we designed several strategies to synthesize an appropriate macrocyclic precursor for the [2+2+2] cycloaddition reaction. We explored the different strategies to finally encounter success with a method relying on ether formation by substitution reaction. The macrocyclization took advantage of both the Thorpe Ingold effect of the ether tails on the bridge of the diol building block, and the sodium templating effect of the flexible triethylene glycol ditosylate building block (Scheme 29).



**Scheme 29:** Design of the macrocyclic precursor

When applying our optimized protocol of the [2+2+2] cycloaddition reaction to the strained system **66** a different product than the expected [2+2+2] cycloaddition product was obtained (Scheme 30). The structure of this unexpected product was determined by spectroscopic methods and X-ray diffraction analysis.



**Scheme 30:** Cycloaddition reaction of the macrocyclic precursor **66**

We suspect that the reaction is taking place through a rhodium-cyclobutadiene intermediate to lead to the less strained product, following a [(2+2)+2] cycloaddition pathway instead of the classical [2+2+2] cycloaddition mechanism. This shows that strained systems undergo a different reaction than their unstrained analogs. The same reaction was observed for a number of monoynes proceeding in moderate to good yields. Noteworthy, when terminal alkynes were used, one major regioisomer was obtained. Different conditions were screened in order to tune the reaction into the direction of the desired [2+2+2] cycloaddition product, but only the [(2+2)+2] products were formed.

These results show that the [2+2+2] cycloaddition reaction is not a suitable method to bring strain to a system such as it was devised for the synthesis of CPP. However, the molecules obtained via the modified mechanism show attractive properties such as cation coordination and UV-fluorescence, making them interesting candidates for application in molecular electronics and nanotechnology. Moreover, this outcome offers a new insight into the reaction mechanism involved in the [2+2+2] cycloaddition.

**1.5 REFERENCES**

- [1] Bertholet, P. E. M. *C. R. Hebd. Seances Acad. Sci.* **1866**, *63*, 515.
- [2] Reppe *Justus Liebigs Annalen der Chemie* **1948**, *560*, 104.
- [3] Müller, E. *Synthesis* **1974**, *1974*, 761.
- [4] Grigg, R.; Scott, R.; Stevenson, P. *J. Chem. Soc., Perkin Trans. 1* **1988**, 1357.
- [5] Grigg, R.; Scott, R.; Stevenson, P. *Tetrahedron Lett.* **1982**, *23*, 2691.
- [6] Chopade, P. R.; Louie, J. *Adv. Synth. Catal.* **2006**, *348*, 2307.
- [7] Tanaka, K. *Synlett* **2007**, *2007*, 1977.
- [8] Shibata, Y.; Tanaka, K. *Synthesis* **2012**, *44*, 323.
- [9] Saito, S.; Yamamoto, Y. *Chem. Rev.* **2000**, *100*, 2901.
- [10] Broere, D. L. J.; Ruijter, E. *Synthesis* **2012**, *44*, 2639.
- [11] Takeuchi, R.; Nakaya, Y. *Org. Lett.* **2003**, *5*, 3659.
- [12] Galan, B. R.; Rovis, T. *Angew. Chem. Int. Ed.* **2009**, *48*, 2830.
- [13] Hill, J. E.; Balaich, G.; Fanwick, P. E.; Rothwell, I. P. *Organometallics* **1993**, *12*, 2911.
- [14] Clayden, J.; Moran, W. J. *Org. Biomol. Chem.* **2007**, *5*, 1028.
- [15] Garcia, L.; Pla-Quintana, A.; Roglans, A.; Parella, T. *Eur. J. Org. Chem.* **2010**, *2010*, 3407.
- [16] Hilt, G.; Hengst, C.; Hess, W. *Eur. J. Org. Chem.* **2008**, 2293.
- [17] Tanaka, K.; Fukawa, N.; Suda, T.; Noguchi, K. *Angew. Chem. Int. Ed.* **2009**, *48*, 5470.
- [18] Nishida, G.; Noguchi, K.; Hirano, M.; Tanaka, K. *Angew. Chem. Int. Ed.* **2008**, *47*, 3410.
- [19] McDonald, F. E.; Smolentsev, V. *Org. Lett.* **2002**, *4*, 745.
- [20] Müller, M.; Kübel, C.; Müllen, K. *Chem. Eur. J.* **1998**, *4*, 2099.
- [21] Bharat; Bhola, R.; Bally, T.; Valente, A.; Cyrański, M. K.; Dobrzycki, Ł.; Spain, S. M.; Rempała, P.; Chin, M. R.; King, B. T. *Angew. Chem. Int. Ed.* **2010**, *49*, 399.
- [22] Dachs, A.; Torrent, A.; Roglans, A.; Parella, T.; Osuna, S.; Solà, M. *Chem. Eur. J.* **2009**, *15*, 5289.
- [23] Torrent, A.; González, I.; Pla-Quintana, A.; Roglans, A.; Moreno-Mañas, M.; Parella, T.; Benet-Buchholz, J. *J. Org. Chem.* **2005**, *70*, 2033.
- [24] Boñaga, L. V. R.; Zhang, H.-C.; Moretto, A. F.; Ye, H.; Gauthier, D. A.; Li, J.; Leo, G. C.; Maryanoff, B. E. *J. Am. Chem. Soc.* **2005**, *127*, 3473.
- [25] Shibata, T.; Miyoshi, M.; Uchiyama, T.; Endo, K.; Miura, N.; Monde, K. *Tetrahedron* **2012**, *68*, 2679.
- [26] Araki, T.; Noguchi, K.; Tanaka, K. *Angew. Chem. Int. Ed.* **2013**, *52*, 5617.
- [27] Dachs, A.; Osuna, S. I.; Roglans, A.; Solà, M. *Organometallics* **2010**, *29*, 562.
- [28] Agenet, N.; Gandon, V.; Vollhardt, K. P. C.; Malacria, M.; Aubert, C. *J. Am. Chem. Soc.* **2007**, *129*, 8860.
- [29] Varela, J. A.; Saá, C. *J. Organomet. Chem.* **2009**, *694*, 143.
- [30] Dachs, A.; Torrent, A.; Pla-Quintana, A.; Roglans, A.; Jutand, A. *Organometallics* **2009**, *28*, 6036.
- [31] Parera, M.; Dachs, A.; Solà, M.; Pla-Quintana, A.; Roglans, A. *Chem. Eur. J.* **2012**, *18*, 13097.
- [32] Yu, X.; Sun, D. *Molecules* **2013**, *18*, 6230.
- [33] Gulder, T.; Baran, P. S. *Natural Product Reports* **2012**, *29*, 899.
- [34] Marsault, E.; Peterson, M. L. *J. Med. Chem.* **2011**, *54*, 1961.
- [35] Terrett, N. K. *Drug Discovery Today: Technologies* **2010**, *7*, e97.
- [36] Lindoy, L. F.; Park, K.-M.; Lee, S. S. *Chem. Soc. Rev.* **2013**, *42*, 1713.
- [37] Kralj, M.; Tušek-Božić, L.; Frkanec, L. *ChemMedChem* **2008**, *3*, 1478.

- [38] Gokel, G. W.; Leevy, W. M.; Weber, M. E. *Chem. Rev.* **2004**, *104*, 2723.
- [39] Shinkai, S. *Tetrahedron* **1993**, *49*, 8933.
- [40] Fery-Forgues, S.; Al-Ali, F. *Journal of Photochemistry and Photobiology C: Photochemistry Reviews* **2004**, *5*, 139.
- [41] An, H.; Bradshaw, J. S.; Izatt, R. M.; Yan, Z. *Chem. Rev.* **1994**, *94*, 939.
- [42] Shukla, R.; Lindeman, S. V.; Rathore, R. *Chem. Commun.* **2009**, 5600.
- [43] Pigge, F. C.; Schmitt, A.; Rath, N. *J. Inclu. Phenom. Macro.* **2008**, *62*, 105.
- [44] Zhang, W.; Moore, J. S. *Angew. Chem. Int. Ed.* **2006**, *45*, 4416.
- [45] Iyoda, M.; Yamakawa, J.; Rahman, M. J. *Angew. Chem. Int. Ed.* **2011**, *50*, 10522.
- [46] Wessjohann, L. A.; Rivera, D. G.; Vercillo, O. E. *Chem. Rev.* **2009**, *109*, 796.
- [47] Kawase, T. *Synlett* **2007**, *2007*, 2609.
- [48] Cárdenas, D. J.; Livoreil, A.; Sauvage, J.-P. *J. Am. Chem. Soc.* **1996**, *118*, 11980.
- [49] Sauvage, J.-P. *Acc. Chem. Res.* **1998**, *31*, 611.
- [50] O'Sullivan, M. C.; Sprafke, J. K.; Kondratuk, D. V.; Rinfray, C.; Claridge, T. D. W.; Saywell, A.; Blunt, M. O.; O'Shea, J. N.; Beton, P. H.; Malfois, M.; Anderson, H. L. *Nature* **2011**, *469*, 72.
- [51] Blankenstein, J.; Zhu, J. *Eur. J. Org. Chem.* **2005**, *2005*, 1949.
- [52] Collins, J. C.; James, K. *MedChemComm* **2012**, *3*, 1489.
- [53] Basler, J. M., University of Basel, 2011.
- [54] Brun, S.; Garcia, L.; Gonzalez, I.; Torrent, A.; Dachs, A.; Pla-Quintana, A.; Parella, T.; Roglans, A. *Chem. Commun.* **2008**, 4339.
- [55] Kappe, C. O. *Angew. Chem. Int. Ed.* **2004**, *43*, 6250.
- [56] de la Hoz, A.; Diaz-Ortiz, A.; Moreno, A. *Chem. Soc. Rev.* **2005**, *34*, 164.
- [57] Caddick, S.; Fitzmaurice, R. *Tetrahedron* **2009**, *65*, 3325.
- [58] Yamamoto, Y.; Hayashi, H. *Tetrahedron* **2007**, *63*, 10149.
- [59] Novák, P.; Číhalová, S.; Otmar, M.; Hocek, M.; Kotora, M. *Tetrahedron* **2008**, *64*, 5200.
- [60] Nicolaus, N.; Strauss, S.; Neudörfl, J. r.-M.; Prokop, A.; Schmalz, H.-G. n. *Org. Lett.* **2008**, *11*, 341.
- [61] Jones, A. L.; Snyder, J. K. *J. Org. Chem.* **2009**, *74*, 2907.
- [62] Wakayama, N. I. *Chem. Phys. Lett.* **1980**, *70*, 397.
- [63] Baudour, J. L.; Cailleau, H.; Yelon, W. B. *Acta Crystallographica Section B* **1977**, *33*, 1773.
- [64] Rietveld, H. M.; Maslen, E. N.; Clews, C. J. B. *Acta Crystallographica Section B* **1970**, *26*, 693.
- [65] Suzuki, H. *Bull. Chem. Soc. Jpn.* **1960**, *33*, 109.
- [66] May, F.; Marcon, V.; Hansen, M. R.; Grozema, F.; Andrienko, D. *J. Mater. Chem.* **2011**, *21*, 9538.
- [67] Abe, A.; Furuya, H.; Mitra, M. K.; Hiejima, T. *Comput. Theor. Polym. Sci.* **1998**, *8*, 253.
- [68] Burton, B. A.; Brant, D. A. *Biopolymers* **1983**, *22*, 1769.
- [69] Ouchi, M.; Inoue, Y.; Liu, Y.; Nagamune, S.; Nakamura, S.; Wada, K.; Hakushi, T. *Bull. Chem. Soc. Jpn.* **1990**, *63*, 1260.
- [70] Beesley, R. M.; Ingold, C. K.; Thorpe, J. F. *Journal of the Chemical Society, Transactions* **1915**, *107*, 1080.
- [71] Guan, J. T.; Yu, G.-A.; Chen, L.; Qing Weng, T.; Yuan, J. J.; Liu, S. H. *Appl. Organomet. Chem.* **2009**, *23*, 75.
- [72] Schaefer, C.; Scholz, G.; Gleiter, R.; Oeser, T.; Rominger, F. *Eur. J. Inorg. Chem.* **2005**, *2005*, 1274.

- [73] Veiros, L. F.; Dazinger, G.; Kirchner, K.; Calhorda, M. J.; Schmid, R. *Chem. Eur. J.* **2004**, *10*, 5860.
- [74] Wesendrup, R.; Schwarz, H. *Organometallics* **1997**, *16*, 461.
- [75] Lamata, M. P.; San José, E.; Carmona, D.; Lahoz, F. J.; Atencio, R.; Oro, L. A. *Organometallics* **1996**, *15*, 4852.
- [76] Reisner, G. M.; Bernal, I.; Rausch, M. D.; Gardner, S. A.; Clearfield, A. *J. Organomet. Chem.* **1980**, *184*, 237.
- [77] Rausch, M. D.; Gardner, S. A.; Tokas, E. F.; Bernal, I.; Reisner, G. M.; Clearfield, A. *J. Chem. Soc., Chem. Commun.* **1978**, 187.
- [78] Nixon, J. F.; Kooti, M. *J. Organomet. Chem.* **1976**, *104*, 231.
- [79] King, R. B.; Ackermann, M. N. *J. Organomet. Chem.* **1974**, *67*, 431.
- [80] Gardner, S. A.; Rausch, M. D. *J. Organomet. Chem.* **1973**, *56*, 365.
- [81] Lautens, M.; Klute, W.; Tam, W. *Chem. Rev.* **1996**, *96*, 49.
- [82] Vollhardt, K. P. C. *Angewandte Chemie International Edition in English* **1984**, *23*, 539.
- [83] Schore, N. E. *Chem. Rev.* **1988**, *88*, 1081.
- [84] Kotha, S.; Brahmachary, E.; Lahiri, K. *Eur. J. Org. Chem.* **2005**, *2005*, 4741.
- [85] Booth, G.; Chatt, J. *Journal of the Chemical Society (Resumed)* **1965**, 3238.
- [86] Turek, P.; Novák, P.; Pohl, R.; Hocek, M.; Kotora, M. *J. Org. Chem.* **2006**, *71*, 8978.
- [87] Turek, P.; Kotora, M.; Tišlerová, I.; Hocek, M.; Votruba, I.; Císařová, I. *J. Org. Chem.* **2004**, *69*, 9224.
- [88] Saino, N.; Amemiya, F.; Tanabe, E.; Kase, K.; Okamoto, S. *Org. Lett.* **2006**, *8*, 1439.
- [89] Doszczak, L.; Fey, P.; Tacke, R. *Synlett* **2007**, *2007*, 0753.
- [90] Geny, A.; Agenet, N.; Iannazzo, L.; Malacria, M.; Aubert, C.; Gandon, V. *Angew. Chem. Int. Ed.* **2009**, *48*, 1810.



**Chapter 2:**  
**Synthesis of Substituted**  
**Cycloparaphenylenes**





## 2.1 INTRODUCTION

### 2.1.1 Carbon

Carbon is for the organic chemist the essential element. Indeed, it constitutes the scaffold of all organic molecules. Finding its origin in the heart of stars, this indispensable element exists in different allotropes (Figure 33). Besides amorphous carbon, the most common allotrope is graphite, but more valuable forms such as diamonds are extremely popular for their beauty and worth. Recently, scientists have discovered more surprising forms such as fullerene,<sup>1</sup> graphene<sup>2</sup> or carbon nanotubes.<sup>3</sup>

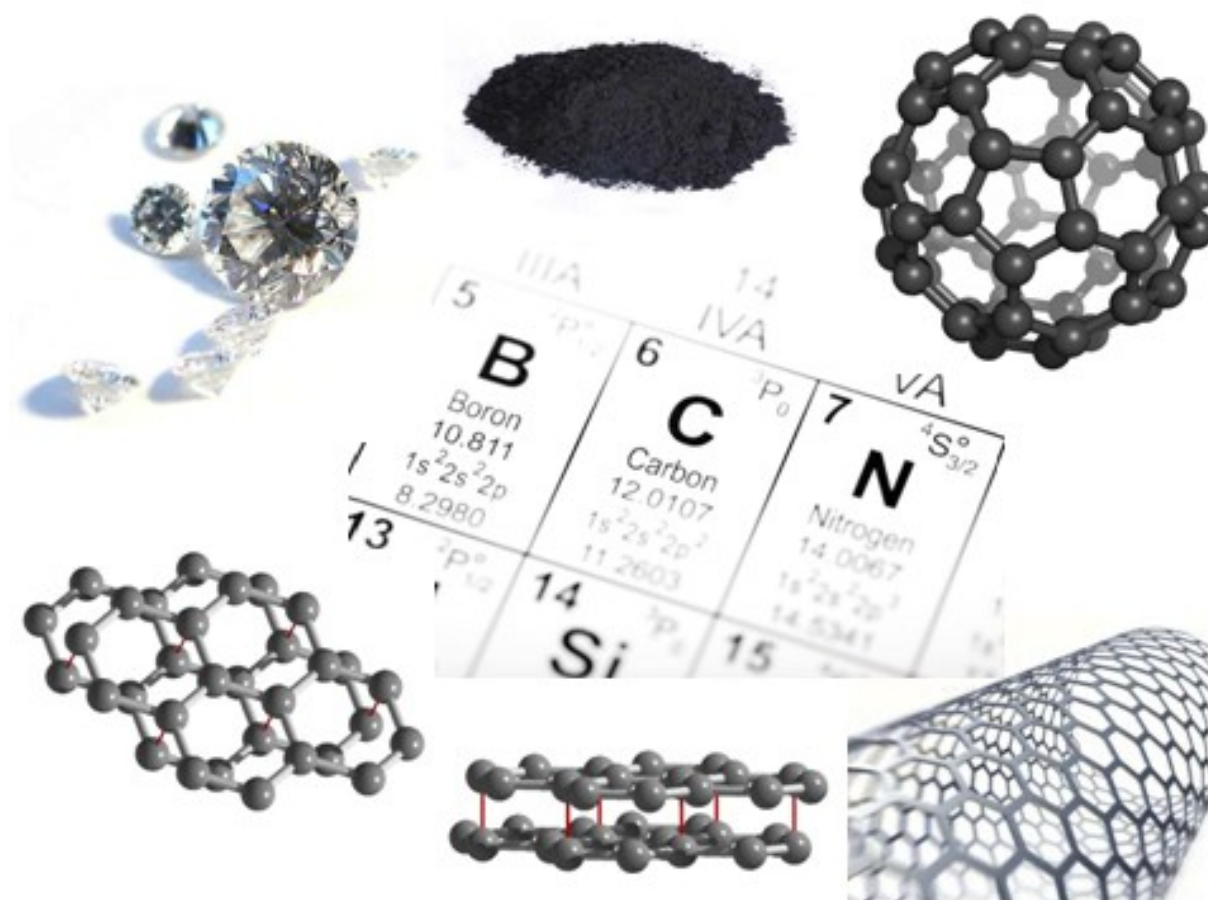


**Figure 33:** Allotropes of carbon

### 2.1.2 Carbon Nanotubes

Carbon nanotubes (CNT), cylindrical carbon molecules, have been discovered in 1991 by Sumio Iijima,<sup>3</sup> from fullerene soot. There are two categories of CNTs, Single Wall Carbon NanoTube (SWCNT) and Multi Wall Carbon NanoTube (MWCNT). SWCNTs consist in a single graphite sheet rolled into a cylindrical tube. Whereas MWCNTs comprise several concentric SWCNTs, enclosed within each other in a Russian doll fashion (Figure 34).

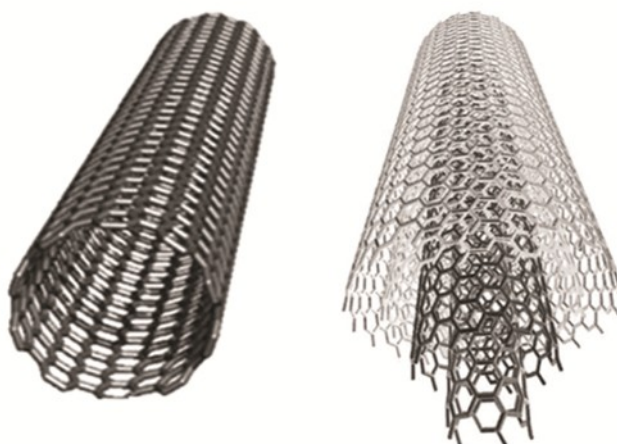


**Figure 34:** Single Wall CNT (left) and Multi Wall CNT (right)

Each CNT can exist in different types, depending on the direction about which the graphite sheet is rolled to form the tube (Figure 35 left). Three types (chirality) of CNTs are distinguishable: armchair, zigzag and chiral CNTs. The properties of CNTs depend directly from their structures more precisely from their diameter and chirality.

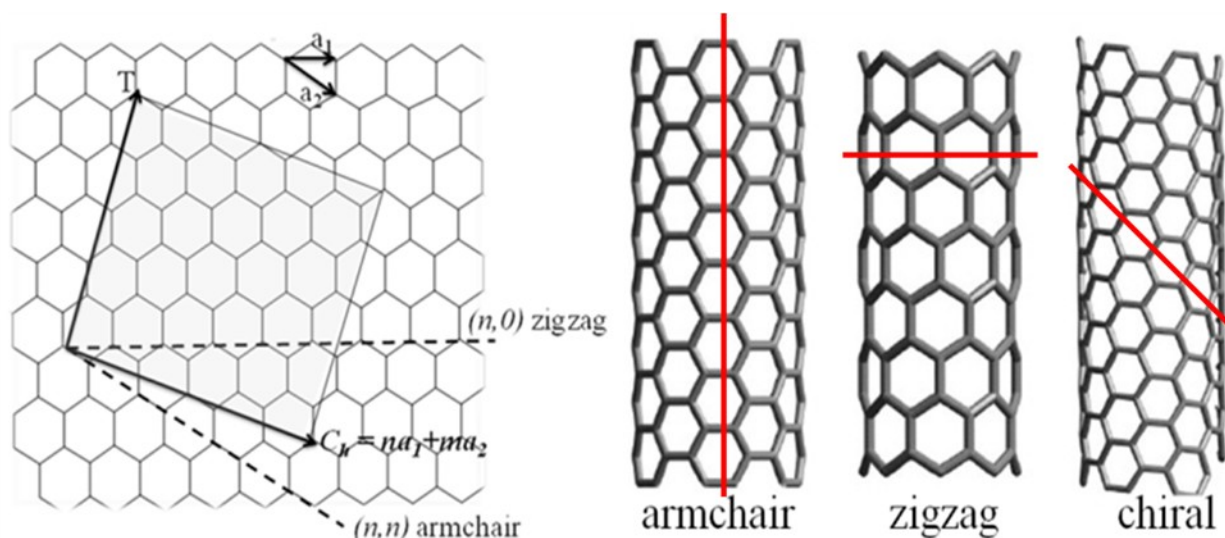


**Figure 35:** Different types of carbon nanotubes

CNTs exhibit impressive properties such as incredible strength; indeed, they are one to twice as strong as steel for approximately six times less weight. They also present excellent mechanical, electrical (conducting, supra-conducting), thermal and magnetic properties. All these features provide them with the necessary qualities to be a much desirable material. Many potential applications of CNT could be imagined in various fields like: semiconductor, electronic memory, medical delivery system, coating, composite material, energy storage, and biotechnology.<sup>4-7</sup>

CNTs are produced by physical processes<sup>8,9</sup> as described below:

### - **CVD: Chemical Vapor Deposition**

A substrate consisting of metal catalyst particles (eg. Ni, Co, Fe...) is heated to 500–1000°C. Gaseous carbon source (acetylene, ethylene, methane, ethanol...) is bled into the reactor. The gas breaks at the surface of the catalyst where carbon nanotubes are forming. The type of CNTs produced depends on the working conditions (temperature, pressure, volume, concentration of gas, metal catalyst, duration, etc.)

### - **Arc Discharge**

An electric arc discharge is generated between two graphite electrodes under inert atmosphere (helium or argon). The carbon is sublimating at high temperature forming CNTs on the cold surface of the reactor.

### - **Laser Ablation**

A graphite piece is vaporized by laser irradiation under inert atmosphere. The soot containing CNTs are collected at the cold wall of a quartz tube.

After the synthesis of CNTs, purification processes are necessary as some impurities such as carbon, graphite, fullerene and metal contamination are present, but also as carbon nanotubes of different types and diameter are produced.

In order to use the promising properties of CNTs, chirality pure CNTs of defined diameter are needed. However, with the above described production methods, the availability of such CNTs is limited. A solution to this problem would be to synthesize CNTs using bottom up approaches.

### 2.1.3 Nanobelts

The first step into a rational synthesis of CNTs, the synthesis of nanobelts have recently challenged organic chemists.<sup>10-14</sup> Besides the ambitious goal of chemical synthesis of CNTs, nanobelts exhibit interesting properties themselves with novel optoelectronic features and host-guest behavior. Moreover, because of the poor solubility and inhomogeneity of CNTs, only very few are really understood from their properties. Thus nanobelts could serve as model to better understand the fundamental properties of CNTs. This emerging field is also connected to a deeper understanding of the concept of aromaticity, electron delocalization,  $\pi$ -interactions and strain.

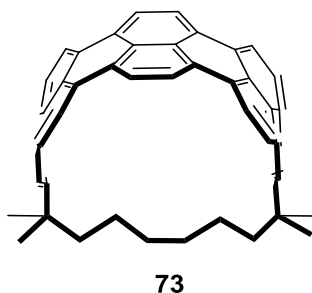


**Figure 36:** Bodwell half belt

Bodwell et al. synthesized an aromatic half belt molecule **73** which imitates perfectly the wall of a (8,8) armchair nanotube (Figure 36).<sup>15</sup> The synthesis of different types of nanobelts has been achieved in the last decades.<sup>10-12,14</sup> A few examples are shown on Figure 37 with cycloparaphenylacetylene **69**, cycloparaphenylene (CPP) **70**, cyclacene **71**, and phenacene **72**.

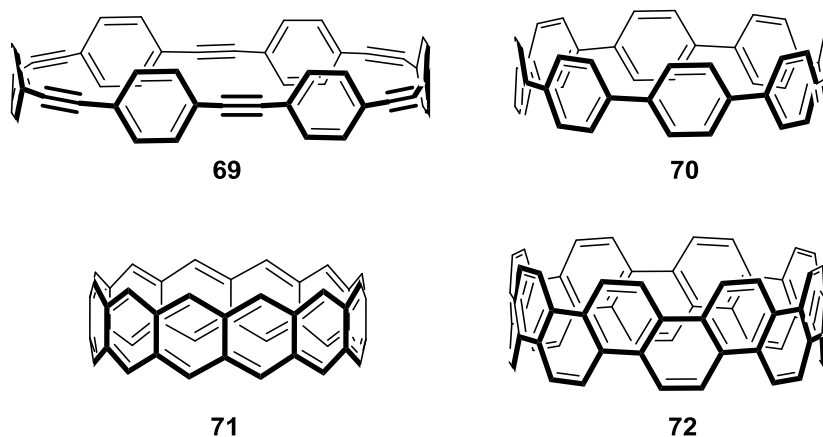


**Figure 37:** Cycloparaphenylacetylene (top left), cycloparaphenylene (top right), cyclacene(bottom left), and phenacene (bottom right).

### 2.1.4 From nanobelts to nanotubes

Cycloparaphenylene (CPP) is the smallest fragment of an armchair CNT. Therefore, such an interesting molecule could serve as template to synthesize longer armchair CNTs. Until very recently, the possibility to grow CNTs from belt template or CNT cap fragment<sup>16</sup> remained only a dream, even if theoretical studies back upped this possible strategy (Figure 38). Lately, the dream has come true: Itami et al. presented the first CPP-templated CNT growth leading to CNTs with an average diameter close to the template ring. Furthermore, this method uses a metal-free approach.

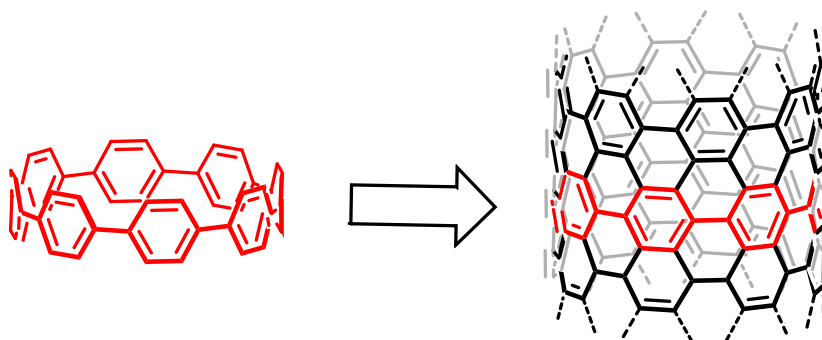


**Figure 38:** Elongation from CPP

As for the other production methods, reaction parameters are important (reaction temperature, nature of the reaction plate and carbon source). They treated [9] and [12]CPP coated C-plane sapphire substrate with ethanol gas under vacuum (1 torr) at 500°C for 15 minutes to afford the corresponding CNTs. However, the small scale of their system and imperfection in diameter and chirality are still to be improved in order for this method to be really applicable for semi-industrial applications. Concerning the mechanism of such a strategy for elongation, three possible mechanisms are proposed (Figure 39):

- Diels Alder /dehydrogenative aromatization was suggested by Scott et al.<sup>17-19</sup>
- Ethynyl radical addition as postulated by Irle Murokum et al.<sup>19</sup>
- CPP-radical mechanism as proposed by Itami et al.<sup>20</sup>

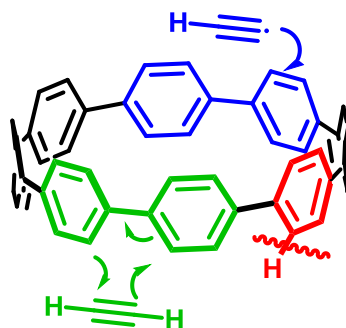


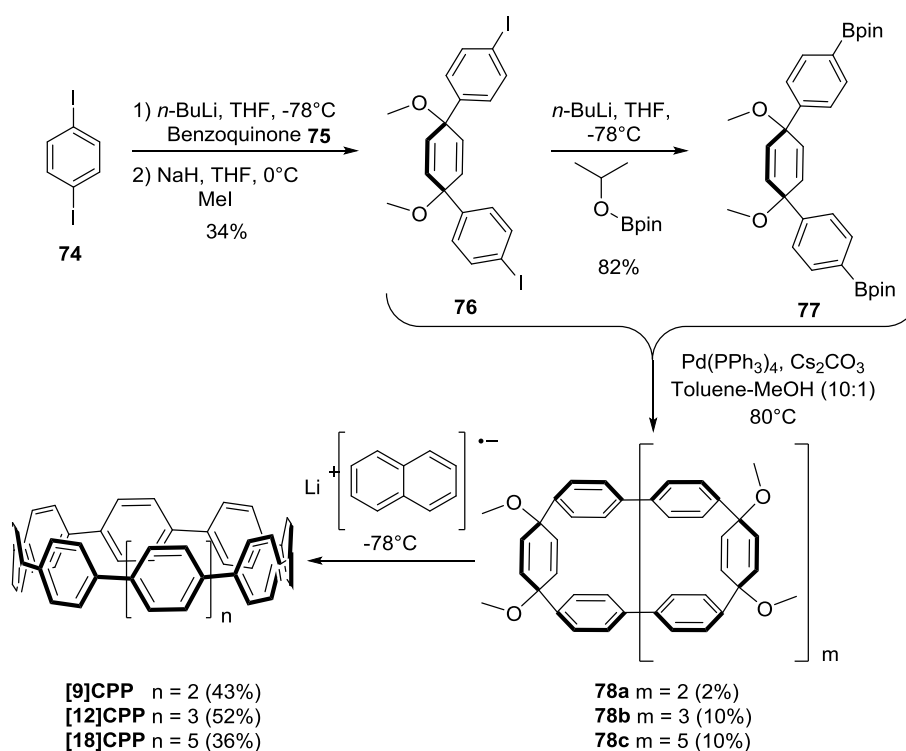
**Figure 39:** Possible mechanisms of CPP initiated CNT growth: Diels-Alder (green), Ethynyl radical addition (blue) and CPP radical (red).

### 2.1.5 Cycloparaphenylene syntheses

The challenge of all CPP syntheses lies in the high strain energy to overcome in the ring-closing step. Indeed, the calculated ring strain is in the range of 29–97 kcal/mol for [20]–[6]CPPs. Therefore, to circumvent this problem several strategies have been elaborated. They all rely on the synthesis of a macrocyclic precursor which is reaching full conjugation only in the last step, hence the strain is built up sequentially.<sup>10,21-23</sup> The different strategies to synthesize CPPs are presented in the following sections.

#### 2.1.5.1 Synthesis by Bertozzi and Jasti

In 2003, Hopf and coworkers devised the use of a dimethoxy-cyclohexadiene, a masked benzene convertible unit as building block for the synthesis of poly-yne cyclophanes.<sup>24</sup> Later, in 2008, Bertozzi and Jasti used a similar strategy for the very first CPP synthesis.<sup>25,26</sup> The macrocyclic precursor **78** could be synthesized by taking advantage of the curvature of the building blocks **76** and **77**. The iodide building block **76** was synthesized by double addition of lithiated iodo-benzene to quinone and direct methylation of the resulting *cis*-diol. Subsequently, the iodide **76** was further converted to the boronic ester **77**. The two building blocks were then submitted to macrocyclization under Suzuki reaction conditions to afford macrocycles of different sizes **78a-c** in 2–10% yields. Finally, the resulting macrocyclic precursors were aromatized using lithium naphthalide at  $-78^{\circ}\text{C}$  (single electron reduction) proceeding in moderate yield (36–52%) of the corresponding [9], [12] and [18] CPPs isolated for the very first time.



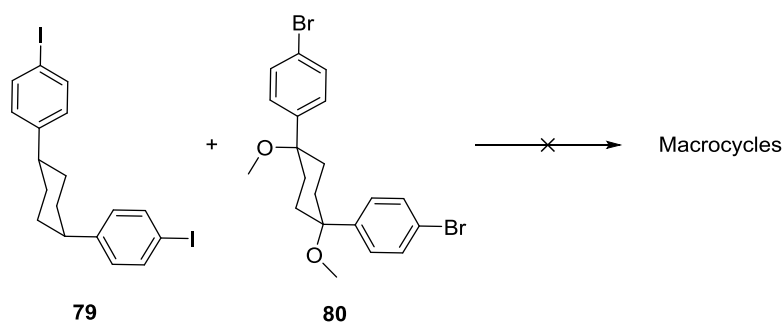
Scheme 31: CPP synthesis by Bertozzi and Jasti

Since this first synthesis, the Jasti group developed this strategy using similar reaction for the selective synthesis of [7]–[12]CPP.<sup>27</sup> They modified the strategy by using orthogonal stepwise reactions rather than the unselective “shotgun” macrocyclization, making the synthesis of the smallest CPP ([7]CPP<sup>28</sup> and [6]CPP<sup>29</sup>) their specialty.

They notably improved the synthesis to provide a gram-scale synthesis of [8] and [10]CPPs.<sup>30</sup> Using a bromide building block and in situ methylation, they improved the scalability and efficiency of the process. Furthermore, they used the inexpensive Pd(OAc)<sub>2</sub> catalyst for the macrocyclization and obtained the CPPs in up to twice better yields than before.

### 2.1.5.2 Synthesis by Itami

Among a number of unsuccessful attempts of synthesizing CPP, Vögtle<sup>31</sup> suggested the use of L-shaped building block for the synthesis of macrocyclic precursor that could be oxidized to the fully aromatic cycloparaphenylenes (Scheme 32). However, the isolation of the desired macrocycle was not successful, demonstrating the part of luck behind the successful synthesis of macrocyclic molecules, as Itami took over the strategy for his successful synthesis of CPPs.

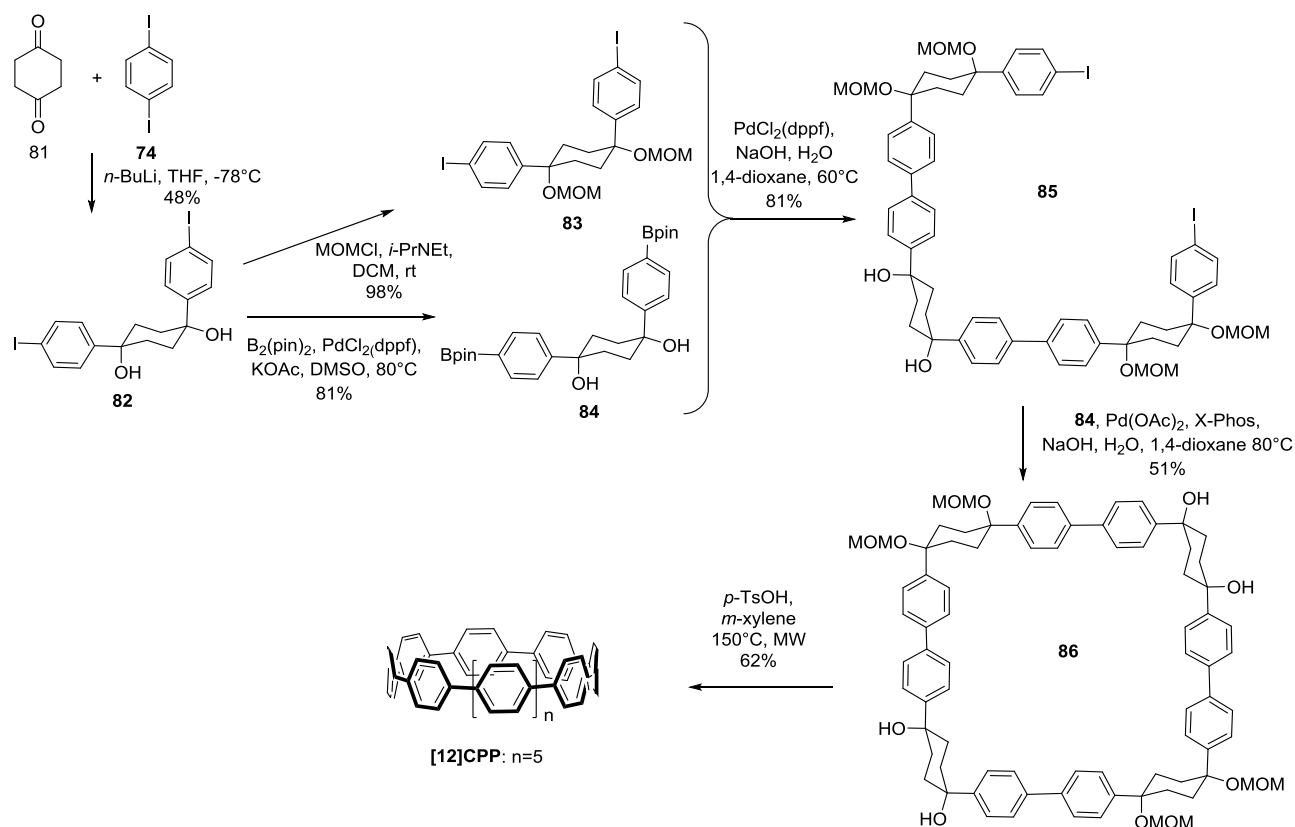


**Scheme 32:** Vögtle’s attempt to synthesize a CPP

Itami and coworkers decided to use L-shaped building block with cyclohexanediol moiety as masked benzene unit. This L-shaped building block presents the ideal curvature to facilitate formation of designed macrocyclic precursors (Scheme 33).

The building block **82** was synthesized by double addition of 4-iodophenyllithium, generated by in situ lithiation of 1,4-diodobenzene, on cyclohexane-1,4-dione. The resulting *cis*-diol **82** was protected with MOM groups. The introduction of MOM groups facilitated handling of the intermediates by increasing their solubility. The building block **82** could be converted to the corresponding boronic ester **84** and the two L-shaped building blocks were coupled by Suzuki coupling reaction in the 2:1 trimer **85**. The macrocycle was then completed by coupling with monomer **85**. The macrocyclic precursor **86** was finally treated with *para*-toluenesulfonic acid under microwave irradiation to obtain the desired [12]CPP by a sequence of deprotection, elimination and oxidation reaction to the aromatic ring.<sup>32</sup>





**Scheme 33: CPP synthesis by Itami<sup>32</sup>**

After this first successful synthesis, the group developed the approach to achieve the modular synthesis of [12], [14]–[16]<sup>33</sup> by taking advantage of the L-shaped building block and combining it with different length of linear phenylene units in a U shaped building block suitable for dimerization macrocyclization. Further applying the strategy and carefully choosing the adequate combination of L-shaped and linear building block the selective synthesis of another series of CPPs was available ([9]–[11] and [13]CPP)<sup>34</sup> In total, by using this method [9]–[16]CPP could be synthesized until now (Figure 40).

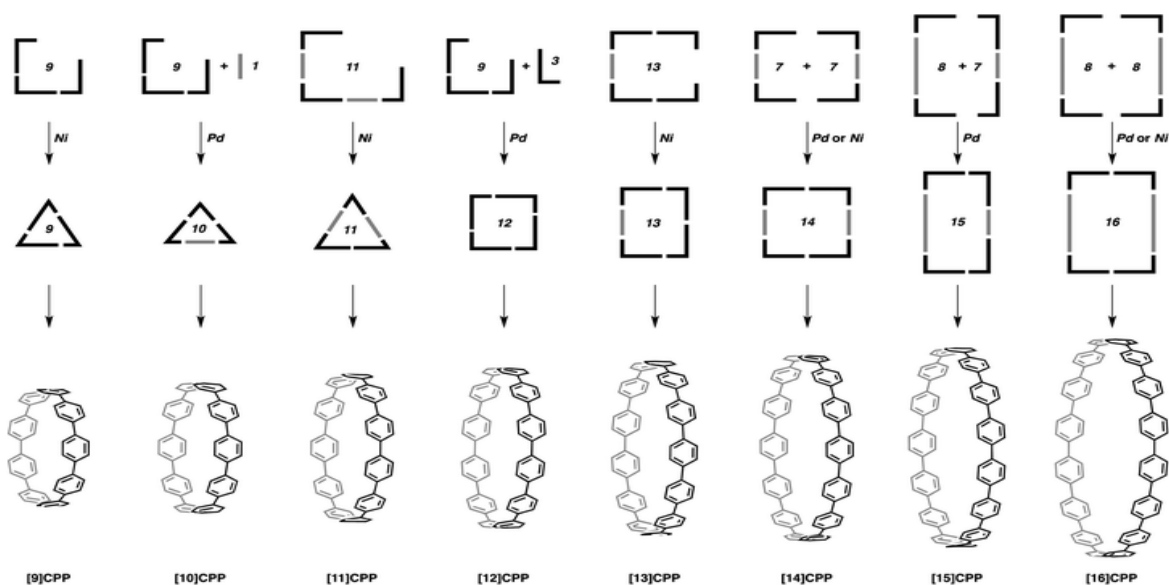
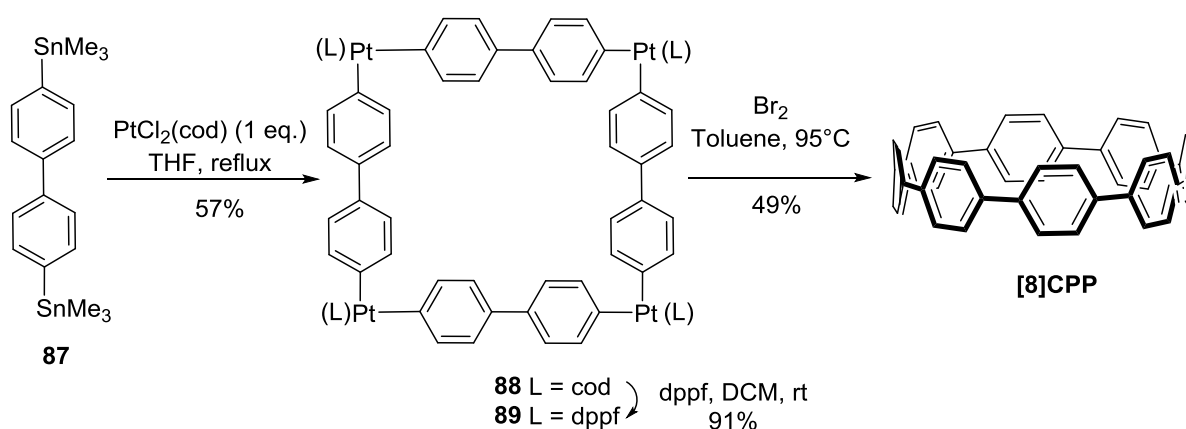


**Figure 40: Strategies to modular synthesis of [9]–[16]CPPs reprinted from literature<sup>34</sup>**

Another improvement was reached using a shotgun approach for the synthesis of [12]CPP<sup>35</sup> and [9]CPP.<sup>36</sup> This new strategy using nickel-promoted macrocyclization of the L-shaped building block furnished a more concise and cost effective scalable synthesis of CPPs.

### 2.1.5.3 Synthesis by Yamago

In 2010, Yamago synthesized [8]CPP<sup>37</sup> using a square-shaped tetra-nuclear platinum complex (Scheme 34). The strain of the macrocyclization was avoided taking advantage of the platinum coordination geometry. The CPP was obtained from the metalla-macrocycle **89** by reductive elimination in 49% yield. This is a very concise synthesis of CPP with only three steps, but to the cost of stoichiometric amount of platinum.



**Scheme 34:** Synthesis of CPP by Yamago

They then modulated the strategy, using terphenyl building blocks to achieve the synthesis of [8]–[13]CPP.<sup>38,39</sup>

### 2.1.5.4 Syntheses of CPP derivatives

Since the syntheses of the wide range of CPPs of different diameters, several derivatives have been designed and synthesized, opening the way for larger CNT fragments, with different chirality and substitutions. Synthesis of  $\pi$ -extended belts would also permit to explore structural and electronic effects in more rigid nanobelts. Moreover, such nanobelts would constitute closer precursors to nanotubes. In the present section selected examples of CPP derivatives recently synthesized are presented.

Jasti et al. synthesized a tetraphenyl-substituted CPP **90** (Figure 41, left) modifying their cyclohexadiene building block by using a tetraphenyl-substituted benzoquinone derivative. They performed the synthesis of the tetraphenyl-substituted [12]CPP using their Suzuki coupling strategy.<sup>40</sup>

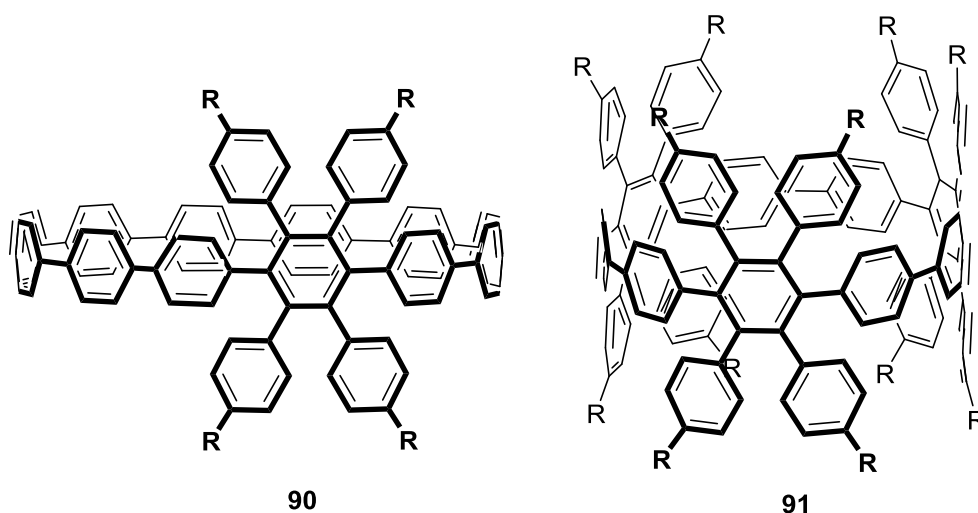


**Figure 41:** Tetraphenylsubstituted CPP: syntheses by Jasti (left) and Müllen (right)

Müllen et al.<sup>41</sup> had a similar idea to use tetraphenyl-substituted cyclohexadiene building block and combine them via nickel mediated Yamamoto coupling reaction. They obtained trimeric macrocycles which were consequently aromatized via low covalent titanium mediated reductive aromatization to produce the substituted CPP **91** in good yields (73–81%) (Figure 41, right). They also tried to perform the cyclodehydrogenation reaction on this CPP to access [3]cyclohexabenzocoronene ([3]CHBC). However, the reaction proved to be quite challenging and led to complex mixture of partially dehydrogenated and chlorinated products. The clear evidence of formation of [3]CHBC was not yet obtained.

A first  $\pi$ -extended belt was synthesized by the Itami group. They choose to apply the cyclohexadiene strategy incorporating naphthalene derivative to synthesize the cyclonaphtylene nanoring **92** (Figure 42). They combined the designed L-shaped building block in a nickel-mediated “shotgun” macrocyclization. Final aromatization under reductive condition afforded desired  $\pi$ -extended [9]NCPP.<sup>42</sup>

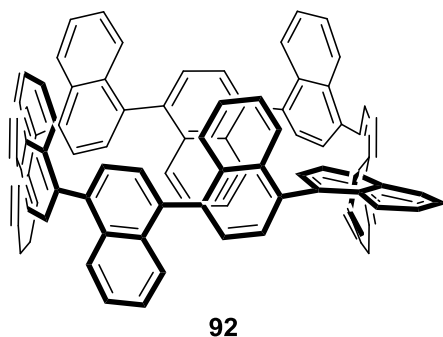


**Figure 42:** Cyclonaphtylene [9]NCPP

Itami recently proved that the concept of the synthesis of CPP can be extended to the synthesis of short chiral CNTs, by inserting an acene unit in a CPP structure.<sup>43</sup> As a concrete example they

synthesized the cyclo[13]*para*-phenylene-2,6-naphthylene **93** ([13]CPPN) using their L-shaped cyclohexane building block based methodology (Figure 43). This strategy can be extended with the use of other acenes and thus opens the way to the synthesis of all chiral nanohoops.

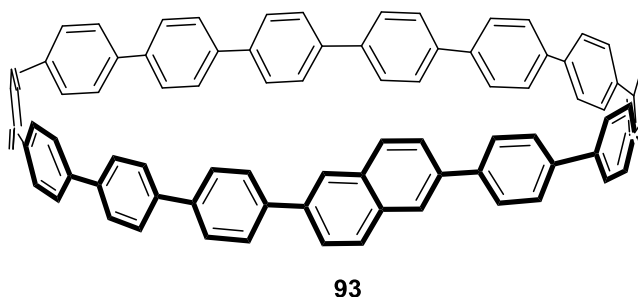


**Figure 43:** Chiral CNT fragment ([13]CPPN)

With the strategies available, it is also possible to synthesize heteroatom-containing CPP such as the nitrogen-containing CPP **94** (Figure 44) synthesized by Itami et al. using bipyridine linear building block.<sup>44</sup>

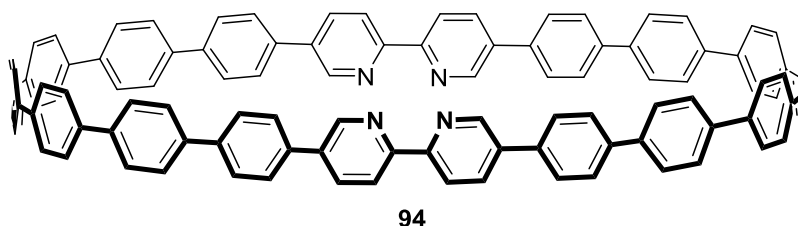


**Figure 44:** Nitrogen containing CPP

## 2.1.6 Properties of Cycloparaphenylenes

### 2.1.6.1 Structural properties

The most stable conformations were determined by calculation.<sup>45</sup> For even [n]CPP the best conformation is when the phenyl units adopt an alternating zig-zag orientation with a nearly  $D_{(n/2)h}$  point group, whereas odd CPPs have helical arrangement of phenylene units with  $C_1$  point group.

The strain energies of CPPs have been estimated by different methods based on the energy of homodesmotic reactions:

- Linear oligo-*para*phenylene is produced from [n]CPP and biphenyl.
- [n]Poly-*para*phenylene is produced from [n]CPP.
- Biphenyls and *paraterphenyls* are obtained from CPP. This last method has the advantage to avoid the calculation of the different conformation of poly-*para*phenylenes.

All the calculation methods give similar results. The most complete list of strain energies was calculated by Yamago et al.<sup>39</sup> and is reported in Table 6.

**Table 6:** Strain energy of CPP

<b>[n]CPP</b>	<b>Strain energy (kcal/mol) <sup>39</sup></b>
<b>[4]CPP</b>	114.1
<b>[5]CPP</b>	117.2
<b>[6]CPP</b>	97.23
<b>[7]CPP</b>	85.20
<b>[8]CPP</b>	73.40
<b>[9]CPP</b>	66.82
<b>[10]CPP</b>	58.93
<b>[11]CPP</b>	54.83
<b>[12]CPP</b>	49.05
<b>[13]CPP</b>	46.45
<b>[14]CPP</b>	42.10
<b>[15]CPP</b>	40.23
<b>[16]CPP</b>	36.76
<b>[17]CPP</b>	35.44
<b>[18]CPP</b>	32.65
<b>[19]CPP</b>	31.73
<b>[20]CPP</b>	29.39

Obviously, the strain energy of CPP increases with decreasing ring size. There is a small odd-even effect: the strain of odd CPP is slightly higher than for even CPPs. This effect is due to the helical conformation of odd CPPs.

The structures and energies of molecular frontier orbitals have also been calculated.<sup>45</sup> The HOMO is mainly localized on individual benzene unit as a  $\pi$  orbital and the LUMO is delocalized mainly to the inter ring bonds as a  $\pi^*$  orbital. The energy of HOMO-1 and HOMO-2 are degenerated as well as LUMO+1 and LUMO+2, therefore commonly the degenerated orbitals are designated by HOMO-1 and LUMO+1. As a typical example, structures of the main orbitals of [12]CPP are depicted on Figure 45.

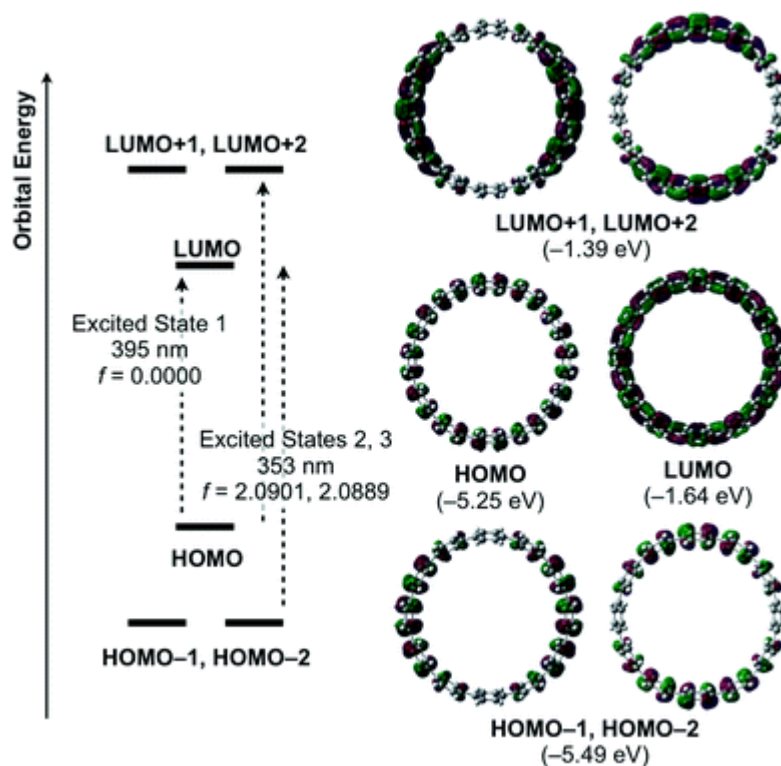


**Figure 45:** Energy diagrams and pictorial representations of the frontier MOs for [12]CPP, calculated at the B3LYP/6-31G(d) level of theory. Excitation energies were computed by TD-DFT at the same level. (reprinted from literature)<sup>45</sup>

The energies of the orbitals of the different size of CPP that have been calculated by Itami et al. are shown on Figure 46.

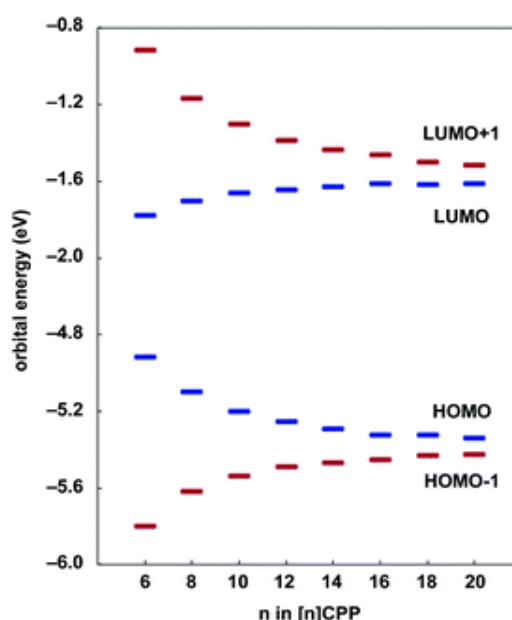


**Figure 46:** Energy diagram of CPPs orbitals calculated by Itami et al. (reprinted from literature)<sup>45</sup>

The energy of HOMO decreases and LUMO increases as the CPP becomes larger which is in big contrast with the case of linear polyphenylenes for which the HOMO increases and LUMO decreases with the number of phenylene unit because of the increase of effective conjugation

(length of conjugation). In CPPs, the aromaticity of individual phenyl unit tends to decrease with decreasing ring size due to deformation of the benzene ring. The distortion of a benzene ring can be estimated with bent angles  $\alpha$  and  $\beta$  as described on Figure 47 which give the deviation of the benzene ring from planarity (bending effect). The torsion angle  $\theta$  between neighboring phenyl ring also influences the conjugation (torsion effect).

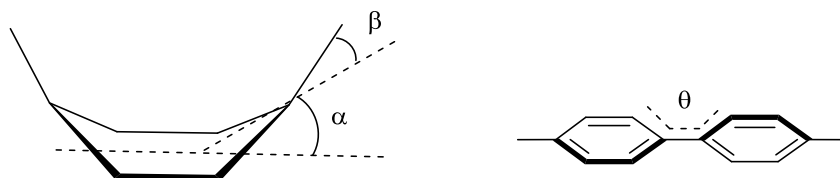


**Figure 47:** Definition of bent angles  $\alpha$  and  $\beta$  and torsion angle  $\theta$

Those angles have been measured for a range of calculated structures of CPPs by Itami et al.<sup>45</sup> and are reported in Table 7. The smaller the ring, the larger the bent angles, hence the distortion from planarity. On the contrary, the torsion angles tend to get larger as the ring size increases.

**Table 7:** Bent and torsion angles (in degree) in various CPP optimized structure

[n]CPP	6	8	10	12	14	16	18	20
<b>Bent angle <math>\alpha</math></b>	12.5	9.3	7.3	6.1	5.2	4.6	4.0	3.6
<b>Bent angle <math>\beta</math></b>	18.0	13.7	11.1	9.3	8.0	6.9	6.3	5.6
<b>Torsion angle <math>\theta</math></b>	27.4	30.7	32.7	33.4	34.4	35.0	34.9	35.1

These factors have an effect on the orbital energies. Intuitively, we expect that the energy of an occupied MO increases and the energy of an unoccupied MO decreases as the number of conjugated phenyl increases, as the torsion angle decreases and the benzene ring are more distorted. However, the contrary effects are observed in the case of CPPs. The influence of the conjugation length should be very small as the conjugation in a CPP is in principle infinite. However, torsion and bending effects are expected to play a large role in the observed trend in MO energies of CPPs.

Indeed, as CPPs become smaller, the benzene rings become more bent resulting in a destabilization of the HOMO ( $\pi$ ) and stabilization of LUMO ( $\pi^*$ ). As for the torsion angle, the increase of ring size allows more flexibility of the neighboring phenyls which can adopt a more twisted angle, resulting in stabilization of the HOMO and destabilization of the LUMO because of reduced conjugation between the phenyl rings.

Itami et al. conducted modeling studies to understand how the parameters influence the energy level of HOMO and LUMO. They found that then bending effect is more pronounced for HOMO energies and the torsion effect has more effect on the LUMO.<sup>45</sup>

This explains why the HOMO-LUMO gap increases with ring size, which is exactly opposite to the trend observed for linear poly-*paraphenylenes*.

### 2.1.6.2 UV and Fluorescence properties

All the CPPs have their absorption maxima around 340 nm regardless to their ring size (see Table 8). This result is counterintuitive considering the size dependence of the HOMO-LUMO gap discussed above.

**Table 8:** UV-Vis properties of CPPs

[n]CPP	$\lambda_{\text{abs}}/\text{nm}$	$\lambda_{\text{fl}}/\text{nm}$
[6]CPP <sup>29</sup>	338	no fluorescence
[7]CPP <sup>28</sup>	339	592
[8]CPP <sup>46</sup>	338	533
[9]CPP <sup>46</sup>	340	494
[10]CPP <sup>46</sup>	340	470
[11]CPP <sup>46</sup>	339	437, 458
[12]CPP <sup>46</sup>	338	428, 450
[13]CPP <sup>46</sup>	337	424, 446
[14]CPP <sup>45</sup>	338	418, 443
[15]CPP <sup>45</sup>	339	416, 440
[16]CPP <sup>45</sup>	339	415, 438

DFT-calculations were undertaken by different groups to clarify this point. All the studies revealed that the HOMO-LUMO transition is symmetry forbidden (small oscillator strength). The transition observed on the absorption spectra can be assigned to the degenerated HOMO-1/LUMO and HOMO/LUMO+1 transition.<sup>39,46-48</sup>

Analysis of the fluorescence spectra is however more complicated. The fluorescence presents a blue shift with increasing ring size. Two points need to be clarified: the increase of the Stokes shift with decrease of ring size and the multipeak emission. A probable explanation for the enlarged Stokes shift would be that smaller rings are more strained and could undergo more structural changes in the excited state.

In a recent work from Kanemitsu et al.,<sup>47</sup> the one and two photon luminescence was experimentally studied. The results show that the photoluminescence of CPP comes from the LUMO state. The transition between LUMO and HOMO is dipole forbidden because of the symmetry. However, phonon assisted optical processes enable luminescence to occur. Thus the



HOMO–LUMO gap explains the Stokes shifts. As for the multipeak emission, it is due to the coupling of exciton/vibration during radiative recombination of excitons.

In another theoretical study by Irle et al.,<sup>49</sup> a slightly different explanation is given. The multipeak of the large CPP are due to vibronic coupling with Jahn-Teller effect of the  $S_2/S_3$  to  $S_0$  radiative transition, the LUMO to HOMO ( $S_1$  to  $S_0$ ) transition being forbidden. However, the symmetry rule governing emission are more relaxed for smaller CPP for which it is possible that the main transition is due to the  $S_1$ - $S_0$  transition with low efficiency, hence the low quantum yield of small CPPs. To explain the blue fluorescence shift of larger CPPs, dynamic relaxations have to be taken into account. The larger CPPs are more rigid because of their greater aromatic character and therefore smaller CPPs can undertake more structural changes with larger vibrational amplitudes thus larger stokes shift.

### 2.1.6.3 Redox properties

Yamago et al. measured the oxidation potential using cyclic voltametry in  $Bu_4NPF_6/C_2H_2Cl_4$  at room temperature. The oxidation potentials are reported in Table 9.

**Table 9:** Half-wave oxidation potential of CPPs

nCPP	8	9	10	11	12	13
E (vs Fc/Fc <sup>+</sup> )/V	0.59	0.70	0.74	0.79	0.83	0.85

All CPPs show reversible oxidation wave indicating stable intermediates. The oxidation potential increases with increasing ring size. A maximum is reached around 0.85 V. This trend is in good agreement with the HOMO energy trend.

## 2.2 PROJECT AND STRATEGY

### 2.2.1 Initial strategy

The synthesis of CPP using [2+2+2] cycloaddition reaction as the key step was a long sought goal in our group. Initially, we wanted to apply this reaction to bring strain in the system, taking advantage of the aromaticity gain to overcome the strain energy. Jonathan Basler made several attempts to synthesize macrocyclic precursor such as the macrocycle **95** in Figure 48.<sup>50</sup> He encountered difficulties notably for the macrocyclization step. One of the problems was the low solubility of the products hampering the purification process. Another problem could be the flexibility of the building blocks which did not favor the formation of the desired macrocycle. He also tried the [2+2+2] cycloaddition reaction on macrocyclic precursor mixture, with no conclusive proof of the presence of CPP product.

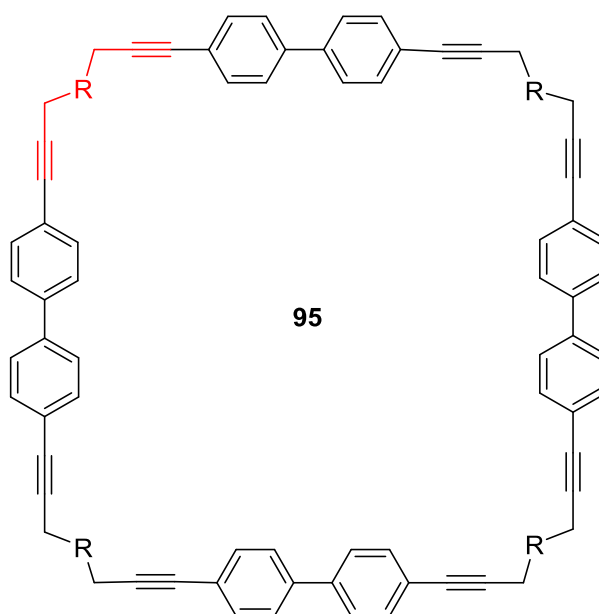
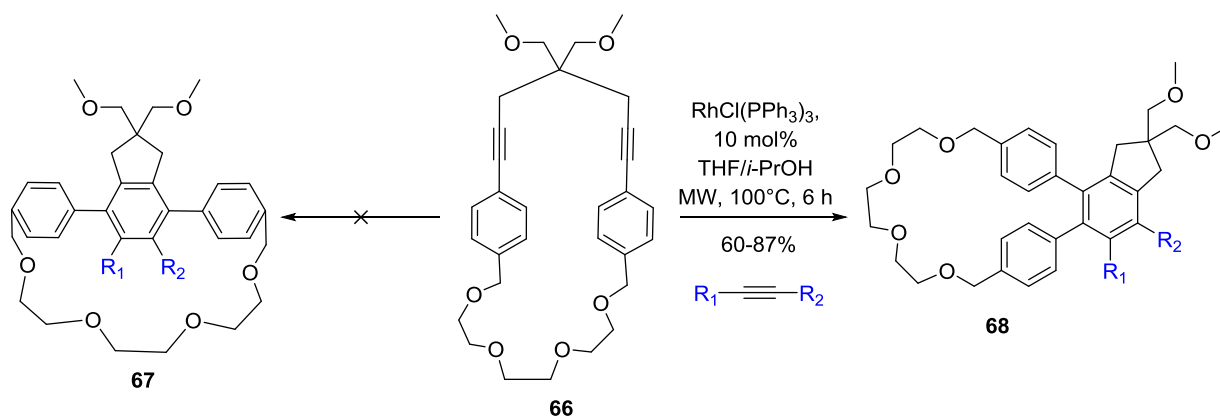


**Figure 48:** Initial strategy for the synthesis of CPP: macrocyclic precursor

Due to the complexity of the system, the strategy was probed on a more controllable macrocyclic system. The outcome was presented in Chapter 1. Those results showed that strained systems tend to follow a different mechanism pathway than the expected [2+2+2] cycloaddition reaction (Scheme 35). Therefore, this method is no longer suitable to bring strain in the system. Nevertheless, the [2+2+2] cycloaddition reaction can be used as a versatile method to introduce substituents in the system, allowing accessing substituted CPPs and choosing substituents at a late stage of the synthesis.



**Scheme 35:** Cycloaddition on strained system

### 2.2.2 Combined strategy

As a consequence of this preliminary study, we had to modify our initial strategy to incorporate another building block being able to account for the strain. Previous CPP syntheses relied on such building blocks in order to synthesize macrocyclic precursors that could be aromatized in a last step. Combining one of those building blocks with a diyne building block should provide a precursor for the synthesis of substituted CPP (Figure 49). The aim of the project discussed in this chapter is to develop a highly modular synthesis of substituted CPPs based on this strategy.

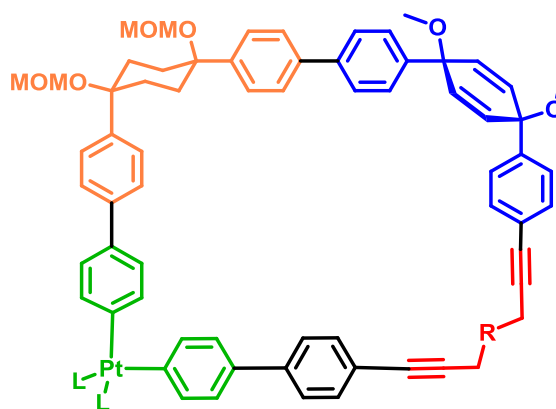


**Figure 49:** Schematic combination of the different building blocks used for CPP synthesis by (Itami in orange, Jasti in blue, Yamago in green, and our group in red)

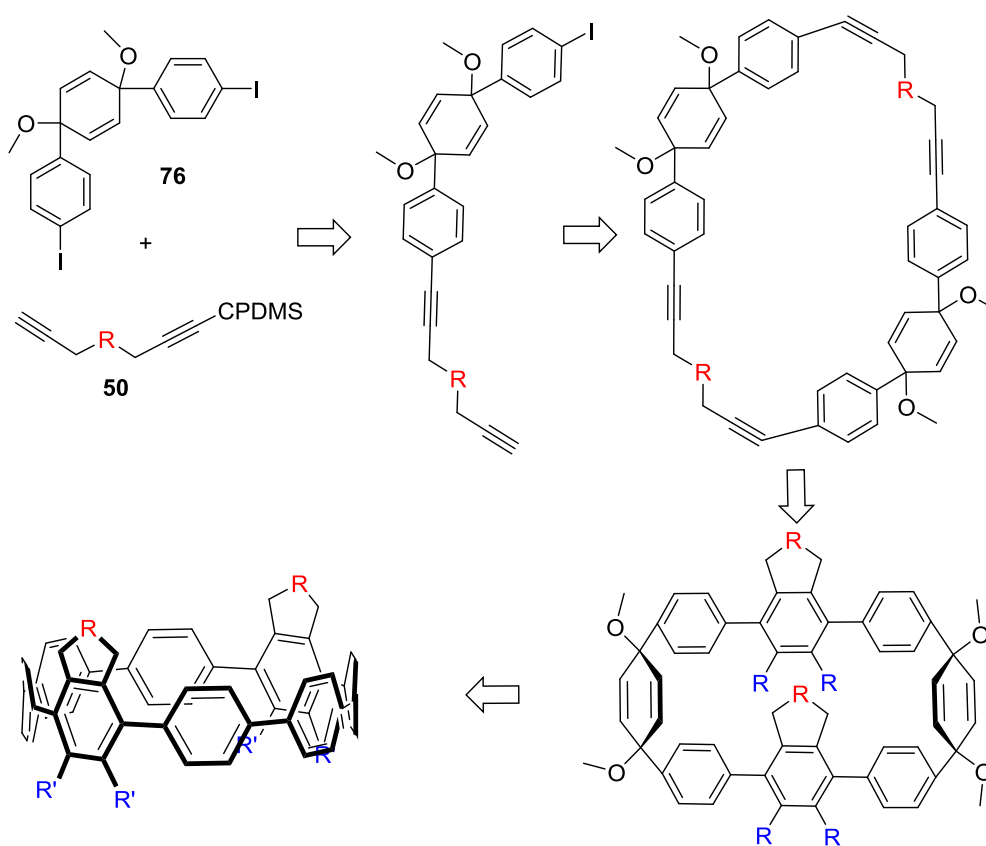
First, a synthesis of the macrocyclic precursor has to be designed. This macrocycle must contain a diyne building block to introduce substituent via [2+2+2] cycloaddition and another building block to bring the strain. Then, the [2+2+2] cycloaddition reaction will be applied, followed by the corresponding aromatization reaction to bring the final strain in the system.

## 2.3 RESULTS AND DISCUSSION

### 2.3.1 Macrocycle synthesis

#### 2.3.1.1 Synthesis of the macrocyclic precursor using Jasti method

Bertozzi and Jasti were the first to offer a successful strategy for the synthesis of CPPs, with cyclohexadiene as a bent benzene convertible unit. To take advantage of their method to bring strain in the system in the last step of the synthesis, we decided to combine their strategy with ours, by coupling their building block **76** with our diyne **50**. Then, after deprotection and macrocyclization, we could introduce substituent via [2+2+2] cycloaddition reaction before aromatizing the molecule to the desired CPP via reductive aromatization as last step (Scheme 36).

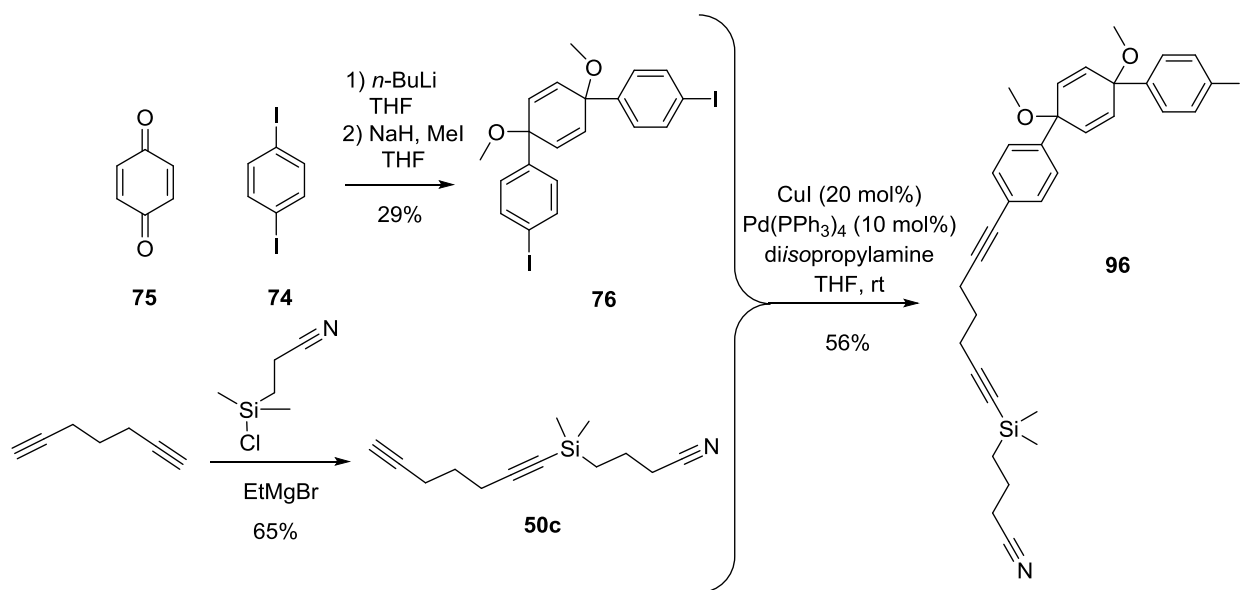


**Scheme 36:** Synthetic strategy using cyclohexadiene building block

The synthesis of the building block **76** designed by Jasti et al. was performed using literature procedure (Scheme 37).<sup>26</sup> The synthesis of this building proceeded in only 29% yield. However, this protocol presents the advantage to be easily performed in one pot and on large scale, affording readily available quantities of the required building block to explore further the strategy.

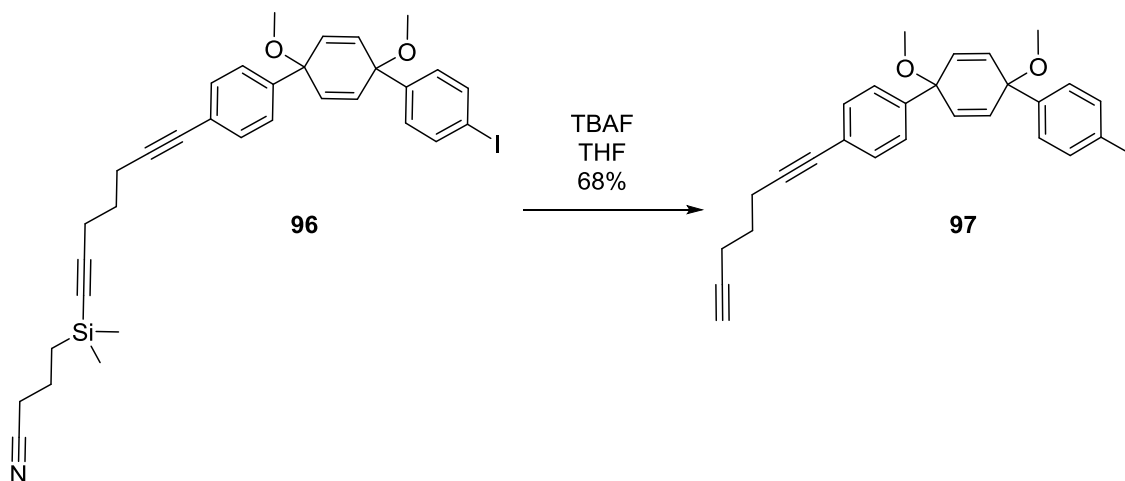
The diyne building block **50c** was obtained by protection with CPDMS protecting group ([3-cyanopropyl]dimethylsilyl) in 65% yield. As already mentioned, the choice of CPDMS as protecting group is crucial in order to facilitate the isolation of the desired product from the

statistical mixture of di-, mono-coupled and unreacted starting material.<sup>51</sup> The two building blocks were then combined via Sonogashira reaction in 56% yield.



**Scheme 37:** Synthesis of the cyclohexadiene combined building block

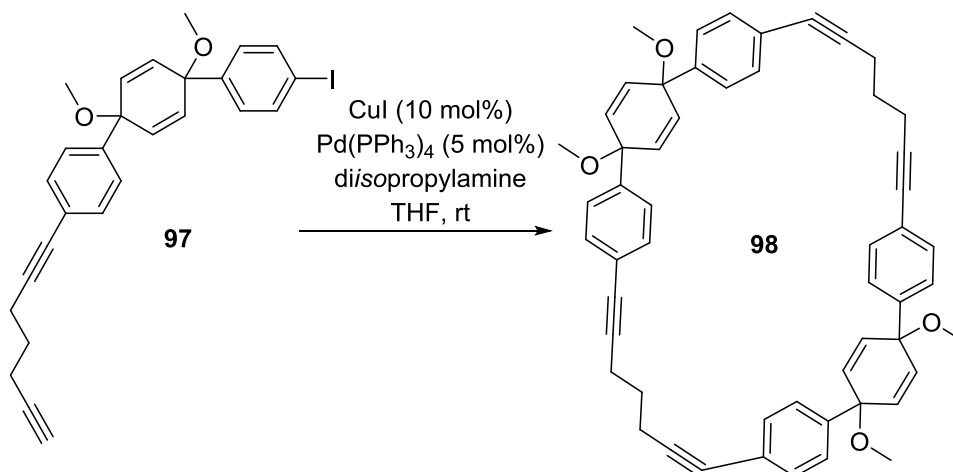
Deprotection of the diyne building block **96** turned out to be quite challenging. First potassium carbonate was used for deprotection, but the first test reaction led mostly to degradation, with only 7% yield of the deprotected product. The reaction time seemed to be a critical parameter.



**Scheme 38:** Deprotection of building block **96**

Despite this fact, the yield could be improved by reducing the reaction time to one hour, the product **97** was then isolated in 29% yield, but still 38% of starting material was recovered. After three hours of reaction, the yield decreased to 24% and 18% of starting material was re-isolated. Thus, the improvements were not satisfying. Switching to TBAF as deprotecting agent led to better yield of 57% after only 30 minutes. On larger scale, yields up to 68% could be obtained. (Scheme 38)

With the monomeric building block **97** in hands, the macrocyclization via Sonogashira reaction was attempted (Scheme 39).



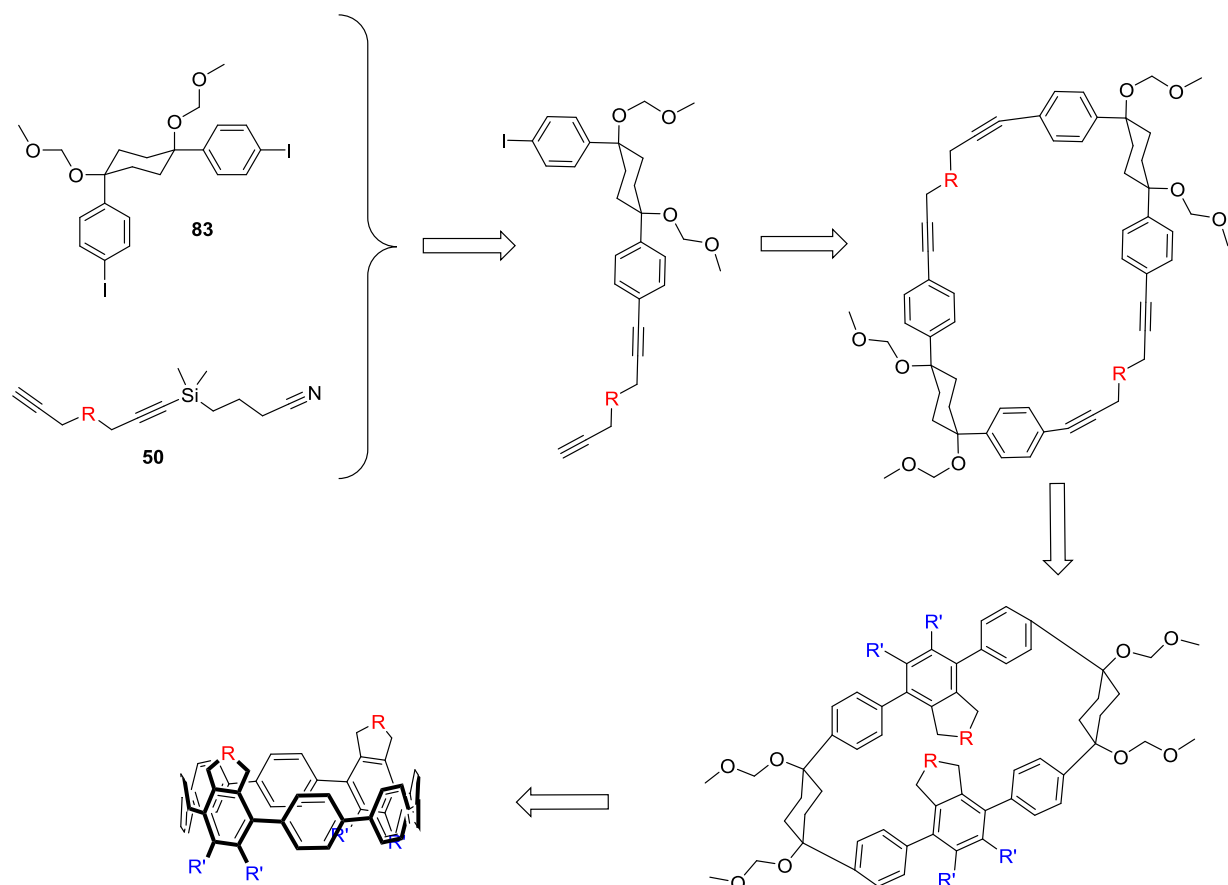
**Scheme 39:** Macrocyclization

A product which could correspond to the desired macrocycle **98** was isolated in approximately 15% yield. However, complete purification could never be achieved. The H-NMR spectrum looked very promising but the corresponding mass spectrometry signal could not be confirmed (ESI/MALDI-MS). We also tried to vary the concentration in order to get a mixture that would be easier to purify but the concentration did not have a large influence on the result. Furthermore, when removing all traces of solvent under high vacuum, the product was not soluble anymore. A [2+2+2] test reaction was performed with the impure macrocycle fraction without much success. Starting material was still present together with insoluble brown solid.

In parallel to this approach, the strategy using Itami's building block was also investigated. Due to the difficulties encountered using the building block of Jasti, the efforts were further focused on the cyclohexane strategy described in the following section.

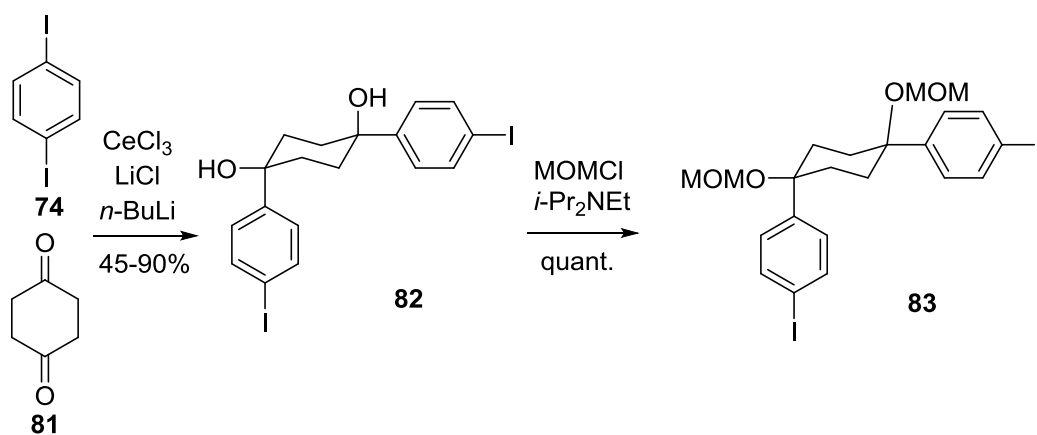
### 2.3.1.2 Synthesis of the macrocyclic precursor using Itami's method

By combining the building block **83** initially designed by Vögtle<sup>31</sup> and later applied successfully by Itami, with our diyne building block **50**, we should be able to access a macrocyclic precursor through a series of protection, combination via Sonogashira coupling, deprotection and macrocyclization reactions. Then, applying the optimized [2+2+2] cycloaddition reaction and finally aromatizing should deliver the substituted CPP (Scheme 40). The advantage of the *cis*-cyclohexane-1,4-diol building block is that it provides a L-shape curvature suitable for the macrocyclization, as it preorganizes the building block in the proper way to close the ring. Moreover, the cyclohexane moiety can be converted to the benzene ring by a one pot elimination-oxidation reaction.



**Scheme 40:** Strategy using cyclohexane combined building block

The building block **83** described by Itami et al. was synthesized following their literature procedure.<sup>33</sup> *Cis*-selective addition of an in situ monolithiated diiodobenzene on cyclohexane-1,4-dione was promoted by coordination to a  $\text{CeCl}_3 \cdot (\text{LiCl})_2$  complex. The reaction usually proceeded in poorer yield (38%) than in the reported protocols.

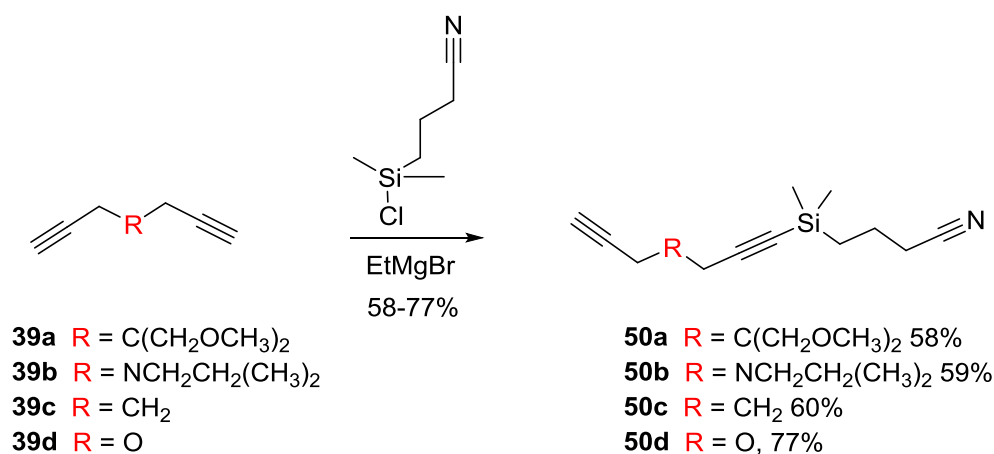


**Scheme 41:** Synthesis of the cyclohexane building block **83**

The cerium complex had to be prepared by stirring previously dried  $\text{CeCl}_3$  and  $\text{LiCl}$  in THF overnight. When increasing the temperature for the complex preparation, an improvement of the yield was observed (72–90%) (Scheme 41). The complex is described in the literature to be fully

soluble in THF, however, it always remained as a suspension in our case. The outcome of the reaction was strongly depending on the quality and dryness of  $\text{CeCl}_3$ . The reaction was not very reproducible and yield as bad as 7% were sometimes observed. Thus we also performed the synthesis of this building block with the classical non *cis*-selective procedure described in their first synthesis of [12]CPP.<sup>32</sup> The yield of this reaction (43%, lit. 48%) was not as good as the excellent yields that could sometimes be obtained with the *cis*-selective protocol due to the non selectivity of the reaction. Nevertheless, the reaction was actually less time consuming, easier to set up, scalable, more reproducible and was therefore more convenient to prepare large quantities of building block for further synthesis. The subsequent protection with MOMCl was always performed in excellent yields. Itami et al. chose MOM protecting group in order to enhance the solubility of the products based on this building block thus facilitating their handling and purifications.

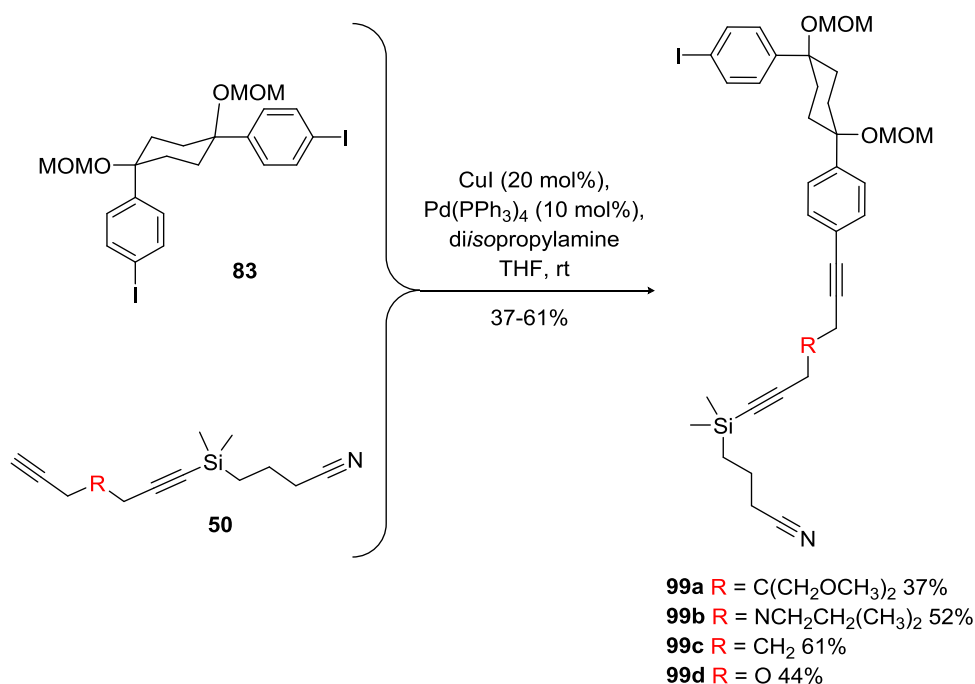
The syntheses of the diynes **50** were previously discussed. The protection of the different diynes with CPDMS proceeded in moderate yields (58–77%) (Scheme 42), which could be expected for a statistical reaction. Indeed, three different products can be isolated from this reaction: the mono-protected product (formed “twice” as two functional groups are present in the molecule), the di-protected product and the un-protected starting material. Here again, the choice of CPDMS as protecting group is crucial as it adds a polar group to the molecule facilitating the separation of the different products obtained in the reaction.



**Scheme 42:** CPDMS-Protection of the diynes

The two building blocks were combined via Sonogashira coupling reaction. Different combined building blocks were obtained from the reaction with various protected diynes in moderate yields (37–61%). Here again it relates to a statistical reaction, which accounts for the limited yields (Scheme 43).





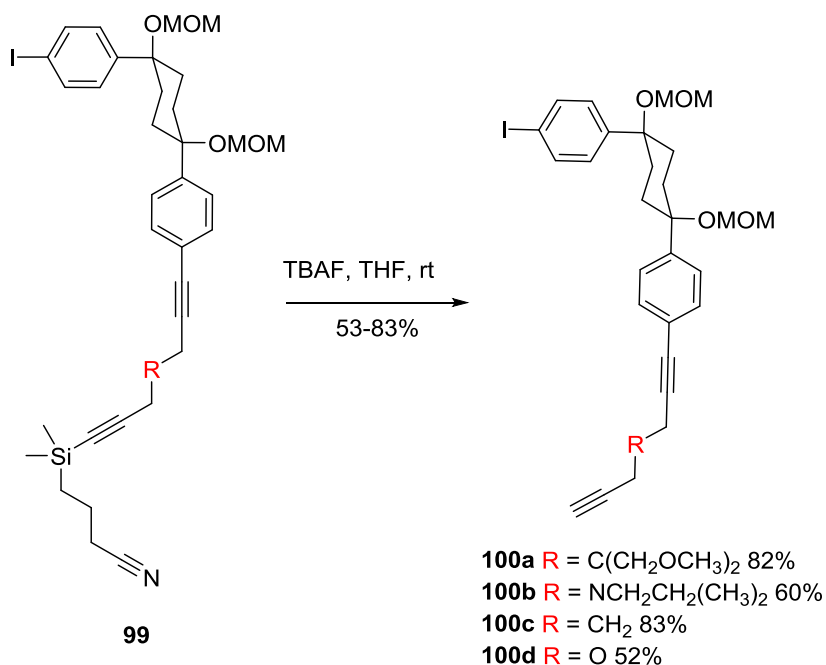
**Scheme 43:** Combination of the protected diynes with the cyclohexane building block

The combined building block **99** had to be subsequently deprotected. Initially, the CPDMS was removed using potassium carbonate in MeOH/THF mixture, but the reaction led to partial degradation and afforded the desired product around only 50% yield. Therefore, a screening to optimize those reaction conditions was undertaken with building block **99c** (Table 10).

**Table 10:** Screening for deprotection conditions

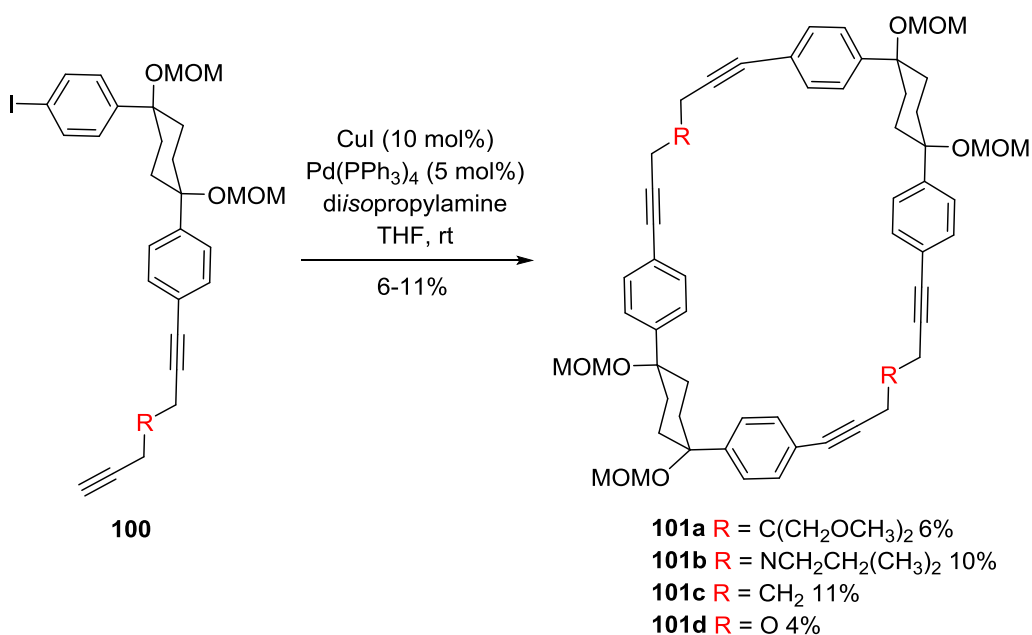
Entry	Conditions	Time	Isolated product	Isolated Starting material
1	4 eq. K <sub>2</sub> CO <sub>3</sub> , MeOH/THF	5 min	7 %	34 %
2	4 eq. K <sub>2</sub> CO <sub>3</sub> , MeOH/THF	30 min	32 %	9 %
3	4 eq. K <sub>2</sub> CO <sub>3</sub> , MeOH/THF	45 min	40 %	1 %
4	4 eq. K <sub>2</sub> CO <sub>3</sub> , MeOH/THF	1 h	50 %	1 %
5	4 eq. K <sub>2</sub> CO <sub>3</sub> , MeOH/THF	1.5 h	54 %	0%
6	4 eq. K <sub>2</sub> CO <sub>3</sub> , MeOH/THF	2 h	59 %	0%
7	1 eq. K <sub>2</sub> CO <sub>3</sub> , MeOH/THF	3 h	49 %	0%
8	3 eq. K <sub>2</sub> CO <sub>3</sub> , MeOH/THF	2 h	56 %	0%
9	3 eq. TBAF dry THF	30 min	73 %	0%

First the reaction time was evaluated and the maximum yield was obtained after two hours (59%, Entry 6), this yield was still only moderate. Then, the amount of potassium carbonate was varied. With one equivalent the reaction needed more time to reach completion (3 h) and gave similar yield as with three or four equivalents (Entries 6–8). As no satisfying improvement was achieved, another deprotecting agent was tried. Using TBAF (Entry 9) significant improvement was observed. The reaction performed with 73% yield in only 30 minutes. Moreover, less degradation occurred, facilitating the purification. Furthermore, the reaction could be performed on larger scale (12 mmol) with even better yield (83%) and in shorter time (5 min). This further proves that the reaction requires careful monitoring in order to be stopped before degradation occurred. The differently substituted building blocks **99a–d** were successfully deprotected using the TBAF procedure in good yields (Scheme 44).



**Scheme 44:** Deprotection of the building block **99**

With the monomer fragments **100a–d** available, macrocycles **101a–d** were prepared by dimerization via Sonogashira coupling. Treatment of **100a–d** with Pd(PPh<sub>3</sub>)<sub>4</sub> and copper iodide in THF (37 mM) in the presence of diisopropylamine generated the desired macrocycles **101a–d** in yields between 4–11% (Scheme 45). Suspension in ethylacetate/hexane mixture and filtration gave the pure product after an initial purification by column chromatography on silica gel. Halving the mixture concentration did not change the resultant yield. However, doubling the concentration dropped the yield to 2%.



**Scheme 45:** Macrocyclization reaction

The trimeric macrocycle was also observed in smaller amount. However, the purification of this macrocycle was more complicated than for the dimer. Therefore, further work only focused on the macrocyclic dimer.

The useful characteristic of the macrocycle to easily precipitate from its solution allowed getting suitable single crystal for X-ray analysis from a solution of **101c** in chloroform. The structure is shown on Figure 50. The macrocycle showed a unique rectangular shape and no deformations due to the strain were observed.

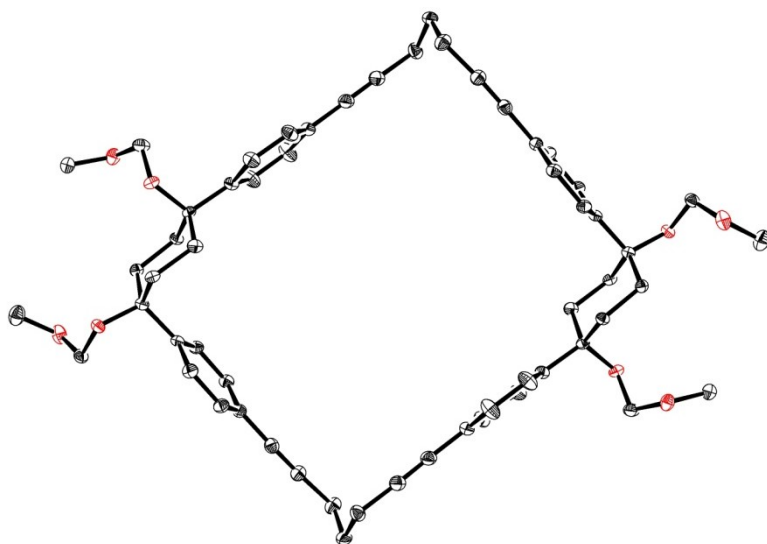


**Figure 50:** X-Ray structure of macrocycle **101c** (Ortep drawing, hydrogens and solvent omitted)

### 2.3.1.3 Shotgun approach to the synthesis of macrocyclic precursor

As the macrocycle **101** was formally identified and successfully isolated via stepwise approach, we could explore a more direct approach. Combining the unprotected building blocks without any pre-combination should also result in the desired macrocycle (Scheme 46).

This shotgun approach was tested with hepta-1,6-diyne **39c** and building block **83** with the same macrocyclization conditions used in the stepwise strategy described in the previous section (37 mM). The macrocyclic dimer could be isolated in 3% yield. However, the purification was more complicated than for the stepwise strategy due to the presence of several linear oligomers. The test reaction provided promising results; consequently, we performed a screening of the reaction conditions to find optimum conditions for the macrocyclization (Table 11).

**Table 11:** Screening for shotgun macrocyclization conditions with iodide building block

n°	Scale	Hepta-1,6-diyne	Conc.	Yield
1	822 $\mu$ mol	1.0 eq.	37 mM	2.6 %
2	6.17 mmol	1.0 eq.	37 mM	2 %
3	822 $\mu$ mol	1.0 eq.	16 mM	8 %
4	822 $\mu$ mol	1.0 eq. (+0.25 eq.)	6 mM	1.9 % <sup>a</sup>
5	822 $\mu$ mol	1.0 eq. (+0.25 eq.)	11 mM	1.6 % <sup>a</sup>
6	822 $\mu$ mol	2.0 eq.	16 mM	8.5 %
7	822 $\mu$ mol	10 eq.	16 mM	6 %
9	8.22 mmol *	1.1 eq.	16 mM	9.5%

<sup>a</sup> 0.25 eq. of heptadiyne were added after 20 h, \* non dry THF was used

On larger scale (6 mmol), the reaction performed with comparable yields (Table 11, Entry 2). Different concentrations were tried. Surprisingly, the best result was obtained when diluting the reaction mixture by a factor of two (16 mM) with 8% yield (Table 11, Entry 3). Further dilution did not improve the yield; on the contrary, more linear oligomers were obtained complicating the purification. In order to convert linear oligomers into macrocycle 0.25 eq. hepta-1,6-diyne more were added after 20 hours without much success (Table 11, Entries 4 and 5). The use of different excesses of hepta-1,6-diyne was probed: while the addition of small excess (1.1–2.0 eq.) of hepta-

1,6-diyne was beneficial (Table 11, Entries 6 and 9), the addition of large excess (10 eq.) led to complex mixture and reduced yield (Table 11, Entry 7).

As we aimed to perform larger batches of reaction in order to have a stock of macrocycle to explore the last two steps of the synthesis of our CPP, we also tested practical and economical conditions. Trying to reduce the catalyst loading led to a more complex mixture. For practical reasons, we also tried the reaction with non dry solvent. The results were similar as with dry THF. We therefore performed the reaction on larger scale (Table 11, Entry 9) with 8.22 mmol (5.00 g of **83**) which afforded the desired macrocycle **101** in 9.5% yield.

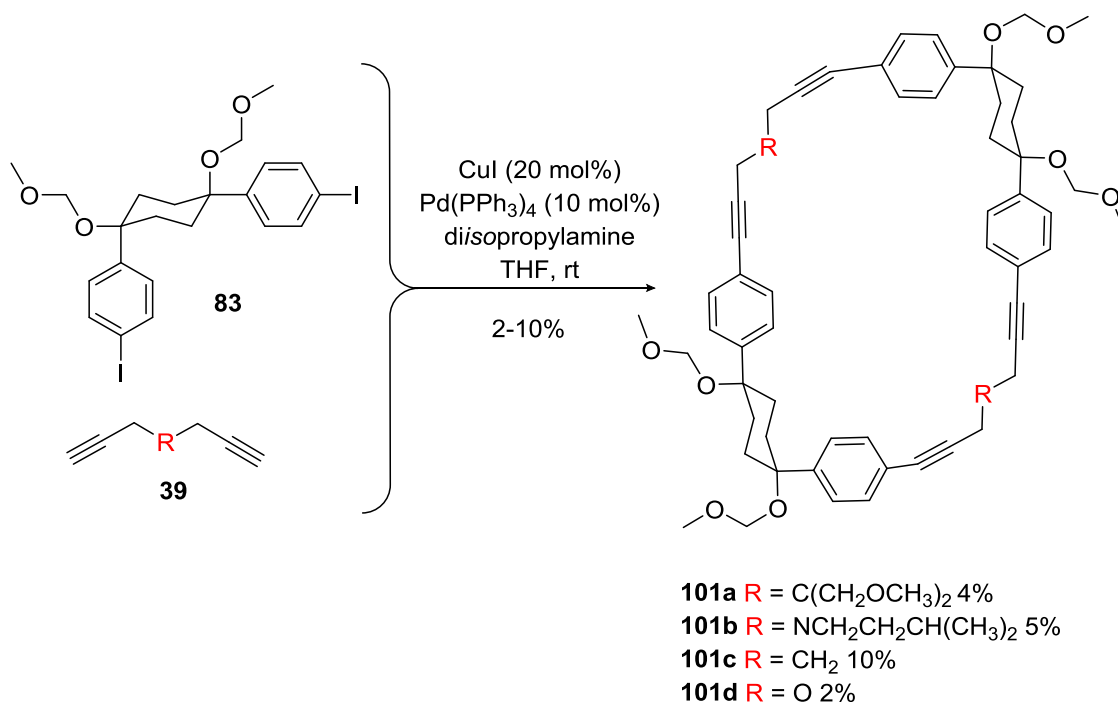
As the use of bromide starting material would be more economic than the corresponding iodide, we also explored the possibility to replace the iodo-compound with the bromide (Table 12). The bromo-building block was synthesized according to the non *cis*-selective addition procedure in 43% yield.

**Table 12:** Screening for shotgun macrocyclization conditions with bromide

n°	Solvent	Conc.	Temperature	Yield
1	THF	16 mM	rt	0 %
2	THF	16 mM	66°C	0 %
3	Dioxane	16 mM	90°C	Linear dimer (20%)
4	Dioxane Pd(PPh <sub>3</sub> ) <sub>2</sub> Cl <sub>2</sub>	16 mM	90°C	Linear dimer
5	Dioxane (not dried)	16 mM	90°C	Linear dimer (18%)

However, this bromide building block turned out to be far less reactive than the corresponding iodide. In THF at room temperature or reflux, no conversion was observed (Table 12, Entry 1–2). Switching to dioxane as solvent and heating the reaction mixture to 90°C, the open dimer was isolated (Table 12, Entry 3). We also tried a different catalyst (Table 12, Entry 4), without success.

From these screening experiments, an optimized protocol for the macrocycle was achieved using the iodide **83** and 1.1 eq. of hepta-1,6-diyne in THF (16 mM). The reaction could be conducted on larger scale with non-dry solvent without altering the yield (around 10%).



**Scheme 46:** Shotgun macrocyclization

Test reactions were performed with the optimized conditions on the other diynes. However, the mixture were more complex than for the hepta-1,6-diyne analog. Therefore, the reactions were performed on larger scale to facilitate the isolation of the products and using the same concentration as for the stepwise strategy macrocyclization (37 mM). This time, the desired macrocycles could be isolated in 2–5% yield (Scheme 46).

Although the purification with this shotgun macrocyclization strategy was more difficult and the yield was lower than for the macrocyclization step of the stepwise approach, this strategy offers a quick entry into the synthesis of the macrocyclic precursor. Indeed, instead of the four steps procedure (protection of the diyne, combination of the building blocks, deprotection and macrocyclization) with purification between each step, we only have one single step. Considering the overall yield, the stepwise approach afforded the macrocycle **101c** with only 3% yield over four steps, whereas the new shotgun approach gives macrocycle in 10% in only one step. Therefore, the yield is improved by a factor of three. This method is not only more interesting from a time saving point of view, but also from an economical and ecological point of view, as less solvent and less reagents are used.

### 2.3.2 [2+2+2] Cycloaddition reaction

With the macrocyclic precursor available, the first [2+2+2] cycloaddition test reaction with macrocycle **101c** and diphenylacetylene was performed with the optimized conditions (microwave, 100°C, 6 h). Conversion to the desired [2+2+2] cycloaddition product was observed on the crude <sup>1</sup>H-NMR spectrum. However, the purification by column chromatography was not successful. Another attempt was made, using smaller excess of alkyne (10 eq.) in order to facilitate the purification. This time, the product was isolated in pure form by simple filtration of the reaction mixture in 67% yield. The [2+2+2] cycloaddition protocol could be applied for differently substituted macrocycles and monoynes in moderate to good yields (46–80%). The results are presented in Table 13. In cases where the alkynes were solids, the product had to be further purified by chromatography. The reaction proceeds for a wide range of precursors, offering a reliable method for the functionalization of this type of molecules.

**Table 13:** Scope of the [2+2+2] reaction

Entry	Product	R	R'	Yield
1	<b>102a</b>	CH <sub>2</sub>	Et	52%
2	<b>102b</b>	CH <sub>2</sub>	Me	80%
3	<b>102c</b>	CH <sub>2</sub>	Ph	67%
4	<b>102d</b>	CH <sub>2</sub>	CH <sub>2</sub> OH	61%
5	<b>102e</b>	CH <sub>2</sub>	<i>p</i> -Ph( <i>n</i> -Bu)	54%
6	<b>102f</b>	CH <sub>2</sub>	<i>p</i> -PhOCH <sub>2</sub> CH <sub>2</sub> OCH <sub>3</sub>	47%
7	<b>102g</b>	CH <sub>2</sub>	<i>m</i> -biph	74%
8	<b>102h</b>	O	Et	46%
9	<b>102i</b>	C(CH <sub>2</sub> OCH <sub>3</sub> ) <sub>2</sub>	Et	68%
10	<b>102j</b>	N(CH <sub>2</sub> CH <sub>3</sub> CH(CH <sub>3</sub> ) <sub>2</sub> )	Et	37%

A suitable crystal for X-ray analysis was obtained for one example (**102b**). The structure is depicted in Figure 51.

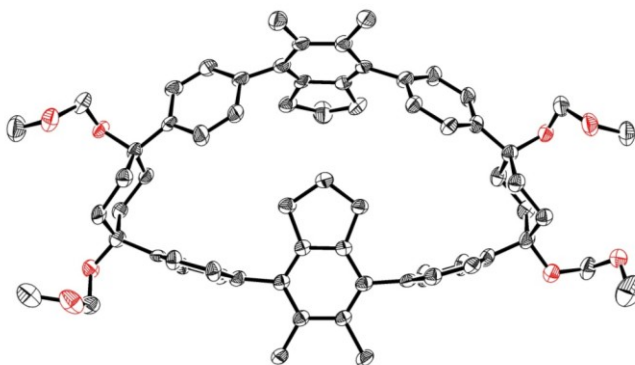


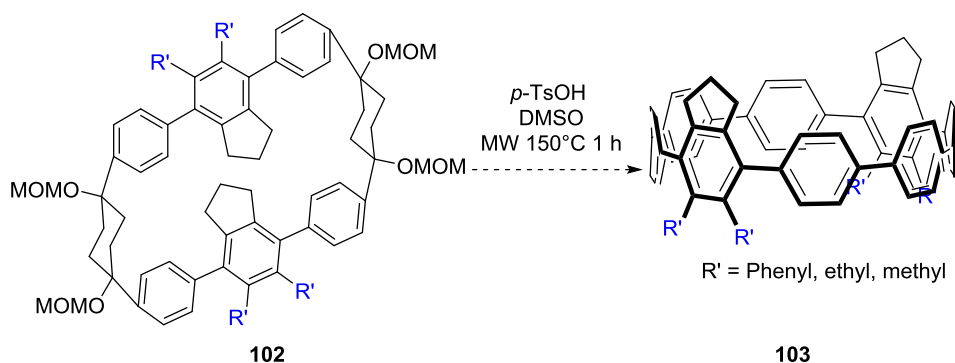
**Figure 51:** X-ray structure of the [2+2+2] cycloaddition product (**102b**) (Ortep drawing, hydrogens and solvent omitted)

Already in this molecule some hint of the strain can be observed. Indeed, the phenyl rings are already slightly distorted with  $\alpha=3.7^\circ$  and one of the phenyl ring shows a deviation from planarity similar to the CPP ( $\alpha=8^\circ$ ). The torsion angles between most of the phenyl rings are around  $80.3^\circ$ . This proves the large steric demand of the substituent on each side of the ring, forcing the twisting of the phenyl rings to an extreme. Usually, in linear *p*-terphenylene the torsion angle in gas phase is around  $40^\circ$ .<sup>52</sup> On another side, it also shows that the molecule is flexible enough to allow the phenyl to adopt a nearly perpendicular arrangement. This is only possible thanks to the remaining flexibility of the molecule provided by the cyclohexane moieties. Indeed, in CPP the strain is such that the torsion angles are limited to  $57^\circ$ .

### 2.3.3 Aromatisation Reaction

#### 2.3.3.1 Microwave mediated aromatization

With different precursors in hands, we then explored the aromatization reaction. First the microwave conditions reported by Itami et al. were tried on different precursors (Scheme 47).<sup>32</sup>



**Scheme 47:** Microwave mediated aromatization reaction

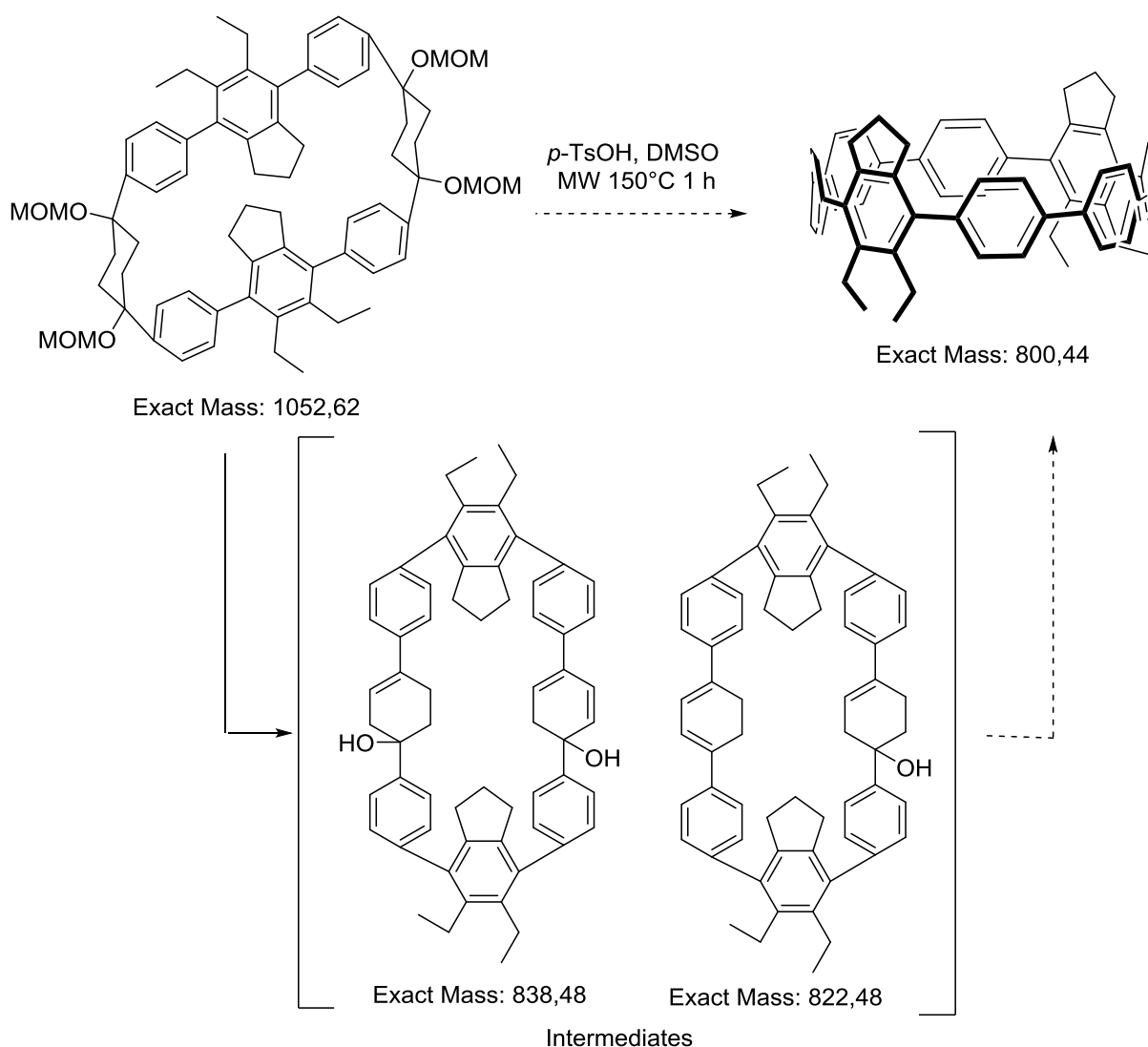
We always obtained an insoluble solid as major product of the reaction. This material was UV-active and gave a fluorescent suspension in chlorinated solvent when irradiated at 306 nm or 365



nm. Because of its insolubility in all common solvents tested, the analysis was complicated. Only MALDI-MS spectrometry could be performed. Encouragingly, the masses corresponding to  $[M+Na]^+$  and  $[M+K]^+$  were found on the MALDI spectra for each molecule tested. However, in the absence of more analytical data, two hypotheses can be envisaged:

- 1) The insoluble material is the CPP product.
- 2) The insoluble material is not the desired CPP and the masses are either traces of the desired product on insoluble solid or the solid is some intermediate with the corresponding masses.

The reaction proceeds through a fourfold deprotection elimination oxidation sequence. Taking a closer look to the structure and masses of the possible intermediates, we realized that  $M+23$  and  $M+39$  can also correspond to the masses of some intermediates (Scheme 48)



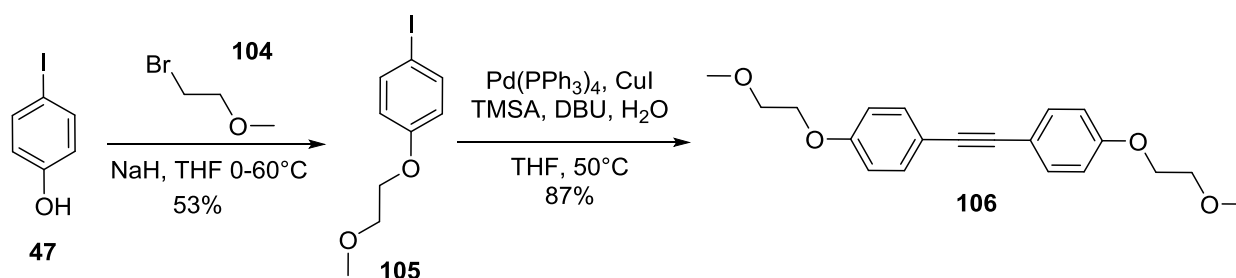
**Scheme 48:** Possible intermediates of the aromatization reaction

In order to identify the product, we tried to recrystallize the insoluble material. All attempts were unfruitful as the crystals that could be obtained were too small for X-ray crystallography.

Resubmitting the insoluble material to the reaction conditions under prolonged reaction time did not lead to different products. This would rather speak for the first hypothesis.

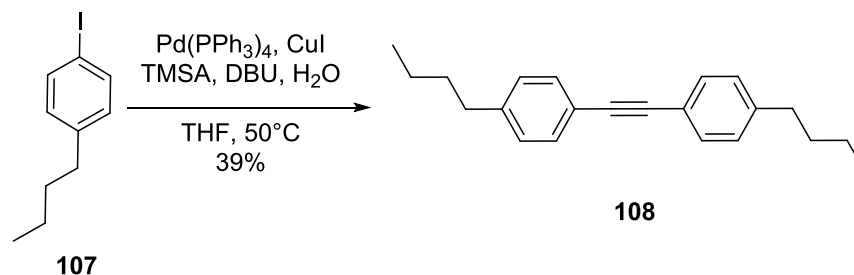
Therefore, to further test this hypothesis (1), alkynes with solubilizing group were designed and synthesized: one bearing ethylene glycol chains and another with *n*-butyl chains. The aim was to be able to isolate a soluble CPP which could then be fully characterized.

The ethylene glycol substituted alkyne **106** was synthesized in two steps (Scheme 49), starting with a substitution reaction of 4-iodophenol and 1-bromo-2-methoxyethane to give 1-iodo-4-(2-methoxyethoxy)benzene **105** in 53%. Then, the corresponding alkyne **106** was obtained via a one pot Sonogashira dicoupling with TMS-acetylene (TMSA). This very convenient method of aryl-substituted acetylene permitted the synthesis of the desired alkyne in 87% yield.



**Scheme 49:** Synthesis of ethyleneglycol substituted alkyne **106**

The one pot Sonogashira dicoupling was also used for the synthesis of the *n*-butyl substituted alkyne **108** in 39% yield (Scheme 50).



**Scheme 50:** Synthesis of *n*-butyl substituted alkyne **108**

The [2+2+2] cycloaddition reaction was performed with these solubilizing alkynes in 47% and 54% with **106** and **108** respectively (Table 13).

The subsequent aromatization reaction under microwave afforded the same kind of insoluble solid. All efforts to dissolve the products were unsuccessful. This result speaks against the first hypothesis (1). Moreover, all CPPs synthesized up to now by other groups were all extremely soluble in organic solvent due to the ring curvature. Therefore, there are good chances that these insoluble products are not the desired CPPs but rather some insoluble intermediates, side products or decomposition products.

### 2.3.3.2 Aromatization via non microwave methods

Itami et al. mentioned some difficulties when applying their microwave reaction for the synthesis of other CPP than [12]CPP. Notably, they mentioned the insolubility of intermediates of the reaction and the need of polar co-solvent such as DMSO.<sup>32,34</sup> They therefore developed another aromatization reaction, using sodium bisulfate in DMSO/xylene at 130°C under air. The same conditions were tried on our precursor **102c**. Insoluble solid was present on the cold part of the reflux condenser. This material was different than the insoluble material observed from the microwave experiment. Indeed, the solid in this case is not UV active and never formed a fine suspension. It probably comes from a side reaction of the solvent (considering the large quantity of material). Beside this solid, a rather complex mixture was obtained, on the TLC control, the main product was sticking to the baseline and some other strongly fluorescent spots were also observed.

Isolation of the eluting products afforded two different identifiable fluorescent products. One (isolated in 25%) had a mass of 816 m/z which could correspond to one of the oxidized product shown in Figure 52. We will use the name CPPOH for this kind of molecule.

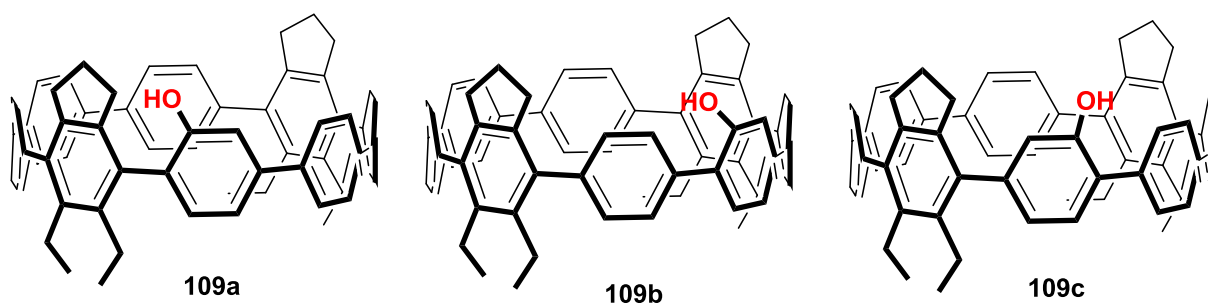


Figure 52: Possible CPPOH structures

Interestingly, another fluorescent product isolated from the mixture corresponded to the oxidized solvent (*m*-xylene) shown in Figure 53. Which supports the hypothesis that an over oxidized CPP product could be obtained.

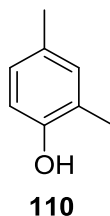
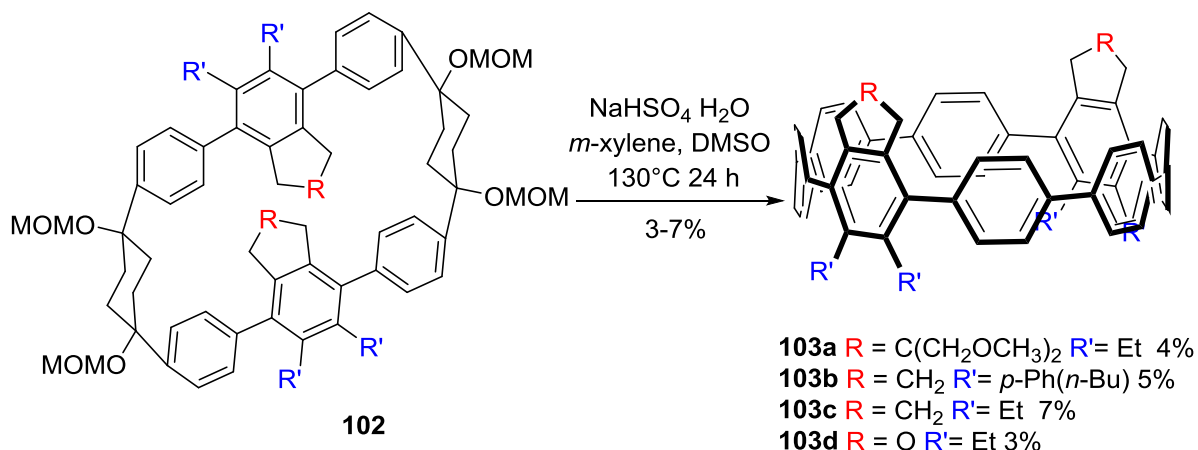


Figure 53: Oxidized solvent

The second fluorescent product was isolated in 7%. All the analytical data were in accordance with the structure of the CPP product. This product was extremely soluble in most organic solvent in contrast to the insoluble material isolated with microwave conditions.

Using these conditions, the reaction was performed with different precursors, notably **102a**, **102e**, **102h**, **102i**. The corresponding desired CPP could be isolated in 3–7% yields (Scheme 51).



**Scheme 51:** Aromatization reaction with sodium bisulfate

As the yields for this reaction were rather poor, a screening of different conditions was undertaken.

### 2.3.3.3 Screening aromatization conditions

The reactions were performed on 10-20 mg of starting material **102c**. The mixtures were controlled by TLC (DCM/Hexane: 1/1) for CPP and CPPOH, and (EtOAc/hexane: 1/1) for starting material. When spots were observed with DCM/hexane system, crude H-NMR and MALDI-TOF-MS were measured.

#### - Acid or base mediated aromatization

Some test reactions were made varying the reaction conditions described by Itami et al.. Varying the time (after 24 h), the scale, the amount of solvent, or the excess of NaHSO<sub>4</sub> did not affect the outcome of the reaction. Indeed, the non eluting product was always the major product.

Some microwave reaction reaction mixtures were checked again for traces of CPP. The filtrate of the microwave reaction (*p*-TsOH) also contained traces of CPP, however, the mixture was a lot more complicated (smearing products) than in the case of the non microwave condition (NaHSO<sub>4</sub>). Reaction using *p*-TsOH as acid in the presence of DDQ as oxidant led to no improvement compared to the conditions developed by Itami et al.

MOM protecting group is commonly removed by reaction with strong acid. Some variations were attempted, using H<sub>2</sub>SO<sub>4</sub>, but the reaction gave only non eluting product.

The MOM protecting group should be stable toward bases, however, a DBU mediated deprotection of alcohol was reported in a total synthesis.<sup>53</sup> If the deprotection were successful, the

elimination could be facilitated under basic conditions. However, basic conditions were not efficient for the deprotection, and only starting material was observed by TLC and  $^1\text{H-NMR}$ .

Reaction in nitrobenzene were also performed, indeed, it has been reported that nitrobenzene/acid mixture could oxidize cyclohexadiene to benzene.<sup>54</sup> Moreover, nitrobenzene at high temperature dissolves the insoluble solid formed under the microwave reaction conditions. Unfortunately, the use of nitrobenzene did not improve the reaction outcome, only non eluting product was observed.

#### - Selenium mediated aromatization

In the earliest work by Vögtle et al.,<sup>31</sup> selenium was used for the aromatization of linear *cis*-bisphenylcyclohexanediol. A similar approach was attempted here. Reactions with selenium were not complete; starting material was still present after extended reaction time. This is probably due to the lack of interaction between the starting material and the selenium (solid state reaction). However, traces of CPP could be observed. With  $\text{SeO}_2$  after prolonged reaction time traces of CPP-OH were observed (TLC).

#### - Lewis acid mediated aromatization

The deprotection of ether protected alcohol with Lewis acid is a well known method.<sup>55</sup> The idea was to see if a Lewis acid could also activate the alcohol to promote the elimination. Oxidation could be performed simply by oxygen as suggested in the method used by Itami et al. The first experiment with  $\text{AlCl}_3$  in acetonitrile gave promising results as a spot higher than CPP (non fluorescent) was observed. This spot could be the eliminated product (before oxidation to the aromatic ring). This hypothesis tends to be confirmed by MALDI-MS. The mass of the eliminated product was found. The H-NMR spectra presented a complicated range of aromatic signals which could be explained by a mixture of the possible isomers. The change of solvent gave no improved result. The presence of acetonitrile seems to be crucial for the reaction to proceed.

#### - Aromatization experiences with other conditions

Some other conditions were tried. Notably attempts to activate the alcohol to make it a better leaving group for the elimination, using thionylchlorid. Unfortunately, this did not change the outcome of the reaction; only non eluting product were obtained no trace of CPP was observed.

Finally, reductive conditions used for the aromatization reaction of anthracene precursor, were tried as well.<sup>56</sup> The use of reductive conditions did not led to the desired CPP, principally non eluting products were obtained. However, this result was not really surprising as oxidative conditions would be needed to complete the last oxidation step, but no useful intermediates that could be oxidizable were observed.

As a conclusion the best results were still the conditions using  $\text{NaHSO}_4$ . The low yield of the reaction can be attributed to the higher strain energy to overcome. Indeed Itami et al. synthesized CPP down to [9]CPP but never a [8]CPP was obtained by this method. Already the aromatization to the [9]CPP suffered from lower yield (24%), compared to 65% for [12]CPP.

### 2.3.4 Properties of substituted CPPs


#### 2.3.4.1 Structural properties

A suitable single crystal of **103d** was obtained by slow evaporation of a solution in dichloromethane, and measured by X-ray spectroscopy (Figure 54, left). The packing arrangement (Figure 54, right) is different to unsubstituted CPPs, where channels are sometimes observed. Here, pairs of rings arrange parallel to each other, and these pairs assemble forming a basket weave motif.

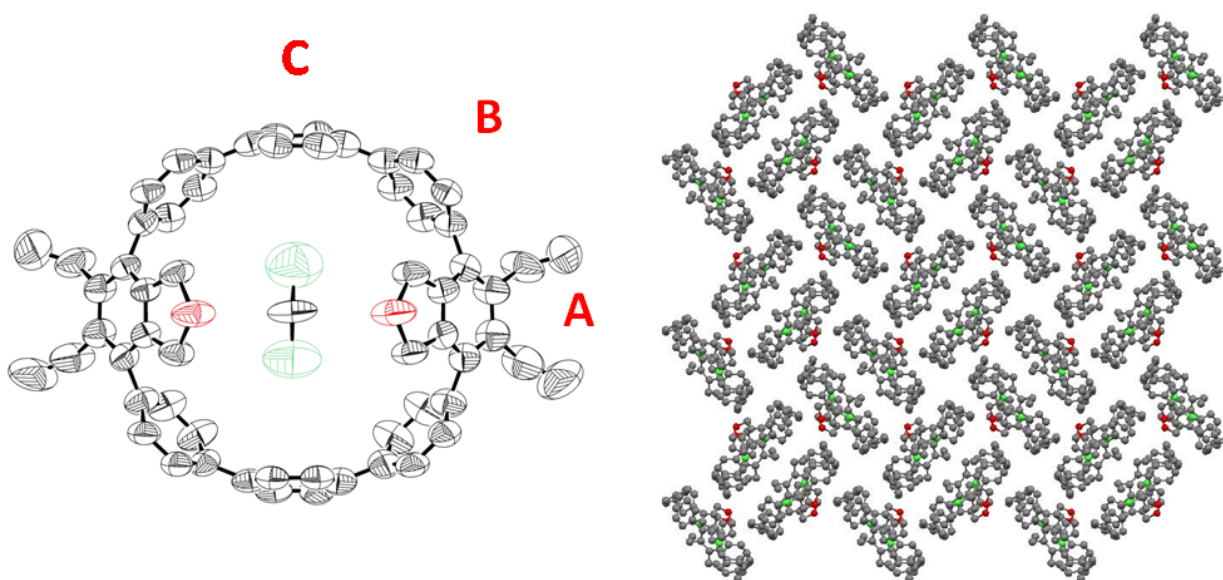


**Figure 54:** Solid state structure of CPP **103d**

A X-ray structure of [8]CPP have been published by Jasti et al.<sup>30</sup> Moreover, the distortion parameters have been measured on a calculated structure by Itami et al.,<sup>45</sup> allowing us to compare the structural parameters of our substituted CPP with the corresponding unsubstituted molecule. The data are summarized in Table 14.

**Table 14:** Comparison of structural properties of substituted CPP and unsubstituted CPP


		<b>103d</b>			<b>[8]CPP</b>	
<b><math>\alpha</math></b>		8.5°			9.3° <sup>45</sup>	
<b><math>\beta</math></b>		14.4°			13.7° <sup>45</sup>	
<b><math>\theta</math></b>		33.0°–57.5°			30.7° <sup>45</sup>	
<b>Diameter</b>		10.95 Å			10.89 Å <sup>30</sup>	
<b>Bond length</b>	$C_{ipso}-C_{ortho}$	$C_{ortho}-C_{ortho}$	$C_{ipso}-C_{ipso}$	$C_{ipso}-C_{ortho}$	$C_{ortho}-C_{ortho}$	$C_{ipso}-C_{ipso}$
	1.400 Å	1.379 Å	1.489 Å	1.401 Å <sup>30</sup>	1.383 Å <sup>30</sup>	1.486 Å <sup>30</sup>

The ring has a round shape with a diameter of 10.95 Å (average calculated between the *ipso*-bonds and the centers of the phenyl rings). This value is comparable to the diameter calculated for [8]CPP.<sup>39</sup> The bond lengths are 1.400 Å, 1.379 Å and 1.489 Å for the  $C_{ipso}-C_{ortho}$ ,  $C_{ortho}-C_{ortho}$  and  $C_{ipso}-C_{ipso}$  bonds respectively. The  $C_{ipso}-C_{ortho}$  and  $C_{ortho}-C_{ortho}$  have a double bond character whereas, the  $C_{ipso}-C_{ipso}$  have more a single bond character, suggesting benzenoid character, as for unsubstituted CPPs.

In all CPPs the phenyl ring are distorted. The angles between the normal benzene plane and the distorted out-of-plane atoms ( $\alpha$ ), respectively the  $C_{ipso}-C_{ipso}$  bond ( $\beta$ ), display the degree of distortion. These angles were defined on Figure 47 in the introduction). In the substituted CPP **103d**  $\alpha$  equals 8.5°, and  $\beta$  equals 14.4° which are comparable to the value for [8]CPP ( $\alpha=9.3^\circ$ ,  $\beta=13.7^\circ$ ).<sup>45</sup> The torsion angle between the middle unsubstituted ring **C** (Figure 54) and the other unsubstituted rings **B** is 32.8°, which is close to the value measured for [8]CPP.<sup>45</sup> The angle between the substituted ring **A** and its adjacent rings **B** is 53.8°. This value is larger than for unsubstituted CPP, but smaller than the value measured by Müllen et al. in their tetraphenyl-substituted [9]CPP (78.7°).<sup>41</sup> This can be explained by the difference in steric hindrance and ring size. Based on all these results, even less  $\pi$ -conjugation can be expected in the substituted CPP than the unsubstituted CPPs.

As a conclusion, the structure of the substituted CPP is relatively similar to the unsubstituted analog. The deformation of the ring and the individual phenyl units are the same for both

molecules. The only significant difference is the torsion angle between the substituted phenyl ring and the adjacent rings which is larger than for unsubstituted phenyl ring in the CPP.

### 2.3.4.2 Strain energy

In previous theoretical studies strain energies have been calculated based on homodesmotic reaction of [n]CPP and n biphenyls giving n *p*-terphenyls.<sup>57</sup> In our collaboration with the group of Prof. Ewels in Nantes,<sup>58</sup> they adopted a different approach to calculate the strain energy of **103a–d**, which seems more appropriate, due to the fact that only the strain energy of the two relevant structures, the cyclic and the infinite linear poly-*para*-phenylene, are calculated. This is achieved by breaking a bond in the CPP and straightening the fragment (Figure 55).

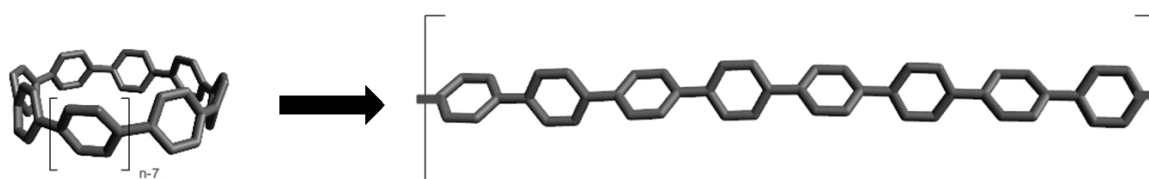


**Figure 55:** Reaction used for the calculation of the strain energies of the investigated structure

This structure was placed in a repeating supercell such that the broken bonds connect to each other across opposite sides of the cell. This approach avoids any additional energetic terms due to changes in conjugation that may be present in the hypothetical homodesmotic reaction approach and is better adapted to substituted rings. With this method, via DFT optimization, the strain energies obtained were 73.6, 51.1, 63.7 and 62.4 kcal·mol<sup>-1</sup> for **103a**, **103b**, **103c** and **103d** respectively (Table 15). The results show an effect of the side-group functionalization on the ring strain. However, differences are small as the benzenoid rings are not conjugated and hence ring strain is primarily a function of ring curvature.

**Table 15:** Diameters, dihedral angles and strain energies of the related structures

	<b>[8]CPP</b>	<b>103a</b>	<b>103b</b>	<b>103c</b>	<b>103d</b>
<b>Strain Energy (kCal/mol)</b>	62.9	73.6	51.1	63.7	62.4
<b>Diameter</b>	11.16 Å	11.21 Å	11.30 Å	11.16 Å	11.15 Å
<b>Torsion angle <math>\theta</math></b>	29.5°	37.4°/51.8°	43.4°/45.8°	39.1°/49.9°	35.1°/45.1°



The torsion angle between the substituted ring and its adjacent ring was also estimated on the calculated structures shown in Table 15. In general, the torsion angles between the substituted ring and the adjacent rings are larger than the torsion angles measured in the unsubstituted [8]CPP by  $18^\circ$  in average. The angles between the middle unsubstituted ring (B/C) are also slightly larger but only by  $9^\circ$  in average. These values are closer to the angles in the unsubstituted CPP. However, the torsion angles of the phenyl rings in the more hindered **103b** tend to the same value ( $43^\circ/46^\circ$ ).

The values of torsion angles for the calculated structure are somewhat different from the value measured on the X-Ray structure. This can be rationalized by the intrinsic difference between X-ray structure and calculated structures. Indeed, the X-ray structure represents the molecule in its solid crystal form, interacting with solvent molecules in the crystal and with other molecules (stacking interaction, H-bonding etc.), whereas the calculated structures represents the most stable conformer of the molecule in vacuum, without any exterior interactions. However, the same trend is observed in both cases. In general, the substituted ring of the CPP is more twisted than the other unsubstituted phenyl in the ring.

### 2.3.4.3 Optical properties

The optical properties (UV-Vis absorption and fluorescence) of the different substituted CPPs **103a–d** were measured (Figure 56).

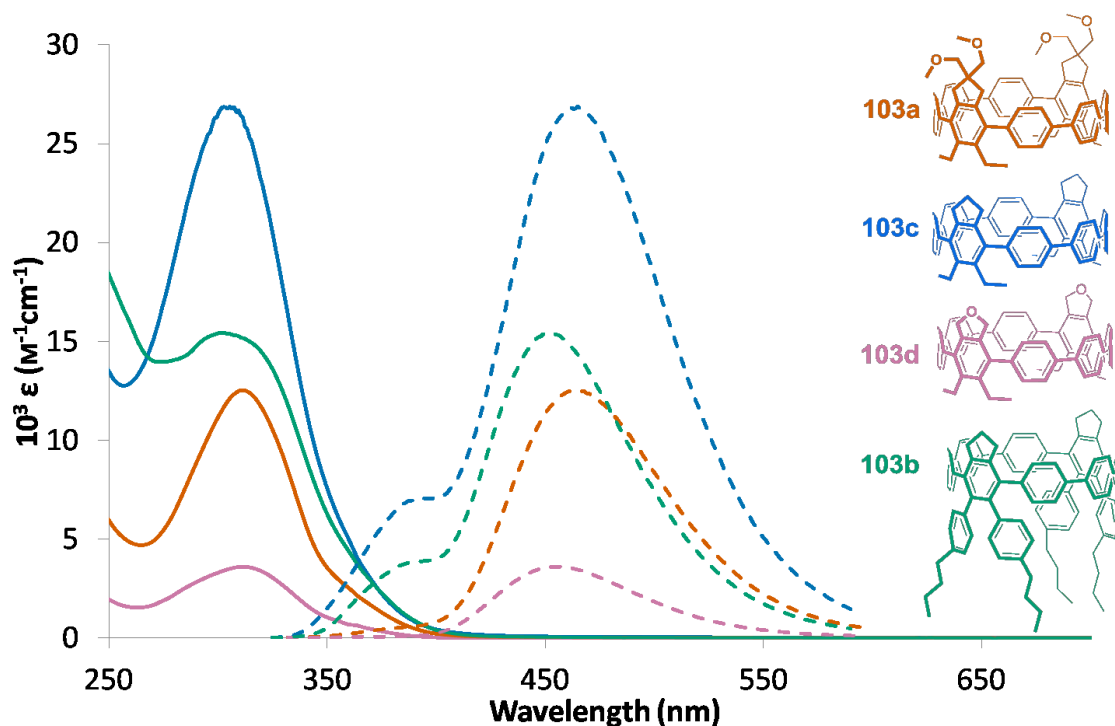


**Figure 56:** UV absorption spectra (plain lines) and emission spectra (dashed lines) of substituted CPPs

The absorbance maxima ( $\lambda_{\text{abs}}$ ) of the substituted CPPs lie between 301–312 nm (Table 16). These occur at shorter wavelengths than for the corresponding unsubstituted [8]CPP (340 nm). The

extinction coefficients are also considerably smaller than for [8]CPP.<sup>39</sup> The emission maxima ( $\lambda_{em}$ ) were observed between 451–465 nm (Table 16). These values are again smaller than for the unsubstituted [8]CPP (540 nm)<sup>45</sup> which can be rationalized by the larger torsion angle compared to the unsubstituted CPP. Indeed, the torsion has a stabilization effect on the HOMO and a destabilization effect on the LUMO, resulting in a larger HOMO-LUMO gap than for the corresponding unsubstituted CPP.

Absorption can occur to several excited states of the molecule, but according to the Kasha rule, the fluorescence emission normally occurs from the lowest excited state (LUMO-HOMO). Former studies on unsubstituted CPPs predicted that this transition was forbidden. However, in small and distorted CPPs, the symmetry rules tend to be more flexible and thus the transition becomes possible with low oscillator strength, hence low efficiency (quantum yield).<sup>47,49</sup>

In our case, the excitation spectra had different shape than the absorption spectra. This can be attributed to the different conformation possible of the substituted CPPs. Therefore, it is advisable to take the interpretation of UV absorption and emission spectra with great prudence. Indeed, as it was the case for the unsubstituted CPPs, the interpretation of the spectra has to be founded on computational studies in order to understand the possible transitions that are occurring in those very unique molecules.

**Table 16:** Optical properties of substituted CPPs

	$\lambda_{abs}$	$\lambda_{em}$	Quantum Yield $\Phi_F$	Fluorescence Lifetime $\tau_s$	$k_r$ ( $\times 10^7 \text{ s}^{-1}$ )	$k_{nr}$ ( $\times 10^7 \text{ s}^{-1}$ )
<b>9a</b>	306 nm	465 nm	0.24	3.5 ns	6.9	22
<b>9b</b>	301 nm	451 nm	0.06	3.3 ns	1.8	29
<b>9c</b>	312 nm	465 nm	0.36	3.7 ns	9.7	17
<b>9d</b>	312 nm	453 nm	0.46	4.3 ns	11	13

The absolute fluorescence quantum yields were measured in chloroform using a calibrated integrating sphere. These yields are smaller than those measured for [9]CPP (0.73) using the same method,<sup>45</sup> indicating an influence of the substitution on the photoluminescence pathways.

In spite of the low fluorescence quantum yields, the fluorescence lifetimes of the substituted molecules are quite short. Additionally, the decay rate constants were determined from the quantum yield and fluorescence life time according to the equations below.

$$\Phi_F = k_r \times \tau_s$$

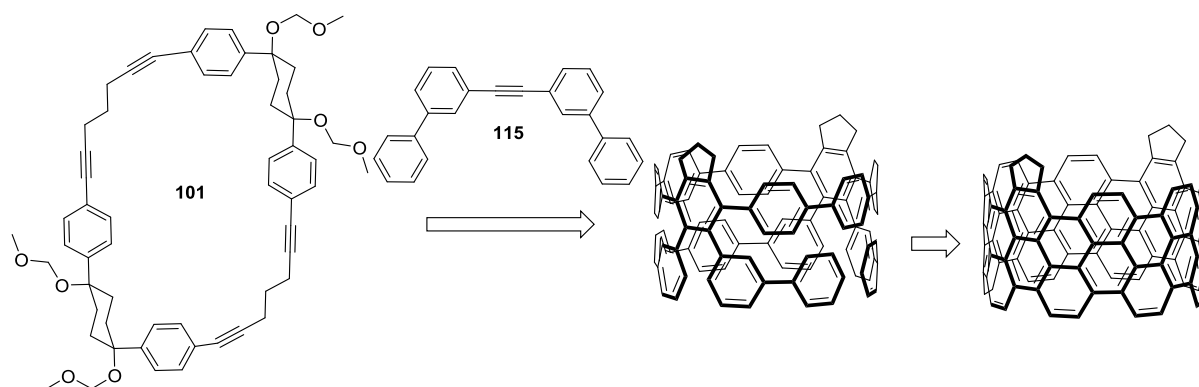
$$k_r + k_{nr} = \frac{1}{\tau_s}$$

The non radiative relaxation plays an important role as can be seen from the calculated decay rate constants  $k_r$  and  $k_{nr}$  shown in Table 16. The very low quantum yield of the phenyl substituted CPP is probably due to the larger substituents which make the molecule more likely to relax through non radiative pathways (rotation, vibration).

With these values our CPPs fit perfectly into the expected range. They match the trend amongst CPPs synthesized to date, namely the larger the diameter and the larger the torsion angles due to substitution, the lower the emission wavelength.

### 2.3.5 Toward the Nanobelt

Using our developed method for the synthesis of substituted CPP, we can envision the synthesis of a more ambitious target: the nanobelt (Scheme 52).

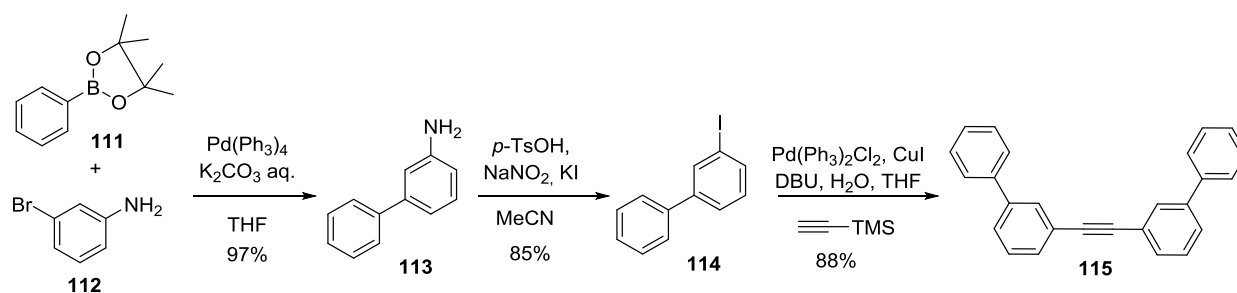


**Scheme 52:** Strategy toward the synthesis of a nanobelt

With an appropriate alkyne, applying the [2+2+2] cycloaddition, the aromatization and finally a cyclodehydrogenation (Scholl reaction) to close the bond between the phenyl rings, we could achieve the bottom up synthesis of a short fragment of CNT. This kind of molecule would provide an interesting rigid model of a CNT, and could as well serve as template for CNT growth.

#### 2.3.5.1 Bis-biphenylacetylene strategy

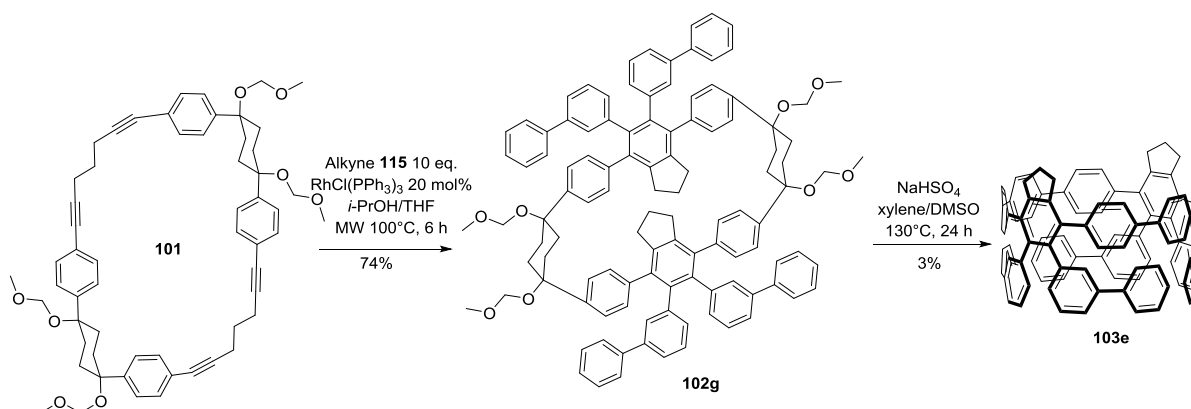
For the synthesis of the required 1,2-di([1,1'-biphenyl]-3-yl)ethyne **115**, we first envisioned a statistical Suzuki coupling with 1,3-diiodobenzene and phenylboronic acid pinacol ester **111**. However, we were surprised that each attempt led to the di-coupled product as major product (together with uncoupled starting material). Therefore, we turned to a stepwise approach with an amine as masked iodide (Scheme 53). The Suzuki reaction between **112** and phenylboronic acid pinacol ester **111** afforded the desired product **113** in 97%. Subsequently, a Sandmeyer reaction converted the amine **113** into the desired iodide compound **114** in 85% yield. Finally, the one pot Sonogashira di-coupling with TMSA delivered the desired alkyne **115** in good yield.



**Scheme 53:** Synthesis of 1,2-di([1,1'-biphenyl]-3-yl)ethyne

The [2+2+2] cycloaddition reaction of the macrocycle **101** with this alkyne afforded the precursor **102g** in 74% yield (Scheme 54). The purification of this compound was however quite challenging because simple filtration led to isolation of product together with some remaining alkyne used in excess in the reaction. This had to be separated by column chromatography which was complicated due to solubility and potential stacking issues.

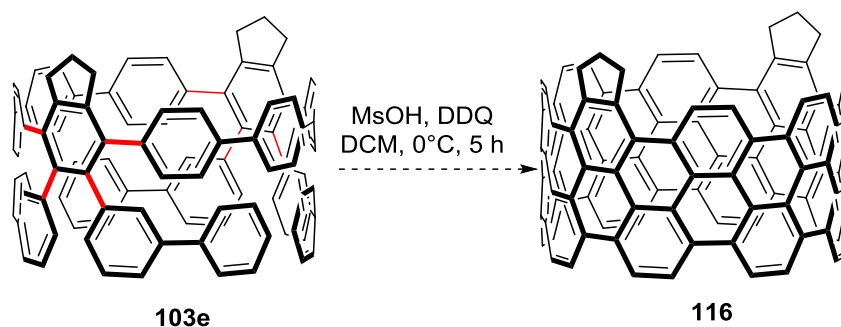
The aromatization reaction proceeded in only 3% yield, meaning only small amount (1.5 mg) of material **103e** were available for test experiment of the next step.



**Scheme 54:** Synthesis of the tetrabiphenyl substituted CPP

The Scholl reaction on substrate **103e** might be challenging, indeed, due to the free rotation around the bond between the phenyls (marked in red on Scheme 55), 14 different isomers can in principle be obtained, depending on which bonds are closed first. Moreover, the Scholl reaction is known to suffer from formation of side products such as polymerization, incomplete reaction and chlorination (when  $\text{FeCl}_3$  is used). However, the different isomers of the complete reaction should present different masses; therefore, analysis by MALDI-MS spectrometry should be possible.

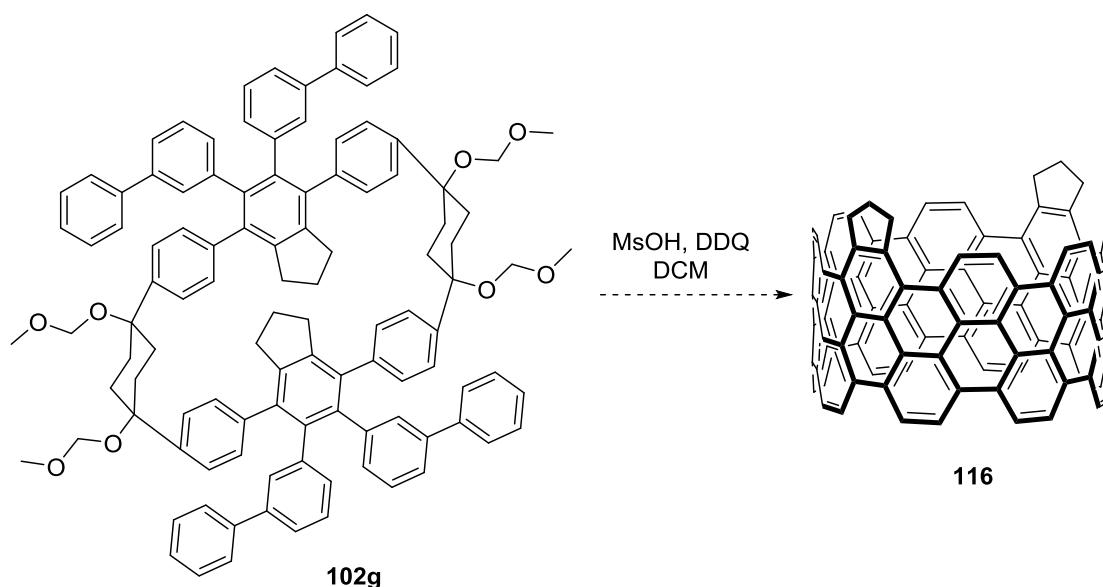
We decided to use the method described in the literature<sup>59</sup> with DDQ and MsOH on the precursor **103e**, to avoid eventual chlorination problems (Scheme 55).



**Scheme 55:** Cyclodehydrogenation reaction

After five hours at 0°C, a mixture of several products was observed by TLC. MALDI-MS spectrometry did not show the complete formation of any of the isomers. Therefore, the reaction mixture was further stirred two more days at room temperature. As a result, a smearing green yellow fluorescent mixture of products was observed on TLC control when irradiated at 306 nm. No reliable data could be obtained by MALDI spectrometry. Considering the small scale of the reaction and the complexity of the observed mixture, no isolation could be performed. The MALDI spectrum and the crude H-NMR spectra did not give any clear evidence that the desired product was formed, although it can also not be excluded.

As the conditions for the aromatization proposed by Itami et al. are composed of an acid (NaHSO<sub>4</sub> or *p*-TsOH) and in some cases chloranil was used as oxidant, it should be possible to use the Scholl conditions (MsOH and DDQ) to promote the aromatization as well. We thus could perform a one pot aromatization-Scholl reaction in one step. With this method we could also circumvent the low yield of the aromatization reaction and the reaction could be performed on more convenient scale for analysis. We tested this strategy on the [2+2+2] cycloaddition product **102g** (Scheme 56).



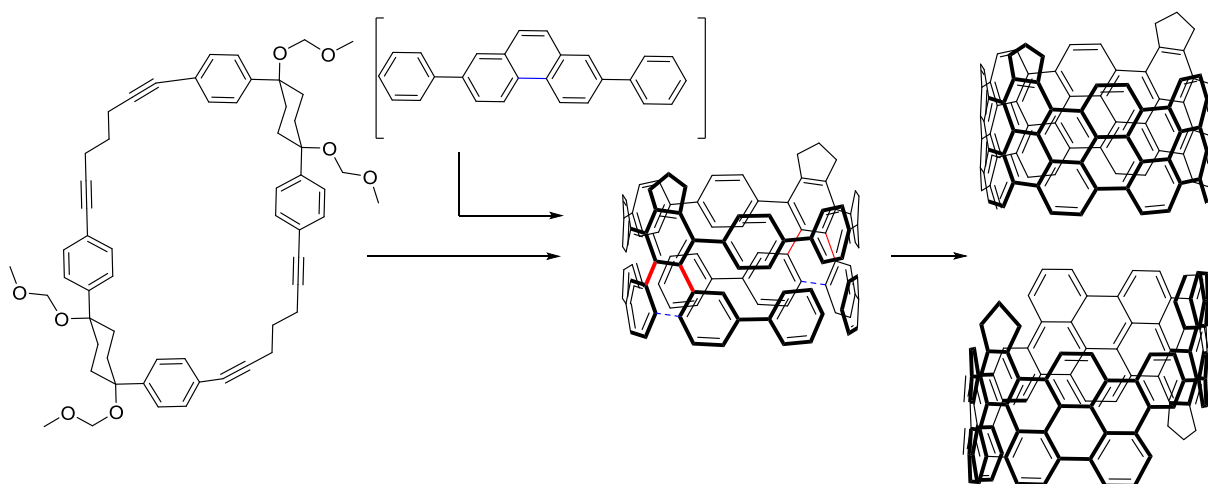
**Scheme 56:** One-pot aromatization-cyclodehydrogenation reaction

After two days at room temperature, neither starting material, nor CPP were detected. A similar result as for the prolonged Scholl reaction was obtained (smearing mixture of fluorescent products on TLC, but no clear product could be identified). Therefore, no isolation could be performed. MALDI-MS analysis did not give any conclusive results.

In spite of the absence of convincing evidence for the formation of the desired molecule, the results can still be regarded as promising. Indeed, no traces of CPP or starting material were observed and new UV active products were formed, which certainly give a hint that conjugated products are formed. As a conclusion, the outcome of the Scholl reaction with biphenyl substituted molecules is difficult to analyze as many products could be obtained by this reaction. Not only different isomer (no less than 14) could in theory be obtained but also incomplete product dimers or larger polymers may be formed. For this reason, it would be helpful to reduce the number of possible isomers by choosing a suitable building block.

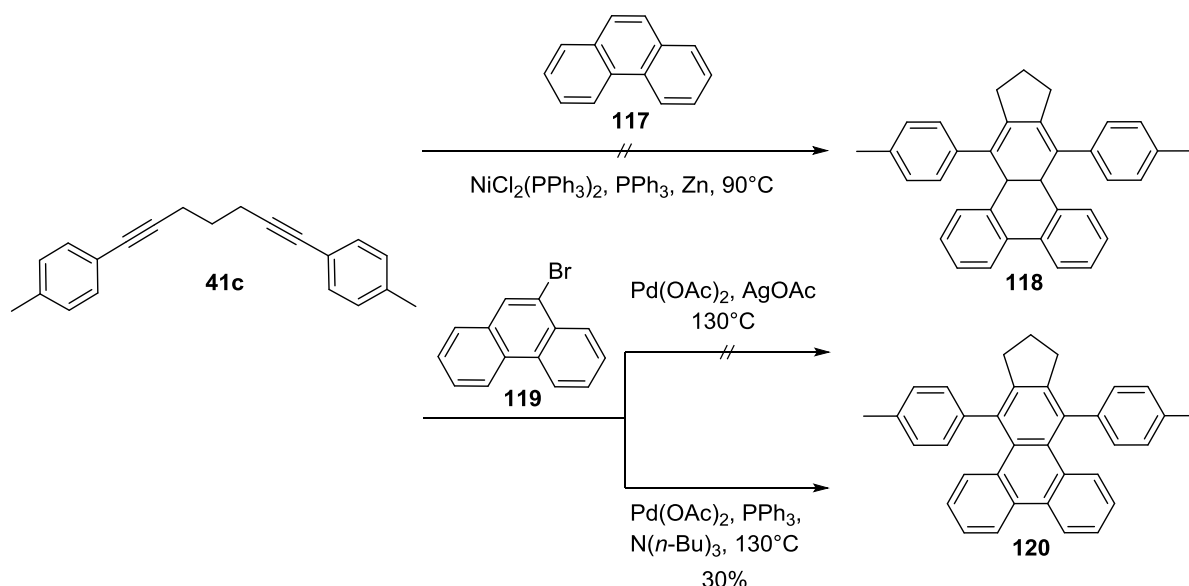
### 2.3.5.2 Diphenylphenanthrene strategy

Using a phenanthrene unit would block the rotation around four bonds (marked in red on Scheme 57) in the precursor, resulting in only two possible isomers remaining.



**Scheme 57:** Phenanthrene strategy for the synthesis of the nanobelt

A different reaction than the alkyne cyclotrimerization has to be envisaged. We tested alternative reactions on the linear precursor **41c** with phenanthrene partners (**117** and **119**) (Scheme 58).

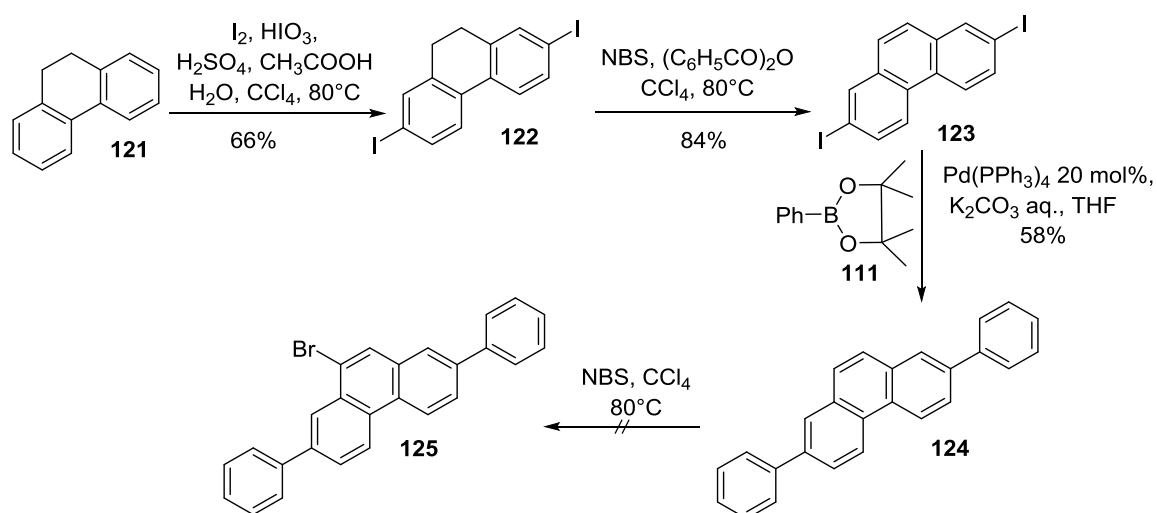


**Scheme 58:** Reaction on a model molecule

In the literature an ene-diyne cycloaddition reaction with fullerene was described and was leading to a cyclohexadiene product.<sup>60</sup> A similar reaction with phenanthrene **117**, followed by an aromatization reaction could provide the desired product. Similar conditions were tried with the linear model, but only starting material were observed. A Pd/Ag promoted cycloaddition with 9-bromophenanthrene **119** and a diyne was performed in the literature.<sup>61</sup> This reaction was attempted on the linear model but here again, only starting material was observed. Finally, we tried a domino inter-intramolecular Heck type reaction<sup>62</sup> with 9-bromophenanthrene **119** on the linear model. This time, the desired product was obtained in around 30% yield.

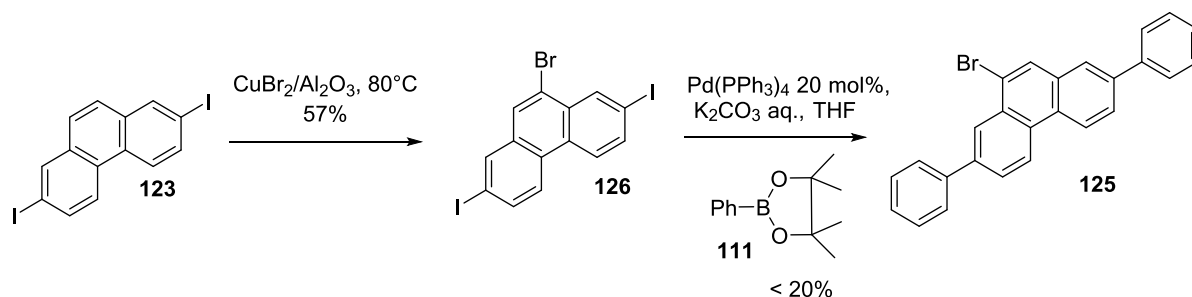
Aware of these encouraging results, we started the synthesis of the new building block: 9-bromo-2,7-diphenylphenanthrene **125**. Several strategies were designed relying on different sequence order of the coupling, bromination and aromatization reactions.

In the first strategy, the building block **123** was synthesized according to a literature procedure from **121** by iodination followed by NBS mediated aromatization.<sup>63</sup> The Suzuki coupling with phenylboronic acid pinacol ester **111** was then performed in 58% yield (Scheme 59). This product **124** was poorly soluble and had to be isolated by filtration of the reaction mixture. Further bromination of **124** turned out to be difficult, presumably in part because of its low solubility.



**Scheme 59:** Synthesis of 9-bromo-2,7-diphenylphenanthrene: strategy 1

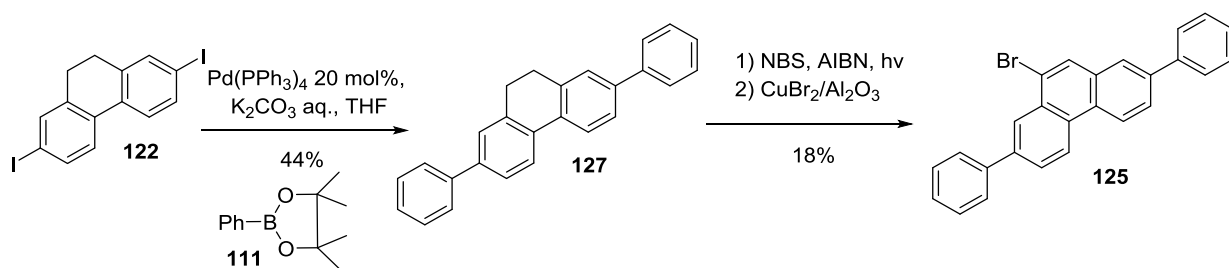
Another strategy was to first brominate compound **123** and then to perform the Suzuki coupling (Scheme 60). Several bromination reaction conditions were tried (bromine, NBS) but only a method using  $\text{CuBr}_2$  on aluminum oxide<sup>64</sup> afforded the desired brominated product **126** in 57% yield. This product was then submitted to the Suzuki coupling, but the purification of the product was complicated as triphenylphosphine co-eluted with the product.



**Scheme 60:** Synthesis of 9-bromo-2,7-diphenylphenanthrene: strategy 2

For the last strategy (Scheme 61), we planned to take advantage of the better solubility of compound **122** to perform the Suzuki reaction which worked in 89% yield. Stepwise aromatization and bromination of the molecule **127** were not successful. Therefore, we explored the possibility of using a one-pot aromatization-bromination reaction procedure. Indeed, we expected that the reaction may proceed through double bromination followed by elimination of one bromine to give the mono-brominated molecule **125**.



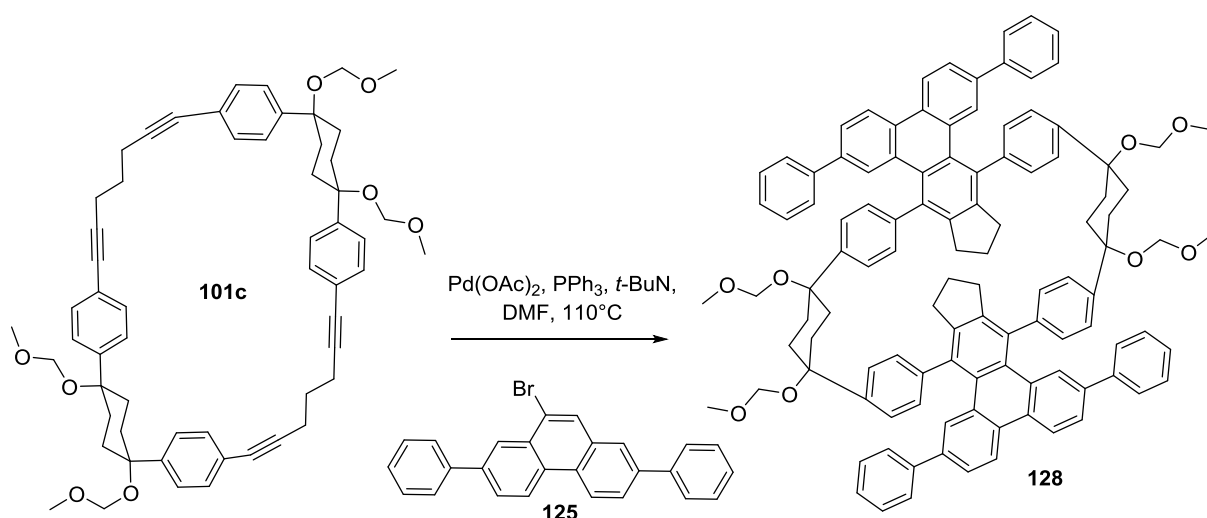


**Scheme 61:** Synthesis of 9-bromo-2,7-diphenylphenanthrene: strategy 3

Different conditions were tried: the use of bromine in presence of acetic acid at  $80^\circ\text{C}$  afforded the desired product **125**, however, the reaction was not very reproducible and when mixture of brominated product were obtained, their separation was not always possible. Performing the reaction at room temperature led only to aromatized product **124**. The same result was observed for NBS with different activation methods.

Finally, the brominated product was obtained using  $\text{CuBr}_2$  on aluminum oxide,<sup>64</sup> but when this method was used alone, bromination occurred on the phenyl moiety giving a mixture of brominated products. Therefore, a one pot reaction was performed: the starting material **127** was first aromatized with NBS and subsequently brominated with  $\text{CuBr}_2/\text{Al}_2\text{O}_3$ , giving the desired building block **125** in 23% yield.

This building block was used in the Heck-type reaction (Scheme 62). The reaction was controlled by TLC and showed full conversion of the macrocycle. A base-line product (yellow fluorescent) was observed on the TLC control. The formed product was too insoluble to be characterized (fine suspension).



**Scheme 62:** Domino Heck type reaction

Nonetheless, it was assumed that this material was the desired product **128** and it was taken as such for the next step: the one pot aromatization-Scholl reaction. The reaction resulted in a complex mixture. However, an interesting orange fluorescent product was isolated by preparative thin layer

chromatography, the product eluted only when a polar mixture (addition of methanol) was used. The  $^1\text{H-NMR}$  spectrum could correspond to the product, however, the proton chemical shifts of such a molecule would be difficult to predict. The mass of the desired product was not detected by MALDI mass spectrometry, even when using different matrices. Another way to characterize the product would be to measure an X-ray structure, therefore, several attempts of recrystallization were done but without success to date. Further work will be needed in order to identify this product. Indeed, this product could also be another isomer, an intermediate of the reaction, an oxidized product, or the product of a polymerization reaction.

To sum up, we tried to apply our synthetic strategy of substituted CPP to synthesize larger nanobelts molecule. First, we explored the possibility to use biphenyl substituted alkyne. However, the number of possible isomers was quite discouraging. We finally envisioned the use of a phenanthrene building block in a domino-Heck type reaction to reduce the number of isomers. Still, the last two steps of the synthesis were difficult to analyze and no clear evidence for the formation of the desired nanobelt has been found yet.

## 2.4 CONCLUSION

Our group initially planned to use the [2+2+2] cycloaddition as a key step for the synthesis of substituted cycloparaphenylenes. However, we discovered that such reaction were not suitable to bring strain in a system (Chapter 1). We overcame this problem by combining our strategy to introduce substituents with the strategy of Itami to bring the final strain in the system (Figure 57).

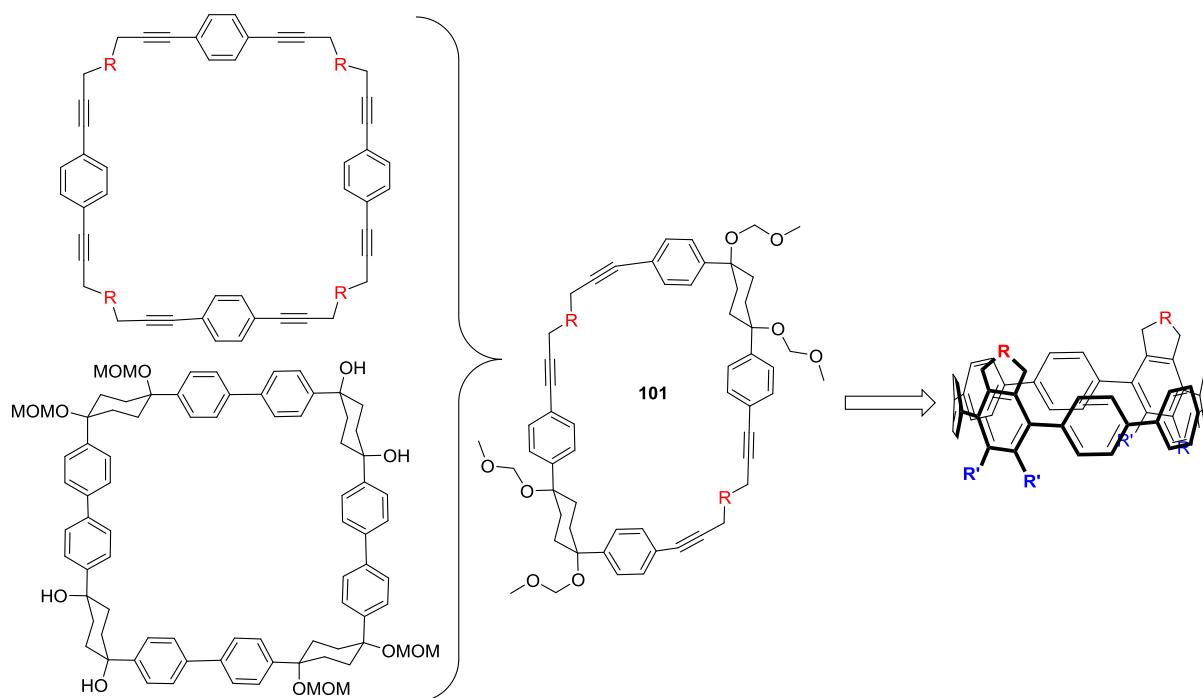


**Figure 57:** Combined strategy for the synthesis of substituted CPP

First we developed a stepwise strategy to the desired macrocyclic precursor **101**. Combining the L-shaped cyclohexane building block with our CPDMS-protected diyne via Sonogashira coupling. Deprotection afforded the monomeric unit which was subsequently submitted to macrocyclization reaction. The macrocyclic dimer was successfully isolated for differently substituted diynes. After this first success with the macrocyclization reaction, we devised a shotgun approach to the macrocycle. Combining directly the unprotected diyne with the L-shaped building block under macrocyclization conditions provided a rapid entry into the macrocyclic precursor synthesis. The [2+2+2] cycloaddition could be performed with several macrocyclic precursors and alkynes in moderate to good yields. This method thus proved its efficiency in functionalizing this kind of molecules. The final strain was brought in the aromatization reaction which afforded the desired substituted CPP in up to 7% yield. The low yield reflects the difficulty to overcome the ring strain in this last step. An oxidized CPP product could also be isolated during this reaction. Differently substituted CPPs were synthesized using this method (Figure 58).

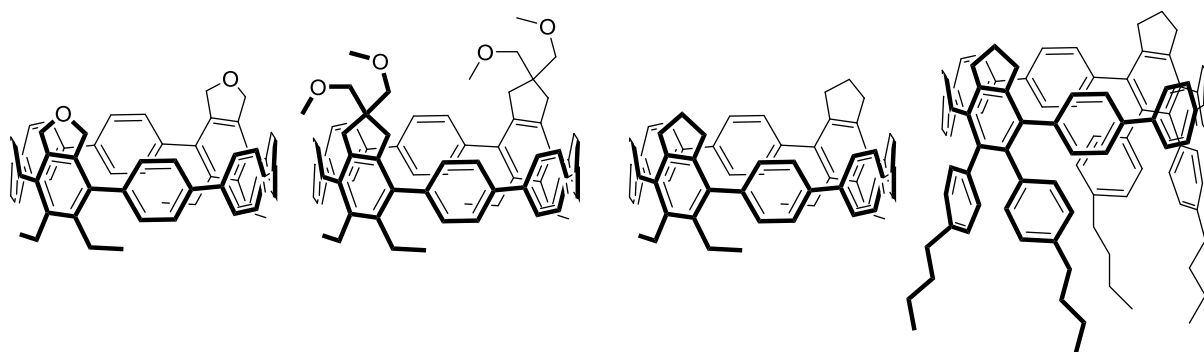


**Figure 58:** Substituted CPPs synthesized using our method

The structural properties of the different CPPs were similar to the corresponding unsubstituted [8]CPP. However, the optical properties presented some variations mainly attributable to the larger torsion angles.

In summary, we provided a highly modular synthesis of substituted CPP, which allows accessing CPPs with different functional group for further chemistry. Besides new host-guest possibilities, substituted CPPs could find applications in nanoporous materials with defined pore size but also as chemosensors.<sup>65,66</sup> The advantage of our strategy is that the substitution can be chosen at a late stage of the synthesis, providing therefore a highly modular method to synthesize functionalized CPPs. The use of this general strategy for the synthesis of larger belt molecule was also explored. Unfortunately, until now no clear proof of the formation of the desired nanobelts was found (Figure 59).

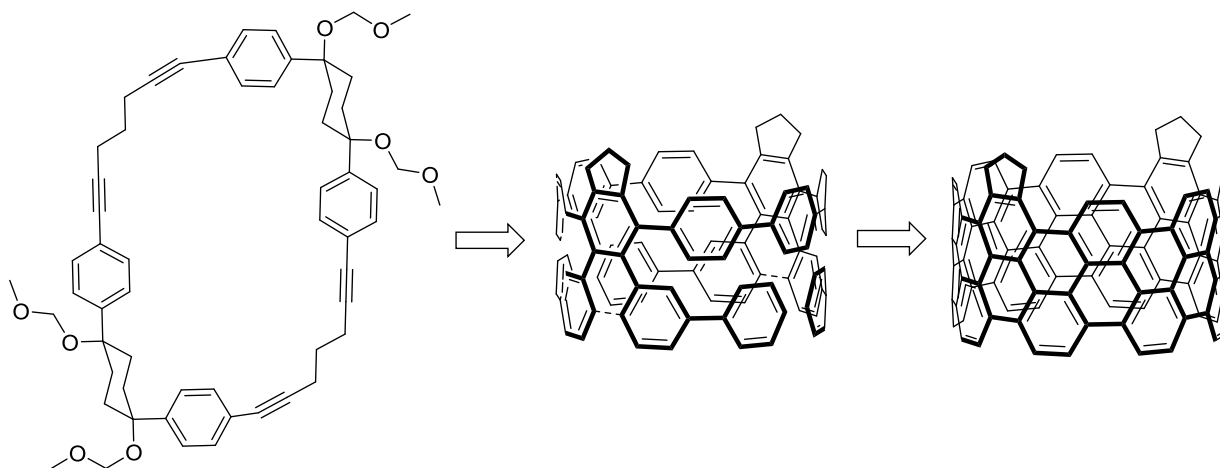


**Figure 59:** Strategy toward the synthesis of a nanobelt

**2.5 REFERENCES**

- [1] Kroto, H. W.; Heath, J. R.; O'Brien, S. C.; Curl, R. F.; Smalley, R. E. *Nature* **1985**, *318*, 162.
- [2] Novoselov, K. S.; Geim, A. K.; Morozov, S. V.; Jiang, D.; Zhang, Y.; Dubonos, S. V.; Grigorieva, I. V.; Firsov, A. A. *Science* **2004**, *306*, 666.
- [3] Iijima, S. *Nature* **1991**, *354*, 56.
- [4] Bianco, A.; Kostarelos, K.; Prato, M. *Curr. Opin. Chem. Biol.* **2005**, *9*, 674.
- [5] Katz, E.; Willner, I. *ChemPhysChem* **2004**, *5*, 1084.
- [6] Baughman, R. H.; Zakhidov, A. A.; de Heer, W. A. *Science* **2002**, *297*, 787.
- [7] Lieber, C. M. *Solid State Commun.* **1998**, *107*, 607.
- [8] Huang, J.; Zhang, Q.; Zhao, M.; Wei, F. *Chin. Sci. Bull.* **2012**, *57*, 157.
- [9] Paradise, M.; Goswami, T. *Materials & Design* **2007**, *28*, 1477.
- [10] Evans, P.; Jasti, R.; Springer Berlin Heidelberg: 2013, p 1.
- [11] Eisenberg, D.; Shenhav, R.; Rabinovitz, M. *Chem. Soc. Rev.* **2010**, *39*, 2879.
- [12] Kawase, T.; Kurata, H. *Chem. Rev.* **2006**, *106*, 5250.
- [13] Cuesta, I. G.; Pedersen, T. B.; Koch, H.; Sánchez de Merás, A. *ChemPhysChem* **2006**, *7*, 2503.
- [14] Scott, L. T. *Angew. Chem. Int. Ed.* **2003**, *42*, 4133.
- [15] Bodwell, G. J.; Miller, D. O.; Vermeij, R. J. *Org. Lett.* **2001**, *3*, 2093.
- [16] Scott, L. T.; Jackson, E. A.; Zhang, Q.; Steinberg, B. D.; Bancu, M.; Li, B. *J. Am. Chem. Soc.* **2011**, *134*, 107.
- [17] Steinberg, B. D.; Scott, L. T. *Angew. Chem. Int. Ed.* **2009**, *48*, 5400.
- [18] Fort, E. H.; Donovan, P. M.; Scott, L. T. *J. Am. Chem. Soc.* **2009**, *131*, 16006.
- [19] Li, H.-B.; Page, A. J.; Irle, S.; Morokuma, K. *ChemPhysChem* **2012**, *13*, 1479.
- [20] Omachi, H.; Nakayama, T.; Takahashi, E.; Segawa, Y.; Itami, K. *Nat. Chem.* **2013**, *5*, 572.
- [21] Omachi, H.; Segawa, Y.; Itami, K. *Acc. Chem. Res.* **2012**, *45*, 1378.
- [22] Sisto, T. J.; Jasti, R. *Synlett* **2012**, *23*, 483.
- [23] Hirst, E. S.; Jasti, R. *J. Org. Chem.* **2012**, *77*, 10473.
- [24] Srinivasan, M.; Sankararaman, S.; Hopf, H.; Varghese, B. *Eur. J. Org. Chem.* **2003**, *2003*, 660.
- [25] Jasti, R.; Bertozzi, C. R. *Chem. Phys. Lett.* **2010**, *494*, 1.
- [26] Jasti, R.; Bhattacharjee, J.; Neaton, J. B.; Bertozzi, C. R. *J. Am. Chem. Soc.* **2008**, *130*, 17646.
- [27] Darzi, E. R.; Sisto, T. J.; Jasti, R. *J. Org. Chem.* **2012**, *77*, 6624.
- [28] Sisto, T. J.; Golder, M. R.; Hirst, E. S.; Jasti, R. *J. Am. Chem. Soc.* **2011**, *133*, 15800.
- [29] Xia, J.; Jasti, R. *Angew. Chem. Int. Ed.* **2012**, *51*, 2474.
- [30] Xia, J.; Bacon, J. W.; Jasti, R. *Chem. Sci.* **2012**, *3*, 3018.
- [31] Friederich, R.; Nieger, M.; Vögtle, F. *Chem. Ber.* **1993**, *126*, 1723.

- [32] Takaba, H.; Omachi, H.; Yamamoto, Y.; Bouffard, J.; Itami, K. *Angew. Chem. Int. Ed.* **2009**, *48*, 6112.
- [33] Omachi, H.; Matsuura, S.; Segawa, Y.; Itami, K. *Angew. Chem. Int. Ed.* **2010**, *49*, 10202.
- [34] Ishii, Y.; Nakanishi, Y.; Omachi, H.; Matsuura, S.; Matsui, K.; Shinohara, H.; Segawa, Y.; Itami, K. *Chem. Sci.* **2012**, *3*, 2340.
- [35] Segawa, Y.; Miyamoto, S.; Omachi, H.; Matsuura, S.; Šenel, P.; Sasamori, T.; Tokitoh, N.; Itami, K. *Angew. Chem. Int. Ed.* **2011**, *50*, 3244.
- [36] Segawa, Y.; Šenel, P.; Matsuura, S.; Omachi, H.; Itami, K. *Chem. Lett.* **2011**, *40*, 423.
- [37] Yamago, S.; Watanabe, Y.; Iwamoto, T. *Angew. Chem. Int. Ed.* **2010**, *49*, 757.
- [38] Kayahara, E.; Sakamoto, Y.; Suzuki, T.; Yamago, S. *Org. Lett.* **2012**, *14*, 3284.
- [39] Iwamoto, T.; Watanabe, Y.; Sakamoto, Y.; Suzuki, T.; Yamago, S. *J. Am. Chem. Soc.* **2011**, *133*, 8354.
- [40] Sisto, T. J.; Tian, X.; Jasti, R. *J. Org. Chem.* **2012**, *77*, 5857.
- [41] Nishiuchi, T.; Feng, X.; Enkelmann, V.; Wagner, M.; Müllen, K. *Chem. Eur. J.* **2012**, *18*, 16621.
- [42] Yagi, A.; Segawa, Y.; Itami, K. *J. Am. Chem. Soc.* **2012**, *134*, 2962.
- [43] Omachi, H.; Segawa, Y.; Itami, K. *Org. Lett.* **2011**, *13*, 2480.
- [44] Matsui, K.; Segawa, Y.; Itami, K. *Org. Lett.* **2012**, *14*, 1888.
- [45] Segawa, Y.; Fukazawa, A.; Matsuura, S.; Omachi, H.; Yamaguchi, S.; Irle, S.; Itami, K. *Org. Biomol. Chem.* **2012**, *10*, 5979.
- [46] Fujitsuka, M.; Cho, D. W.; Iwamoto, T.; Yamago, S.; Majima, T. *Phys. Chem. Chem. Phys.* **2012**, *14*, 14585.
- [47] Nishihara, T.; Segawa, Y.; Itami, K.; Kanemitsu, Y. *J. Phys. Chem. Lett.* **2012**, *3*, 3125.
- [48] Wong, B. M.; Lee, J. W. *J. Phys. Chem. Lett.* **2011**, *2*, 2702.
- [49] Camacho, C.; Niehaus, T. A.; Itami, K.; Irle, S. *Chem. Sci.* **2013**, *4*, 187.
- [50] Basler, J. M., University of Basel, 2011.
- [51] Höger, S.; Bonrad, K. *J. Org. Chem.* **2000**, *65*, 2243.
- [52] Katō, M.; Taniguchi, Y. *The Journal of Chemical Physics* **1990**, *92*, 887.
- [53] Weiss, M. E.; Carreira, E. M. *Angew. Chem. Int. Ed.* **2011**, *50*, 11501.
- [54] Cristiano, M. L. S.; Gago, D. J. P.; d'A. Rocha Gonsalves, A. M.; Johnstone, R. A. W.; McCarron, M.; Varejao, J. M. T. B. *Org. Biomol. Chem.* **2003**, *1*, 565.
- [55] Wuts, P. G. M.; Greene, T. W. In *Greene's Protective Groups in Organic Synthesis*; John Wiley & Sons, Inc.: 2006, p 986.
- [56] Kaur, I.; Jia, W.; Koprski, R. P.; Selvarasah, S.; Dokmeci, M. R.; Pramanik, C.; McGruer, N. E.; Miller, G. P. *J. Am. Chem. Soc.* **2008**, *130*, 16274.

- [57] Segawa, Y.; Omachi, H.; Itami, K. *Org. Lett.* **2010**, *12*, 2262.
- [58] Chris P. Ewels and Jean-Joseph Adjizian, IMN, CNRS, Université de Nantes, 2, rue de la Houssinière, BP32229, F-44322 Nantes, France.
- [59] Zhai, L.; Shukla, R.; Rathore, R. *Org. Lett.* **2009**, *11*, 3474.
- [60] Hsiao, T.-Y.; Santhosh, K. C.; Liou, K.-F.; Cheng, C.-H. *J. Am. Chem. Soc.* **1998**, *120*, 12232.
- [61] Kung, Y.-H.; Cheng, Y.-S.; Tai, C.-C.; Liu, W.-S.; Shin, C.-C.; Ma, C.-C.; Tsai, Y.-C.; Wu, T.-C.; Kuo, M.-Y.; Wu, Y.-T. *Chem. Eur. J.* **2010**, *16*, 5909.
- [62] Hu, Y.; Yao, H.; Sun, Y.; Wan, J.; Lin, X.; Zhu, T. *Chem. Eur. J.* **2010**, *16*, 7635.
- [63] Shaporenko, A.; Elbing, M.; Błaszczuk, A.; von Hänisch, C.; Mayor, M.; Zharnikov, M. *The Journal of Physical Chemistry B* **2006**, *110*, 4307.
- [64] Ma, Y.; Song, C.; Jiang, W.; Wu, Q.; Wang, Y.; Liu, X.; Andrus, M. B. *Org. Lett.* **2003**, *5*, 3317.
- [65] O'Mahony, A. M.; Wang, J. *Analytical Methods* **2013**, *5*, 4296.
- [66] Miles, B. N.; Ivanov, A. P.; Wilson, K. A.; Doğan, F.; Japrun, D.; Edel, J. B. *Chem. Soc. Rev.* **2013**, *42*, 15.

## **Chapter 3:**

# **Experimental part**





### **3.1 GENERAL INFORMATION:**

**Reagents and Solvents:** All chemicals and solvents for reactions were purchased from one of the following commercial sources: Acros, Alfa Aesar, Fluka, Fluorochem, Sigma-Aldrich, Strem or VWR and used without further purification. Pd(PPh<sub>3</sub>)<sub>4</sub> was prepared from PdCl<sub>2</sub> according to a literature procedure.<sup>1</sup> Dry solvents were obtained from a solvent purification system (Pure-Solv™). Dry solvent for small scale reactions was purchased from Aldrich (crown cap over molecular sieves). For extraction and chromatography technical solvents were redistilled once with a rotator evaporator prior to usage.

**Reactions:** All reactions were performed under ambient atmosphere if not stated otherwise. All reactions dealing with air and moisture sensitive compounds were carried out under an inert atmosphere of argon using schlenck techniques. For moisture sensitive reactions the glass material was heated at 110 °C in a drying oven over night before usage.

**Microwave Reactions:** Microwave reactions were carried out in an Initiator 8 (400 W) from Biotage.

**Chromatography:** The thin layer chromatography was conducted on aluminum supported silica gel 60 F254 with a thickness of 0.2 mm from Merck and detected with a CAMAG UV lamp at 254 nm or 365 nm or developed with KMnO<sub>4</sub>. For the preparative scale thin layer chromatography was used 1 or 2 mm silica gel coated glass plates (20 × 20 cm) from Analtech. For the column chromatography silica gel 60 (40 – 63 μm) from Fluka, Sigma-Aldrich, Merck, SiliCycle Inc was used.

**Gel Permeation Chromatography (GPC):** Gel Permeation Chromatography (GPC) was performed on a Shimadzu Prominence System with PSS SDV preparative columns from PSS (2 columns in series: 600 mm x 20.0 mm, 5 μm particles, linear porosity “S”, operating ranges: 100 – 100 000 g mol<sup>-1</sup>) using chloroform as eluent.

**NMR-Spectroscopy:** Bruker DRX-NMR (600 MHz or 500/126 MHz), Bruker DPX-NMR (400/101 MHz) and Bruker BZH-NMR (250 MHz) instruments were used to record the spectra. The measurements were performed at room temperature unless otherwise stated. The carbon shifts marked with \* were determined from 2D HMQC and HMBC data with increments in the indirect dimension. The chemical shift  $\delta$  values were corrected to the signal of the deuterated solvents: 7.26 ppm (<sup>1</sup>H-NMR) and 77.16 ppm (<sup>13</sup>C-NMR) for CDCl<sub>3</sub>; 5.32 ppm (<sup>1</sup>H-NMR) and 53.5 ppm (<sup>13</sup>C-NMR) for CD<sub>2</sub>Cl<sub>2</sub>; 5.91 ppm (<sup>1</sup>H-NMR) and 74.2 ppm (<sup>13</sup>C-NMR) for CD<sub>2</sub>Cl<sub>4</sub>. Coupling constants (*J*) are reported in Hertz (Hz). Multiplets are assigned as: s (singlet), d (doublet), t (triplet), q

(quartet), p (pentuplet) and m (multiplet). Broad signals are assigned with: b (broad). NMR-solvents were obtained from Cambridge Isotope Laboratories, Inc. (Andover, MA, USA).

**UV-Vis and Fluorescence Spectroscopy:** UV-Vis absorption was measured on a Agilent UV-Vis single beam Spectrophotometer Emission spectra were measured on a Shimadzu RF-5301PC Spectrofluorophotometer. Quantum yield measurements were done on a Hamamatsu Absolute PL Quantum Yield Spectrometer C11347, and Fluorescence lifetimes were measured using a Hamamatsu Compact Fluorescence Lifetime Spectrometer C11367-11.

**Mass Spectrometry:** Electron spray mass spectrometry was measured on a Bruker esquire 3000 plus. For GC/MS-analysis a Hewlett Packard 5890 Series II gas chromatography system, with a Macherey Nagel OPTIMA 1 Me2Si column (25 m × 0.2 mm × 0.35 m), at 1 mL/min He-flow rate (split = 20:1) with a Hewlett Packard 5971 Series mass selective detector (EI 70 eV) was used. Matrix Assisted Laser Desorption Ionization Time of Flight (MALDI-ToF) mass spectra were performed on an Applied Bio Systems Voyager-De™ Pro mass spectrometer or a Bruker microflex mass spectrometer. Fast atom bombardment (FAB) mass spectrometry was measured on a MAR 312 and Electron Impact (EI) mass spectra were recorded on a Finnigan MAT 95Q by Dr. H. Nadig.

High-resolution mass (HR-ESI MS) spectra were recorded using a Bruker maXis 4G QTOF-ESI Spectrometer by Dr. H. Nadig or by the MS-service of ETH zurich on a Bruker's solariX (ESI/MALDI-FTICR-MS) and EI.

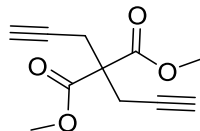
**IR-Spectroscopy:** Spectra were recorded on a Fourier transform infrared spectrometer Shimadzu FTIR-8400S by which the compounds were measured through a Specac Golden Gate ATR sampling system.

**Elementary analysis:** The elemental analyses were performed by Mr. W. Kirsch on a Leco CHN-900 or by Mrs Sylvie Mittelheisser on a Vario Micro Cube.

**Melting Point:** Measurements of melting points were made with a SRS EZ-Melt MPA 120 or Büchi 530 instrument.

## 3.2 EXPERIMENTAL PROCEDURES

### 3.2.1 Diyne synthesis



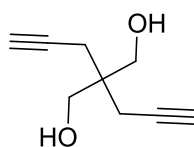
#### Synthesis of dipropargyl methylmalonate 37<sup>2</sup>

Under an inert atmosphere of argon NaH (2.86 g, 71.5 mmol, 1.10 eq., 60 wt.% in mineral oil) was added portion wise at 0°C to a solution of dimethyl malonate **35** (7.43 mL, 65.0 mmol, 1.00 eq.) in 150 mL anhydrous THF. The mixture was allowed to warm to rt (over 30 min), whereas the mixture became cloudy. Then, propargyl bromide (7.70 mL, 71.5 mmol, 1.10 eq.) was slowly added and the mixture turned brown. The mixture was stirred for 2.5 h at rt. Then, the solution was cooled down to 0°C and NaH (2.86 g, 71.5 mmol, 1.10 eq., 60 wt% in mineral oil) was added portion wise. The mixture was warmed and propargyl bromide **36** (7.70 mL, 71.5 mmol, 1.10 eq.) was slowly added. The mixture was stirred for 5 h, quenched with water and extracted twice with TBME. The combined organic layers were washed with brine and the combined aqueous layers were reextracted with TBME. The organic layers were dried over MgSO<sub>4</sub> and concentrated under reduced pressure. The crude product was recrystallized from hexane and to obtain 9.65 g of dipropargylester as a yellowish solid (71%).

<sup>1</sup>H NMR (400 MHz, CDCl<sub>3</sub>, δ/ppm): 3.74 (s, 6H); 2.97 (d, *J* = 2.6 Hz, 4H); 2.01 (t, *J* = 2.6 Hz, 2H).

<sup>13</sup>C NMR (101 MHz, CDCl<sub>3</sub>, δ/ppm): 169.3 (2C), 78.6 (2C), 72.0 (2C), 56.6, 53.5, (2C), 23.0 (2C).

Analytical data are in accordance with the literature.<sup>3</sup>



### **Synthesis of bis(homopropargyl)dialcohol 38<sup>2</sup>**

Dipropargylester **37** (3.00 g, 14.4 mmol, 0.95 eq.) was dissolved in 60 mL dry THF and cooled to  $-10^{\circ}\text{C}$  -  $-20^{\circ}\text{C}$  (gas bubbler attached). Then,  $\text{LiAlH}_4$  (1.76 g, 45.0 mmol, 3.00 eq.) was added over 1 h at this temperature. The mixture was allowed to warm to rt and stirred overnight. Afterwards, it was carefully quenched with water and 6% NaOH was added. Then, the suspension was acidified with 1 M HCl, extracted three times with TBME, and the organic layer was dried over  $\text{MgSO}_4$  and evaporated. Recrystallization from hexane and ethyl acetate yielded the title compound as white needles (1.83 g, 12.0 mmol, 84%).

**<sup>1</sup>H NMR** (400 MHz,  $\text{CDCl}_3$ ,  $\delta/\text{ppm}$ ): 3.77 (d,  $J = 5.7$  Hz, 1H), 2.40 (d,  $J = 2.7$  Hz, 1H), 2.13 (t,  $J = 5.7$  Hz, 1H), 2.07 (t,  $J = 2.7$  Hz, 1H).

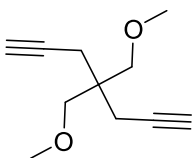
**<sup>13</sup>C NMR** (101 MHz,  $\text{CDCl}_3$ ,  $\delta/\text{ppm}$ ): 80.4, 71.4, 66.7, 42.2, 21.9.

**MS** (FAB)  $m/z$  (%): 153 (100%) [ $\text{M}+\text{H}^+$ ], 137, 91, 43.

**EA** (%): calc. C, 71.03; H, 7.95; found C, 70.96; H, 8.04.

**IR** ( $\nu/\text{cm}^{-1}$ ): 3333, 3277, 3264, 3257, 3245, 3243, 3211, 3207, 3203, 3200, 3194, 3187, 3133, 2938, 2886, 2885, 1467, 1460, 1428, 1372, 1367, 1313, 1127, 1106, 1024, 1003.

**Mp**: 61-62 $^{\circ}\text{C}$ .



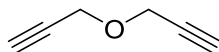
### Synthesis of 4,4-bis(methoxymethyl)hepta-1,6-diyne 39a<sup>2</sup>

A solution of bis(homopropargyl)dialcohol **38** (4.90 g, 32.2 mmol, 0.976 eq.) and iodomethane (8.1 mL, 129 mmol, 3.90 eq.) in dry THF (100 mL) was added dropwise at 0°C to a suspension of sodium hydride (60% in oil, 3.63 g, 90.8 mmol) in THF (100 mL). The mixture was stirred for 1 h at rt, diluted with Et<sub>2</sub>O and slowly quenched with water. Then, a few milliliters of sat. NH<sub>4</sub>Cl were added, the organic layer was washed twice with sat. NH<sub>4</sub>Cl solution and brine, dried over MgSO<sub>4</sub> and concentrated. The crude mixture was purified by distillation under reduced pressure (85°C, 5 mbar) to furnish 4.84 g of the title compound as a colorless liquid (78%).

<sup>1</sup>H NMR (400 MHz, CDCl<sub>3</sub>, δ/ppm): 3.35 (d, *J* = 3.4 Hz, 4H), 3.34 (s, 6H), 2.35 (d, *J* = 2.7 Hz, 4H), 1.98 (t, *J* = 2.7 Hz, 2H).

<sup>13</sup>C NMR (126 MHz, CDCl<sub>3</sub>, δ/ppm): 80.8, 73.5, 70.6, 59.5, 41.7, 21.9

Analytical data are in accordance with the literature.<sup>4</sup>



### Synthesis of propargylether 39d

Propargylic alcohol (34.4 mL, 585 mmol, 1.40 eq) and propargylbromide (36.0 mL, 418 mmol, 1.00 eq.) were placed in a flask. Freshly powdered NaOH (25.0 g, 625 mmol, 1.50 eq.) were added in small portions with vigorous stirring. The temperature was kept between 60 and 70°C, 5 mL of THF were added to facilitate stirring. When, the reaction subsided, the mixture was heated for an additional 1 h at 70-80°C. Again 15 mL THF were added. After cooling to 30°C, 50 mL of icewater was added with vigorous stirring. The product was isolated by extraction with Et<sub>2</sub>O (2x) and the extracts washed with water. After drying the organic solution over MgSO<sub>4</sub>, most of the ether was distilled off at normal pressure. The remaining liquid was purified by distillation to give 40.1 g (95%) dipropargyl ether as coloureless liquid, bp. 40-60°C/100mbar.

<sup>1</sup>H NMR (400 MHz, CDCl<sub>3</sub>, δ/ppm): 4.24 (d, *J* = 1.0 Hz, 4H), 2.45 (t, *J* = 1.0 Hz, 2H).

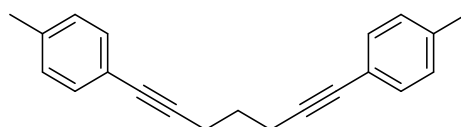
<sup>13</sup>C NMR (126 MHz, CDCl<sub>3</sub>, δ/ppm): 79.1, 75.5, 56.8.

Analytical data are in accordance with the literature<sup>5</sup>

### 3.2.2 Linear precursor synthesis

#### General procedure for the synthesis of the linear precursor

An oven dried two-necked flask was placed Pd(PPh<sub>3</sub>)<sub>4</sub> (10 mol%) and CuI (, 20 mol%) in dry THF. The mixture was degassed by bubbling argon through the solution. Then, 4-iodotoluene (2.10 eq.) and diyne **39** (1.00 eq.) and diisopropylamine were added with argon counterflow. The reaction was stirred overnight at rt. Afterwards, the reaction mixture was poured on sat. NH<sub>4</sub>Cl and extracted with ethyl acetate (3 x). The combined organic layers were washed with sat. NH<sub>4</sub>Cl, brine, dried over MgSO<sub>4</sub> and concentrated under reduced pressure. The crude material was purified by column chromatography on silica gel and hexane/EtOAc was used as eluent.



#### Synthesis of 1,7-di-p-tolylhepta-1,6-diyne 41c

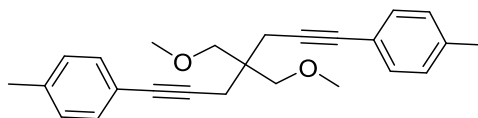
According to the general procedure, Pd(PPh<sub>3</sub>)<sub>4</sub> (2.53 g, 2.17 mmol, 10 mol%), CuI (0.827 g, 4.34 mmol, 20 mol%), 4-iodotoluene (9.94 g, 45.6 mmol, 2.10 eq.), hepta-1,6-diyne (2.00 g, 27.7 mmol, 1.00 eq.) and 40 mL diisopropylamine were added in dry THF (100 mL) and stirred overnight at rt. After work up, the crude material was purified by column chromatography on silica gel and hexane/EtOAc: 20/1 was used as eluent. The product was then recrystallized from EtOH to afford 2.70 g of the product as yellow solid (69%).

<sup>1</sup>H-NMR (400 MHz, CDCl<sub>3</sub>, δ/ppm): 7.30 (m, 4H), 7.09 (m, 4H), 2.58 (t, *J* = 7.03 Hz, 4H), 2.33 (s, 6H), 1.90 (t, *J* = 7.03 Hz, 2H).

<sup>13</sup>C-NMR (101 MHz, CDCl<sub>3</sub>, δ/ppm): 137.7, 131.6, 129.1, 120.9, 88.6, 81.4, 28.2, 21.6, 18.9

EA (%): calc. C, 92.60; H, 7.40; found C, 92.39; H, 7.44.

Mp: 48-50°C.



### Synthesis of 41a

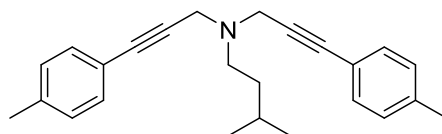
According to the general procedure, Pd(PPh<sub>3</sub>)<sub>4</sub> (324 mg, 0.277 mmol, 10 mol%), CuI (106 mg, 0.555 mmol, 20 mol%), 10 mL diisopropylamine, 4-iodotoluene (1.27 g, 5.83 mmol, 2.10 eq) and **39a** (500 mg, 2.77 mmol, 1.00 eq) were added in dry THF (10 mL). The solution was stirred at rt overnight. After standard workup, the crude product was purified by column chromatography (cyclohexane/EtOAc: 20/1) to give 722 mg of product as yellow oil (72%).

<sup>1</sup>H-NMR (400 MHz, CDCl<sub>3</sub>, δ/ppm): 7.31, (m, 4H), 7.10 (m, 4H), 3.48 (s, 4H), 3.39 (s, 6H), 2.61 (s, 4H), 2.34 (s, 6H).

<sup>13</sup>C-NMR (101 MHz, CDCl<sub>3</sub>, δ/ppm): 138.0, 131.9, 129.3, 121.2, 86.2, 83.0, 74.5, 59.9, 43.0, 23.5, 21.8.

MS (EI, 70eV) *m/z* (%): 360.2 (15), 315.2 (65), 283.2 (100).

HR-MS (ESI): calc. for [C<sub>25</sub>H<sub>29</sub>NaO<sub>2</sub>]<sup>+</sup>: [M+Na]<sup>+</sup> 383.1982; found: 383.1983.



### Synthesis of 41b

According to the general procedure, Pd(PPh<sub>3</sub>)<sub>4</sub> (357 mg, 0.306 mmol, 10 mol%), CuI (117 mg, 0.613 mmol, 20 mol%), 4-iodotoluene (1.40 g, 6.43 mmol, 2.10 eq.) and **39b** (500 mg, 3.06 mmol, 1.00 eq.), 11 mL diisopropylamine were added in dry THF (20 mL). The reaction mixture was stirred overnight at rt. After standard work up, the crude product was purified on column chromatography (cyclohexane/ EtOAc) to lead 918 mg of the title compound as an orange-red oil (87%).

<sup>1</sup>H-NMR (400 MHz, CDCl<sub>3</sub>, δ/ppm): 7.34 (m, 4H), 7.10 (m, 4H), 3.69 (s, 4H), 2.68 (m, 2H), 2.34 (s, 6H), 1.66 (m, 1H), 1.45 (m, 2H), 0.94 (d, *J* = 6.62 Hz, 6H).

<sup>13</sup>C-NMR (101 MHz, CDCl<sub>3</sub>, δ/ppm): 138.5, 132.0, 129.4, 120.6, 85.5, 84.4, 51.7, 43.7, 36.9, 36.9, 26.8, 23.1, 21.8.

EA (%): calc. C, 87.41; H, 8.51; N, 4.08 found C, 85.10; H, 8.40; N, 4.34.

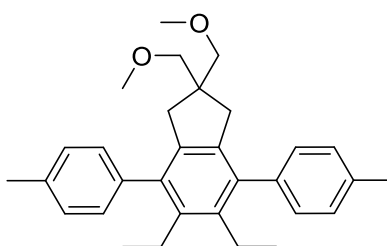
MS (FAB), *m/z*: 342.3[M+H].



### 3.2.3 [2+2+2] cycloaddition reaction on linear molecules

#### General procedure for the [2+2+2] cycloaddition

The linear precursor **41** (100 mg, 1,00 eq.), the alkyne (30.0 eq.), anhydrous 2-propanol (10 mL), and THF (10 mL) were placed in a 20 mL microwave flask equipped with a spin bar. The reaction mixture was degassed by bubbling Ar through the solution for 15 min. Then, RhCl(PPh<sub>3</sub>)<sub>3</sub> (0.10 eq.) was added and the reaction flask was put in the microwave reactor at 100°C for 6h. The reaction mixture was then diluted with DCM and washed with brine. The aqueous phase was extracted by DCM and the combined organic phases were washed with sat NaHCO<sub>3</sub> (2x) and brine. After drying over MgSO<sub>4</sub> the volatiles were evaporated. The product was then purified by flash chromatography (EtOAc/Cyclohexane) to lead product according to the yield in table 1.



#### Synthesis of 42a

According to the general procedure, the linear precursor **41a** (100 mg, 0.277 mmol, 1,00 eq.), hex-3-yne (959  $\mu$ L, 8.32 mmol, 30.0 eq.), anhydrous 2-propanol (10 mL), and anhydrous THF (10 mL) were placed in a 20 mL microwave flask equipped with a spin bar. The reaction mixture was degassed by bubbling argon through the solution for 15 min. Then, RhCl(PPh<sub>3</sub>)<sub>3</sub> (25.9 mg, 13.9  $\mu$ mol, 10.0 mol%) was added and the reaction flask was placed in the microwave reactor at 100°C for 6h. After standard workup, the product was purified by flash chromatography (cyclohexane/EtOAc: 30/1) to give 105 mg of product as white solid (85%).

**<sup>1</sup>H-NMR** (400 MHz, CDCl<sub>3</sub>,  $\delta$ /ppm): 7.20 (m, 4H), 7.13 (m, 4H), 3.25 (s, 6H), 3.23 (s, 4H), 2.51 (q,  $J$  = 7.44 Hz, 4H), 2.48 (s, 4H), 2.39 (s, 6H), 0.96 (t,  $J$  = 7.44 Hz, 6H).

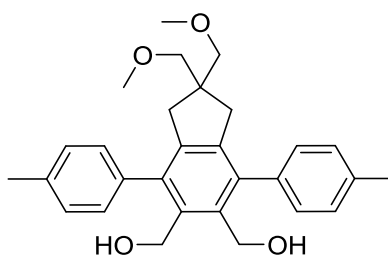
**<sup>13</sup>C-NMR** (101 MHz, CDCl<sub>3</sub>,  $\delta$ /ppm): 138.8, 138.7, 138.6, 138.6, 136.3, 129.4, 129.4, 76.6, 59.6, 47.2, 39.7, 23.3, 21.6, 16.4.

**EA (%)**: calc. C 84.12 H 8.65, found C 83.88 H 8.61.

**MS** (EI, 70eV),  $m/z$  (%): 442 (17) [M<sup>+</sup>], 365 (100).

**IR** ( $\nu$  /cm<sup>-1</sup>): 2959, 2868, 1516, 1432, 1372, 1101.

**Mp**: 122-125°C.



### Synthesis of 42b

According to the general procedure, the linear precursor **41a** (100 mg, 0.264 mmol, 1.00 eq.), 2-butyne-1,4-diol (689 mg, 7.92 mmol, 30.0 eq.), anhydrous 2-propanol (10 mL), and anhydrous THF (10 mL) were placed in a 20 mL microwave flask equipped with a spin bar. The reaction mixture was degassed by bubbling Ar through the solution for 15 min. Then,  $\text{RhCl}(\text{PPh}_3)_3$  (24.6 mg, 26.4  $\mu\text{mol}$ , 10 mol%) was added and the reaction flask was placed in the microwave reactor at 100°C for 6h. After standard workup, the product was purified by flash chromatography (cyclohexane/EtOAc: 3/7) to give 57 mg of product as white solid (48%).

**$^1\text{H-NMR}$**  (400 MHz,  $\text{CDCl}_3$ ,  $\delta/\text{ppm}$ ): 7.24 (m, 4H), 7.19 (m, 4H), 4.60 (d,  $J = 5.11$  Hz, 4H), 3.26 (s, 6H), 3.24 (s, 4H), 2.62 (s, 4H), 2.41 (s, 6H).

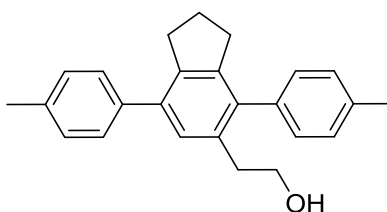
**$^{13}\text{C-NMR}$**  (101 MHz,  $\text{CDCl}_3$ ,  $\delta/\text{ppm}$ ): 141.3, 139.2, 136.8, 136.6, 136.5, 129.2, 129.1, 76.1, 60.8, 59.3, 47.3, 39.4, 21.4

**MS** (EI, 70eV)  $m/z$  (%): 446 (8) [ $\text{M}^+$ ], 321 (100).

**HR-MS** (ESI): calc. for  $[\text{C}_{29}\text{H}_{34}\text{NaO}_4]^+$ : [ $\text{M}+\text{Na}$ ] $^+$  469.2349; found: 469.2349.

**IR** ( $\nu/\text{cm}^{-1}$ ): 3293, 2989, 2873, 1115, 1010.

**Mp**: 210-215°C.



### Synthesis of 42c

According to the general procedure, the linear precursor **41c** (100 mg, 0.367 mmol, 1.00 eq.), 3-butyl-1-ol (859  $\mu$ L, 11.0 mmol, 30.0 eq.), anhydrous 2-propanol (10 mL), and anhydrous THF (10 mL) were placed in a 20 mL microwave flask equipped with a spin bar. The reaction mixture was degassed by bubbling Ar through the solution for 15 min. Then,  $\text{RhCl}(\text{PPh}_3)_3$  (34.2 mg, 36.8  $\mu$ mol, 10 mol%) was added and the reaction flask was placed in the microwave reactor at 100°C for 6h. After standard workup, the product was purified by flash chromatography (cyclohexane/EtOAc: 1/1) to give 80 mg of product as white solid (64%).

**$^1\text{H-NMR}$**  (400 MHz,  $\text{CDCl}_3$ ,  $\delta$ /ppm): 7.41 (m, 2H), 7.26 (m, 2H), 7.24 (m, 2H), 7.18 (s, 1H), 7.15 (m, 2H), 3.66 (t,  $J = 6.9$  Hz, 2H), 3.02 (t,  $J = 7.3$  Hz, 2H), 2.80 (t,  $J = 6.9$  Hz, 4H), 2.67 (t,  $J = 7.3$  Hz, 2H), 2.42 (s, 6H), 1.98 (p,  $J = 7.3$  Hz, 2H).

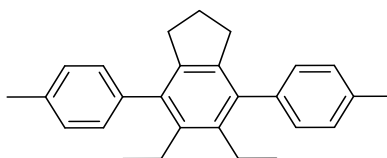
**$^{13}\text{C-NMR}$**  (101 MHz,  $\text{CDCl}_3$ ,  $\delta$ /ppm): 144.9, 140.3, 138.7, 138.1, 137.5, 137.0, 136.8, 134.8, 129.4, 128.9, 128.6, 64.0, 36.7, 33.5, 26.1, 21.6.

**MS** (EI, 70eV),  $m/z$  (%): 342 (78) [ $\text{M}^+$ ], 311 (100).

**HR-MS** (ESI): calc. for  $[\text{C}_{25}\text{H}_{26}\text{NaO}]^+$ :  $[\text{M}+\text{Na}]^+$  365.1876; found: 365.1878.

**IR** ( $\nu/\text{cm}^{-1}$ ): 3312, 3025, 2931, 1464, 1033.

**Mp**: 76.2°C.



### Synthesis of 42d

According to the general procedure, the linear precursor **41c** (100 mg, 0.367 mmol, 1.00 eq.), hex-3-yne (1.27 mL, 11.0 mmol, 30.0 eq.), anhydrous 2-propanol (10 mL), and anhydrous THF (10 mL) were placed in a 20 mL microwave flask equipped with a spin bar. The reaction mixture was degassed by bubbling Ar through the solution for 15 min. Then, RhCl(PPh<sub>3</sub>)<sub>3</sub> (34.3 mg, 36.7 μmol, 10 mol%) was added and the reaction flask was placed in the microwave reactor at 100°C for 6h. After standard workup, the product was purified by flash chromatography (cyclohexane) to give 96 mg of product as white solid (87%).

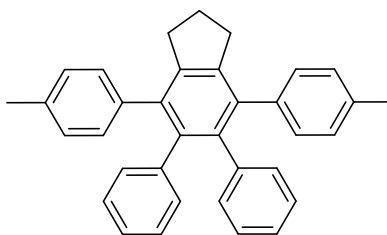
**<sup>1</sup>H-NMR** (400 MHz, CDCl<sub>3</sub>, δ/ppm): 7.22 (m, 4H), 7.17 (m, 4H), 2.59 (t, *J* = 7.20 Hz, 4H), 2.54 (q, *J* = 7.3 Hz, 4H), 2.41 (s, 6H), 1.85 (m, 2H), 0.97 (t, *J* = 7.3 Hz, 6H).

**<sup>13</sup>C-NMR** (101 MHz, CDCl<sub>3</sub>, δ/ppm): 140.6, 138.7, 138.3, 138.1, 136.1, 129.3, 129.0, 33.4, 24.8, 23.1, 21.5, 16.2.

**EA (%)**: calc. C 91.47 H 8.53, found C 91.10 H 8.55.

**MS** (EI, 70eV) *m/z* (%): 354 (100) [M<sup>+</sup>].

**IR** (ν /cm<sup>-1</sup>): 3044, 2966, 2920, 1517, 1458, 1438, 1370.



### Synthesis of 42e

According to the general procedure, the linear precursor **41c** (100 mg, 0.367 mmol, 1.00 eq.), diphenylacetylene (661 mg, 3.67 mmol, 30.0 eq.), anhydrous 2-propanol (10 mL), and anhydrous THF (10 mL) were placed in a 20 mL microwave flask equipped with a spin bar. The reaction mixture was degassed by bubbling Ar through the solution for 15 min. Then, RhCl(PPh<sub>3</sub>)<sub>3</sub> (34.3 mg, 36.7 μmol, 10 mol%) was added and the reaction flask was placed in the microwave reactor at 100°C for 6h. After standard workup, the product was purified by flash chromatography (cyclohexane) to lead 126 mg of product as white solid (76%).

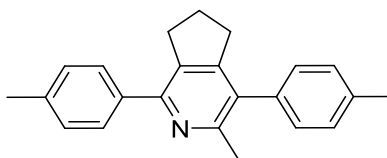
**<sup>1</sup>H-NMR** (400 MHz, CDCl<sub>3</sub>, δ/ppm): 6.97 (m, 8H), 6.84 (m, 6H), 6.78 (m, 4H), 2.87 (t, *J* = 7.4 Hz, 4H), 2.25 (s, 6H), 2.03 (p, *J* = 7.4 Hz, 2H).

**<sup>13</sup>C-NMR** (126 MHz, CDCl<sub>3</sub>, δ/ppm): 142.4, 140.7, 139.3, 137.7, 137.2, 135.5, 131.7, 129.9, 128.3, 126.7, 125.2, 33.7, 25.3, 21.3.

**EA (%)**: calc. C 93.29 H 6.71, found C 90.14 H 6.72.

**IR** (ν /cm<sup>-1</sup>): 3025, 2955, 1516, 1447, 1241.

**Mp**: 214-217°C.



### **Synthesis of 42g**

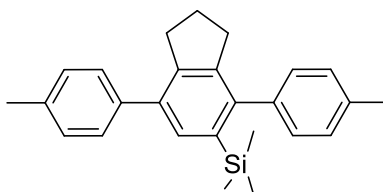
According to the general procedure, the linear precursor **41c** (100 mg, 0.367 mmol, 1.00 eq.), acetonitrile (600  $\mu$ L, 11.0 mmol, 30.0 eq.), anhydrous 2-propanol (10 mL), and anhydrous THF (10 mL) were placed in a 20 mL microwave flask equipped with a spin bar. The reaction mixture was degassed by bubbling Ar through the solution for 15 min. Then,  $\text{RhCl}(\text{PPh}_3)_3$  (34.3 mg, 36.7  $\mu$ mol, 10 mol%) was added and the reaction flask was placed in the microwave reactor at 100°C for 6h. After standard workup, the product was purified by flash chromatography (cyclohexane/EtOAc: 50/1) to give 17 mg of product as yellow solid (14%).

**$^1\text{H-NMR}$**  (400 MHz,  $\text{CDCl}_3$ ,  $\delta$ /ppm): 7.70 (m, 2H), 7.26 (m, 4H), 7.15 (m, 2H), 3.11 (t,  $J = 7.29$  Hz, 2H), 2.70 (t,  $J = 7.44$  Hz, 2H), 2.42 (s, 6H), 2.41 (s, 3H), 2.01 (p,  $J = 7.38$  Hz, 2H).

**$^{13}\text{C-NMR}$**  (101 MHz,  $\text{CDCl}_3$ ,  $\delta$ /ppm): 154.0, 153.8, 152.1, 137.8, 137.7, 136.9, 136.1, 134.5, 132.2, 129.3 (2C), 129.1 (2C), 129.0 (2C), 128.5 (2C), 33.1, 32.8, 25.8, 23.2, 21.5, 21.4.

**HR-MS** (ESI): calc. for  $[\text{C}_{23}\text{H}_{23}\text{NNa}]^+$ :  $[\text{M}+\text{Na}]^+$  336.1723; found: 336.2409.

**Mp**: 101.8°C.



### **Synthesis of 42f**

According to the general procedure, the linear precursor **41c** (150 mg, 0.551 mmol, 1.00 eq.), ethynyltrimethylsilane (784  $\mu\text{L}$ , 5.51 mmol, 10.0 eq.), anhydrous 2-propanol (3 mL), and anhydrous THF (3 mL) were placed in a 10 mL microwave flask equipped with a spin bar. The reaction mixture was degassed by bubbling Ar through the solution for 15 min. Then,  $\text{RhCl}(\text{PPh}_3)_3$  (52.4 mg, 55.1  $\mu\text{mol}$ , 10 mol%) was added and the reaction flask was placed in the microwave reactor at 100°C for 6h. After standard workup, the product was purified by flash chromatography (cyclohexane/EtOAc: 7/2) to give 152 mg of product as yellow solid (74.5%).

**$^1\text{H-NMR}$**  (400 MHz,  $\text{CDCl}_3$ ,  $\delta/\text{ppm}$ ): 7.48 (s, 1H), 7.43 (m, 2H), 7.28 (m, 2H), 7.23 (m, 2H), 7.18 (m, 2H), 3.05 (t,  $J = 7.4$  Hz, 2H), 2.69 (t,  $J = 7.4$  Hz, 2H), 2.44 (s, 6 H), 1.98 (p,  $J = 7.4$  Hz, 2H), 0.01 (s, 12H)

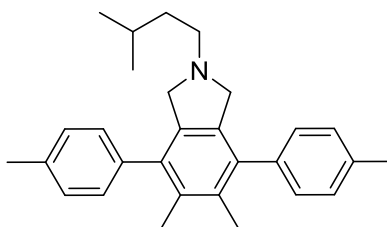
**$^{13}\text{C-NMR}$**  (101 MHz,  $\text{CDCl}_3$ ,  $\delta/\text{ppm}$ ): 144.2, 143.7, 142.8, 139.8, 138.8, 137.1, 136.6 (2C), 133.5 (2C), 129.5 (2C), 129.1 (2C), 128.7 (2C), 128.6 (2C), 33.5, 33.0, 25.5, 21.4, 21.3, 0.89 (3C).

**EA (%)**: calc. C 84.26 H 8.16, found C 83.93 H 8.18.

**MS** (EI, 70eV),  $m/z$  (%): 355.2 (100), 370.2 (41), 339.1 (25).

**IR** ( $\nu/\text{cm}^{-1}$ ): 3024, 2955, 2862, 2839, 1515, 1460, 1447, 1240, 1106, 1019.

**Mp**: 90°C.

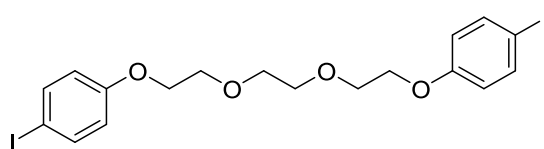


### Synthesis of 42h

According to the general procedure, the linear precursor **41b** (150 mg, 0.291 mmol, 1.00 eq.), hex-3-yne (1.00 mL, 8.73 mmol, 30.0 eq.), anhydrous 2-propanol (3 mL), and anhydrous THF (3 mL) were placed in a 10 mL microwave flask equipped with a spin bar. The reaction mixture was degassed by bubbling Ar through the solution for 15 min. Then, RhCl(PPh<sub>3</sub>)<sub>3</sub> (27 mg, 29.1 μmol, 10 mol%) was added and the reaction flask was placed in the microwave reactor at 100°C for 6h. After standard workup, the product was purified by flash chromatography (Cyclohexane/EtOAc: 9/1) to give 116 mg of product as yellow solid (85%).

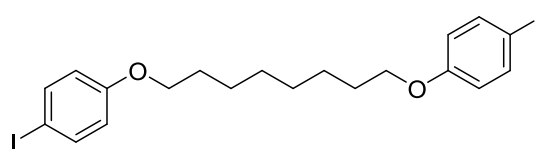
<sup>1</sup>H-NMR (400 MHz, CDCl<sub>3</sub>, δ/ppm): 7.22 (m, 4H), 7.16 (m, 2H), 3.59 (s, 4H), 2.52 (m, 4+2H), 2.41 (s, 6H), 1.53 (m, 1H), 1.27 (m, 2H), 0.95 (t, *J* = 7.4 Hz, 6H), 0.81 (d, *J* = 6.6 Hz, 6H).



**3.2.4 Macrocycle synthesis via Sonogashira****Synthesis of 1,2-bis[2-(4-iodophenoxy)ethoxy]ethane 48**

A suspension of 4-iodophenol (530 mg, 2.40 mmol, 2.20 eq.), di-*p*-tosylatetriethylene glycol (501 mg, 1.09 mmol, 1.00 eq.) and KOH (177 mg, 2.84 mmol, 2.60 eq.) in 5 mL *n*-butanol was heated to reflux for 3 days with vigorous stirring. The mixture was then allowed to cool and the precipitated was filtered off and washed with *n*-butanol to remove the unreacted starting material. The remaining solid was suspended in THF and the insoluble solid were removed by filtration. The organic phase was evaporated to afford 216 mg of the title product as light yellow solid in 36% yield.

<sup>1</sup>H-NMR (400 MHz, CDCl<sub>3</sub>, δ/ppm): 7.53 (m, 4H), 6.68 (m, 4H), 4.07 (m, 4H), 3.84 (m, 4H), 3.73 (s, 4H).

**Synthesis of 1,8-bis(4-iodophenoxy)octane 43**<sup>2</sup>

A solution of 1,8-dibromooctane (1.86 mL, 10.0 mmol, 1.00 eq), 4-iodophenol (4.51 g, 20.5 mmol, 2.05 eq) and KOH (1.16 g, 20.6 mmol, 2.06 eq) in *n*-butanol (25 mL) was refluxed overnight. Then, water and DCM were added until the formed precipitate was dissolved. Then, the organic layer was washed with 0.5 M NaOH (3x), with brine and dried over MgSO<sub>4</sub>. The crude residue was recrystallized from hot acetone yielding 2.96 g of title as a colorless solid (54%).

<sup>1</sup>H-NMR (400 MHz, CDCl<sub>3</sub>, δ/ppm): 7.56 (m, 4H), 6.69 (m, 4H), 3.93 (t, *J* = 6.5 Hz, 4H), 1.79 (m, 4H), 1.43 (m, 8H).

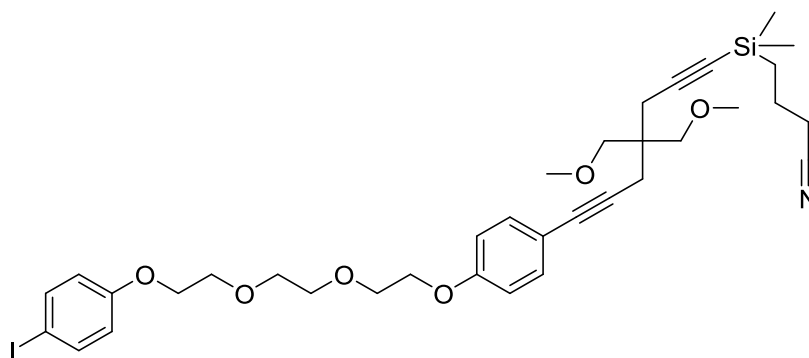
<sup>13</sup>C-NMR (126 MHz, CDCl<sub>3</sub>, δ/ppm): 159.2, 138.4, 117.1, 82.6, 68.2, 29.5, 29.3, 26.1.

EA (%): calc. C, 43.66; H, 4.40; found C, 43.73; H, 4.30.

MS (EI, 70 eV) *m/z*: 550 (100%) [M<sup>+</sup>], 330, 219, 69.

IR (ν /cm<sup>-1</sup>): 2936, 2903, 1585, 1569, 1484, 1471, 1284, 1239, 1226, 1173, 1100, 1029, 988.

Mp: 103-105°C.



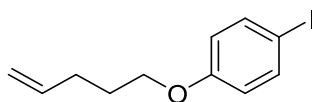
### Synthesis of 51

An oven dried two-necked flask was charged dry THF (10 mL). Then, Pd(PPh<sub>3</sub>)<sub>4</sub> (21.1 mg, 18.0 μmol, 10 mol%), CuI (6.87 mg, 36.1 μmol, 20 mol%), the diiodo compound **48** (100 mg, 0.180 mmol, 1.00 eq.), the monoprotected diyne **50a** (55.1 mg, 0.180 mmol, 1.00 eq.) and diisopropylamine (5.0 mL) were added. The solution was degassed by bubbling argon through the solution for 15 min. The reaction mixture was stirred at rt overnight. After that it was poured on sat. NH<sub>4</sub>Cl and extracted with EtOAc (3x). The organic layers were washed with sat. NH<sub>4</sub>Cl and brine, dried over MgSO<sub>4</sub> and the volatiles were evaporated under reduced pressure. The crude mixture was purified by column chromatography (cyclohexane/EtOAc: 7/3) to yield 38 mg of the product as yellow oil (29%).

<sup>1</sup>H-NMR (400 MHz, CDCl<sub>3</sub>, δ/ppm): 7.52 (m, 2H), 7.31 (m, 2H), 6.82 (m, 2H), 6.68 (m, 2H), 4.08 (m, 4H), 3.84 (m, 4H), 3.73 (s, 4H), 3.39 (s, 4H), 3.35 (s, 6H), 2.51 (s, 2H), 2.42 (s, 2H), 2.38 (m, 2H), 1.77 (m, 2H), 0.75 (m, 2H), 0.16 (s, 6H).

<sup>13</sup>C-NMR (101 MHz, CDCl<sub>3</sub>, δ/ppm): 159.1, 158.7, 138.6, 133.3, 120.2, 117.5, 116.6, 114.9, 105.7, 85.2, 85.2, 83.4, 82.8, 74.3, 71.3, 70.1, 70.1, 67.8, 67.9, 59.9, 42.7, 23.9, 23.4, 21.1, 20.9, 16.3, -1.2.

### 3.2.5 Synthesis of Macrocycle by Ring closure metathesis



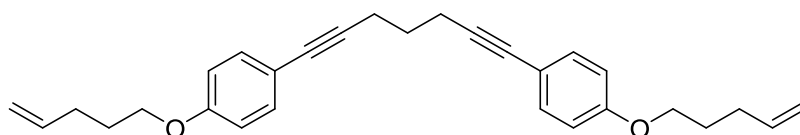
#### Synthesis of 1-iodo-4-(pent-4-en-1-yloxy)benzene 53

A solution of 4-iodophenol (500 mg, 2.27 mmol, 1.00 eq.), KOH (140 mg, 2.50 mmol, 1.10 eq.) and KI (11.3 mg, 68.0  $\mu\text{mol}$ , 3.00 mol%) in ethanol (5 mL) was stirred for 1h at reflux. Then, bromopentene (337 mg, 2.25 mmol, 1.00 eq.) was slowly added to the mixture and it was refluxed overnight. After removal of the solvent the residue was purified by column chromatography (cyclohexane/DCM: 7/2) to give 477 mg of the title product as a colorless oil (72%).

$^1\text{H-NMR}$  (400 MHz,  $\text{CDCl}_3$ ,  $\delta/\text{ppm}$ ): 7.54 (m, 2H), 6.67 (m, 2H), 5.84 (m, 1H), 5.05 (m, 1H), 5.00 (m, 1H), 3.93 (t  $J = 6.44$  Hz, 2H), 2.22 (m, 2H), 1.87 (m, 2H).

$^{13}\text{C-NMR}$  (101 MHz,  $\text{CDCl}_3$ ,  $\delta/\text{ppm}$ ): 159.3, 138.6, 138.1, 117.3, 115.7, 82.9, 67.7, 30.4, 28.7.

Analytical data are in accordance with the literature<sup>6</sup>



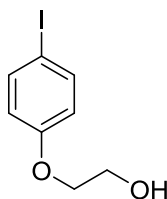
#### Synthesis of 1,7-bis[4-(pent-4-en-1-yloxy)phenyl]hepta-1,6-diyne 54

In a 50 mL flask under nitrogen 1-iodo-4-(pent-4-en-1-yloxy)benzene **53** (250 mg, 0.868 mmol, 2.00 eq.),  $\text{Pd}(\text{PPh}_3)_4$  (50.6 mg, 43.0  $\mu\text{mol}$ , 10.0 mol%), CuI (16.5 mg, 87.0  $\mu\text{mol}$ , 20.0 mol%), diisopropylamine (3 mL) and dry THF (20 mL) were added, argon was bubbled through the solution for 15 min. Then, hepta-1,6-diyne (40.0 mg, 0.434 mmol, 1.00 eq.) was added and the reaction mixture was stirred at rt overnight. At reaction completion, the reaction mixture was diluted with sat.  $\text{NH}_4\text{Cl}$  and EtOAc, the aqueous phase was extracted with EtOAc (3x) and the combined organic phases are washed with sat.  $\text{NH}_4\text{Cl}$ , dried over  $\text{Na}_2\text{SO}_4$  and concentrated under reduced pressure. The crude product was purified by column chromatography (cyclohexane/ DCM: 1/1) to give 107 mg of title compound as a yellow oil (60%).

$^1\text{H-NMR}$  (400 MHz,  $\text{CDCl}_3$ ,  $\delta/\text{ppm}$ ): 7.32 (m, 4H), 6.80 (m, 4H), 5.84 (dd,  $J = 10.2$  Hz,  $J = 17.0$  Hz, 2H), 5.06 (d,  $J = 17.0$  Hz, 2H), 5.00 (d,  $J = 10.2$  Hz, 2H), 3.95 (t,  $J = 6.5$  Hz, 4H), 2.56 (t,  $J = 7.01$  Hz, 4H), 2.22 (m, 4H), 1.87 (m, 6H).

$^{13}\text{C-NMR}$  (101 MHz,  $\text{CDCl}_3$ ,  $\delta/\text{ppm}$ ): 158.9, 138.1, 133.3, 116.3, 115.7, 114.8, 88.0, 81.3, 67.6, 30.5, 28.8, 28.6, 19.1.

### 3.2.6 Synthesis of macrocycle by ether formation



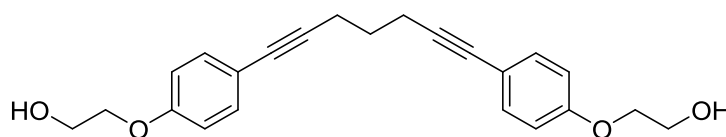
#### Synthesis of 2-(4-iodophenoxy)ethanol 57

To a mixture of 4-iodophenol (1.00 g, 4.50 mmol, 1.00 eq.) in DMF (5 mL) was added 2-bromoethanol (870 mg, 6.75 mmol, 1.50 eq.) and  $K_2CO_3$  (1.00 g, 6.75 mmol, 1.50 eq.). The reaction mixture was heated in a microwave reactor at 180 °C for 0.5 h. After cooling to rt the mixture was partitioned in DCM and water, the organic layer was dried over  $MgSO_4$  and concentrated under reduced pressure. The residue was purified by column chromatography (hexane/EtOAc, 6/4) to afford 824 mg of product as white solid (69%).

$^1H$ -NMR (400 MHz,  $CDCl_3$ ,  $\delta$ /ppm): 7.56 (m, 2H), 7.28 (m, 2H), 4.05 (m, 2H), 3.96 (m, 2H), 1.98 (t,  $J = 6.2$  Hz, 1H).

$^{13}C$ -NMR (101 MHz,  $CDCl_3$ ,  $\delta$ /ppm): 160.0, 138.7, 117.4, 83.4, 69.7, 61.8.

Analytical data are in accordance with the literature<sup>7</sup>

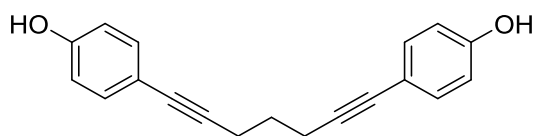


#### Synthesis of 1,7-bis[4-(2-hydroxyethoxy)phenyl]hepta-1,6-diyne 58

In a 50 mL flask under nitrogen 2-(4-iodophenoxy)ethanol **57** (680 mg, 2.45 mmol, 2.50 eq.),  $Pd(PPh_3)_4$  (114 mg, 97.9  $\mu$ mol, 10.0 mol%),  $CuI$  (37.3 mg, 196  $\mu$ mol, 20.0 mol%), diisopropylamine (4 mL) was added, then dry THF (10 mL) was added and argon was bubbled through the solution for 15 min. Hepta-1,6-diyne (90.2 mg, 979  $\mu$ mol, 1.00 eq.) was added and the reaction mixture was stirred at rt overnight. At reaction completion, the reaction mixture was diluted with sat.  $NH_4Cl$  and EtOAc, the aqueous phase was extracted with EtOAc (3x) and the combined organic phases were washed with sat.  $NH_4Cl$ , dried over  $Na_2SO_4$  and concentrated under reduced pressure. The crude product was purified by column chromatography (cyclohexane/EtOAc/MeOH: 1/1/5%) to give 230 mg of title compound as a yellow oil (65%).

$^1H$ -NMR (500 MHz,  $CDCl_3$ ,  $\delta$ /ppm): 7.33 (m, 4H), 6.82 (m, 4H), 4.05 (m, 2H), 3.94 (m, 2H), 2.56 (t,  $J = 7.0$  Hz, 4H), 2.41 (bs, 2H), 1.88 (p,  $J = 7.0$  Hz, 2H).

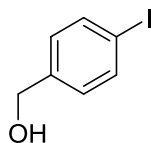
$^{13}C$ -NMR (126 MHz,  $CDCl_3$ ,  $\delta$ /ppm): 158.2 (2C), 133.1 (4C), 116.5 (2C), 114.5 (4C), 87.9 (2C), 80.9 (2C), 69.3 (2C), 61.4 (2C), 28.2 (1C), 18.8 (2C).



### Synthesis of 4,4'-(hepta-1,6-diyne-1,7-diyl)diphenol 61

An oven dried two-necked flask was charged with dry THF (20 mL) which was degassed by bubbling argon through the solvent for 15 min. Then, Pd(PPh<sub>3</sub>)<sub>4</sub> (253 mg, 217 μmol, 10.0 mol%), CuI (82.7 mg, 434 μmol, 20.0 mol%) were added under argon. Then 4-iodophenol (983 mg, 4.56 mmol, 2.10 eq.) and hepta-1,6-diyne (200 mg, 2.17 mmol, 1.00 eq.) were added, followed by diisopropylamine (8 mL). The reaction mixture was stirred overnight at rt. Afterwards, it was poured on sat. NH<sub>4</sub>Cl, and extracted with EtOAc (5x). Combined organic layers were washed with sat. NH<sub>4</sub>Cl, brine, dried over MgSO<sub>4</sub> and concentrated under reduced pressure. The dried product was black; it was purified on column chromatography (cyclohexane/EtOAc 3/7 and 0.5% MeOH). The product turned red with time (degradation).

<sup>1</sup>H-NMR (400 MHz, CDCl<sub>3</sub>, δ/ppm): 7.28 (m, 4H), 6.74 (m, 4H), 4.85 (s, 2H), 2.56 (t, *J* = 7.03 Hz, 4H), 1.88 (p, *J* = 7.03 Hz, 2H).



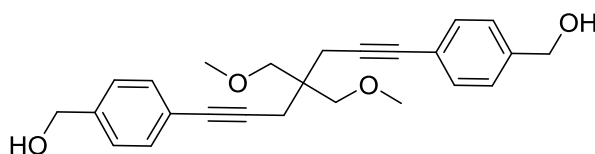
### Synthesis of (4-iodophenyl)methanol 64

A 2M solution of BH<sub>3</sub>•Me<sub>2</sub>S complex (31.4 mL, 62.7 mmol, 2.00 eq.) was added to a solution of 4-iodobenzoic acid (8.00 g, 31.6 mmol, 1.00 eq.) in dry THF (64 mL) under an inert atmosphere of argon. The reaction mixture was stirred over night and was then quenched with a 2 M HCl solution (160 mL). The mixture was then extracted with DCM (2x), the combined organic phases were washed with sat. NaHCO<sub>3</sub> (2x) and brine (2x). The organic phase was then dried over Na<sub>2</sub>SO<sub>4</sub> and the solvent was removed under reduced pressure to lead the product as white solid (99%).

<sup>1</sup>H-NMR (400 MHz, CDCl<sub>3</sub>, δ/ppm): 7.68 (m, 2H), 7.10 (m, 2H), 4.63 (d, *J* = 5.09 Hz, 2H), 1.85 (t, *J* = 5.50 Hz, 1H).

<sup>13</sup>C-NMR (101 MHz, CDCl<sub>3</sub>, δ/ppm): 140.8, 138.0, 129.2, 93.4, 65.0.

Analytical data are in accordance with the literature<sup>8</sup>



### **Synthesis of 65a**

An oven dried two-necked flask was charged with dry THF (120 mL) which was degassed by bubbling argon through the solvent. Pd(PPh<sub>3</sub>)<sub>4</sub> (1.30 g, 1.11 mmol, 10.0 mol%), CuI (425 mg, 2.23 mmol, 20.0 mol%) were added with argon counter flow. Then 40 mL diisopropylamine and (4-iodophenyl)methanol **64** (6.00 g, 25.6 mmol, 2.30 eq.) were added, followed by 4,4-bis(methoxymethyl)hepta-1,6-diyne **39a** (2.01 g, 11.1 mmol, 1.00 eq.). The solution was stirred at rt overnight. Afterwards, it was poured on sat NH<sub>4</sub>Cl, and extracted with EtOAc (3x). Combined organic layers were washed with sat. NH<sub>4</sub>Cl, brine, dried over MgSO<sub>4</sub> and concentrated under reduced pressure. The crude product was suspended in EtOAc and the insoluble solid was filtrated off. The filtrate was concentrated and purified by column chromatography (cyclohexane/EtOAc: 4/6) to give 4.12 g of product as yellow oil (94%).

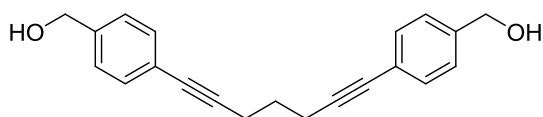
**<sup>1</sup>H-NMR** (400 MHz, CDCl<sub>3</sub>, δ/ppm): 7.39 (m, 4H), 7.28 (m, 4H), 4.68 (d, *J* = 5.66 Hz, 4H), 3.482.60 (t, *J* = 7.01 Hz, 4H), 1.91 (p, *J* = 6.92 Hz, 2H), 1.66 (t, *J* = 5.84 Hz, 2H).

**<sup>13</sup>C-NMR** (101 MHz, CDCl<sub>3</sub>, δ/ppm): 140.7, 132.15, 127.2, 123.5, 89.7, 81.5, 65.4, 28.3, 19.0.

**MS** (EI, 70eV) *m/z* (%): 392.2 (12) [M<sup>+</sup>], 347.2 (100), 315.1 (76), 285 (36), 255 (58).

**EA** (%): calc. C, 76.50; H, 7.19; found C, 76.24; H, 7.17.

**IR** (ν /cm<sup>-1</sup>): 3269, 3017, 2924, 2881, 2823, 1445, 1409, 1365, 1287, 1108, 1105, 999.

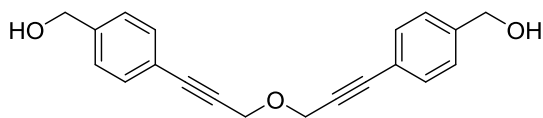


### Synthesis of 65c

An oven dried flask was charged with dry THF (250 mL) which was degassed by bubbling argon through the solvent for 15 min. Pd(PPh<sub>3</sub>)<sub>4</sub> (1.42 g, 1.22 mmol, 10.0 mol%), CuI (465 mg, 2.44 mmol, 20.0 mol%), 4-iodobenzylalcohol **64** (6.57 g, 28.1 mmol, 2.30 eq.), hepta-1,6-diyne (2.20 g, 12.2 mmol, 1.00 eq.) and diisopropylamine (44 mL) were added under argon. The reaction mixture was stirred overnight at rt. Afterwards, it was poured on sat. NH<sub>4</sub>Cl, and extracted with EtOAc (2x). The combined organic layers were washed with sat. NH<sub>4</sub>Cl, brine, dried over Na<sub>2</sub>SO<sub>4</sub> and concentrated under reduced pressure. The residue was suspended in EtOAc and the solid was filtrated off and washed with EtOAc. The filtrate was concentrated and purified by column chromatography (cyclohexane/EtOAc: 4/6) to afford 4.68 g of product as yellow solid (98%).

<sup>1</sup>H-NMR (400 MHz, CDCl<sub>3</sub>, δ/ppm): 7.39 (m, 4H), 7.28 (m, 4H), 4.68 (d, *J* = 5.7 Hz, 4H), 2.60 (t, *J* = 7.0 Hz, 4H), 1.91 (p, *J* = 6.9 Hz, 2H), 1.66 (t, *J* = 5.8 Hz, 2H).

<sup>13</sup>C-NMR (101 MHz, CDCl<sub>3</sub>, δ/ppm): 140.7, 132.15, 127.2, 123.5, 89.7, 81.5, 65.4, 28.3, 19.0.



### Synthesis of 65d

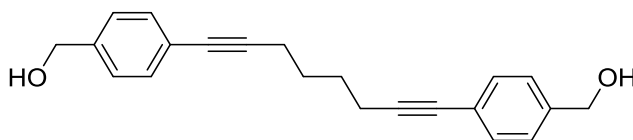
An oven dried two-necked flask was charged with dry THF (50 mL) which was degassed by bubbling argon through the solvent for 15 min. Pd(PPh<sub>3</sub>)<sub>4</sub> (598 mg, 513 μmol, 10.0 mol%), CuI (195 mg, 1.03 mmol, 20.0 mol%), 4-iodobenzylalcohol **64** (3.00 g, 12.8 mmol, 2.50 eq.) the diyne **39d** (93% in toluene, 519 mg, 5.13 mmol, 1.00 eq.) and diisopropylamine (20 mL) were added. The reaction mixture was stirred at rt overnight. After that it was poured on sat. NH<sub>4</sub>Cl and extracted with EtOAc (3x). The organic layers were washed with sat. NH<sub>4</sub>Cl (2x) and brine, dried over MgSO<sub>4</sub> and the volatiles were evaporated under reduced pressure. The crude mixture was purified by column chromatography (5/5/0.05, cyclohexane/EtOAc/MeOH) to afford 1.19 g of the titled compound as yellow solid (76%).

<sup>1</sup>H-NMR (400 MHz, CDCl<sub>3</sub>, δ/ppm): 7.45 (m, 4H), 7.31 (m, 4H), 4.70 (d, *J* = 5.9 Hz, 4H), 4.54 (s, 4H), 1.71 (t, *J* = 5.9 Hz, 2H).

<sup>13</sup>C-NMR (101 MHz, CDCl<sub>3</sub>, δ/ppm): 141.72, 132.4, 127.2, 122.1, 87.1, 84.8, 65.3, 57.9.

MS (EI, 70 eV) *m/z*: 245 (100%), 277 (82%), 306 (25%) [M<sup>+</sup>].

Mp: 108-111°C.



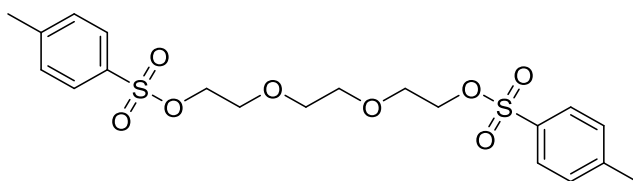
### Synthesis of 65b

An oven dried two-necked flask was charged with dry THF (40 mL). Then Pd(PPh<sub>3</sub>)<sub>4</sub> (434 mg, 372 μmol, 10.0 mol%), CuI (142 mg, 473 μmol, 20.0 mol%), 4-iodobenzylalcohol **64** (2.00 g, 8.55 mmol, 2.30 eq.) and the octa-1,7-diyne (394 mg, 3.72 mmol, 1.00 eq.) and diisopropylamine (15.0 mL) were added. The solution was degassed by bubbling argon through the mixture for 15 min. The reaction mixture was stirred at rt overnight. After that it was poured on sat. NH<sub>4</sub>Cl and extracted with EtOAc (3x). The organic layers were washed with sat. NH<sub>4</sub>Cl (2x) and brine, dried over MgSO<sub>4</sub> and the volatiles were evaporated under reduced pressure. The crude mixture was purified by column chromatography (5/5/0.05, cyclohexane/EtOAc/MeOH) to afford 810 mg of the titled compound as yellow solid (68%).

<sup>1</sup>H-NMR (400 MHz, CDCl<sub>3</sub>, δ/ppm): 7.39 (m, 4H), 7.28 (m, 4H), 4.68 (d, *J* = 5.9 Hz, 4H), 2.48 (t, *J* = 6.5 Hz, 4H), 1.79 (m, 4H), 1.64 (t, *J* = 5.9 Hz, 2H).

<sup>13</sup>C-NMR (101 MHz, CDCl<sub>3</sub>, δ/ppm): 140.6, 132.1, 127.2, 123.6, 90.3, 81.1, 65.4, 28.3, 19.4.

MS (EI, 70 eV) *m/z*: 318 (100%) [M<sup>+</sup>].



### Synthesis of 46

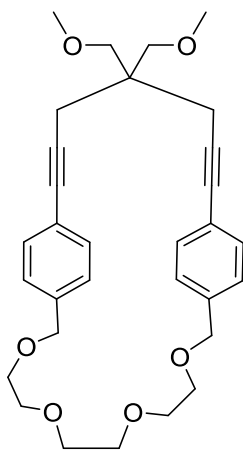
NaOH (7.99 g, 200 mmol, 3.00 eq.) dissolved in water (40 mL) and triethylenglycol (10 g, 66.6 mmol, 1.00 eq.) in THF (40 mL) were placed in a flask and the mixture was cooled to 0°C with magnetic stirring. To the mixture was added dropwise *p*-toluenesulfonyl chloride (22.9 g, 120 mmol, 1.80 eq.) in 40 mL THF over 2h (cooling below 5°C). The mixture was stirred at 0-5°C for an additional 2 h and then poured into ice-water (100 mL). The solidified tosylate was filtered and washed thoroughly with water and dried under vacuum. The crude product was recrystallized from MeOH to afford the product as white crystals (66%).

<sup>1</sup>H-NMR (400 MHz, CDCl<sub>3</sub>, δ/ppm): 7.77 (m, 4H), 7.33 (m, 4H), 4.12 (m, 4H), 3.64 (m, 4H), 3.51 (s, 4H), 2.43 (s, 6H).

<sup>13</sup>C-NMR (101 MHz, CDCl<sub>3</sub>, δ/ppm): 145.3, 133.3, 130.3, 128.4, 71.1, 69.6, 69.1.

Analytical data are in accordance with the literature<sup>9</sup>





### **Synthesis of macrocycle 66**

In an oven dried three necked flask was suspended NaH, 60% in mineral oil (129 mg, 5.10 mmol 4.00 eq.) in anhydrous THF (25 mL) and cooled in an ice bath under nitrogen. To this mixture a solution of the diol **65a** (500 mg, 1.27 mmol, 1.00 eq.) in 10 mL THF was added dropwise and stirred for an additionnal 3h at rt. Then a solution of triethylene glycol p-ditosylate **46** (584 mg, 1.27 mmol, 1.00 eq.) in THF (40 mL) was added dropwise. After the addition was complete the reaction mixture was heated to reflux overnight. After that, it was cooled to rt and quenched with water. The aqueous layer was extracted with DCM (3 x) and the combined organic phases were dried over MgSO<sub>4</sub> and the solvent was removed by rotatory evaporation. The crude product was purified by flash column chromatography (cyclohexane/EtOAc: 6/4) to yield 210 mg of product as yellow solid (33%).

**<sup>1</sup>H-NMR** (400 MHz, CDCl<sub>3</sub>, δ/ppm): 7.21 (m, 4H), 7.10 (m, 4H), 4.51 (s, 4H), 3.68 (m, 4H), 3.67 (s, 4H), 3.57 (m, 4H), 3.44 (s, 4H), 3.37 (s, 6H), 2.59 (s, 4H).

**<sup>13</sup>C-NMR** (101 MHz, CDCl<sub>3</sub>, δ/ppm): 138.2 (2C), 132.1(2C), 127.8 (4C), 123.6 (4C), 87.5 (2C), 83.3(2C), 75.8 (2C), 73.2 (2C), 71.3 (2C), 71.2 (2C), 69.8 (2C), 59.7 (2C), 42.0, 25.4 (2C).

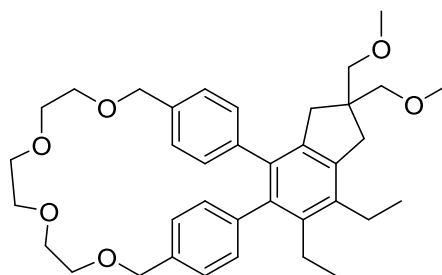
**HR-MS** (ESI): calc. for [C<sub>31</sub>H<sub>38</sub>NaO<sub>6</sub>]<sup>+</sup>: [M+Na]<sup>+</sup> 529.2561; found: 529.2566.

**Mp**: 77-80°C

### 3.2.7 Cycloaddition reaction on macrocycle 66

#### General procedure for the cycloaddition on strained precursor 66

The macrocyclic precursor **66** (100 mg, 1,00 eq.), the alkyne (10.0 eq.), anhydrous 2-propanol (3 mL), and THF (3 mL) were placed in a 5 mL microwave flask equipped with a spin bar. The reaction mixture was degassed by bubbling Ar through the solution for 15 min. Then, RhCl(PPh<sub>3</sub>)<sub>3</sub> (0.10 eq.) was added and the reaction flask was placed in the microwave reactor at 100°C for 6h. The reaction mixture was then diluted with DCM and washed with brine and dried over MgSO<sub>4</sub>. The volatiles were evaporated. The product was then purified by flash chromatography (cyclohexane/EtOAc) to lead product according to the yield in Table 3.



#### Synthesis of 68a

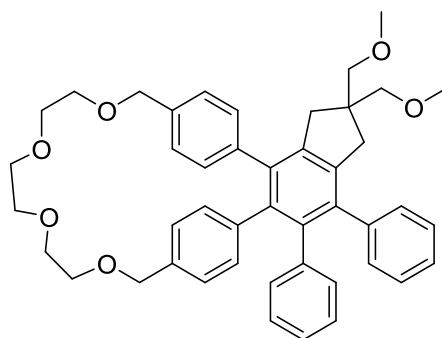
According to the general procedure, the macrocyclic precursor **66** (100 mg, 215 μmol, 1,00 eq.), hex-3-yne (742 μL, 6.44 mmol, 10.0 eq.), anhydrous 2-propanol (3.5 mL) and anhydrous THF (3.5 mL) were placed in a 10 mL microwave flask equipped with a spin bar. The reaction mixture was degassed by bubbling Ar through the solution for 15 min. Then, RhCl(PPh<sub>3</sub>)<sub>3</sub> (20.4 mg, 21.5 μmol, 10.0 mol %) was added and the reaction flask was placed in the microwave reactor at 100°C for 6 h. After the standard workup, the crude product was purified by flash chromatography (cyclohexane/EtOAc: 1/1) to give 107 mg of product as yellow oil (88%). Further purification by preparative TLC led to white crystal solid.

**<sup>1</sup>H-NMR** (400 MHz, CDCl<sub>3</sub>, δ/ppm): 7.08 (m, 2H), 7.02 (m, 2H), 6.97 (m, 2H), 6.86 (m, 2H), 4.47 (s, 2H), 4.42 (s, 2H), 3.64 (m, 8H), 3.60-3.41 (m, 4H), 3.36 (s, 4H), 3.34 (s, 6H), 2.93 (s, 2H), 2.70 (q, *J* = 7.52 Hz, 2H), 2.62 (s, 2H), 2.54 (q, *J* = 7.34 Hz, 2H), 1.23 (t, *J* = 7.52 Hz, 3H), 0.95 (t, *J* = 7.34 Hz, 3H).

**<sup>13</sup>C-NMR** (126 MHz, CDCl<sub>3</sub>, δ/ppm): 140.5, 140.0, 139.9, 139.6, 138.0, 137.8, 137.5, 136.2, 135.2, 135.1, 130.7 (2C), 129.7 (2C), 127.2 (2C), 127.1 (2C), 76.2 (2C), 73.0, 72.9, 70.5 (4C), 68.7, 68.2, 59.2 (2C), 47.1, 39.1, 37.9, 23.3, 22.8, 15.8, 14.5.

**MS** (MALDI-TOF): *m/z* = 587 [M], 612 [M+Na]<sup>+</sup>, 626 [M+K]<sup>+</sup>.

**HR-MS** (ESI): calc. for [C<sub>37</sub>H<sub>48</sub>NaO<sub>6</sub>]<sup>+</sup>: [M+Na]<sup>+</sup> 611.3343; found: 611.3345.



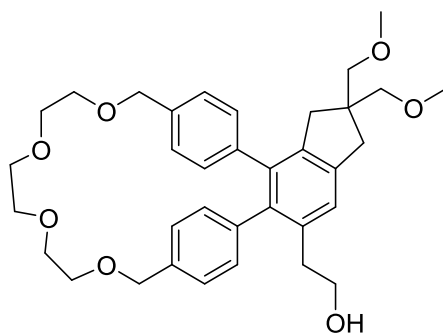
### **Synthesis of 68b**

According to the general procedure, the macrocyclic precursor **66** (100 mg, 0.197 mmol, 1.00 eq.), diphenylacetylene (355 mg, 1.97 mmol, 10.0 eq.), anhydrous 2-propanol (3 mL), and anhydrous THF (3 mL) were placed in a 5 mL microwave flask equipped with a spin bar. The reaction mixture was degassed by bubbling Ar through the solution for 15 min. Then,  $\text{RhCl}(\text{PPh}_3)_3$  (18.4 mg, 19.7  $\mu\text{mol}$ , 10.0 mol%) was added and the reaction flask was placed in the microwave reactor at 100°C for 6h. After standard workup, the crude product was purified by flash chromatography (cyclohexane/EtOAc: 1/1) to give 86 mg of product as colorless oil (64%).

**$^1\text{H-NMR}$**  (400 MHz,  $\text{CDCl}_3$ ,  $\delta/\text{ppm}$ ): 7.14 (m, 2H), 7.10 (m, 2H), 7.05(m, 2H), 6.98 (m, 2H), 6.82 (m, 8H), 6.71 (m, 2H), 4.47 (s, 2H), 4.31 (s, 2H), 3.63 (m, 8H), 3.47 (m, 2H), 3.37 (s, 4H), 3.32 (s, 6H), 3.31 (m, 2H), 2.83 (s, 2H), 2.79 (s, 2H).

**$^{13}\text{C-NMR}$**  (126 MHz,  $\text{CDCl}_3$ ,  $\delta/\text{ppm}$ ): 140.4 (2C), 140.3, 140.1, 140.0, 139.9, 139.3, 139.2, 137.9, 137.7, 135.8, 134.7, 131.7 (4C), 130.1 (2C), 130.0 (2C), 127.6 (2C), 127.5 (2C), 126.9 (2C), 126.8 (2C), 126.1, 125.3, 76.3 (2C), 73.2, 73.1, 70.9, 70.6 (3C), 68.9, 68.4, 59.4 (2C), 47.4, 39.5 (2C).

**HR-MS** (ESI): calc. for  $[\text{C}_{45}\text{H}_{52}\text{NO}_6]^+$ :  $[\text{M}+\text{NH}_4]^+$  702.3789; found: 702.3791.



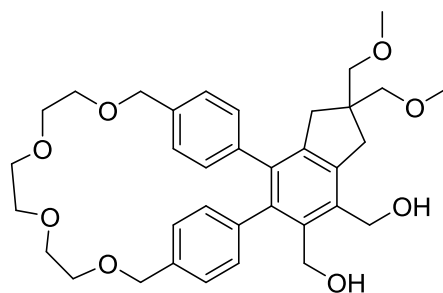
### **Synthesis of 68g:**

According to the general procedure, the macrocyclic precursor **66** (100 mg, 0.197 mmol, 1.00 eq.), 3-butyn-1-ol (149  $\mu$ L, 1.97 mmol, 10.0 eq.), anhydrous 2-propanol (3 mL), and anhydrous THF (3 mL) were placed in a 5 mL microwave flask equipped with a spin bar. The reaction mixture was degassed by bubbling Ar through the solution for 15 min. Then,  $\text{RhCl}(\text{PPh}_3)_3$  (18.4 mg, 19.7  $\mu$ mol, 10.0 mol%) was added and the reaction flask was placed in the microwave reactor at 100°C for 6h. After standard workup, the crude product was purified by flash chromatography (cyclohexane/EtOAc: 1/9) and preparative TLC (DCM/MeCN: 7/3) to give 48.1 mg of product as light yellow oil (43%)

**$^1\text{H-NMR}$**  (400 MHz,  $\text{CDCl}_3$ ,  $\delta$ /ppm): 7.16 (s, 1H), 7.09 (m, 2H), 7.05 (m, 2H), 6.93 (m, 2H), 6.87 (m, 2H), 4.45 (s, 2H), 4.43 (s, 2H), 3.64 (m, 8H), 3.44 (m, 2H), 3.39 (m, 2H), 3.35 (s, 2H), 3.34 (s, 2H), 3.33 (s, 6H), 2.94 (s, 2H), 2.78 (t,  $J = 6.9$  Hz, 2H), 2.63 (s, 2H), 1.26 (m, 2H).

**$^{13}\text{C-NMR}$**  (126 MHz,  $\text{CDCl}_3$ ,  $\delta$ /ppm \*): 141.3, 139.5, 139.4, 139.2 (2C), 138.8, 135.7, 135.5, 134.4, 130.7 (2H), 129.7 (2C), 127.6 (2C), 127.3 (2C), 125.2, 76.0 (2C), 72.9 (2C), 70.5 (4C), 68.6, 68.3, 63.3, 59.2 (2C), 47.5, 39.0, 38.7, 37.0.

**HR-MS** (ESI): calc. for  $[\text{C}_{35}\text{H}_{48}\text{NO}_7]^+$ :  $[\text{M}+\text{NH}_4]^+$  594.3425; found: 594.3425.



### **Synthesis of 68c:**

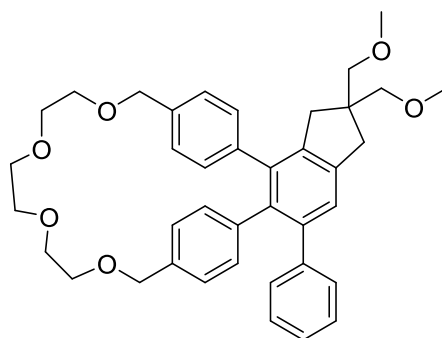
According to the general procedure, the macrocyclic precursor **66** (100 mg, 0.197 mmol, 1.00 eq.), 2-butyn-1,4-diol (172 mg, 1.97 mmol, 10.0 eq.), anhydrous 2-propanol (3 mL), and anhydrous THF (3 mL) were placed in a 5 mL microwave flask equipped with a spin bar. The reaction mixture was degassed by bubbling Ar through the solution for 15 min. Then,  $\text{RhCl}(\text{PPh}_3)_3$  (18.4 mg, 19.7  $\mu\text{mol}$ , 10.0 mol%) was added and the reaction flask was placed in the microwave reactor at 100°C for 6 h. After standard workup, the crude product was purified by flash chromatographies (EtOAc/Cyclohexane: 9/1) and (EtOAc/Cyclohexane 1/1 +10% MeOH) to give 69 mg of product as light yellow oil (59%)

**$^1\text{H-NMR}$**  (400 MHz,  $\text{CDCl}_3$ ,  $\delta/\text{ppm}$ ): 7.09 (m, 2H), 7.06 (m, 2H), 6.97 (m, 2H), 6.84 (m, 2H), 4.80 (s, 2H), 4.55 (s, 2H), 4.45 (s, 2H), 4.43 (s, 2H), 3.63 (m, 8H), 3.43 (m, 2H), 3.38 (m, 2H), 3.35 (s, 4H), 3.31 (s, 6H), 3.06 (s, 2H), 3.14 (bs, 1H), 2.80 (bs, 1H), 2.68 (s, 2H).

**$^{13}\text{C-NMR}$**  (126 MHz,  $\text{CDCl}_3$ ,  $\delta/\text{ppm}$ ): 141.2 (2C), 140.7, 139.3, 139.0, 138.6, 136.1, 136.0, 135.7, 135.3, 130.7 (2C), 129.6 (2C), 127.5 (4C), 76.0 (2C), 73.0, 70.4 (4C), 68.8, 68.5, 60.8, 60.5, 59.2 (2C), 47.2, 39.4, 37.4.

**MS** (ESI)  $m/z$  : 615  $[\text{M}+\text{Na}]^+$ , 631 $[\text{M}+\text{K}]^+$ .

**HR-MS** (ESI): calc. for  $[\text{C}_{35}\text{H}_{44}\text{NaO}_8]^+$ :  $[\text{M}+\text{Na}]^+$  615.2928; found: 615.2934.



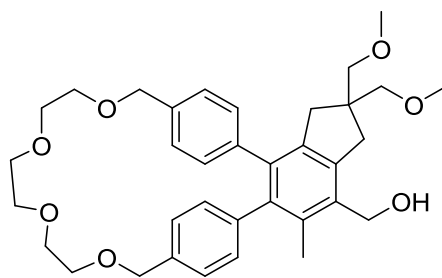
### **Synthesis of 68d:**

According to the general procedure, the macrocyclic precursor **9** (100 mg, 0.197 mmol, 1.00 eq.), phenylacetylene (217  $\mu$ L, 1.97 mmol, 10.0 eq.), anhydrous 2-propanol (3 mL), and anhydrous THF (3 mL) were placed in a 5 mL microwave flask equipped with a spin bar. The reaction mixture was degassed by bubbling Ar through the solution for 15 min. Then,  $\text{RhCl}(\text{PPh}_3)_3$  (18.4 mg, 19.7  $\mu$ mol, 10.0 mol%) was added and the reaction flask was placed in the microwave reactor at 100°C for 6h. After standard workup, the crude product was purified by flash chromatography (cyclohexane/EtOAc: 1/1) to lead 80 mg of product as light yellow oil (67%).

**<sup>1</sup>H-NMR** (400 MHz,  $\text{CD}_2\text{Cl}_2$ ,  $\delta$ /ppm): 7.21 (s, 1H), 7.12 (m, 2H), 7.10 (m, 5H), 6.92 (m, 2H), 6.89 (m, 2H), 6.75 (m, 2H), 4.43 (s, 2H), 4.31 (s, 2H), 3.57 (m, 8H), 3.46 (m, 2H), 3.36 (m, 2H), 3.35 (s, 2H), 3.35 (s, 2H), 3.32 (s, 6H), 2.97 (s, 2H), 2.68 (s, 2H).

**<sup>13</sup>C-NMR** (126 MHz,  $\text{CDCl}_3$ ,  $\delta$ /ppm \*): 143.0, 140.9 (2C), 140.0 (2C), 139.0, 138.0, 136.5, 135.8, 132.0 (2C), 130.2 (2C), 130.1 (2C), 127.6 (5C), 127.1 (2C), 126.1, 76.4 (2C), 73.0 (2C), 70.5 (4C), 68.9, 69.2, 59.2 (2C), 48.4, 39.4, 39.1.

**HR-MS** (ESI): calc. for  $[\text{C}_{39}\text{H}_{44}\text{NaO}_6]^+$ :  $[\text{M}+\text{Na}]^+$  631.3030; found: 631.3023.



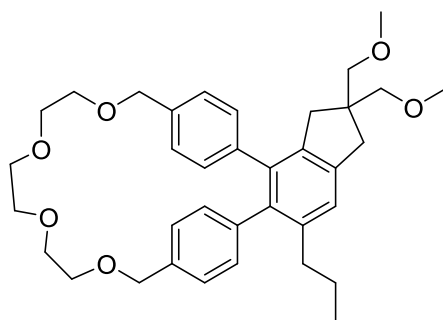
### **Synthesis of 68h:**

According to the general procedure, the macrocyclic precursor **66** (100 mg, 0.197 mmol, 1.00 eq.), 2-butyne-1-ol (153  $\mu$ L, 1.97 mmol, 10.0 eq.), anhydrous 2-propanol (3 mL), and anhydrous THF (3 mL) were placed in a 5 mL microwave flask equipped with a spin bar. The reaction mixture was degassed by bubbling Ar through the solution for 15 min. Then,  $\text{RhCl}(\text{PPh}_3)_3$  (18.4 mg, 19.7  $\mu$ mol, 10.0 mol%) was added and the reaction flask was placed in the microwave reactor at 100°C for 6h. After standard workup, the crude product was purified by flash chromatography (cyclohexane/EtOAc: 1/9) to give 73 mg of product as light yellow oil (64%)

**$^1\text{H-NMR}$**  (400 MHz,  $\text{CDCl}_3$ ,  $\delta$ /ppm): 7.09 (m, 2H), 7.04 (m, 2H), 6.89 (m, 2H), 6.85 (m, 2H), 4.77 (s, 2H), 4.46 (s, 2H), 4.42 (s, 2H), 3.63 (m, 8H), 3.43 (m, 2H), 3.37 (m, 2H), 3.35 (s, 2H), 3.35 (s, 2H), 3.32 (s, 6H), 3.05 (s, 2H), 2.65 (s, 2H), 2.23 (s, 3H).

**$^{13}\text{C-NMR}$**  (126 MHz,  $\text{CDCl}_3$ ,  $\delta$ /ppm \*): 140.6, 140.2, 140.0, 139.4, 138.3, 138.2, 135.4, 135.2, 133.5 (2C), 130.6 (2C), 129.7 (2C), 127.6 (2C), 127.3 (2C), 76.0 (2C), 72.9 (2C), 70.5 (4C), 68.7, 68.4, 60.8, 59.1 (2C), 47.0, 39.2, 37.6, 16.7.

**HR-MS** (ESI): calc. for  $[\text{C}_{35}\text{H}_{48}\text{NO}_7]^+$ :  $[\text{M}+\text{NH}_4]^+$  594.3425; found: 594.3429.

**Synthesis of 68f:**

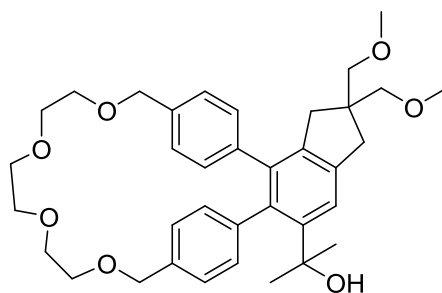
According to the general procedure, the macrocyclic precursor **66** (100 mg, 0.197 mmol, 1.00 eq.), 1-pentyn (195  $\mu$ L, 1.97 mmol, 10.0 eq.), anhydrous 2-propanol (3 mL), and anhydrous THF (3 mL) were placed in a 5 mL microwave flask equipped with a spin bar. The reaction mixture was degassed by bubbling Ar through the solution for 15 min. Then, RhCl(PPh<sub>3</sub>)<sub>3</sub> (18.4 mg, 19.7  $\mu$ mol, 10.0 mol%) was added and the reaction flask was placed in the microwave reactor at 100°C for 6h. After standard workup, the crude product was purified by flash chromatography (cyclohexane/EtOAc: 1/1) to give 73 mg of product as colorless oil (64%)

**<sup>1</sup>H-NMR** (400 MHz, CDCl<sub>3</sub>,  $\delta$ /ppm): 7.12 (s, 1H), 7.08 (m, 2H), 7.04 (m, 2H), 6.92 (m, 2H), 6.87 (m, 2H), 4.47 (s, 2H), 4.43 (s, 2H), 3.64 (m, 8H), 3.44 (m, 2H), 3.37 (m, 2H), 3.35 (s, 2H), 3.35 (s, 2H), 3.33 (s, 6H), 2.93 (s, 2H), 2.63 (s, 2H), 2.43 (m, 2H), 1.46 (m, 2H), 0.79 (t,  $J = 7.3$  Hz, 3H).

**<sup>13</sup>C-NMR** (126 MHz, CDCl<sub>3</sub>,  $\delta$ /ppm \*): 141.1, 139.8 (2C), 139.0, 138.6, 138.3, 138.2, 135.4 (2C), 135.3, 130.7 (2C), 129.7, 127.4 (2C), 127.3 (2C), 124.5, 76.1 (2C), 73.1, 73.0, 70.5 (4C), 68.7, 68.2, 59.2 (2C), 47.7, 39.0, 38.8, 35.9, 24.5, 14.1.

**HR-MS** (ESI): calc. for [C<sub>36</sub>H<sub>46</sub>NaO<sub>6</sub>]<sup>+</sup>: [M+Na]<sup>+</sup> 597.3187; found: 597.3187.





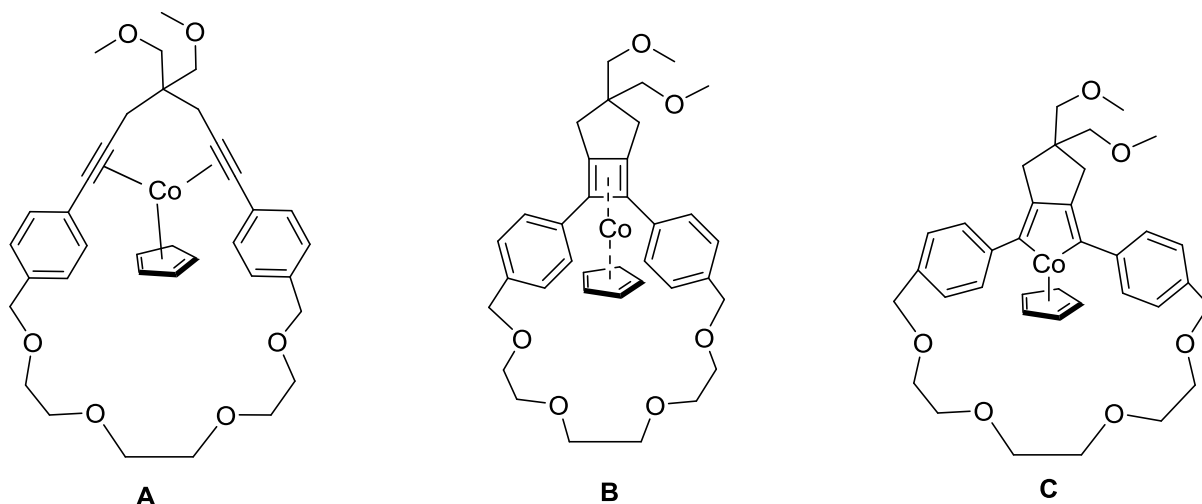
### **Synthesis of 68e:**

According to the general procedure, the macrocyclic precursor **66** (100 mg, 0.197 mmol, 1.00 eq.), 2-methyl-3-butyn-2-ol (193  $\mu$ L, 1.97 mmol, 10.0 eq.), anhydrous 2-propanol (3 mL), and anhydrous THF (3 mL) were placed in a 5 mL microwave flask equipped with a spin bar. The reaction mixture was degassed by bubbling Ar through the solution for 15 min. Then,  $\text{RhCl}(\text{PPh}_3)_3$  (18.4 mg, 19.7  $\mu$ mol, 10.0 mol%) was added and the reaction flask was placed in the microwave reactor at 100°C for 6h. After standard workup, the crude product was purified by flash chromatography (cyclohexane/EtOAc: 1/9) to give 86 mg of product as colorless oil (64%)

**$^1\text{H-NMR}$**  (400 MHz,  $\text{CDCl}_3$ ,  $\delta$ /ppm): 7.47 (s, 1H), 7.07 (m, 2H), 7.02 (m, 4H), 6.81 (m, 2H), 4.44 (s, 2H), 4.41 (s, 2H), 3.65 (m, 8H), 3.44 (m, 2H), 3.35 (m, 2H), 3.34 (s, 2H), ), 3.33 (s, 2H), 3.32 (s, 6H), 2.95 (s, 2H), 2.52 (s, 2H), 1.89 (bs, 1H), 1.48 (s, 6H).

**$^{13}\text{C-NMR}$**  (126 MHz,  $\text{CDCl}_3$ ,  $\delta$ /ppm \*): 144.8, 141.1, 140.4, 140.0, 139.4, 136.5, 136.1, 135.4, 131.5 (2C), 129.5, 127.1 (4C), 126.4 (2C), 121.3, 76.0 (2C), 74.3, 73.0, 72.9, 70.5 (4C), 68.7, 68.3, 59.2 (2C), 47.7, 39.0, 38.9, 32.7 (2C)

**HR-MS** (ESI): calc. for  $[\text{C}_{36}\text{H}_{46}\text{NaO}_7]^+$ :  $[\text{M}+\text{NH}_4]^+$  6.13.3136; found: 6.13.3139.



### Cobalt complex synthesis:

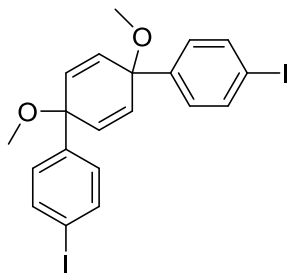
A degassed solution of macrocycle **66** (1.00 eq., 20.0 mg, 0.04 mmol) 2-butyne-1,4-diol (20.0 eq., 68.7 mg, 0.790 mmol) and anhydrous mesitylene (10 mL) was heated at 140 °C for 20 min. Then, cyclopenta-dienylcobalt dicarbonyl (2.00 eq., 0.024 mL, 0.1 mmol) was added and the mixture was heated at 140°C for 24 h. After the reaction mixture was cooled to rt, a solid precipitated and was filtered off. The residue was purified by column chromatography (cyclohexane/EtOAc: 4/6) to afford 14 mg of complex **A**, **B** or **C** as yellow oil (54%).

<sup>1</sup>H-NMR (400 MHz, CDCl<sub>3</sub>, δ/ppm): 7.31 (m, 4H), 7.20 (m, 4H), 4.66 (s, 5H), 4.63 (d, *J* = 13.5 Hz, 2H), 4.44 (d, *J* = 13.5 Hz, 2H), 3.72 (s, 2H), 3.60 (m, 2H), 3.54 (s, 4H), 3.50 (m, 2H), 3.46 (s, 3H), 3.35 (bs, 5H), 2.41 (d, *J* = 16.7 Hz 2H), 2.15 (d, *J* = 16.7 Hz, 2H).

<sup>13</sup>C-NMR (125 MHz, CDCl<sub>3</sub>, δ/ppm): 137.7, 136.1, 127.7, 127.2, 84.7, 81.8, 76.7, 72.5, 70.7, 70.1, 67.9, 66.9, 59.3, 60.0, 32.8.

MS (ESI), *m/z*: 653.3.

### 3.2.8 Synthesis of substituted CPP Jasti strategy



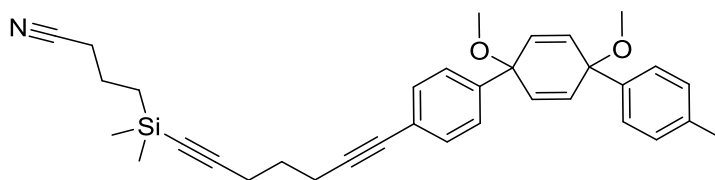
#### Synthesis of the building block76

In a dried 500 mL flask cooled to  $-78^{\circ}\text{C}$ , was added 200 mL dry THF, 1,4-diiodobenzene (5.00 g 15.2 mmol, 2.05 eq.), then, *n*-BuLi (2.5 M in hexane, 6.51 mL, 16.3 mmol, 2.20 eq.) was added dropwise. The mixture was stirred for 25 min, then 1,4-benzoquinone (799 mg, 7.39 mmol, 1.00 eq) was added portion-wise as a solid. The resulting mixture was further stirred 1.5 h after which the mixture was poured on 100 mL ice and  $\text{Et}_2\text{O}$  was added. This biphasic mixture was stirred for another 1.5h. The layers were separated and the aqueous layer was extracted with  $\text{Et}_2\text{O}$ . Combined organic layers were dried over  $\text{Na}_2\text{SO}_4$  and concentrated under reduced pressure. This crude material was subjected directly to the next step:

In a 100 mL flask was added NaH (60% in mineral oil, 800 mg, 18.5 mmol, 2.50 eq.) in 25 mL dry THF. The crude diol was added as a THF solution at  $0^{\circ}\text{C}$ , under nitrogen. The mixture was stirred for 30 min, then MeI (1.86 mL, 29.6, 4.00 eq.) was added. The mixture was allowed to warm up to rt and was stirred overnight. Then, water was added and the layers were separated. The aqueous layer was extracted with  $\text{Et}_2\text{O}$  (3x), combined organic layers were dried over  $\text{Na}_2\text{SO}_4$  and concentrated under reduced pressure. The crude product was purified by column chromatography (cyclohexane/ $\text{EtOAc}$ : 9/1) and recrystallization in hexane (60 mL) to give 1.15 g of the product as white crystals (29%).

$^1\text{H-NMR}$  (400 MHz,  $\text{CDCl}_3$ ,  $\delta$ /ppm): 7.64 (m, 4H), 7.11 (m, 4H), 6.05 (s, 4H), 3.42 (s, 6H).

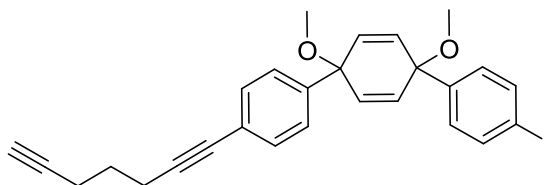
Analytical data are in accordance with the literature<sup>10,11</sup>



### **Synthesis of 96:**

In an oven-dried flask was added the iodo-compound **76** (1.14 g, 2.09 mmol, 1.00 eq.), 50 mL dry THF and the alkyne **50c** (0.455 g, 2.09 mmol, 1.00 eq.). Nitrogen was bubbled through the mixture for 10 min. Then Pd(PPh<sub>3</sub>)<sub>4</sub> (242 mg, 0.209 mmol, 10.0 mol%) and CuI (79.8 mg, 0.419 mmol, 20.0 mol%) were added with nitrogen counterflow followed by 8 mL diisopropylamine. The reaction mixture was stirred overnight at rt. Afterwards, it was poured on sat. NH<sub>4</sub>Cl, and extracted with ethyl acetate (3x). The combined organic layers were washed with sat. NH<sub>4</sub>Cl, brine, dried over MgSO<sub>4</sub> and concentrated under reduced pressure. The crude product was purified on column chromatography to lead 739 mg of the title compound (56%).

<sup>1</sup>H NMR (400 MHz, CDCl<sub>3</sub>, δ/ppm): 7.62 (m, 2H), 7.34 (m, 2H), 7.28 (m, 2H), 7.10 (m, 2H), 6.09 (m, 2H), 6.04 (m, 2H), 3.42 (s, 6 H), 2.51 (t, *J* = 7.0 Hz, 2H), 2.40 (m, 4H), 1.82 (m, 2H), 1.76 (m, 2H), 0.75 (m, 2H), 0.16 (s, 6H).

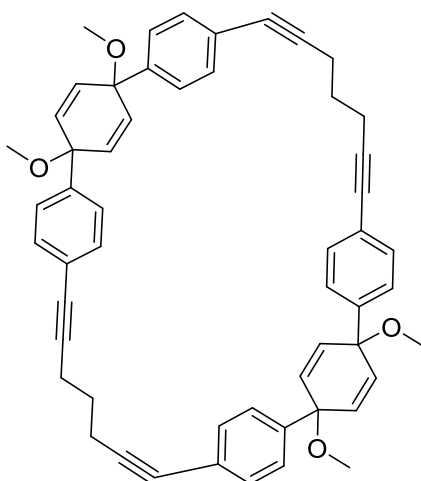


### **Synthesis of 97:**

Compound **96** (4.57 g, 7.21 mmol, 1.00 eq.) was dissolved in dry THF (80 mL), and distributed equally in 4 flasks. Then the mixtures were degassed by bubbling nitrogen through the solution for 30 min and TBAF (1 M in THF, 70 μL, 0.07 mmol) was added. The reaction mixtures were stirred for 30 min at rt after which they were combined and diluted with EtOAc and brine. The aqueous phase was extracted with EtOAc (3x) and the combined organic layers were dried over Na<sub>2</sub>SO<sub>4</sub>. After removal of the solvent under reduced pressure the crude product was purified by column chromatography (cyclohexane/EtOAc: 9/1) to give 2.50 g of product as a yellow oil (68%).

<sup>1</sup>H NMR (400 MHz, CDCl<sub>3</sub>, δ/ppm): 7.62 (m, 2H), 7.34 (m, 2H), 7.28 (m, 2H), 7.10 (m, 2H), 6.09 (m, 2H), 6.04 (m, 2H), 3.42 (s, 6 H), 2.54 (t, *J* = 7.0 Hz, 2H), 2.37 (m, 4H), 1.99 (t, *J* = 2.6 Hz, 1H), 1.83 (q, *J* = 7.0 Hz, 2H).

<sup>13</sup>C-NMR (126 MHz, CDCl<sub>3</sub>, δ/ppm): 143.1, 142.6, 137.5, 133.5, 133.2, 131.7, 128.1, 125.9, 123.2, 93.4, 89.4, 83.6, 81.1, 74.7, 74.6, 69.1, 52.1, 27.7, 27.0, 18.6, 17.7.

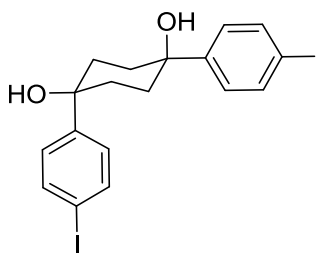


### **Synthesis of 98:**

An oven dried flask was charged with dry THF (5 mL). Then, **97** (80 mg, 157  $\mu\text{mol}$ , 1.00 eq.), CuI (5.99 mg, 31.0  $\mu\text{mol}$ , 20.0 mol%), Pd(PPh<sub>3</sub>)<sub>4</sub> (18.2 mg, 15.7  $\mu\text{mol}$ , 10.0 mol%) and 0.6 mL diisopropylamine were added under inert atmosphere. The flask was degassed for 15 min by bubbling nitrogen through the solution, and stirred at rt overnight. Afterwards, the solution was quenched with sat. NH<sub>4</sub>Cl solution, the two phases were separated and the aqueous layer was extracted with ethyl acetate (3x). Combined organic layers were washed with sat. NH<sub>4</sub>Cl, brine, dried over Na<sub>2</sub>SO<sub>4</sub> and concentrated under reduced pressure. The residue was purified by column chromatography (cyclohexane/EtOAc: 8/2) to yield the not totally pure product in around 12% yield.

<sup>1</sup>H NMR (400 MHz, CDCl<sub>3</sub>):  $\delta$  7.35 (m, 4H), 7.27 (m, 4H), 6.08 (s, 8H), 3.42 (s, 12H), 2.57 (t,  $J$  = 7.0 Hz, 8H), 1.89 (m, 4H).

### 3.2.9 Synthesis of Substituted CPP Itami strategy



#### Cis selective synthesis of 82

LiCl (3.56 g, 83.2 mmol, 5.2 eq.) and predried  $\text{CeCl}_3$  (10.3 g, 41.6 mmol, 2.60 eq.) were added in a 1 L three necks flask under nitrogen and heated to  $150^\circ\text{C}$  under vacuum for 2h. Then, 200 mL dry THF were added under nitrogen and the suspension was stirred at  $45^\circ\text{C}$  overnight.

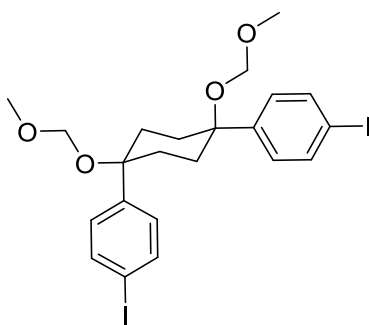
To a solution of 1,4-diiodobenzene (13.2 g, 40.0 mmol, 2.50 eq.) in 400 mL dry THF was added *n*-BuLi (1.6 M in hexane, 25.0 mL, 40.0 mmol, 2.50 eq.) dropwise at  $-70^\circ\text{C}$ . The resulting mixture was stirred 1h at  $-70^\circ$  and then was added dropwise to the previously prepared LiCl  $\text{CeCl}_3$  complex solution at  $-70^\circ\text{C}$ . At the end of the addition the mixture was further stirred at  $-70^\circ\text{C}$  for 1h at  $0^\circ\text{C}$  for 30 min. Then, 1,4-cyclohexanedione (1.79 g, 16.0 mmol, 1.00 eq.) in 50 mL dry THF was added dropwise. The mixture was stirred at  $0^\circ\text{C}$  for 30 min. Then sat.  $\text{NH}_4\text{Cl}$  was added and the mixture was extracted with EtOAc (3x). Combined organic layers were washed with brine, dried over  $\text{Na}_2\text{SO}_4$  and concentrated under reduced pressure. The crude product was purified by column chromatography (cyclohexane/EtOAc: 3/7) to give 7.38 g of product as white solid (89%).

#### Non cis selective synthesis of 82

In a 1 L two-necked flask 1,4-diiodobenzene (21.6 g, 65.5 mmol, 2.50 eq.) was added in 300 mL dry THF under argon. Then *n*-BuLi (2.5 M in hexane, 26.2 mL, 65.5 mmol, 2.50 eq.) was added dropwise, keeping the temperature below  $-50^\circ\text{C}$ . At the end of the addition the reaction mixture was stirred at  $-60^\circ\text{C}$  for 1h. Then 1,4-cyclohexanedione (3.00 g, 26.2 mmol, 1.00 eq.) in 125 mL dry THF was added dropwise at  $-60^\circ\text{C}$ . The reaction was further stirred at rt for 1h30. When the reaction was complete, the mixture was quenched with  $\text{H}_2\text{O}$ , extracted with EtOAc (3x), dried over  $\text{Na}_2\text{SO}_4$  and concentrated under reduced pressure. The crude product was purified by column chromatography (cyclohexane/EtOAc: 3/7), the impure fraction was again filtrated after concentration to give 5.22 g of pure *cis*-product as white solid (38%).

$^1\text{H NMR}$  (400 MHz,  $\text{CDCl}_3$ ,  $\delta/\text{ppm}$ ): 7.67 (m, 4H), 7.21 (m, 4H), 2.06 (s, 8H), 1.70 (s, 2H).

Analytical data are in accordance with the literature<sup>12,13</sup>

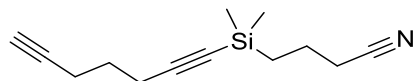


### Synthesis of 83

In a flask was placed **82** (5.22 g, 10.0 mmol, 1.00 eq.) in 50 mL dry DCM and N-ethyl-diisopropylamine (7.00 mL, 40.1 mmol, 4.00 eq.) under argon. To this mixture was added dropwise MOMCl (3.00 mL, 40.1 mmol, 4.00 eq.). The mixture was stirred at rt overnight. After this, sat. NH<sub>4</sub>Cl was added and the mixture was extracted with DCM (3x). The combined organic phases were dried over Na<sub>2</sub>SO<sub>4</sub> and concentrated under reduced pressure. The crude product was purified by column chromatography (cyclohexane/EtOAc: 7/3) to afford 6.01 g of product as white solid (99%)

<sup>1</sup>H NMR (400 MHz, CDCl<sub>3</sub>, δ/ppm): 7.67 (m, 4H), 7.21 (m, 4H), 4.45 (s, 4H), 3.40 (s, 6H), 2.28 (bs, 4H), 2.01 (bs, 4H), 1.70 (s, 2H).

Analytical data are in accordance with the literature<sup>12</sup>



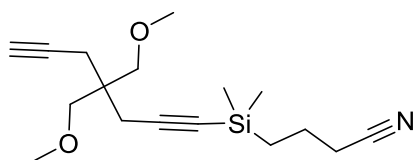
### Synthesis of CPDMS-hepta-1,6-diyne 50c

Hepta-1,6-diyne (8.70 mL, 76.0 mmol, 1.30 eq.) was dissolved in 180 mL dry THF and ethylmagnesium bromide (1 M in THF, 40.0 mL and 3 M in Et<sub>2</sub>O, 8.50 mL, 65.5 mmol, 1.10 eq.) was added dropwise at 0°C. The mixture was stirred for 30 min at 0°C and 1h at rt, then CPDMS-Cl (9.50 mL, 57.9 mmol, 1.00 eq.) was added dropwise at 0°C. After 1d at rt the solution was slowly quenched with water and diluted with EtOAc. After workup, the crude oil was purified by column chromatography on silica gel (EtOAc/hexane 1/15 to 1/1) to yield 7.60 g of the title compound as colorless oil (60%).

<sup>1</sup>H NMR (400 MHz, CDCl<sub>3</sub>, δ/ppm): 2.39 (t, *J* = 7.0 Hz, 2H), 2.35 (t, *J* = 7.1 Hz, 2H), 2.29 (td, *J* = 7.1 Hz, *J* = 2.4 Hz, 2H), 1.96 (td, *J* = 2.6 Hz, *J* = 0.6 Hz, 1H), 1.74 (m, 4H), 0.73 (m, 2H), 0.14 (s, 6H).

<sup>13</sup>C NMR (101 MHz, CDCl<sub>3</sub>, δ/ppm): 119.9, 107.8, 83.5, 83.4, 69.1, 27.6, 20.8, 20.6, 19.1, 17.7, 16.0, -1.5.

Analytical data are in accordance with the literature<sup>14</sup>



### Synthesis of CPDMS-4,4-bis(methoxymethyl)hepta-1,6-diyne 50a<sup>2</sup>

4,4-Bis(methoxymethyl)hepta-1,6-diyne **39a** (3.72 g, 20.0 mmol, 1.00 eq.) was dissolved in 100 mL dry THF and ethylmagnesium bromide (3 M in Et<sub>2</sub>O, 5.87 mL, 17.6 mmol, 0.880 eq.) was added dropwise at 0°C. The mixture was stirred for 30 min at 0°C and 1h at rt, then CPDMS-Cl (2.71 g, 16.6 mmol, 0.830 eq.) was added dropwise at 0°C. After 2d at rt the solution was diluted with ether and slowly quenched with water. The organic layer was washed twice with sat. NH<sub>4</sub>Cl, the aqueous layer was re-extracted with TBME and the combined organic phases were washed with brine, dried over MgSO<sub>4</sub> and concentrated under reduced pressure. The crude mixture was purified by column chromatography (hexane/ethyl acetate: 6/1) to obtain 2.94 g of the monoprotected alkyne as a colorless liquid (58%).

<sup>1</sup>H NMR (500 MHz, CDCl<sub>3</sub>, δ/ppm): 3.17 (s, 10H), 2.25 (t, *J* = 7.0 Hz, 2H), 2.21 (s, 2H), 2.16 (d, *J* = 2.7 Hz, 2H), 1.82 (t, *J* = 2.6 Hz, 1H), 1.62 (ddd, *J* = 19.0 Hz, 9.5 Hz, 6.3 Hz, 2H), 0.64 – 0.55 (m, 2H).

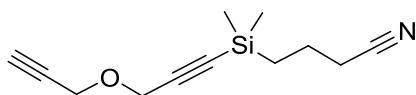
<sup>13</sup>C NMR (126 MHz, CDCl<sub>3</sub>, δ/ppm): 121.4, 106.7, 86.5, 82.2, 75.2, 72.1, 61.1, 43.4, 24.9, 23.6, 22.3, 22.1, 17.5, 1.6 (2C).

MS (FAB) *m/z*: 306 (100%) [M+H<sup>+</sup>], 126, 98, 45.

EA (%): calc. C, 66.84; H, 8.91; N, 4.59; found C, 66.00; H, 8.78; N, 4.49.

IR (ν /cm<sup>-1</sup>): 3291, 2926, 2887, 2812, 2177, 1733, 1477, 1455, 1428, 1250, 1195, 1174, 1101, 1031





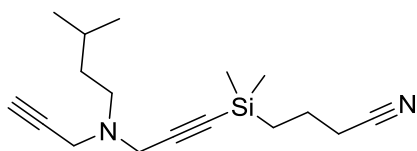
### **Synthesis of CPDMS-dipropargylether 39d**

To a solution of 1,1,1,3,3,3-hexamethyldisilazane (18.8 mL, 88.6 mmol, 1.00 eq.) in THF (8 mL) cooled to  $-78^{\circ}\text{C}$  was added *n*-butyllithium (2.5 M in hexane, 35.5 mL, 477 mmol, 5.00 eq.) under nitrogen dropwise. After stirring for 15 min at that temperature, the cooling bath was removed and the pale yellow solution was stirred for an additional 15 min. Then it was added via syringe to a solution of CPDMS-Cl (15.2 mL, 92.8 mmol, 1.05 eq.) in THF  $-78^{\circ}\text{C}$ . The mixture was stirred for 1h, then dipropargylether **39d** (9.20 g, 97.8 mmol, 1.10 eq.) was added and stirring was continued for 2h. Sat.  $\text{NH}_4\text{Cl}$  was then added to the reaction, the aqueous layer was extracted with ether, dried over  $\text{MgSO}_4$ , and the solvent removed in vacuo. The crude product was purified by distillation ( $142^{\circ}\text{C}/0.7\text{mbar}$ ) to give 14.9 g, 77%.

**$^1\text{H}$  NMR**(400 MHz,  $\text{CDCl}_3$ ,  $\delta/\text{ppm}$ ): 4.23 (m, 4H), 2.45 (t,  $J = 2.4$  Hz 1H), 2.39 (t,  $J = 7.0$  Hz, 2H), 1.75 (m, 2H), 0.77 (m, 2H), 0.17 (s, 6H).

**$^{13}\text{C}$  NMR** (126 MHz,  $\text{CDCl}_3$ ,  $\delta/\text{ppm}$ ): 120.1, 102.3, 90.6, 79.2, 75.6, 57.7, 57.0, 20.9, 20.9, 15.9, -1.69.

**HR-MS** (ESI): calc. for  $[\text{C}_{12}\text{H}_{17}\text{NNaOSi}]^+$ :  $[\text{M}+\text{Na}]^+$  242.0972; found 242.0972.



### **Synthesis of CPDMS-dipropargyl-isoamyl amine 50b<sup>2</sup>**

Dipropargyl-isoamylamine **39b** (2.32 g, 142 mmol, 1.00 eq.) was dissolved in 100 mL dry THF and ethylmagnesium bromide (3 M in Et<sub>2</sub>O, 4.17 mL, 12.5 mmol, 0.880 eq.) was added dropwise at 0°C. The mixture was stirred for 30 min at 0°C and 1h at rt, then CPDMS-Cl (1.91 g, 11.8 mmol, 0.830 eq.) was added dropwise at 0°C. After 1d at rt the solution was slowly quenched with water and diluted with EtOAc. The organic layer was washed with sat. NH<sub>4</sub>Cl (2x), the aqueous layer was re-extracted with TBME and the combined organic phases were washed with brine, dried over MgSO<sub>4</sub>, and concentrated under reduced pressure. The crude mixture was purified by column chromatography (hexane/EtOAc: 4/1) to obtain 2.01 g of the monoprotected alkyne as a colorless liquid (59%).

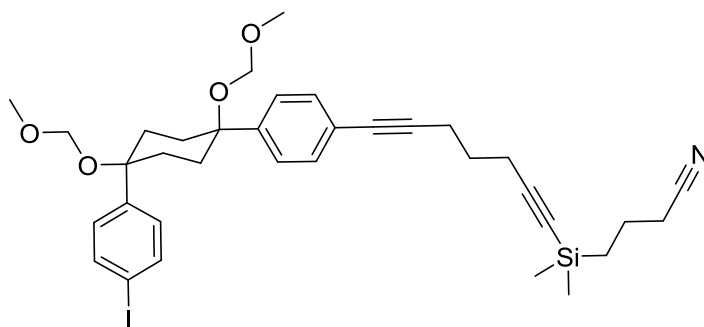
<sup>1</sup>H NMR (400 MHz, CDCl<sub>3</sub>, δ/ppm): 3.45 (s, 1H), 3.44 (d, *J* = 2.4 Hz, 1H), 2.58 – 2.53 (m, 1H), 2.42 (t, *J* = 7.0 Hz, 1H), 2.24 (t, *J* = 2.4 Hz, 1H), 1.84 – 1.74 (m, 1H), 1.69 – 1.59 (m, 1H), 1.38 (dd, *J* = 15.1 Hz, 7.1 Hz, 1H), 0.93 (d, *J* = 6.6 Hz, 3H), 0.83 – 0.75 (m, 1H), 0.19 (s, 3H).

<sup>13</sup>C NMR (126 MHz, CDCl<sub>3</sub>, δ/ppm): 119.9, 102.9, 87.8, 79.0, 73.2, 51.2, 43.5, 42.5, 36.5, 26.5, 22.9, 20.8, 20.7, 16.0, 0.2.

MS (FAB) *m/z*: 289 (2%) [M+H<sup>+</sup>], 231, 154, 126 (100%), 98, 43.

EA (%): calc. C, 70.77; H, 9.78; N, 9.71; found C, 70.69; H, 9.92; N, 9.71.

IR (ν /cm<sup>-1</sup>): 3330, 2953, 2868, 1464, 1426, 1361, 1317, 1250, 1171, 1139, 1116, 1088, 975.



### Synthesis of 99c

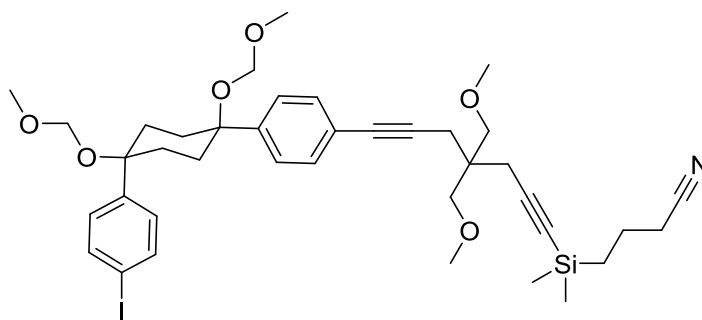
To an oven-dried flask was added **83** (12.0 g, 19.7 mmol, 1.00 eq.), 200 mL dry THF and the protected alkyne **50c** (4.29 g, 19.7 mmol, 1.00 eq.). Argon was bubbled through the solution for 15 min. Then, Pd(PPh<sub>3</sub>)<sub>4</sub> (1.14 g, 0.986 mmol, 5 mol%), CuI (376 mg, 1.97 mmol, 10.0 mol%) were added with argon counterflow followed by 100 mL diisopropylamine. The reaction mixture was stirred overnight at rt. Afterwards, it was poured on sat. NH<sub>4</sub>Cl, and extracted with EtOAc (3x). The combined organic layers were washed with sat. NH<sub>4</sub>Cl, brine, dried over Na<sub>2</sub>SO<sub>4</sub> and concentrated under reduced pressure. The crude product was purified on column chromatography (cyclohexane/EtOAc: 8/2) to give 8.32 g of the title compound as colorless oil (61%).

<sup>1</sup>H NMR (400 MHz, CDCl<sub>3</sub>, δ/ppm): 7.64 (m, 2H), 7.35 (s, 4H), 7.15 (m, 2H), 4.44 – 4.38 (m, 4H), 3.42 – 3.35 (m, 6H), 2.51 (t, *J* = 7.0 Hz, 2H), 2.40 (t, *J* = 7.0 Hz, 4H), 2.27 (s, 4H), 2.04 (d, *J* = 4.3 Hz, 4H), 1.86 – 1.76 (m, 2H), 1.77 – 1.71 (m, 2H), 0.79 – 0.70 (m, 2H), 0.18 – 0.12 (m, 6H).

<sup>13</sup>C NMR (101 MHz, CDCl<sub>3</sub>, δ/ppm)\*: 142.3, 141.6, 137.5 (2C), 131.6 (2C), 128.8 (2C), 126.8 (2C), 123.1, 119.8, 107.8, 93.4, 92.2 (2C), 89.5, 83.2, 80.9, 77.9 (2C), 56.1 (2C), 32.8 (4C), 27.7, 20.7, 20.3, 19.1, 18.6, 15.8, -1.5 (2C).

MS (FAB) *m/z* (%): 697 (M<sup>+</sup>, 6%), 126 (100), 574 (82).

HR-MS (ESI): calc. for [C<sub>35</sub>H<sub>44</sub>INaO<sub>4</sub>Si]<sup>+</sup>: [M+Na]<sup>+</sup> 720.1976; found 720.1990.



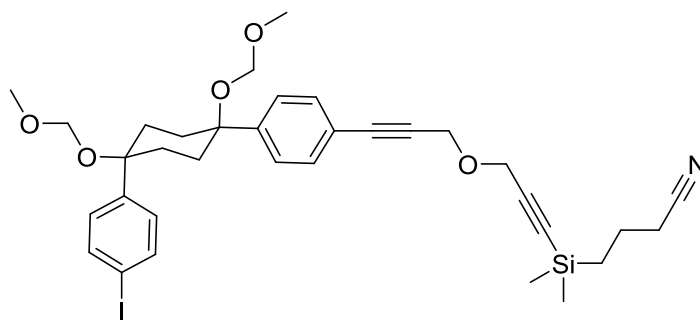
### Synthesis of 99a

To a 250 mL oven-dried flask filled with 80 mL dry THF was added Pd(PPh<sub>3</sub>)<sub>4</sub> (227 mg, 191 μmol, 10.0 mol%), CuI (72.6, 381 μmol, 20.0 mol%). Then, nitrogen was bubbled through the solution for 10 min, after which the diiodide **83** (1.19 g, 1.96 mmol, 1.00 eq.), the protected alkyne **50a** (582 mg 1.91 mmol, 1.00 eq.) and 10 mL diisopropylamine were added. The mixture was stirred at rt overnight. The mixture was then poured on sat. NH<sub>4</sub>Cl and the aqueous phase was extracted with EtOAc (3 x). The combined organic extracts were washed with sat. NH<sub>4</sub>Cl, brine, dried over Na<sub>2</sub>SO<sub>4</sub> and concentrated under reduced pressure. The residue was purified by column chromatography (cyclohexane/EtOAc, 8/2) to yield 560 mg of the product as yellow oil (37%).

<sup>1</sup>H NMR (400 MHz, CDCl<sub>3</sub>, δ/ppm): 7.67 – 7.60 (m, 2H), 7.35 (s, 4H), 7.16 (m, 2H), 4.41 (d, *J* = 5.2 Hz, 4H), 3.39 (d, *J* = 3.1 Hz, 6H), 3.38 (s, 4H), 3.35 (s, 6H), 2.52 (s, 2H), 2.41 (s, 2H), 2.39 (t, *J* = 7.0 Hz, 2H), 2.28 (bs, 4H), 2.01 (bs, 4H), 1.81 – 1.71 (m, 2H), 0.78 – 0.70 (m, 2H), 0.16 (s, 6H).

<sup>13</sup>C NMR (150Hz, C<sub>2</sub>D<sub>2</sub>Cl<sub>4</sub>, 358K, δ/ppm)\*: 142.9, 142.2, 137.5 (2C), 131.6 (2C), 128.7 (2C), 126.6 (2C), 123.2, 119.2, 105.4, 93.1, 91.9 (2C), 87.5, 84.9, 82.4, 77.7 (2C), 74.3, 74.2 (2C), 59.5 (2C), 55.8 (2C), 32.8 (4C), 23.8, 23.6, 20.6, 20.3, 16.0, -1.9 (2C).

**HR-MS** (ESI): calc. for [C<sub>39</sub>H<sub>52</sub>INNaO<sub>6</sub>Si]<sup>+</sup>: [M+Na]<sup>+</sup> 808.2501; found 808.2510.



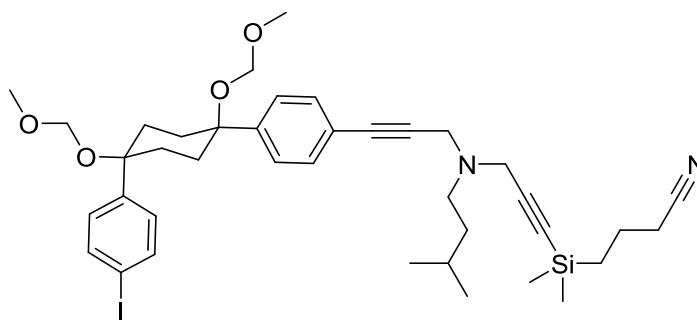
### Synthesis of 99d

To a 250 mL oven dried flask filled with 160 mL dry THF was added  $\text{Pd}(\text{PPh}_3)_4$  (380 mg, 329  $\mu\text{mol}$ , 10.0 mol%),  $\text{CuI}$  (125 mg, 658  $\mu\text{mol}$ , 20.0 mol%). Then nitrogen was bubbled through the solution for 10 min, after which the diiodide **83** (2.00 g, 3.29 mmol, 1.00 eq.), the protected alkyne **50d** (721 mg 3.29 mmol, 1.00 eq.) and 12 mL *diisopropylamine* were added. The mixture was stirred at rt overnight. The mixture was then poured on sat.  $\text{NH}_4\text{Cl}$  and the aqueous phase was extracted with  $\text{EtOAc}$  (3x). The combined organic extracts were washed with sat.  $\text{NH}_4\text{Cl}$  and brine, dried over  $\text{Na}_2\text{SO}_4$  and concentrated under reduced pressure. The residue was purified by column chromatography (cyclohexane/ $\text{EtOAc}$ : 8/2) to yield 1.01 g of the product as a yellow oil (44%).

$^1\text{H NMR}$  (400 MHz,  $\text{CDCl}_3$ ,  $\delta/\text{ppm}$ ): 7.65 (m, 2H), 7.39 (m, 4H), 7.16 (m, 2H), 4.45 (s, 2H), 4.41 (s, 4H), 4.29 (s, 2H), 3.39 (s, 6H), 2.39 (m, 4H), 2.26 (m, 4H), 1.77 (m, 2H), 0.78 (m, 2H), 0.19 (s, 6H).

$^{13}\text{C NMR}$  (150Hz,  $\text{C}_2\text{D}_2\text{Cl}_4$ , 358K,  $\delta/\text{ppm}$ )\*: 143.2, 142.6, 137.4 (2C), 131.8 (2C), 128.6 (2C), 126.6 (2C), 121.6, 119.4, 102.3, 93.1, 92.1 (2C), 90.3, 86.5, 85.0, 77.7 (2C), 57.6 (4C), 57.5 (2C), 55.8 (2C), 15.7, 20.7, 20.3, -2.0 (2C).

**HR-MS** (ESI): calc. for  $[\text{C}_{34}\text{H}_{42}\text{INaO}_5\text{Si}]^+$ :  $[\text{M}+\text{Na}]^+$  722.1769; found 722.1777.



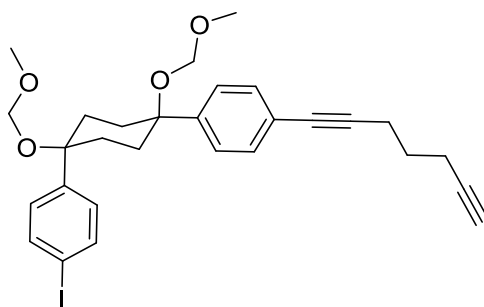
### **Synthesis of 99b**

To an oven-dried flask filled with 160 mL dry THF was added Pd(PPh<sub>3</sub>)<sub>4</sub> (380 mg, 329 μmol, 10.0 mol%), CuI (125 mg, 658 μmol, 20.0 mol%). Nitrogen was bubbled through the solution for 10 min, after which diiodide **83** (2.00 g, 3.29 mmol, 1.00 eq.), protected alkyne **50b** (949 mg 3.29 mmol, 1.00 eq.) and 12 mL diisopropylamine were added. The mixture was stirred at rt overnight. The mixture was then poured on sat. NH<sub>4</sub>Cl and the aqueous phase was extracted with EtOAc (3x). Combined organic extracts were washed with sat. NH<sub>4</sub>Cl and brine then dried over Na<sub>2</sub>SO<sub>4</sub> and concentrated under reduced pressure. The residue was purified by column chromatography (cyclohexane/EtOAc: 8/2) to yield 1.31 g of the product as a yellow oil (52%).

<sup>1</sup>H NMR (400 MHz, CDCl<sub>3</sub>, δ/ppm): 7.64 (m, 2H), 7.37 (m, 4H), 7.16 (m, 2H), 4.41 (d, *J* = 5.0 Hz, 4H), 3.60 (s, 2H), 3.48 (s, 2H), 3.39 (d, *J* = 3.6 Hz, 6H), 2.62 – 2.55 (m, 2H), 2.39 (t, *J* = 7.0 Hz, 2H), 2.27 (bm, 4H), 2.12 – 1.93 (bm, 4H), 1.82 – 1.71 (m, 2H), 1.63 (m, 1H), 1.44 – 1.36 (m, 2H), 0.92 (d, *J* = 6.6 Hz, 6H), 0.79 – 0.73 (m, 2H), 0.17 (s, 6H).

<sup>13</sup>C NMR (150Hz, C<sub>2</sub>D<sub>2</sub>Cl<sub>4</sub>, 358K, δ/ppm)\*: 142.9, 142.8, 137.6, 131.8, 129.0, 126.7, 122.1, 93.4, 92.2, 87.7, 84.7, 84.4, 77.9, 55.7, 51.0, 43.5, 43.2, 36.2, 32.8, 26.1, 22.6, 20.5, 20.3, 15.6, -1.9.

HR-MS (ESI): calc. for [C<sub>39</sub>H<sub>54</sub>IN<sub>2</sub>O<sub>4</sub>Si]<sup>+</sup>: [M+H]<sup>+</sup> 769.2892; found 769.2904.



### Synthesis of 100c

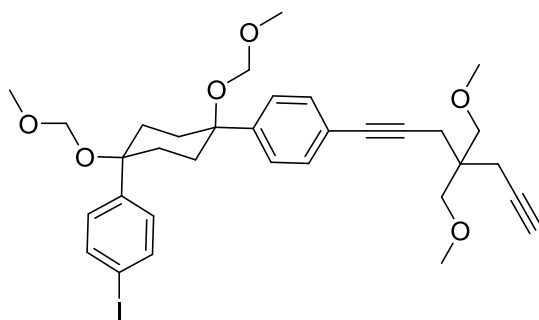
Compound **99c** (8.00 g, 11.5 mmol, 1.00 eq.) was dissolved in dry THF (100 mL). The mixture was degassed with argon for 30 min and TBAF (1 M in THF, 23 mL, 22.9 mmol, 2.00 eq.) was added. The reaction mixture was stirred for 30 min at rt and diluted with EtOAc and brine. The aqueous phase was extracted three times with EtOAc (3x) and the combined organic layers were dried over Na<sub>2</sub>SO<sub>4</sub>. After removal of the solvent under reduced pressure the crude product was purified by column chromatography (cyclohexane/EtOAc: 8/2) to give 5.43 g of the product as a yellow oil (83%).

**<sup>1</sup>H NMR** (400 MHz, CDCl<sub>3</sub>, δ/ppm): 7.65 (d, *J* = 8.3 Hz, 2H), 7.35 (s, 4H), 7.15 (d, *J* = 8.3 Hz, 2H), 4.45 – 4.36 (m, 4H), 3.38 (m, 6H), 2.53 (t, *J* = 7.0 Hz, 2H), 2.42 – 2.32 (m, 4H), 2.28 (d, *J* = 6.3 Hz, 4H), 1.99 (dd, *J* = 13.8, 11.2 Hz, 4H), 1.86 – 1.76 (m, 2H), 1.68 (m, 2H), 0.71 – 0.65 (m, 1H).

**<sup>13</sup>C NMR** (126Hz, CDCl<sub>3</sub>, δ/ppm)\*: 142.5, 141.6, 137.9 (2C), 131.5 (2C), 128.6 (2C), 126.5 (2C), 123.0, 93.3, 92.0 (2C), 89.5, 83.3, 80.5, 77.9 (2C), 68.7, 55.6 (2C), 32.8 (4C), 27.7, 18.1, 17.4.

**MS** (FAB) *m/z* (%): 572 (M<sup>+</sup>16%), 45 (100), 449 (96%).

**HR-MS** (ESI): calc. for [C<sub>29</sub>H<sub>33</sub>INaO<sub>4</sub>]<sup>+</sup>: [M+Na]<sup>+</sup> 595.1316; found 595.1313.



### **Synthesis of 100a**

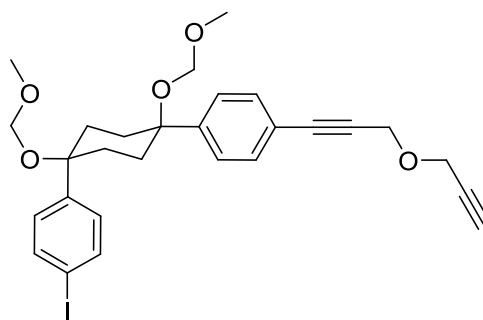
To a 20 mL vial the protected alkyne **99a** (560 mg, 713  $\mu\text{mol}$ , 1.00 eq.) was introduced with dry THF (15 mL). Nitrogen was bubbled through the solution for 20 min, after which TBAF (1 M in THF, 1.5 mL, 1.43 mmol, 2.00 eq.) was added drop-wise. After stirring 30 min at rt, the mixture was quenched with brine. The aqueous phase was extracted with EtOAc (3 x) and the organic extracts were dried over  $\text{Na}_2\text{SO}_4$  and concentrated under reduced pressure. The residue was purified by column chromatography on silica (cyclohexane/EtOAc: 8/2) to give 386 mg of product as yellow oil (82%).

**$^1\text{H}$  NMR** (400 MHz,  $\text{CDCl}_3$ ,  $\delta/\text{ppm}$ ): 7.64 (m, 2H), 7.36 (s, 4H), 7.16 (d, 2H), 4.40 (d, 4H), 3.68 (s, 2H), 3.40 (s, 10H), 3.37 (s, 6H), 2.42 (s, 2H), 2.37 (t, 2H), 2.30 (bs, 4H), 1.99 (m, 4H).

**$^{13}\text{C}$  NMR** (150Hz,  $\text{C}_2\text{D}_2\text{Cl}_4$ , 358K,  $\delta/\text{ppm}$ )\*: 142.8, 142.3, 137.5 (2C), 131.5 (2C), 128.8 (2C), 126.6 (2C), 123.0, 93.3, 92.1 (2C), 86.9, 82.1, 80.7, 77.8 (2C), 73.7 (2C), 70.4, 59.2 (2C), 55.9 (2C), 42.0, 32.8 (4C), 22.8, 21.9.

**HR-MS** (ESI): calc. for  $[\text{C}_{33}\text{H}_{41}\text{INaO}_6]^+$ :  $[\text{M}+\text{Na}]^+$  683.1840; found 683.1850.





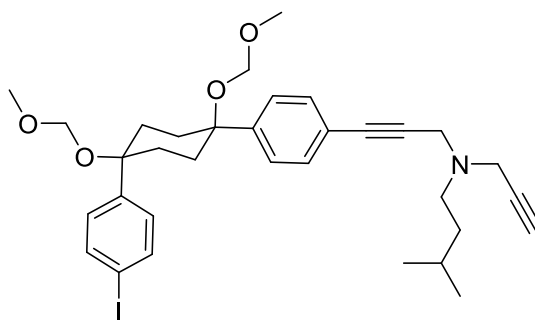
### Synthesis of 100d

The protected alkyne **99d** (1.00 g, 1.43 mmol, 1.00 eq.) was dissolved with dry THF (15 mL). Nitrogen was bubbled through the solution for 20 min, after which TBAF (1 M in THF, 2.86 mL, 2.86 mmol, 2.00 eq.) was added drop-wise. After stirring for 30 min at rt, the mixture was quenched with brine. The aqueous phase was extracted with EtOAc (3 x) the organic extracts were dried over Na<sub>2</sub>SO<sub>4</sub> and concentrated under reduced pressure. The residue was purified by column chromatography (cyclohexane/EtOAc: 8/2) to give 428 mg of product as yellow oil (52%).

<sup>1</sup>H NMR (500 MHz, CDCl<sub>3</sub>, δ/ppm): 7.69 – 7.64 (m, 2H), 7.45 – 7.36 (m, 4H), 7.21 – 7.15 (m, 2H), 4.50 (s, 2H), 4.43 (d, *J* = 3.7 Hz, 4H), 4.33 (d, *J* = 2.3 Hz, 2H), 3.41 (d, *J* = 4.5 Hz, 6H), 2.49 (t, *J* = 2.3 Hz, 1H), 2.31 (s, 4H), 2.11 – 1.97 (m, 1H).

<sup>13</sup>C NMR (150Hz, C<sub>2</sub>D<sub>2</sub>Cl<sub>4</sub>, 358K, δ/ppm)\*: 143.2, 142.7, 137.5 (2C), 131.8 (2C), 128.8 (2C), 126.8 (2C), 121.7, 93.2, 92.1 (2C), 86.3, 84.4, 79.0, 77.8 (2C), 75.0, 57.1, 56.4, 56.0 (2C), 32.6 (4C).

**HR-MS** (ESI): calc. for [C<sub>28</sub>H<sub>31</sub>INaO<sub>5</sub>]<sup>+</sup>: [M+Na]<sup>+</sup> 597.1108; found 597.1114.



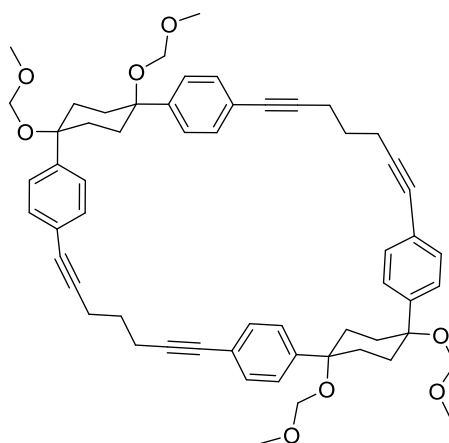
### **Synthesis of 100b**

To a 20 mL vial the protected alkyne **99b** (1.31 g, 1.7 mmol, 1.00 eq.) was dissolved with dry THF (15 mL). Nitrogen was bubbled through the solution for 20 min, after which TBAF (1 M in THF, 3.5 mL, 3.41 mmol, 2.00 eq.) was added drop-wise. After stirring for 30 min at rt, the mixture was quenched with brine. The aqueous phase was extracted with EtOAc (3 x) and the organic extracts were dried over Na<sub>2</sub>SO<sub>4</sub> and concentrated under reduced pressure. The residue was purified by column chromatography (cyclohexane/EtOAc: 8/2) to give 652 mg of product as yellow oil (60%).

**<sup>1</sup>H NMR** (500 MHz, CDCl<sub>3</sub>, δ/ppm): 7.65 (m, 2H), 7.37 (m, 4H), 7.16 (m, 2H), 4.41 (s, 2H), 4.40 (s, 2H), 3.63 (s, 2H), 3.48 (d, *J* = 2.4 Hz, 2H), 3.10 (s, 3H), 3.39 (s, 3H), 2.64 – 2.56 (m, 2H), 2.27 (bm, 4H), 2.24 – 2.22 (m, 1H), 2.01 (m, 4H), 1.63 (m, 2H), 1.46 – 1.35 (m, 2H), 0.92 (d, *J* = 6.5 Hz, 6H).

**<sup>13</sup>C NMR** (150Hz, C<sub>2</sub>D<sub>2</sub>Cl<sub>4</sub>, 358K, δ/ppm)\*: 142.9, 142.7, 137.4, 131.6, 128.7, 126.6, 122.4, 93.3, 91.9, 84.9, 78.9, 77.9, 72.8, 56.0, 51.0, 43.0, 42.1, 36.3, 32.5, 25.7, 22.5.

**HR-MS** (ESI): calc. for [C<sub>33</sub>H<sub>43</sub>INO<sub>4</sub>]<sup>+</sup>: [M+H]<sup>+</sup> 644.2231; found 644.2234.



### **Synthesis of macrocycle 101c**

**From building block 100c:** to an oven-dried flask, compound **100c** (5.43 g, 9.49 mmol, 1.00 eq.) and 250 mL dry THF were added. Argon was bubbled through the solution for 15 min. Then, Pd(PPh<sub>3</sub>)<sub>4</sub> (1.10 g, 949 μmol, 10.0 mol%) and CuI (362 mg, 1.90 μmol, 20.0 mol%) were added with argon counterflow followed by 34 mL of diisopropylamine. The reaction mixture was stirred overnight at rt. Afterwards, the mixture was poured on sat. NH<sub>4</sub>Cl, and extracted with ethyl acetate (3x). The combined organic layers were washed with sat. NH<sub>4</sub>Cl, brine, dried over Na<sub>2</sub>SO<sub>4</sub> and concentrated under reduced pressure. The crude product was purified on column chromatography (cyclohexane/EtOAc, 7/3), the residue was then suspended in cyclohexane/EtOAc and filtrated to give 488 mg of product as a white solid (11%).

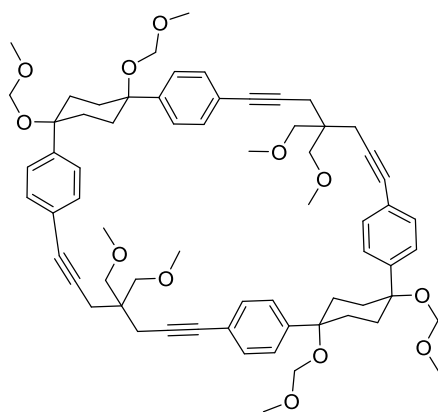
**Shot gun synthesis:** to a 100 mL oven dried flask dry THF (50 mL) was added under argon. Argon was bubbled through the solvent for 10 min. Then, Pd(PPh<sub>3</sub>)<sub>4</sub> (95.0 mg, 82.2 μmol, 10 mol%), CuI (31.3 mg, 164 μmol, 20 mol%), **83** (500 mg, 822 μmol, 1.00 eq.) were added under argon, followed with 1,6-heptadiyne (94 μL, 822 μmol, 1.00 eq.), and diisopropylamine (3 mL). The mixture was stirred at rt overnight. The mixture was poured on sat. NH<sub>4</sub>Cl and the water phase was extracted with EtOAc (3x). Combined organic layers were washed with sat. NH<sub>4</sub>Cl, brine, dried over Na<sub>2</sub>SO<sub>4</sub> and concentrated under reduced pressure. The residue was purified by two flash chromatographies (cyclohexane/EtOAc, 7/3) to give 29 mg product as white solid (8%).

**<sup>1</sup>H NMR** (400 MHz, CDCl<sub>3</sub>, δ/ppm): 7.33 (s, 16H), 4.44 (s, 8H), 3.39 (s, 12H), 2.57 (t, *J* = 7.0 Hz, 8H), 2.38-2.16 (m, 8H), 2.04 (s, 8H), 1.93-1.78 (m, 4H)

**<sup>13</sup>C NMR** (126 MHz, CDCl<sub>3</sub>, δ/ppm) \*: 141.1 (4C), 131.4 (8C), 126.7 (8C), 122.8 (4C), 92.0 (4C), 89.5 (4C), 80.8 (4C), 78.0 (4C), 55.7 (4C), 32.8 (8C), 27.7 (2C), 18.4 (4C).

**HR-MS** (ESI): calc. for [C<sub>58</sub>H<sub>64</sub>NaO<sub>8</sub>]<sup>+</sup>: [M+Na]<sup>+</sup> 911.4493; found 911.4506.

**Mp:** >350°C



### **Synthesis of 101a**

**From building block 100a:** to a 50 mL oven-dried flask the building block **100a** (386 mg, 58.4  $\mu\text{mol}$ , 1.00 eq.) was transferred with THF (20 mL). Then,  $\text{Pd}(\text{PPh}_3)_4$  (67.5 mg, 58.4  $\mu\text{mol}$ , 10 mol%) and  $\text{CuI}$  (22.3 mg, 11.7  $\mu\text{mol}$ , 20 mol%) were added. Nitrogen was bubbled through the solution for 10 min after which 2 mL *diisopropylamine* were added. The mixture was stirred at rt overnight. The mixture was then poured on sat.  $\text{NH}_4\text{Cl}$  and the aqueous phase was extracted with  $\text{EtOAc}$  (3 x). The combined organic extracts were washed with sat.  $\text{NH}_4\text{Cl}$  and brine then, dried over  $\text{Na}_2\text{SO}_4$  and concentrated under reduced pressure. The residue was purified by column chromatography (cyclohexane/ $\text{EtOAc}$ : 7/3) to give 90.0 mg of yellow wet solid. This solid was suspended in few mL cyclohexane and filtrated to give 19 mg of a white solid (6%).

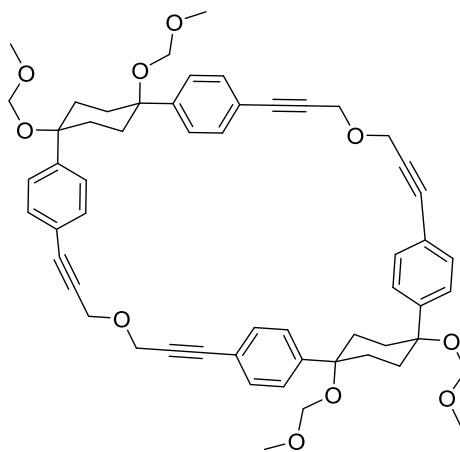
**Shot gun synthesis:** in a flask was placed 200 mL THF and argon was bubbled through the solvent for 30 min. Then,  $\text{Pd}(\text{PPh}_3)_4$  (950 mg, 822  $\mu\text{mol}$ , 10.0 mol%),  $\text{CuI}$  (313 mg, 1.64 mmol, 20.0 mol%) and the iodide building block **83** (5.00 g, 8.22 mmol, 1.00 eq.) were added followed by the diyne **39a** (1.63 g, 9.04 mmol, 1.10 eq.) and 30 mL *diisopropylamine*. The mixture was stirred at rt overnight. The reaction mixture was washed with sat.  $\text{NH}_4\text{Cl}$ . The aqueous phase was extracted with  $\text{EtOAc}$  (3 x). The combined organic extracts were dried over  $\text{Na}_2\text{SO}_4$  and concentrated under reduced pressure. The residue was dissolved in  $\text{EtOAc}$  and the solid was filtrated off before purification on column chromatography on silica (cyclohexane/ $\text{EtOAc}$ : 6/4). After the column the pale yellow solid was suspended in hexane/ $\text{EtOAc}$  and filtrated to give 174 mg of the product as a white solid (4%).

**$^1\text{H NMR}$**  (400 MHz,  $\text{CDCl}_3$ ,  $\delta/\text{ppm}$ ): 7.33 (m, 16H), 4.44 (s, 8H), 3.44 (s, 8H), 3.40 (s, 12 H), 3.37 (s, 12H), 2.59 (s, 8H), 2.27-1.85 (bs, 12H).

**$^{13}\text{C NMR}$**  (150MHz,  $\text{C}_2\text{D}_2\text{Cl}_4$ , 353K,  $\delta/\text{ppm}$ )\*: 141.9 (4C), 131.0 (8C), 126.0 (8C), 122.5 (4C), 91.6 (4C), 86.9 (4C), 82.1 (4C), 77.4 (4C), 73.9 (4C), 59.0 (4C), 55.3 (4C), 42.4 (2C), 32.6 (8C), 22.6 (4C).

**HR-MS** (ESI): calc. for  $[\text{C}_{66}\text{H}_{80}\text{NaO}_{12}]^+$ :  $[\text{M}+\text{Na}]^+$  1087.5542; found 1087.5556.

**Mp**: 230°C (decomposition)



### **Shot gun synthesis of macrocycle 101d**

**From building block 100d:** to a 50 mL oven-dried flask the building block **100d** (386 mg, 58.4  $\mu\text{mol}$ , 1.00 eq.) was transferred with THF (20 mL). Then,  $\text{Pd}(\text{PPh}_3)_4$  (84.1 mg, 72.8  $\mu\text{mol}$ , 10.0 mol%) and  $\text{CuI}$  (27.7 mg, 146  $\mu\text{mol}$ , 20.0 mol%) were added. Nitrogen was bubbled through the solution for 10 min after which 3 mL diisopropylamine were added. The mixture was stirred at rt overnight. The mixture was then poured on sat.  $\text{NH}_4\text{Cl}$  and the aqueous phase was extracted with EtOAc (3 x). The combined organic extracts were washed with sat.  $\text{NH}_4\text{Cl}$  and brine, dried over  $\text{Na}_2\text{SO}_4$  and concentrated under reduced pressure. The residue was purified by column chromatography (cyclohexane/EtOAc: 6/4) to yield 13 mg of pale yellow solid (4%)

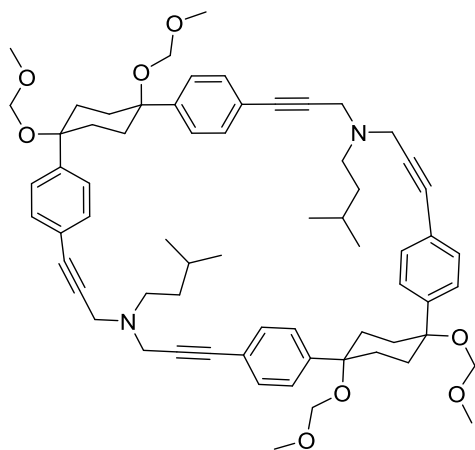
**Shot gun synthesis:** in a flask was placed 200 mL THF and argon was bubbled through the solvent for 30 min. Then,  $\text{Pd}(\text{PPh}_3)_4$  (950 mg, 822  $\mu\text{mol}$ , 10.0 mol%),  $\text{CuI}$  (313 mg, 1.64 mmol, 20.0 mol%) and the iodide building block **83** (5.00 g, 8.22 mmol, 1.00 eq.) were added followed by diyne **39d** (774mg, 8.22 mmol, 1.00 eq.) and 30 mL diisopropylamine. The mixture was stirred at rt overnight. The reaction mixture was washed with sat.  $\text{NH}_4\text{Cl}$ . The aqueous phase was extracted EtOAc (3 x). Combined organic extracts were dried over  $\text{Na}_2\text{SO}_4$  and concentrated under reduced pressure. The residue was dissolved in EtOAc and the solid was filtrated off before purification on column chromatography (cyclohexane/EtOAc: 6/4). After the column the pale yellow solid was suspended in hexane/EtOAc and filtrated to give 83 mg of the product as a white solid (2%).

$^1\text{H NMR}$  (400 MHz,  $\text{CDCl}_3$ ,  $\delta/\text{ppm}$ ): 7.43 – 7.30 (m, 16H), 4.52 (s, 8H), 4.46 (s, 8H), 3.40 (s, 12H), 2.27 (bs, 8H).

$^{13}\text{C NMR}$  (150Hz,  $\text{C}_2\text{D}_2\text{Cl}_4$ , 353K,  $\delta/\text{ppm}$ )\*: 142.8 (4C), 131.0 (8C), 126.1 (8C), 121.3 (4C), 91.6 (4C), 86.5 (4C), 84.4 (4C), 77.4 (4C), 56.5 (4C), 55.4.0 (4C), 32.4 (8C).

**HR-MS** (ESI): calc. for  $[\text{C}_{56}\text{H}_{60}\text{NaO}_{10}]^+$ :  $[\text{M}+\text{Na}]^+$  915.4079; found 915.4085.

**Mp:**  $>350^\circ\text{C}$



### **Synthesis of 101b**

**From building block 100b:** to a 50 mL oven-dried flask the building block **100b** (493 mg, 766  $\mu\text{mol}$ , 1.00 eq.) was transferred and then filled with 20 mL THF. Then,  $\text{Pd}(\text{PPh}_3)_4$  (88.5 mg, 76.6  $\mu\text{mol}$ , 10 mol%),  $\text{CuI}$  (29.2 mg, 153  $\mu\text{mol}$ , 20 mol%) were added. Nitrogen was bubbled through the solution for 10 min after which, 3 mL *diisopropylamine* were added. The mixture was stirred at rt overnight. The mixture was then poured on sat.  $\text{NH}_4\text{Cl}$  and the aqueous phase was extracted with  $\text{EtOAc}$  (3 x). Combined organic extracts were washed with sat.  $\text{NH}_4\text{Cl}$  and brine then, dried over  $\text{Na}_2\text{SO}_4$  and concentrated under reduced pressure. The residue was purified by column chromatography (cyclohexane/ $\text{EtOAc}$ : 3/7) to yield 38 mg of a white solid (9.6%).

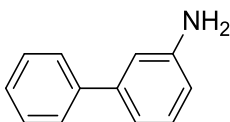
**Shot gun synthesis:** in a flask was placed 200 mL THF and argon was bubbled through the solvent for 30 min. Then,  $\text{Pd}(\text{PPh}_3)_4$  (950 mg, 822  $\mu\text{mol}$ , 10.0 mol%),  $\text{CuI}$  (313 mg, 1.64 mmol, 20.0 mol%) and the iodide building block **83** (5.00 g, 8.22 mmol, 1.00 eq.) were added followed by diyne **39b** (1.48 g, 9.04 mmol, 1.10 eq.) and 30 mL *diisopropylamine*. The mixture was stirred at rt overnight. The reaction mixture was washed with sat.  $\text{NH}_4\text{Cl}$ . The aqueous phase was extracted  $\text{EtOAc}$  (3 x), combined organic extracts were dried over  $\text{Na}_2\text{SO}_4$  and concentrated under reduced pressure. The residue was dissolved in  $\text{EtOAc}$  and the solid was filtrated off before purification on column chromatography (cyclohexane/ $\text{EtOAc}$ : 6/4). After the column the pale yellow solid was suspended in hexane/ $\text{EtOAc}$  and filtrated to give 174 mg of the product as a white solid (5%).

**$^1\text{H}$  NMR** (400 MHz,  $\text{CDCl}_3$ ,  $\delta/\text{ppm}$ ): 7.24 (m, 16H), 4.45 (s, 8H), 3.70 (s, 8H), 3.40 (s, 12H), 2.61 (m, 4H), 2.26-2.00 (bs, 12H), 1.64 (m, 2H), 1.27 (m, 4H), 0.93 (d, 12H,  $J = 6.6$  Hz).

**$^{13}\text{C}$  NMR** (101 MHz,  $\text{CDCl}_3$ ,  $\delta/\text{ppm}$ )\*: 142.4 (4C), 131.7 (8C), 126.5 (8C), 122.4 (4C), 92.2 (4C), 85.1 (4C), 84.8 (4C), 78.1 (4C), 56.0 (4C), 51.9 (2C), 42.9 (4C), 36.5 (2C), 32.6 (8C), 26.4 (2C), 22.7 (4C).

**HR-MS** (ESI): calc. for  $[\text{C}_{66}\text{H}_{84}\text{N}_2\text{O}_8]^{2+}$ :  $[\text{M}+2\text{H}]^{2+}$  516.3108; found 516.3110.

**Mp:** 159°C

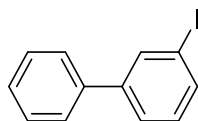


### **Synthesis of [1,1'-biphenyl]-3-amine 113**

A three-necked flask was charged with phenylboronic acid pinacol ester (639 mg, 3.13 mmol, 1.10 eq.), 3-bromoaniline (316  $\mu$ L, 2.85 mmol, 1.00 eq.), Pd(PPh<sub>3</sub>)<sub>4</sub> (165 mg, 0.142 mmol, 5.00 mol%) and flushed with nitrogen. Then, THF (70 mL) and aqueous K<sub>2</sub>CO<sub>3</sub> (2 M, 20 mL) were added to the reaction mixture, which was degassed with a nitrogen stream for 20 min and stirred at 80°C overnight. The reaction was allowed to cool to rt, and the organic layer was separated and washed with water and brine (100 mL). After drying over Na<sub>2</sub>SO<sub>4</sub> and removal of the solvent under reduced pressure, the residue was purified by column chromatography (EtOAc/hexane: 6/4) to yield 372 mg of the product as a yellow oil (77%).

<sup>1</sup>H NMR (400 MHz, CDCl<sub>3</sub>,  $\delta$ /ppm): 7.57 (m, 2H), 7.42 (m, 2H), 7.33 (m, 1H), 7.23 (m, 1H) 7.00 (m, 1H), 6.92 (m, 1H), 6.68 (m, 1H), 3.74 (bs, 2H).

Analytical data are in accordance with the literature.<sup>15</sup>



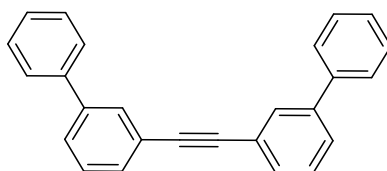
### **Synthesis of 3-iodo-1,1'-biphenyl 114**

To a solution of *p*-TsOH·H<sub>2</sub>O (9.54 g, 50.2 mmol, 3.00 eq.) in MeCN (60 mL) was added (1,1'-biphenyl)-3-amine **113** (2.83 g, 16.7 mmol, 1.00 eq.). The resulting suspension was cooled to 10–15 °C and a solution of NaNO<sub>2</sub> (2.35 mg, 33.4 mmol, 2.00 eq.) and KI (7.01 g, 41.8 mmol, 2.50 eq.) in H<sub>2</sub>O (11 mL) was gradually added. The reaction mixture was stirred for 10 min then allowed to warm to 20°C and stirred for 4h. To the reaction mixture was then added H<sub>2</sub>O (50 mL), NaHCO<sub>3</sub> (1 M; until pH = 9–10) and Na<sub>2</sub>S<sub>2</sub>O<sub>3</sub> (2 M, 40 mL). The aromatic iodide was extracted with EtOAc dried over Na<sub>2</sub>SO<sub>4</sub> and concentrated under reduced pressure. The residue was purified by flash chromatography (cyclohexane) to give 3.98 g of product as pale yellow solid (85%).

<sup>1</sup>H NMR (400 MHz, CDCl<sub>3</sub>,  $\delta$ /ppm): 7.94 (m, 1H), 7.67 (m, 1H), 7.55 (m, 1H), 7.53 (m, 2H) 7.44 (m, 2H), 7.36 (m, 1H), 7.17 (m, 1H).

<sup>13</sup>C NMR (101 MHz, CDCl<sub>3</sub>,  $\delta$ /ppm): 143.4, 139.6, 136.3, 136.3, 130.6, 129.0, 127.9, 127.3, 126.5, 94.9.

Analytical data are in accordance with the literature.<sup>16</sup>



### **Synthesis of 1,2-di[(1,1'-biphenyl)-3-yl]ethyne 115**

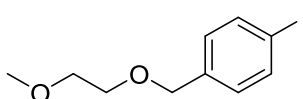
To a 250 mL flask under argon was added 3-iodobiphenyl **114** (3.89 g, 13.9 mmol, 1.00 eq.) in dry THF (125 mL). The mixture was degassed by bubbling argon through the solution for 30 min. Then, CuI (265 mg, 1.39 mmol, 10 mol%), Pd(PPh<sub>3</sub>)<sub>4</sub> (963 mg, 0.834 mmol, 6 mol%), DBU (13 mL, 6.00 eq.), water (81.9 μL, 5.56 mmol, 40 mol%) and TMS acetylene (989 μL, 6.95 mmol, 0.500 eq.) were added. The mixture was stirred at rt for 30 min and then at reflux for 4 days. The mixture was then washed with sat. NH<sub>4</sub>Cl (2x). The organic phase was dried over Na<sub>2</sub>SO<sub>4</sub> and concentrated under reduced pressure. The residue was purified by flash chromatography (cyclohexane) to obtain 2.02 g of product as a white solid (88%).

<sup>1</sup>H NMR (400 MHz, CD<sub>2</sub>Cl<sub>2</sub>, δ/ppm): 7.82 (m, 2H), 7.63 (m, 6H), 7.55 (m, 2H), 7.51 – 7.43 (m, 6H), 7.42 – 7.36 (m, 2H).

<sup>13</sup>C NMR (101 MHz, CDCl<sub>3</sub>, δ/ppm): 141.6 (2C), 140.5 (2C), 130.5 (4C), 129.0 (6C), 127.8 (2C), 127.3 (2C), 127.3 (4C), 123.8 (2C), 89.6 (2C).

HR-MS (EI): calc. for [C<sub>26</sub>H<sub>18</sub>]<sup>+</sup>: [M]<sup>+</sup> 330.1409; found: 330.1387.

Mp: 142.3-144.8°C



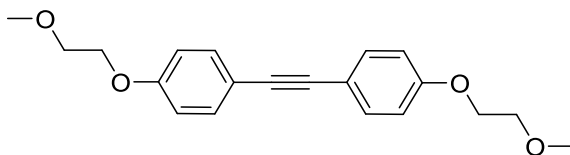
### **Synthesis of 1-iodo-4-(2-methoxyethoxy)benzene 105**

A suspension of NaH (60% in mineral oil, 1.08 g, 27.0 mmol, 2.00 eq) in 100 mL dry THF was prepared. Then, 4-iodophenol (3.00 g, 13.5 mmol, 1.00 eq.) in 10 mL THF was added dropwise at 0°C. The resulting mixture was stirred at rt for 4h. Then, 2-bromomethylether (1.29 mL, 13.5 mmol, 1.00 eq.) was added dropwise at 0°C and the mixture was stirred at 50°C overnight. After that, 2-bromomethylether (2 mL) was added and the mixture was stirred 24h. The mixture was quenched with sat. NaCl and extracted with EtOAc. The organic layer was dried over Na<sub>2</sub>SO<sub>4</sub> and concentrated under reduced pressure. The residue was purified by column chromatography to yield the title product as a transparent liquid (2.00 g, 46%)

<sup>1</sup>H NMR (400 MHz, CDCl<sub>3</sub>, δ/ppm): 7.54 (m, 2H), 6.70 (m, 2H), 4.07 (m, 2H), 3.73 (m, 2H), 3.44 (s, 3H).

Analytical data are in accordance with the literature.<sup>17</sup>





### **Synthesis of 1,2-bis [4-(2-methoxyethoxy)phenyl]ethyne 106**

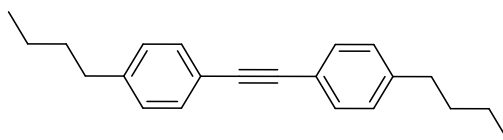
To a 20 mL vial under nitrogen was added CuI (62.3 mg, 327  $\mu$ mol, 10 mol%), Pd(PPh<sub>3</sub>)<sub>4</sub> (227 mg, 196  $\mu$ mol, 6 mol%), 1-iodo-4-(2-methoxyethoxy)benzene **105** (1.00 g, 3.60 mmol, 1.00 eq.) in dry THF (10 mL). Nitrogen was bubbled through the solution for 10 min. Then, DBU (2.93 mL, 19.6 mmol, 6.00 eq.), water (23.6  $\mu$ L, 1.31 mmol, 40 mol%) and TMS-acetylene (237  $\mu$ L, 1.63 mmol, 0.500 eq.) were added. The mixture was stirred at reflux overnight. The cooled mixture was poured on sat. NH<sub>4</sub>Cl and the water phase was extracted with EtOAc (3x). The combined organic layers were washed with sat. NH<sub>4</sub>Cl, brine, dried over Na<sub>2</sub>SO<sub>4</sub> and concentrated under reduced pressure. The residue was purified by flash chromatography (cyclohexane) to give 376.6 mg, as colorless oil (70%).

**<sup>1</sup>H NMR** (400 MHz, CDCl<sub>3</sub>,  $\delta$ /ppm): 7.43 (m, 4H), 6.89 (m, 4H), 4.13 (m, 4H), 3.76 (m, 4H), 3.46 (s, 6H).

**<sup>13</sup>C NMR** (101 MHz, CDCl<sub>3</sub>,  $\delta$ /ppm): 158.5 (2C), 132.9 (4C), 115.9 (2C), 114.6 (4C), 87.9 (2C), 70.9 (2C), 67.3 (2C), 59.3(2C).

**GCMS** (m/z): 326, 210

**HR-MS** (EI): calc. for [C<sub>20</sub>H<sub>22</sub>O<sub>4</sub>]<sup>+</sup>: [M]<sup>+</sup> 326.1518; found: 326.1507.



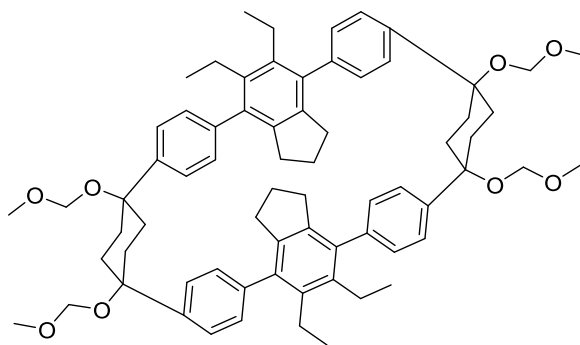
### **Synthesis of 1,2-bis[4-(*n*-butyl)phenyl]ethyne 108**

To a 250 mL flask under argon was added CuI (894 mg, 4.69 mmol, 10 mol%), Pd(PPh<sub>3</sub>)<sub>4</sub> (3.25 g, 2.82 mmol, 6 mol%), 1-bromo-4-*n*-butylbenzene (10.0 g, 46.9 mmol, 1.00 eq.) in dry THF (100 mL). Argon was bubbled through the solution for 10 min. Then DBU (38.0 mL, 251 mmol, 5.35 eq.), water (338 μL, 18.8 mmol, 40 mol%) and TMS-acetylene (3.34 mL, 23.5 mmol, 0.500 eq.) were added. The mixture was stirred at reflux overnight. The mixture was allowed to cool to rt and was poured on sat. NH<sub>4</sub>Cl, and the water phase was extracted with EtOAc (3x). The combined organic layers were washed with sat. NH<sub>4</sub>Cl, brine, dried over Na<sub>2</sub>SO<sub>4</sub> and concentrated under reduced pressure. The residue was purified by flash chromatography (cyclohexane) and recrystallized (ethanol/DCM) to give 2.66 g of the title compound as white solid (39%).

<sup>1</sup>H NMR (400 MHz, CDCl<sub>3</sub>, δ/ppm): 7.43 (m, 4H), 7.15 (m, 4H), 2.61 (t, *J* = 7.6 Hz, 4H), 1.60 (m, 4H), 1.35 (m, 4H), 0.93 (t, *J* = 7.3 Hz, 6H).

<sup>13</sup>C NMR (126 MHz, CDCl<sub>3</sub>, δ/ppm): 143.3 (2C), 131.6 (4C), 128.6 (4C), 120.8 (2C), 89.1 (2C), 35.8 (2C), 33.6 (2C), 22.5 (2C), 14.1 (2C).

Analytical data are in accordance with the literature.<sup>18</sup>



### **Synthesis of 102a**

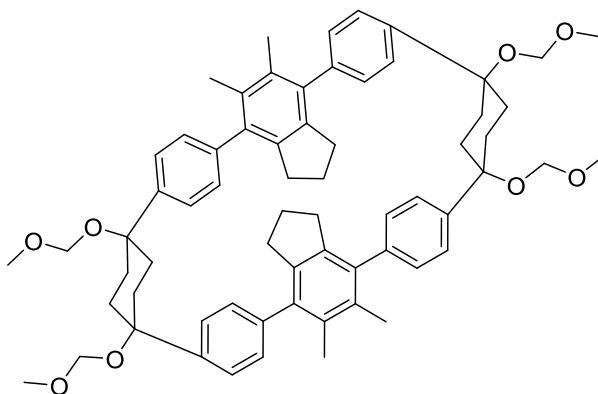
Macrocyclic **101c** (115 mg, 129  $\mu\text{mol}$ , 1.00 eq.), anhydrous 2-propanol (10 mL), and anhydrous THF (10 mL) were placed in a 20 mL microwave flask equipped with a stir bar. The reaction mixture was degassed by bubbling nitrogen through the solution for 15 min. Then,  $\text{RhCl}(\text{PPh}_3)_3$  (24.1 mg, 25.8  $\mu\text{mol}$ , 20 mol%) and hex-3-yne (147  $\mu\text{L}$ , 1.29 mmol, 10.0 eq.) were added and the reaction flask was irradiated with microwave at 100°C for 6 h. The reaction mixture was filtrated and washed with cyclohexane to give 71.0 mg of pure product as an off-white solid (52%).

**$^1\text{H}$  NMR** (400 MHz  $\text{CDCl}_3$ ,  $\delta/\text{ppm}$ ): 7.35 (m, 8H), 7.04 (m, 8H), 4.75 (s, 8H), 3.50 (s, 12H), 2.74 (q,  $J = 7.4$  Hz, 8H), 2.27 (m, 8H), 2.15 – 1.95 (m, 8H), 1.80 (t,  $J = 7.5$  Hz, 8H), 1.09 (m, 16H).

**$^{13}\text{C}$  NMR** (101 MHz,  $\text{CDCl}_3$ ,  $\delta/\text{ppm}$ ): 141.2 (4C), 141.1 (4C), 139.6 (4C), 138.1 (4C), 137.7 (4C), 129.4 (8C), 127.1 (8C), 92.9 (4C), 78.4 (4C), 56.0 (4C), 34.1 (8C), 32.9 (4C), 23.5 (4C), 23.3 (2C), 16.7 (4C).

**HR-MS** (ESI): calc. for  $[\text{C}_{70}\text{H}_{84}\text{NaO}_8]^+$ :  $[\text{M}+\text{Na}]^+$  1075.6058; found 1075.6071.

**Mp**: 278-284°C.



### **Synthesis of 102b**

Macrocycle **101c** (57.0 mg, 64.1  $\mu\text{mol}$ , 1.00 eq.), anhydrous 2-propanol (2 mL), and anhydrous THF (2 mL) were placed in a 5 mL microwave flask equipped with a stir bar. The reaction mixture was degassed by bubbling nitrogen through the solution for 5 min. Then,  $\text{RhCl}(\text{PPh}_3)_3$  (12.0 mg, 10  $\mu\text{mol}$ , 20 mol%) and 2-butyne (50  $\mu\text{L}$ , 641  $\mu\text{mol}$ , 10.0 eq.) were added and the reaction flask was irradiated with microwave at 100°C for 6 h. The reaction mixture was filtrated to give 38 mg of pure product as a white solid (81%).

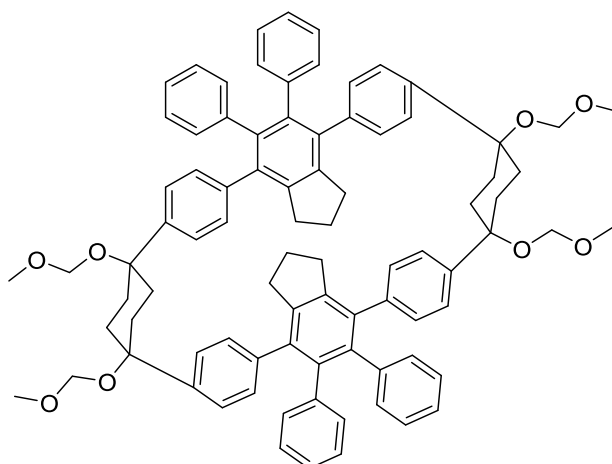
**$^1\text{H}$  NMR** (400 MHz,  $\text{CDCl}_3$ ,  $\delta/\text{ppm}$ ): 7.36 (m, 8H), 7.03 (m, 8H), 4.74 (s, 8H), 3.49 (s, 12H), 2.29 (m, 8H), 2.24 (s, 12H), 2.02 (m, 8H), 1.87 (t,  $J = 7.5$  Hz, 8H), 1.08 (m, 4H).

**$^{13}\text{C}$  NMR** (101 MHz,  $\text{CDCl}_3$ ,  $\delta/\text{ppm}$ ): 140.8 (8C), 139.7 (4C), 137.8 (4C), 132.1 (4C), 129.5 (8C), 127.3 (8C), 92.9 (4C), 78.2 (4C), 56.1 (4C), 34.2 (8C), 33.1 (4C), 23.8 (2C), 18.1 (4C).

**MS** (FAB)  $m/z$  (%): 996.5.

**HR-MS** (ESI): calc. for  $[\text{C}_{66}\text{H}_{76}\text{NaO}_8]^+$ :  $[\text{M}+\text{Na}]^+$  1019.5432; found 1019.5448.

**Mp**: 283-288°C.



### Synthesis of 102c

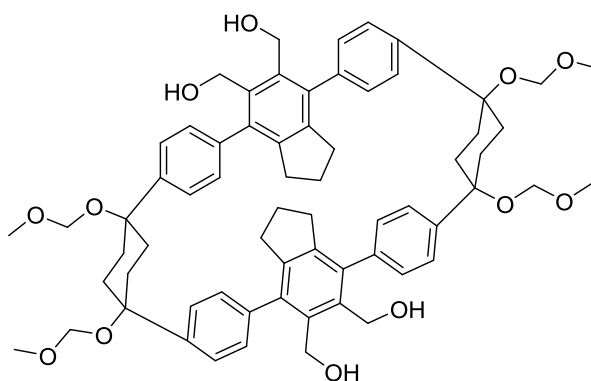
Macrocyclic **101c** (203 mg, 228  $\mu\text{mol}$ , 1.00 eq.), diphenylacetylene (411 mg, 2.28 mmol, 10.0 eq.), anhydrous 2-propanol (10 mL), and anhydrous THF (10 mL) were placed in a 20 mL microwave flask equipped with a stir bar. The reaction mixture was degassed by bubbling argon through the solution for 15 min. Then,  $\text{RhCl}(\text{PPh}_3)_3$  (42.7 mg, 45.7  $\mu\text{mol}$ , 20 mol%) was added and the reaction flask was placed in the microwave reactor at 100°C for 6 h. The reaction mixture was allowed to cool to rt and was filtrated and washed with hexane and EtOAc to give 191 mg of product as white solid (67%).

$^1\text{H NMR}$  (400 MHz,  $\text{CDCl}_3$ ,  $\delta/\text{ppm}$ ): 7.12 (m, 8H), 6.92 (m Hz, 8H), 6.86 (m, 12H), 6.80 (m, 8H), 4.61 (s, 8H), 3.37 (s, 12H), 2.43 (t,  $J = 7.5$  Hz, 8H), 2.15 – 2.05 (m, 8H), 1.94 (m, 8H), 1.59 (m, 4H).

$^{13}\text{C NMR}$  (126 MHz  $\text{CDCl}_3$ ,  $\delta/\text{ppm}$ ): 142.4 (4C), 140.0 (4C), 139.9 (4C), 139.6 (4C), 138.5 (4C) 137.3 (4C), 131.4 (8C), 129.9 (8C), 126.7 (8C), 126.3 (8C), 125.4 (4C), 92.6 (4C), 78.4 (4C), 55.7 (4C), 33.9 (8C), 33.3 (4C), 24.2 (2C).

**HR-MS** (ESI): calc. for  $[\text{C}_{86}\text{H}_{84}\text{NaO}_8]^+$ :  $[\text{M}+\text{Na}]^+$  1267.6058; found 1267.6062

**Mp**: >350°C decomposition.



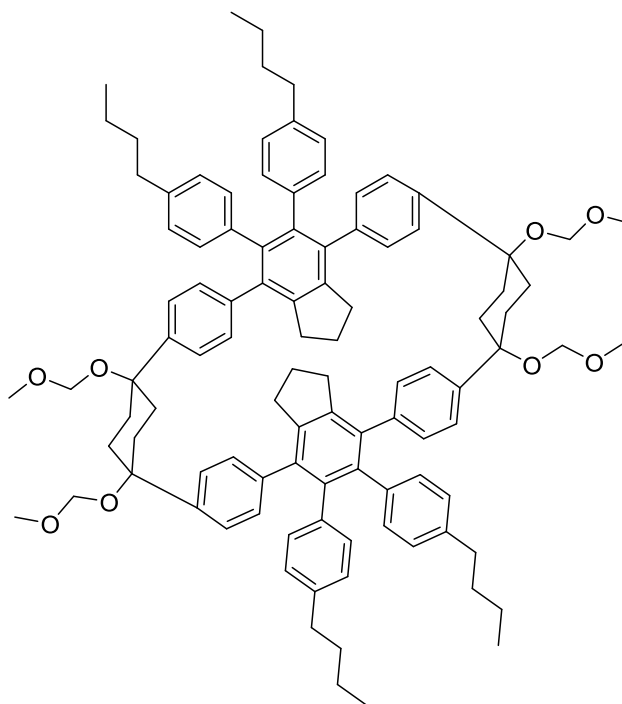
### **Synthesis of 102d**

Macrocycle **101c** (100 mg, 112  $\mu\text{mol}$ , 1.00 eq.), anhydrous 2-propanol (5 mL), and anhydrous THF (5 mL) were placed in a 10 mL microwave flask equipped with a stir bar. The reaction mixture was degassed by bubbling nitrogen through the solution for 15 min. Then,  $\text{RhCl}(\text{PPh}_3)_3$  (21.0 mg, 22.4  $\mu\text{mol}$ , 20 mol%) and 2-butyne-1,4-diol (96.8 mg, 1.12 mmol, 10.0 eq.) were added and the reaction flask was irradiated with microwave at 100°C for 6 h. The reaction mixture was filtrated to give 73 mg of product as a white solid (61%).

$^1\text{H NMR}$  (400 MHz,  $\text{CDCl}_3$ )  $\delta$ : broad signals (insoluble material)

**HR-MS** (ESI): calc. for  $[\text{C}_{66}\text{H}_{76}\text{NaO}_{12}]^+$ :  $[\text{M}+\text{Na}]^+$  1083.5229; found 1083.5242.

**Mp**: 262-273°C.



### Synthesis of 102e

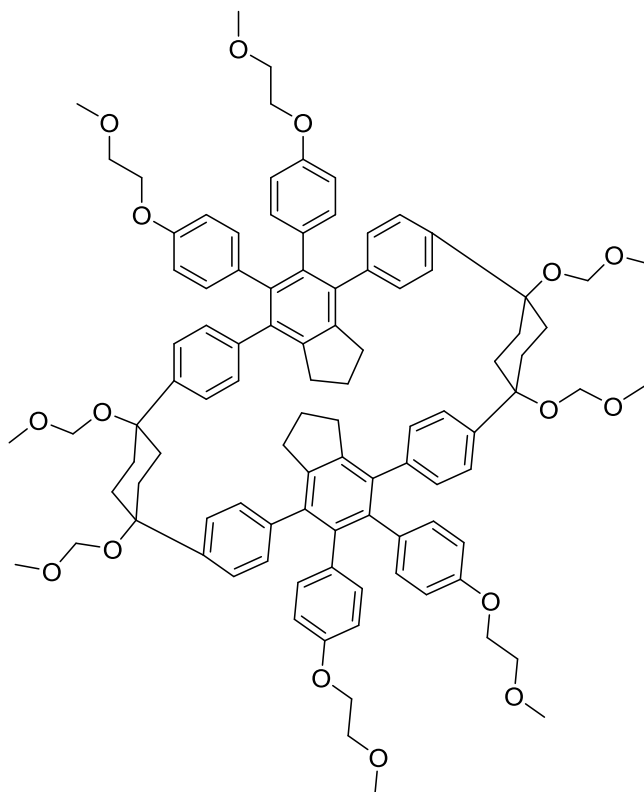
To a microwave vial was added anhydrous THF (5 mL) and anhydrous *isopropanol* (5 mL) and argon was bubbled through the solvent for 15 min. The macrocycle **101c** (100 mg, 112  $\mu\text{mol}$ , 1.00 eq.), 1,2-bis[4-(*n*-butyl)phenyl]ethyne **108** (326 mg, 1.12 mmol, 10.0 eq) and  $\text{RhCl}(\text{PPh}_3)_3$  (20.0 mg, 22.4  $\mu\text{mol}$ , 20 mol%) were added. The vial was sealed and irradiated by microwave at 100°C for 6h. Then, the volatiles were removed under reduced pressure and the crude product was chromatographed on column (cyclohexane/EtOAc, gradient) to afford 89.0 mg of product as white solid (54%).

$^1\text{H NMR}$  (400 MHz,  $\text{CDCl}_3$ ,  $\delta/\text{ppm}$ ): 7.11 (m, 8H), 6.91 (dm, 8H), 6.64 (s, 16H), 4.61 (s, 8H), 3.35 (s, 12H), 2.46 (t,  $J = 7.5$  Hz, 8H), 2.35 (t,  $J = 7.5$  Hz, 8H), 2.05 (m, 8H), 1.93 (m, 8H), 1.37 (m, 8H), 1.16 (m, 8H), 0.83 (t,  $J = 7.3$  Hz, 12H).

$^{13}\text{C NMR}$  (126 MHz,  $\text{CDCl}_3$ ,  $\delta/\text{ppm}$ ): 142.0 (4C), 140.1 (4C), 139.5 (4C), 139.4 (4C), 138.5 (4C), 137.3 (4C), 137.1 (4C), 131.1 (8C), 129.9 (8C), 126.5 (8C), 126.3 (8C), 92.5 (4C), 78.3 (4C), 55.6 (4C), 34.9 (4C), 33.8 (8C), 33.3 (4C), 24.3 (2C), 21.9 (4C), 13.9 (4C).

**HR-MS** (ESI): calc. for  $[\text{C}_{102}\text{H}_{120}\text{NO}_8]^+$ :  $[\text{M}+\text{NH}_4]^+$  1486.9008; found 1486.9004.

**Mp**: 272-274°C.



### Synthesis of 102f

To a microwave vial was added anhydrous THF (3 mL) and anhydrous *isopropanol* (3 mL) and argon was bubbled through the solvent for 15 min. The macrocycle **101c** (60 mg, 57.5  $\mu\text{mol}$ , 1.00 eq.), 1,2-bis [4-(2-methoxyethoxy)phenyl]ethyne **106** (220 mg, 675  $\mu\text{mol}$ , 10.0 eq.) and  $\text{RhCl}(\text{PPh}_3)_3$  (12.6 mg, 13.5  $\mu\text{mol}$ , 20 mol%) were added. The vial was sealed and irradiated by microwave at 100°C for 6h. The solid was filtrated and recrystallization in cyclohexane/DCM afforded 15 mg of pure product as an off-white solid. The rest was chromatographed on column (cyclohexane/EtOAc, gradient) to afford 34 mg of product (47%).

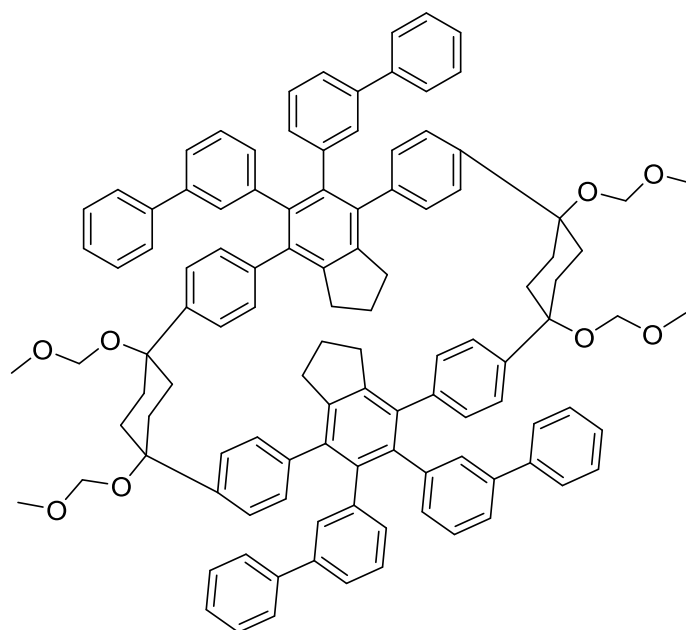
$^1\text{H NMR}$  (400 MHz,  $\text{CDCl}_3$ ,  $\delta/\text{ppm}$ ): 7.12 (m, 8H), 6.90 (m, 8H), 6.72 (m, 8H), 6.45 (m, 8H), 4.63 (s, 8H), 3.92 (m, 8H), 3.65 (m, 8H), 3.40 (s, 12H), 3.39 (s, 12H), 2.33 (t,  $J = 7.5$  Hz, 8H), 2.11 (m, 8H), 1.93 (m, 8H), 1.50 (p,  $J = 7.5$  Hz, 4H).

$^{13}\text{C NMR}$  (126 MHz,  $\text{CDCl}_3$ ,  $\delta/\text{ppm}$ ): 156.3 (4C), 142.2 (4C), 140.1 (4C), 139.3 (4C), 138.2 (4C), 137.8 (4C), 132.6 (4C), 132.4 (8C), 130.1 (8C), 126.2 (8C), 112.9 (8C), 92.7 (4C), 78.3 (4C), 71.1 (4C), 66.7 (4C), 59.2 (4C), 55.7 (4C), 34.0 (8C), 33.3 (4C), 24.1 (2C).

**HR-MS** (ESI): calc. for  $[\text{C}_{98}\text{H}_{108}\text{NaO}_{16}]^+$ :  $[\text{M}+\text{Na}]^+$  1563.7530; found 11563.7527.

**Mp**: 270-272°C.





### **Synthesis of 102g**

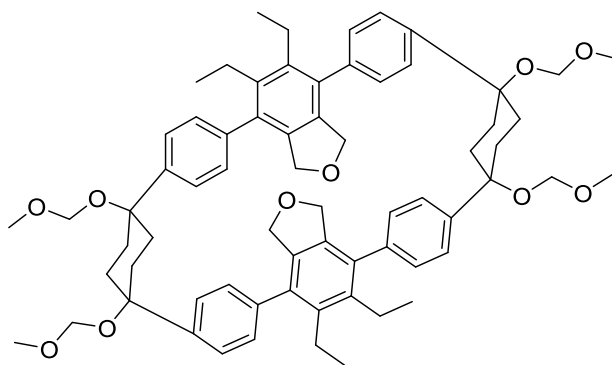
To a microwave vial was added anhydrous THF (10 mL) and anhydrous *isopropanol* (10 mL) and argon was bubbled through the solvent for 15 min. Then macrocycle **101c** (200 mg, 225  $\mu\text{mol}$ , 1.00 eq.), 1,2-di[(1,1'-biphenyl)-3-yl]ethyne **115** (743 mg, 2.25 mmol, 10.0 eq.) and  $\text{Rh}(\text{PPh}_3)_3\text{Cl}$  (41.6 mg, 45  $\mu\text{mol}$ , 20 mol%) were added. The vial was sealed and irradiated by microwave at 100°C for 6h. The volatiles were removed under reduced pressure and the crude product was chromatographed on column (CH/EtOAc, gradient) to afford 258 mg of product as white solid (74%).

**$^1\text{H}$  NMR** (400 MHz  $\text{CDCl}_3$   $\delta/\text{ppm}$ ): 7.20 (m, 12H), 7.13 (m, 12H), 7.07 (m, 12H), 6.94 (m, 12H), 6.86 (m, 4H), 4.63 (s, 8H), 3.37 (s, 12H), 2.46 (m, 8H), 2.03 (m, 8H), 1.92 (m, 8H), 1.62 (s, 4H).

**$^{13}\text{C}$  NMR** (150Hz,  $\text{C}_2\text{D}_2\text{Cl}_4$ , 348K,  $\delta/\text{ppm}$ ): 143.0, 141.2, 140.4, 139.8, 139.5, 138.2, 137.3, 131.4, 131.0, 130.8, 130.4, 130.1, 126.9, 126.3, 125.2, 124.5, 122.3, 92.6, 78.6, 55.6, 34.1, 33.1, 24.3

**HR-MS** (ESI): calc. for  $[\text{C}_{110}\text{H}_{100}\text{NO}_8]^+$ :  $[\text{M}+\text{NH}_4]^+$  1571.7310; found 1571.7317.

**Mp**: 274-276°C.



### **Synthesis of 102h**

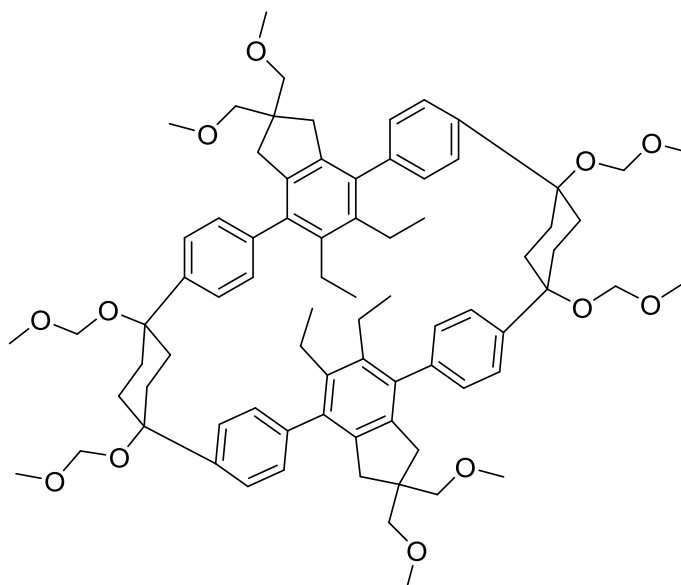
To a 20 mL microwave vial was introduced anhydrous THF (5 mL) and anhydrous *i*-PrOH (5 mL) and argon was bubbled through the solvent for 15 min. Then, **101d** (60 mg, 67.2  $\mu$ mol, 1.00 eq.), 3-hex-3-yne (100  $\mu$ L, 896  $\mu$ mol, 13.0 eq.) and RhCl(PPh<sub>3</sub>)<sub>3</sub> (16.6 mg, 17.9  $\mu$ mol, 27 mol%) were added and the vial was sealed and irradiated in the microwave reactor at 100°C for 6h. The crude mixture was concentrated, suspended in cyclohexane/EtOAc (1/1) and filtrated to give 33 mg of a grey solid (46%).

**<sup>1</sup>H NMR** (400 MHz, CDCl<sub>3</sub>,  $\delta$ /ppm): 7.38 (m, 8H), 7.11 (m, 8H), 4.71 (s, 8H), 3.93 (s, 8H), 3.48 (s, 12H), 2.79 (m, 8H), 2.31 (m, 8H), 1.95 (m, 8H), 1.11 (t,  $J$  = 7.4 Hz, 12H).

**<sup>13</sup>C NMR** (101 MHz, CDCl<sub>3</sub>,  $\delta$ /ppm): 140.0 (4C), 138.8 (4C), 137.0 (4C), 135.2 (8C), 128.9 (8C), 127.5 (8C), 92.8 (4C), 77.8 (4C), 74.1 (4C), 56.0 (4C), 33.9 (8C), 23.2 (4C), 16.6 (4C).

**HR-MS** (ESI): calc. for [C<sub>68</sub>H<sub>80</sub>NaO<sub>10</sub>]<sup>+</sup>: [M+Na]<sup>+</sup> 1079.5644; found 1079.5658.

**Mp**: >350°C decomposition.



### Synthesis of 102i

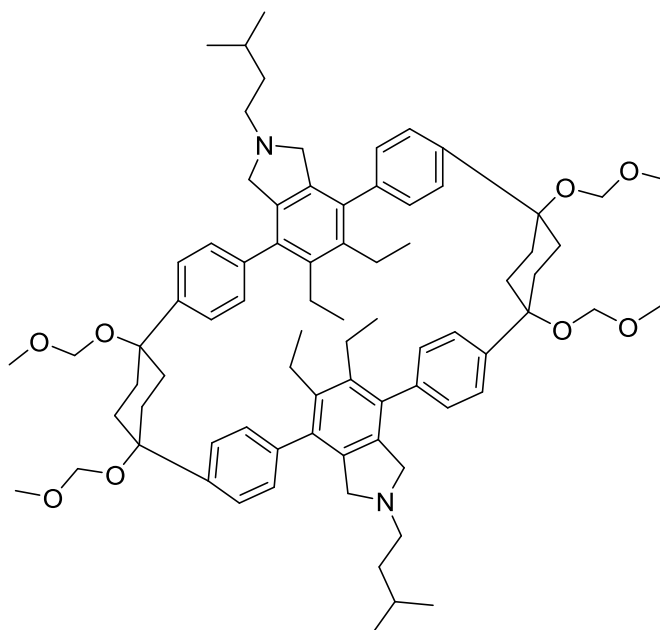
To a microwave vial was added anhydrous THF (10 mL) and anhydrous *isopropanol* (10 mL) and argon was bubbled through the solvent for 15 min. Then, macrocycle **101a** (100 mg, 93.9  $\mu\text{mol}$ , 1.00 eq.), 3-hex-3-yne (107  $\mu\text{L}$ , 939  $\mu\text{mol}$ , 10.0 eq.) and  $\text{Rh}(\text{PPh}_3)_3\text{Cl}$  (17.5 mg, 18.8  $\mu\text{mol}$ , 20 mol%) were added. The vial was sealed and irradiated by microwave at 100°C for 6h. The mixture was concentrated, suspended in cyclohexane/EtOAc (1/1) and filtrated to give 78.5 mg of product as a grey solid (68%).

**$^1\text{H}$  NMR** (600 MHz,  $\text{C}_2\text{D}_2\text{Cl}_4$ , 158 K,  $\delta/\text{ppm}$ ): 7.27 (m, 8H), 6.98 (m, 8H), 4.67 (s, 8H), 3.38 (s, 12H), 3.06 (s, 12H), 2.83 (s, 8H), 2.52 (q,  $J = 7.4$  Hz, 8H), 2.29 (m, 8H), 1.95 (m, 8H), 1.89 (bs, 8H), 0.96 (t,  $J = 7.4$  Hz, 12H).

**$^{13}\text{C}$  NMR** (150Hz,  $\text{C}_2\text{D}_2\text{Cl}_4$ , 358K,  $\delta/\text{ppm}$ ): 140.5 (4C), 140.0 (4C), 138.8 (4C), 138.5 (4C), 138.0 (4C), 129.2 (8C), 126.9 (8C), 92.5 (4C), 77.8 (4C), 75.9 (4C), 59.0 (4C), 55.4 (4C), 46.8 (2C), 38.8 (4C), 33.9 (8C), 23.3 (4C), 16.3 (4C).

**HR-MS** (ESI): calc. for  $[\text{C}_{78}\text{H}_{100}\text{NaO}_{12}]^+$ :  $[\text{M}+\text{Na}]^+$  1251.7107; found 1251.7092.

**Mp**: 272-279°C.



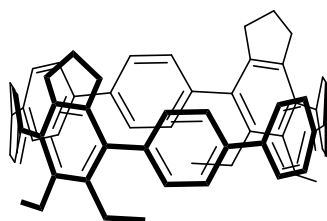
### Synthesis of 102j

To a microwave vial was added anhydrous THF (10 mL) and anhydrous *isopropanol* (10 mL) and argon was bubbled through the solvent for 15 min. Then, macrocycle **101b** (100 mg, 97.0  $\mu\text{mol}$ , 1.00 eq.), 3-hexyne (111  $\mu\text{L}$ , 970  $\mu\text{mol}$ , 10.0 eq.) and  $\text{Rh}(\text{PPh}_3)_3\text{Cl}$  (18.1 mg, 19.4  $\mu\text{mol}$ , 20 mol%) were added. The vial was sealed and irradiated by microwave at 100°C for 6h. The mixture was concentrated and chromatographed on silica (cyclohexane/EtOAc, 1/1) to afford 43.0 mg of product as a yellow solid (37%).

$^1\text{H NMR}$  (400 MHz,  $\text{CDCl}_3$ ,  $\delta/\text{ppm}$ ): 7.29 – 6.56 (m, 16H), 4.72 (s, 8H), 3.47 (s, 12H), 2.74 (s, 8H), 2.38 (m, 8H), 2.04 (m, 8H), 1.80 (m, 3H), 1.05 (t,  $J = 7.3$  Hz, 8H), 0.78 (d,  $J = 6.6$  Hz, 7H), 0.61 (m, 3H).

$^{13}\text{C NMR}$  (101Hz,,  $\text{CDCl}_3$ ): broad signals.

**HR-MS** (ESI): calc. for  $[\text{C}_{78}\text{H}_{103}\text{N}_2\text{O}_8]^+$ :  $[\text{M}+\text{H}]^+$  1095.7709; found 1095.7707.



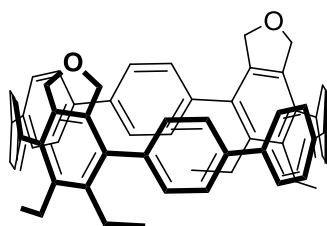
### Synthesis of 103c

In a 20 mL vial **102a** (120 mg, 114  $\mu\text{mol}$ , 1.00 eq.) and  $\text{NaHSO}_4/\text{H}_2\text{O}$  (274 mg, 2.28 mmol, 20.0 eq.) were dissolved in 5 mL *m*-xylene and 5 mL DMSO. The solution was stirred under air at 130°C for 24h. The mixture was cooled to rt and extracted with water and EtOAc. The organic phase was washed with water, dried over  $\text{Na}_2\text{SO}_4$  and concentrated under reduced pressure. The residue was chromatographed on TLC (hexane/DCM: 1/1) to give 6.0 mg of **103c** as a pale yellow solid (7%).

$^1\text{H NMR}$  (500 MHz,  $\text{CD}_2\text{Cl}_2$ ,  $\delta/\text{ppm}$ ): 7.35 (s, 8H), 7.30 – 7.25 (m, 8H), 7.04 – 6.93 (m, 8H), 2.98 (q,  $J = 7.5$  Hz, 8H), 1.90 (t,  $J = 7.7$  Hz, 8H), 1.28 – 1.20 (m, 4H), 1.14 (t,  $J = 7.4$  Hz, 12H).

$^{13}\text{C NMR}$  (126 MHz,  $\text{CD}_2\text{Cl}_2$ ,  $\delta/\text{ppm}$ )\*: 141.9, 139.3, 138.4, 137.9, 137.8, 137.3, 131.1, 127.2, 126.3, 32.4, 23.1, 21.8, 16.2.

**HR-MS** (MALDI): calc. for  $[\text{C}_{62}\text{H}_{56}]^+$ :  $[\text{M}]^+$  800.4377; found 800.4378. (DCTB matrix)



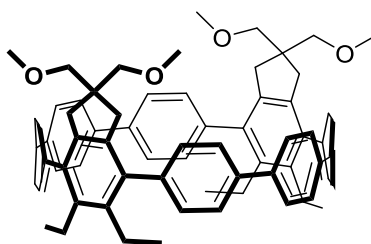
### Synthesis of 103d

In a 20 mL vial **102h** (30.0 mg, 28.4  $\mu\text{mol}$ , 1.00 eq.) and  $\text{NaHSO}_4/\text{H}_2\text{O}$  (78.0 mg, 567  $\mu\text{mol}$ , 20.0 eq.) were dissolved in 5 mL *m*-xylene and 5 mL DMSO. The solution was stirred under air at 130°C for 48h. The mixture was cooled to rt and diluted with water and EtOAc. The organic phase was washed with water, dried over  $\text{Na}_2\text{SO}_4$  and concentrated under reduced pressure. The residue was chromatographed on TLC (hexane/DCM: 1/1 +1% MeOH) to give 0.6 mg of **103d** as a pale yellow solid 3%.

$^1\text{H NMR}$  (500 MHz,  $\text{CD}_2\text{Cl}_2$ ,  $\delta/\text{ppm}$ ): 7.44 (s, 8H), 7.39 (m, 8H), 7.06 (m, 8H), 4.07 (s, 8H), 3.11 (q,  $J = 7.5$  Hz, 8H), 1.26 (m, 12H).

$^{13}\text{C NMR}$  (126 MHz,  $\text{CD}_2\text{Cl}_2$ ,  $\delta/\text{ppm}$ )\*: 139.4 (8C), 139.1 (4C), 138.9 (4C), 138.7 (4C), 135.8 (4C), 131.0 (8C), 128.2 (8C), 127.5 (8C), 74.7 (4C), 23.9 (4C), 17.1 (4C).

**HR-MS** (MALDI): calc. for  $[\text{C}_{60}\text{H}_{52}\text{O}_2]^+$ :  $[\text{M}]^+$  804.3962; found 804.3964. (DCTB matrix)



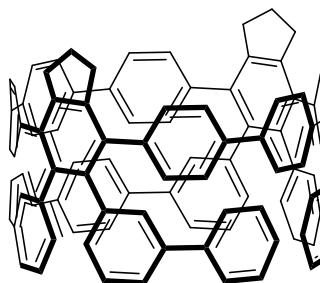
### Synthesis of 103a

In a 20 mL vial **102i** (33.0 mg, 26.8  $\mu\text{mol}$ , 1.00 eq.) and  $\text{NaHSO}_4/\text{H}_2\text{O}$  (64.0 mg, 0.537 mmol, 20.0 eq.) were dissolved in 5 mL *m*-xylene and 5 mL DMSO. The mixture was stirred under air at 130°C for 24h. The solution was cooled to rt and diluted with water and EtOAc. The organic phase was washed with water, dried over  $\text{Na}_2\text{SO}_4$  and concentrated under reduced pressure. The residue was chromatographed on TLC (Hexane/DCM: 1/1 +1%MeOH) to give 1.9 mg of **103a** as white solid (4%).

$^1\text{H NMR}$  (500 MHz,  $\text{CD}_2\text{Cl}_2$ ,  $\delta/\text{ppm}$ ): 7.45 (s, 8H), 7.37 – 7.30 (m, 8H), 7.09 – 7.02 (m, 8H), 3.06 (q,  $J = 7.4$  Hz, 8H), 2.87 (s, 12H), 2.73 (s, 8H), 1.98 (s, 8H), 1.21 (t,  $J = 7.4$  Hz, 12H).

$^{13}\text{C NMR}$  (126 MHz,  $\text{CD}_2\text{Cl}_2$ ,  $\delta/\text{ppm}$ ): 141.0, 140.1, 139.3, 139.0, 138.9, 138.5, 132.1, 128.1, 127.1, 75.9, 59.0, 45.9, 24.4, 17.1.

**HR-MS** (ESI): calc. for  $[\text{C}_{70}\text{H}_{72}\text{NaO}_4]^+$ :  $[\text{M}+\text{Na}]^+$  999.5323; found 999.5340.

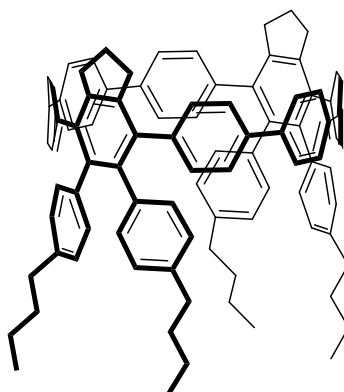


### Synthesis of 103e

In a 20 mL flask **102g** (60.0 mg, 39.0  $\mu\text{mol}$ , 1.00 eq.) and  $\text{NaHSO}_4/\text{H}_2\text{O}$  (94.0 mg, 780  $\mu\text{mol}$ , 20.0 eq.) were dissolved in 5 mL *m*-xylene and 2.5 mL DMSO. The solution was stirred under air at 130°C for 24h. The mixture was concentrated by vacuum distillation. The remaining solid was filtrated off and the resulting filtrate was purified by PTLC (hexane/DCM: 1/1) to give 1.5 mg of product as white solid (3%).

$^1\text{H NMR}$  (500 MHz,  $\text{CD}_2\text{Cl}_2$ ,  $\delta/\text{ppm}$ ): 7.48 (m, 4H), 7.37 – 7.14 (m, 40H), 7.02 (m, 16H), 2.20 (t,  $J = 7.6$  Hz, 8H), 1.45 (t,  $J = 7.6$  Hz, 4H).

**MALDI MS**: 1297.24 (M<sup>+</sup>)



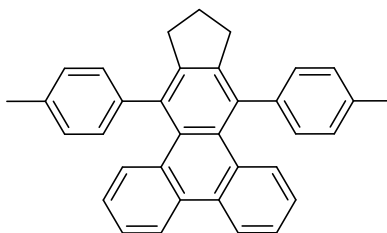
### Synthesis of 103b

In a 20 mL vial **102e** (80.0 mg, 54.4  $\mu\text{mol}$ , 1.00 eq.) and  $\text{NaHSO}_4/\text{H}_2\text{O}$  (150 mg, 1.08 mmol, 20.0 eq.) were dissolved in 7.5 mL *m*-xylene and 7.5 mL DMSO. The solution was stirred under air at 130°C for 48h. The mixture was cooled to rt and extracted with water and EtOAc. The organic phase was washed with water, dried over  $\text{Na}_2\text{SO}_4$  and concentrated under reduced pressure. The residue was chromatographed on TLC (Hexane/DCM: 1/1 +1% MeOH) to give 3.00 mg of **103b** as a pale yellow solid (5%).

**$^1\text{H}$  NMR** (500 MHz,  $\text{CD}_2\text{Cl}_2$ ,  $\delta/\text{ppm}$ ): 7.35 (s, 8H), 7.22 (m, 8H), 7.01 (m, 8H), 6.89 (m, 8H), 6.76 (m, 8H), 2.50 – 2.43 (m, 8H), 2.29 (t,  $J = 7.6$  Hz, 8H), 1.53 (m, 4H), 1.47 (m, 8H), 1.22 (m, 8H), 0.93 – 0.86 (m, 12H).

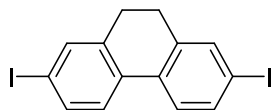
**$^{13}\text{C}$  NMR** (126 MHz,  $\text{CD}_2\text{Cl}_2$ ,  $\delta/\text{ppm}$ )\*: 143.5 (4C), 140.3 (4C), 139.5 (4C), 139.0 (8C), 138.7 (4C), 138.3 (4C), 138.2 (4C), 132.2 (8C), 131.8 (8C), 128.2 (8C), 126.9 (8C), 126.7 (8C), 35.1 (4C), 33.4 (4C), 33.3 (4C), 23.7 (2C), 22.4 (4C), 13.8 (4C).

**HR-MS** (MALDI): calc. for  $[\text{C}_{94}\text{H}_{88}]^+$ :  $[\text{M}]^+$  1216.6881; found 1216.6884. (DCTB matrix)

**3.2.10 Nanobelt synthesis : diphenylphenanthrene strategy****Synthesis of 9,13-di-*p*-tolyl-11,12-dihydro-10*H*-cyclopenta[*b*]triphenylene 120**

1,7-di-*p*-tolylhepta-1,6-diyne **41c** (41.0 mg, 153  $\mu\text{mol}$ , 1.00 eq.), 9-bromophenanthrene **119** (49.2 mg, 184  $\mu\text{mol}$ , 1.20 eq.), Pd(OAc)<sub>2</sub> (1.40 mg, 6.00  $\mu\text{mol}$ , 4.00 mol%) and PPh<sub>3</sub> (1.6 mg, 6.00  $\mu\text{mol}$ , 4.00 mol%) were added to a degassed solution of *n*-Bu<sub>3</sub>N (73.0  $\mu\text{L}$ , 306  $\mu\text{mol}$ , 2.00 eq.) in DMF (3 mL). The solution was stirred at rt for 30 min and heated at 130°C for 20 h. The reaction mixture was cooled, quenched with water, and extracted with EtOAc. The organic phase was washed with Na<sub>2</sub>CO<sub>3</sub> 5%, HCl 7%, brine, dried over Na<sub>2</sub>SO<sub>4</sub> and concentrated under reduced pressure. The residue was purified by column chromatography to give 20 mg of product (30%).

<sup>1</sup>H NMR (400 MHz, CDCl<sub>3</sub>,  $\delta$ /ppm): 8.39 (m, 2H), 7.72 (m, 2H), 7.35 (m, 2H), 7.22 (m, 4H), 7.01 (m, 2H).

**Synthesis of 2,7-diiodo-9,10-dihydrophenanthrene 122**

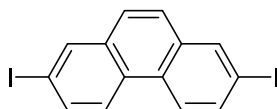
9,10-Dihydrophenanthrene (2.00 g, 11.1 mmol, 1.00 eq.), iodine (2.25 g, 8.88 mmol, 0.800 eq.) and iodic acid (1.05 g, 5.99 mmol, 0.540 eq.) were added subsequently to a solution of 14 mL glacial AcOH, 2 mL H<sub>2</sub>O, 0.5 mL conc. H<sub>2</sub>SO<sub>4</sub> and 1 mL CCl<sub>4</sub>. Then the reaction mixture was heated to 80°C and kept at this temperature for 5h. After quenching with water, the mixture was dissolved in DCM and washed with Na<sub>2</sub>S<sub>2</sub>O<sub>3</sub>, dried over Na<sub>2</sub>SO<sub>4</sub> and concentrated under reduced pressure. The solid was collected by filtration and washed with Et<sub>2</sub>O/MeOH 1/1 and EtOAc to provide the product as light yellow solid (3.15 g, 66%).

<sup>1</sup>H NMR (400 MHz, CDCl<sub>3</sub>,  $\delta$ /ppm): 7.62 (m, 2H), 7.59 (m, 2H), 7.42 (m, 2H).

<sup>13</sup>C NMR (101 MHz, CDCl<sub>3</sub>,  $\delta$ /ppm): 139.5, 137.2, 136.3, 133.4, 125.5, 93.5, 28.5.

Analytical data are in accordance with the literature<sup>19</sup>





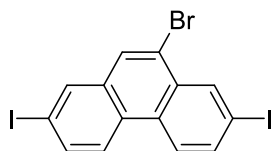
### **Synthesis of 2,7-diiodophenanthrene 123**

2,7-Diiodo-9,10-dihydrophenanthrene **122** (3.15 g, 7.30 mmol, 1.00 eq.) was dissolved in 50 mL  $\text{CCl}_4$ . Then N-bromosuccinimide (1.30 g, 7.30 mmol, 1.00 eq.) and a trace of dibenzoylperoxide were added and the reaction refluxed for 5h. The formed solid was collected by filtration and washed with ethanol to give the product as a white solid (2.23 g, 71%).

$^1\text{H NMR}$  (400 MHz,  $\text{CDCl}_3$ ,  $\delta/\text{ppm}$ ): 8.34 (m, 2 H), 8.25 (m, 2H), 7.91 (m, 2H), 7.62 (s, 2H).

$^{13}\text{C NMR}$  (126 MHz,  $\text{CDCl}_3$ ,  $\delta/\text{ppm}$ ): 137.5, 135.7, 133.8, 129.2, 126.9, 124.4, 92.9

Analytical data are in accordance with the literature<sup>19</sup>



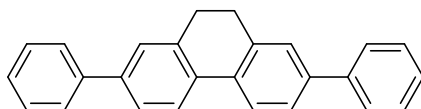
### **9-Bromo-2,7-diiodophenanthrene 126**

In a 100 mL flask was added 2,7-diiodophenanthrene **123** (1.00 g, 2.33 mmol, 1.00 eq.) in 40 mL chlorobenzene. Then  $\text{CuBr}_2$  on alox<sup>20</sup> (5.00 g, 23.3 mmol, 10.0 eq.) was added and the mixture was stirred at 100°C overnight. The cooled mixture was filtrated and washed with toluene and DCM. The filtrate was concentrated under reduced pressure to give 676 mg of product as pale yellow solid (57%).

$^1\text{H NMR}$  (400 MHz,  $\text{CDCl}_3$ ,  $\delta/\text{ppm}$ ): 8.70 (m, 1 H), 8.30 (m, 2H), 8.15 (m, 1H), 7.97 (m, 2H), 7.92 (m, 1H).

$^{13}\text{C NMR}$  (126 MHz,  $\text{CDCl}_3$ ,  $\delta/\text{ppm}$ ): 137.4, 137.1, 136.7, 136.6, 136.2, 130.2, 124.4, 124.3.

**GCMS:** 508 [M], 381, 302, 254, 175.

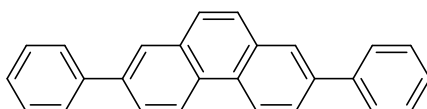


### **2,7-diphenyl-9,10-dihydrophenanthrene 127**

In a 50 mL flask was placed 2,7-diiodo-9,10-dihydrophenanthrene **122** (1.43 g, 3.31 mmol, 1.00 eq.) and phenylboronic acid pinacol ester (1.53 g, 7.28 mmol, 2.20 eq.) in 30 mL THF, argon was bubbled through the solution for 15 min, then Pd(PPh<sub>3</sub>)<sub>4</sub> (622 mg, 622 μmol, 20.0 mol%) and K<sub>2</sub>CO<sub>3</sub> aq. (2M, 23 mL) were added. The solution was refluxed overnight. The mixture was filtrated and washed with EtOH and a few mL of DCM, to give 486 mg of product as white solid (44%).

<sup>1</sup>H NMR (400 MHz, CDCl<sub>3</sub>, δ/ppm): 7.86 (m, 2H), 7.66 (m, 4H), 7.57 (m, 2H), 7.50 (m, 2H), 7.49 (m, 4H), 7.36 (m, 2H).

<sup>13</sup>C NMR (101 MHz, CDCl<sub>3</sub>, δ/ppm): 141.0, 140.3, 137.9, 133.5, 129.0, 127.5, 127.1, 127.0, 125.9, 124.3, 29.5.

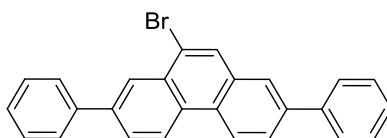


### **2,7-diphenylphenanthrene 124**

In a 50 ml flask was placed 2,7-diiodophenanthrene **123** (500 mg, 1.16 mmol, 1.00 eq.) and phenylboronic acid pinacol ester (538 mg, 2.56 mmol, 2.20 eq.) in 30 mL THF, argon was bubbled through the solution for 15 min. Then, Pd(PPh<sub>3</sub>)<sub>4</sub> (269 mg, 233 μmol, 20.0 mol%) and K<sub>2</sub>CO<sub>3</sub> aq. (2M, 8 mL) were added and the mixture was refluxed overnight. The suspension was filtrated and washed with EtOH and a few mL of DCM, to give 222 mg white solid (58%).

<sup>1</sup>H NMR (400 MHz, CDCl<sub>3</sub>, δ/ppm): 8.72 (m, 2H), 8.07 (m, 2H), 7.89 (m, 2H), 7.80 (s, 2H), 7.74 (m, 4H), 7.48 (m, 4H), 7.38 (m, 2H).

GCMS: 330 [M]



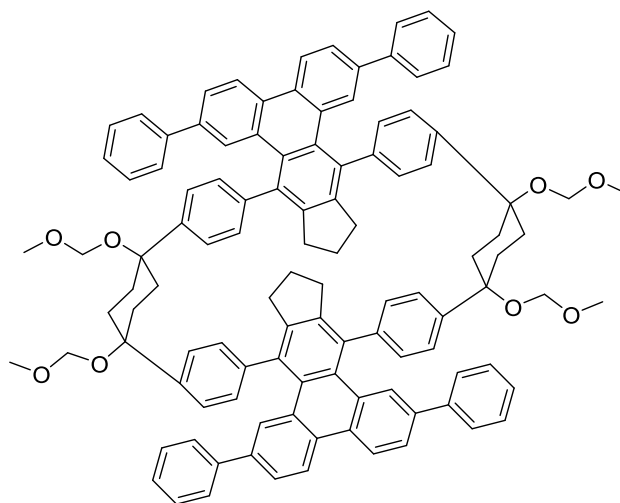
### **9-bromo-2,7-diphenylphenanthrene 125**

In a 25 mL flask was placed 2,7-diphenyl-9,10-dihydrophenanthrene **127** (300 mg, 902  $\mu\text{mol}$ , 1.00 eq.) NBS (161 mg, 902  $\mu\text{mol}$ , 1.00 eq.) and a tip of spatula of AIBN in 7 mL chlorobenzene. The mixture was irradiated with halogen lamp (45°C) overnight. Then  $\text{CuBr}_2$  on alox (1.50 g, 4.51 mmol, 5.00 eq.) was added and the mixture was stirred at 100°C for 24h. After that, the mixture was filtrated, the filtrate was concentrated and purified by column chromatography (cyclohexane/toluene: 9/1) to give 66 mg of product as white crystalline solid (18%)

$^1\text{H NMR}$  (400 MHz,  $\text{CDCl}_3$ ,  $\delta/\text{ppm}$ ): 8.77 (m, 1H), 8.73 (m, 1H), 8.59 (m, 1H), 8.20 (s, 1H), 8.02 (m, 1H), 7.99 (m, 1H), 7.95 (m, 1H), 7.82 (m, 1H), 7.76 (m, 1H), 7.53 (m, 1H), 7.43 (m, 1H).

$^{13}\text{C NMR}$  (101 MHz,  $\text{CDCl}_3$ ,  $\delta/\text{ppm}$ ): 141.5, 140.7, 138.1, 133.9, 129.1, 127.6, 127.5, 127.4, 127.3, 126.2, 124.6.

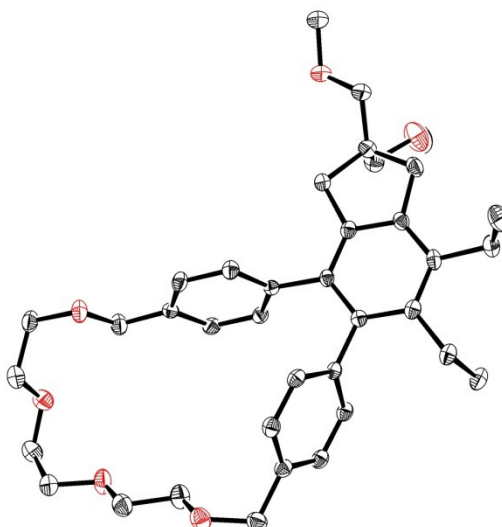
**GCMS:** 408 [M], 326, 252, 205, 163.



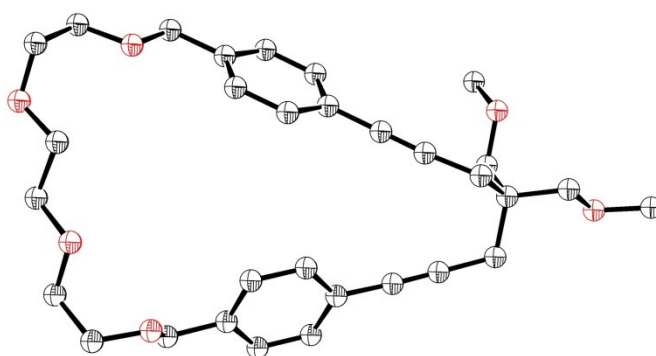
### **Domino-Heck type with 9-bromo-2,7-diphenylphenanthrene 125 and 101c**

Macrocyclic **101c** (91.7 mg, 103  $\mu\text{mol}$ , 1.00 eq.) 9-bromo-2,7-diphenylphenanthrene (93.0 mg, 227  $\mu\text{mol}$ , 2.20 eq.),  $\text{Pd}(\text{OAc})_2$  (0.462 mg, 2.06  $\mu\text{mol}$ , 2.00 mol%),  $\text{PPh}_3$  (1.08 mg, 4.12  $\mu\text{mol}$ , 4.00 mol%) were added to a degassed solution of *n*- $\text{Bu}_3$  (48.0  $\mu\text{L}$ , 206  $\mu\text{mol}$ , 2.00 eq.) in DMF (6 mL). The suspension was further degassed by bubbling argon through for 30 min and the mixture was stirred at 110°C overnight. The cooled mixture was separated in LiCl (5% aq) and DCM. The organic phase was washed with LiCl (5%) 3 x and with brine then, dried over  $\text{Na}_2\text{SO}_4$  and concentrated under reduced pressure. A yellowish solid was obtained which was too insoluble for being analyzed.

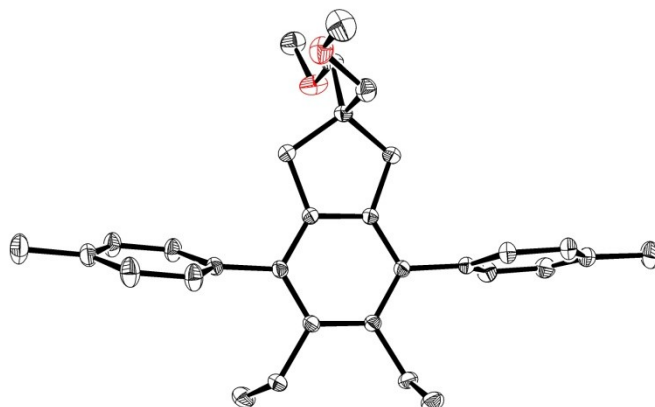
### 3.3 CRYSTALLOGRAPHIC DATA:



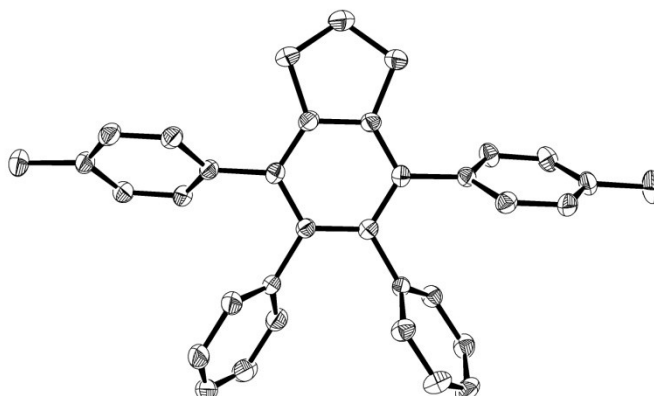
Crystal data for **68a**: formula  $C_{39.93}H_{52.38}O_{6.19}$ ,  $M = 631.43$ ,  $F(000) = 682.959$ , colourless block, size  $0.030 \cdot 0.050 \cdot 0.210 \text{ mm}^3$ , triclinic, space group  $P -1$ ,  $Z = 2$ ,  $a = 9.6066(10) \text{ \AA}$ ,  $b = 11.7824(13) \text{ \AA}$ ,  $c = 15.8331(17) \text{ \AA}$ ,  $\alpha = 90.523(6)^\circ$ ,  $\beta = 95.662(6)^\circ$ ,  $\gamma = 100.184(6)^\circ$ ,  $V = 1754.6(3) \text{ \AA}^3$ ,  $D_{\text{calc.}} = 1.195 \text{ Mg} \cdot \text{m}^{-3}$ . The crystal was measured on a Bruker Kappa Apex2 diffractometer at 123K using graphite-monochromated  $\text{MoK}_\alpha$ -radiation with  $\lambda = 0.71073 \text{ \AA}$ ,  $\Theta_{\text{max}} = 27.478^\circ$ . Minimal/maximal transmission 1.00/1.00,  $\mu = 0.079 \text{ mm}^{-1}$ . The Apex2 suite has been used for datacollection and integration. From a total of 21781 reflections, 7930 were independent (merging  $r = 0.048$ ). From these, 4417 were considered as observed ( $I > 2.0\sigma(I)$ ) and were used to refine 525 parameters. The structure was solved by Other methods using the program Superflip. Least-squares refinement against  $F$  was carried out on all non-hydrogen atoms using the program CRYSTALS.  $R = 0.0610$  (observed data),  $wR = 0.1402$  (all data),  $\text{GOF} = 1.0016$ . Minimal/maximal residual electron density =  $-0.94/0.72 \text{ e \AA}^{-3}$ . Chebychev polynomial weights were used to complete the refinement. Plots were produced using Ortep 3v2.



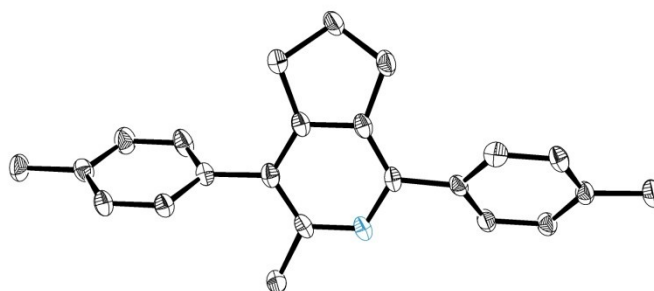
Crystal data for **66**: formula  $C_{31}H_{38}O_6$ ,  $M = 506.64$ ,  $F(000) = 544$ , colourless block, size  $0.050 \cdot 0.140 \cdot 0.210$  mm<sup>3</sup>, triclinic, space group  $P \bar{1}$ ,  $Z = 2$ ,  $a = 8.4549(4)$  Å,  $b = 10.6064(4)$  Å,  $c = 17.4616(7)$  Å,  $\alpha = 72.980(2)^\circ$ ,  $\beta = 76.359(2)^\circ$ ,  $\gamma = 67.627(2)^\circ$ ,  $V = 1370.82(10)$  Å<sup>3</sup>,  $D_{\text{calc.}} = 1.227$  Mg · m<sup>-3</sup>. The crystal was measured on a Bruker Kappa Apex2 diffractometer at 123K using graphite-monochromated Mo  $K_\alpha$ -radiation with  $\lambda = 0.71073$  Å,  $\Theta_{\text{max}} = 30.066^\circ$ . Minimal/maximal transmission 0.99/1.00,  $\mu = 0.084$  mm<sup>-1</sup>. The Apex2 suite has been used for datacollection and integration. From a total of 28795 reflections, 7983 were independent (merging  $r = 0.042$ ). From these, 4264 were considered as observed ( $I > 2.0\sigma(I)$ ) and were used to refine 334 parameters. The structure was solved by direct methods using the program SIR92. Least-squares refinement against  $F$  was carried out on all non-hydrogen atoms using the program CRYSTALS.  $R = 0.0400$  (observed data),  $wR = 0.0945$  (all data),  $GOF = 1.1157$ . Minimal/maximal residual electron density =  $-0.22/0.30$  e Å<sup>-3</sup>. Chebychev polynomial weights were used to complete the refinement. Plots were produced using Ortep 3v2



Crystal data for **42a**: formula  $C_{31}H_{38}O_2$ ,  $M = 442.64$ ,  $F(000) = 960$ , colourless block, size  $0.110 \cdot 0.170 \cdot 0.210 \text{ mm}^3$ , monoclinic, space group  $P 21/c$ ,  $Z = 4$ ,  $a = 10.6213(3) \text{ \AA}$ ,  $b = 20.0058(5) \text{ \AA}$ ,  $c = 13.1220(3) \text{ \AA}$ ,  $\alpha = 90^\circ$ ,  $\beta = 110.6260(10)^\circ$ ,  $\gamma = 90^\circ$ ,  $V = 2609.53(12) \text{ \AA}^3$ ,  $D_{\text{calc.}} = 1.127 \text{ Mg} \cdot \text{m}^{-3}$ . The crystal was measured on a Bruker Kappa Apex2 diffractometer at 123K using graphite-monochromated Mo  $K_\alpha$ -radiation with  $\lambda = 0.71073 \text{ \AA}$ ,  $\Theta_{\text{max}} = 34.971^\circ$ . Minimal/maximal transmission 0.99/0.99,  $\mu = 0.068 \text{ mm}^{-1}$ . The Apex2 suite has been used for datacollection and integration. From a total of 74553 reflections, 11390 were independent (merging  $r = 0.032$ ). From these, 8181 were considered as observed ( $I > 2.0\sigma(I)$ ) and were used to refine 298 parameters. The structure was solved by direct methods using the program SIR92. Least-squares refinement against  $F$  was carried out on all non-hydrogen atoms using the program CRYSTALS.  $R = 0.0521$  (observed data),  $wR = 0.0923$  (all data),  $\text{GOF} = 1.0486$ . Minimal/maximal residual electron density =  $-0.28/0.50 \text{ e \AA}^{-3}$ . Chebychev polynomial weights were used to complete the refinement. Plots were produced using Ortep 3v2

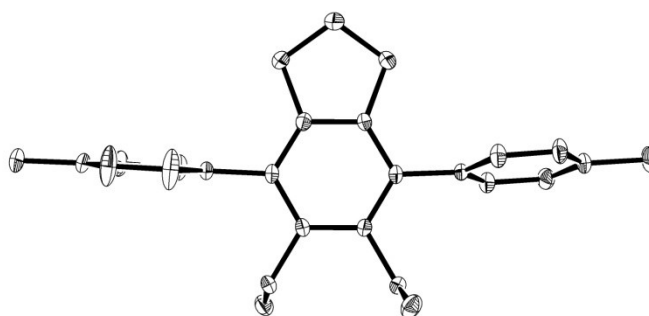


Crystal data for **42e**: formula  $C_{35}H_{30}$ ,  $M = 450.62$ ,  $F(000) = 960$ , yellow block, size  $0.040 \cdot 0.170 \cdot 0.190 \text{ mm}^3$ , monoclinic, space group  $P 2_1/n$ ,  $Z = 4$ ,  $a = 9.9450(5) \text{ \AA}$ ,  $b = 18.2228(9) \text{ \AA}$ ,  $c = 14.5398(8) \text{ \AA}$ ,  $\alpha = 90^\circ$ ,  $\beta = 106.679(2)^\circ$ ,  $\gamma = 90^\circ$ ,  $V = 2524.1(2) \text{ \AA}^3$ ,  $D_{\text{calc.}} = 1.186 \text{ Mg} \cdot \text{m}^{-3}$ . The crystal was measured on a Bruker Kappa Apex2 diffractometer at 123K using graphite-monochromated Mo  $K_\alpha$ -radiation with  $\lambda = 0.71073 \text{ \AA}$ ,  $\Theta_{\text{max}} = 30.042^\circ$ . Minimal/maximal transmission 0.99/1.00,  $\mu = 0.067 \text{ mm}^{-1}$ . The Apex2 suite has been used for datacollection and integration. From a total of 37736 reflections, 7379 were independent (merging  $r = 0.048$ ). From these, 3761 were considered as observed ( $I > 2.0\sigma(I)$ ) and were used to refine 316 parameters. The structure was solved by direct methods using the program SIR92. Least-squares refinement against  $F$  was carried out on all non-hydrogen atoms using the program CRYSTALS.  $R = 0.0546$  (observed data),  $wR = 0.1283$  (all data),  $\text{GOF} = 1.0908$ . Minimal/maximal residual electron density =  $-0.34/0.36 \text{ e \AA}^{-3}$ . Chebychev polynomial weights were used to complete the refinement. Plots were produced using Ortep 3v2

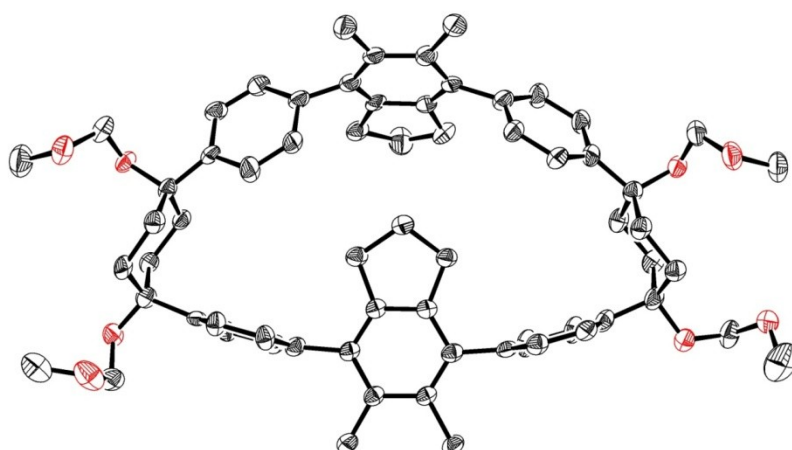


Crystal data for **42g**: formula  $C_{23}H_{23}N_1$ ,  $M = 313.44$ ,  $F(000) = 672$ , colourless plate, size  $0.020 \cdot 0.110 \cdot 0.230 \text{ mm}^3$ , monoclinic, space group  $P 21/c$ ,  $Z = 4$ ,  $a = 12.990(4) \text{ \AA}$ ,  $b = 15.212(4) \text{ \AA}$ ,  $c = 9.107(3) \text{ \AA}$ ,  $\alpha = 90^\circ$ ,  $\beta = 107.22^\circ$ ,  $\gamma = 90^\circ$ ,  $V = 1719.0(9) \text{ \AA}^3$ ,  $D_{\text{calc.}} = 1.211 \text{ Mg} \cdot \text{m}^{-3}$ . The crystal was measured on a Bruker Kappa Apex2 diffractometer at 123K using graphite-monochromated Mo  $K_\alpha$ -radiation with  $\lambda = 0.71073 \text{ \AA}$ ,  $\Theta_{\text{max}} = 25.039^\circ$ . Minimal/maximal transmission 0.99/1.00,  $\mu = 0.069 \text{ mm}^{-1}$ . The Apex2 suite has been used for datacollection and integration. From a total of 14602 reflections, 3026 were independent (merging  $r = 0.130$ ). From these, 3015 were considered as observed ( $I > 2.0\sigma(I)$ ) and were used to refine 217 parameters. The structure was solved by direct methods using the program SIR92. Least-squares refinement against  $F_{\text{sqd}}$  was carried out on all non-hydrogen atoms using the program CRYSTALS.  $R = 0.0559$  (observed data),  $wR = 0.1353$  (all data),  $\text{GOF} = 0.8004$ . Minimal/maximal residual electron density =  $-0.81/0.95 \text{ e \AA}^{-3}$ . Chebychev polynomial weights were used to complete the refinement. Plots were produced using Ortep 3v2.

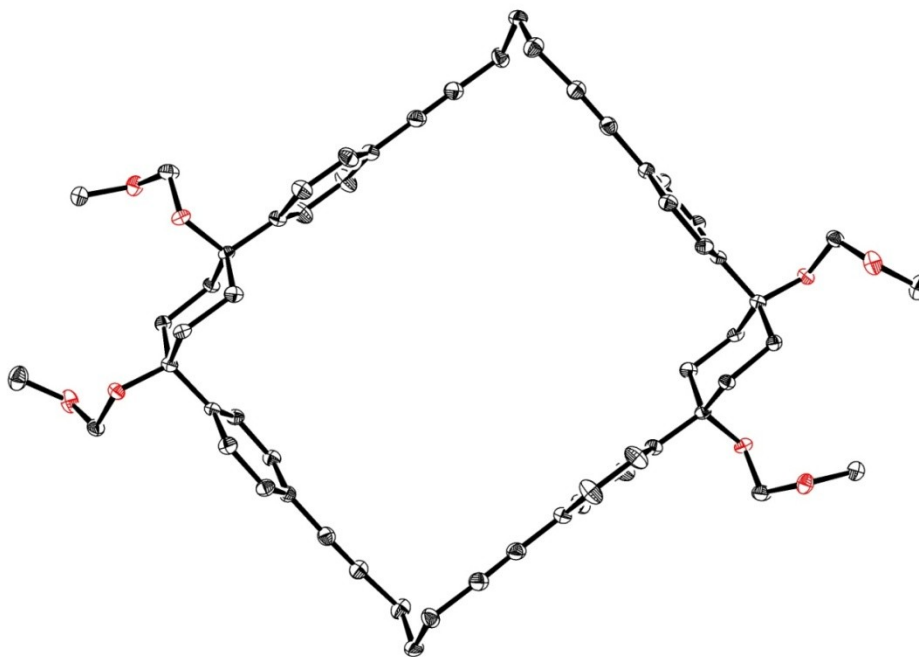




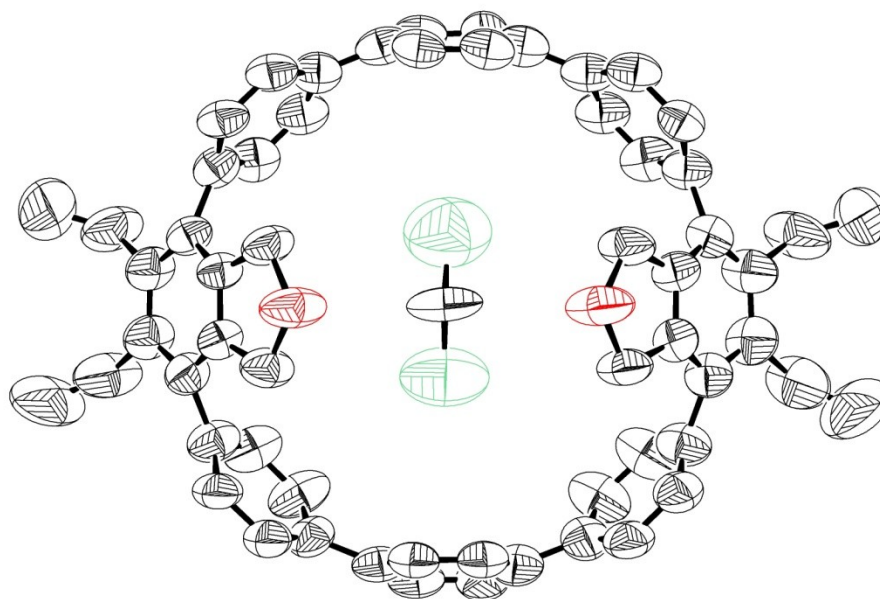
Crystal data for **42d**: formula  $C_{27}H_{30}$ ,  $M = 354.53$ ,  $F(000) = 384$ , colourless block, size  $0.040 \cdot 0.090 \cdot 0.210 \text{ mm}^3$ , triclinic, space group  $P -1$ ,  $Z = 2$ ,  $a = 9.2663(3) \text{ \AA}$ ,  $b = 10.4543(4) \text{ \AA}$ ,  $c = 12.0726(4) \text{ \AA}$ ,  $\alpha = 70.585(2)^\circ$ ,  $\beta = 72.341(2)^\circ$ ,  $\gamma = 74.409(2)^\circ$ ,  $V = 1032.51(6) \text{ \AA}^3$ ,  $D_{\text{calc.}} = 1.140 \text{ Mg} \cdot \text{m}^{-3}$ . The crystal was measured on a Bruker Kappa Apex2 diffractometer at 123K using graphite-monochromated Mo  $K_{\alpha}$ -radiation with  $\lambda = 0.71073 \text{ \AA}$ ,  $\Theta_{\text{max}} = 32.603^\circ$ . Minimal/maximal transmission 0.99/1.00,  $\mu = 0.064 \text{ mm}^{-1}$ . The Apex2 suite has been used for datacollection and integration. From a total of 26834 reflections, 7413 were independent (merging  $r = 0.043$ ). From these, 3790 were considered as observed ( $I > 2.0\sigma(I)$ ) and were used to refine 244 parameters. The structure was solved by direct methods using the program Superflip. Least-squares refinement against  $F$  was carried out on all non-hydrogen atoms using the program CRYSTALS.  $R = 0.0566$  (observed data),  $wR = 0.1275$  (all data),  $\text{GOF} = 1.1107$ . Minimal/maximal residual electron density =  $-0.23/0.37 \text{ e \AA}^{-3}$ . Chebychev polynomial weights were used to complete the refinement. Plots were produced using Ortep 3v2



Crystal data for **102b**: formula  $C_{68}H_{78}Cl_6O_8$ ,  $M = 1236.08$ ,  $F(000) = 2608$ , colourless plate, size  $0.010 \cdot 0.070 \cdot 0.220 \text{ mm}^3$ , monoclinic, space group  $P 2_1/c$ ,  $Z = 4$ ,  $a = 20.300(2) \text{ \AA}$ ,  $b = 13.4605(14) \text{ \AA}$ ,  $c = 23.478(3) \text{ \AA}$ ,  $\alpha = 90^\circ$ ,  $\beta = 99.477(5)^\circ$ ,  $\gamma = 90^\circ$ ,  $V = 6327.9(12) \text{ \AA}^3$ ,  $D_{\text{calc.}} = 1.297 \text{ Mg} \cdot \text{m}^{-3}$ . The crystal was measured on a Bruker Kappa Apex2 diffractometer at 123K using graphite-monochromated Mo  $K_\alpha$ -radiation with  $\lambda = 0.71073 \text{ \AA}$ ,  $\Theta_{\text{max}} = 26.376^\circ$ . Minimal/maximal transmission 0.98/1.00,  $\mu = 0.326 \text{ mm}^{-1}$ . The Apex2 suite has been used for data collection and integration. From a total of 47114 reflections, 12921 were independent (merging  $r = 0.364$ ). From these, 12870 were considered as observed ( $I > 2.0\sigma(I)$ ) and were used to refine 739 parameters. The structure was solved by Direct methods using the program SIR92. Least-squares refinement against  $F_{\text{sqd}}$  was carried out on all non-hydrogen atoms using the program CRYSTALS.  $R = 0.1001$  (observed data),  $wR = 0.2828$  (all data),  $\text{GOF} = 1.0315$ . Minimal/maximal residual electron density =  $-2.62/2.87 \text{ e \AA}^{-3}$ . Chebychev polynomial weights were used to complete the refinement. Plots were produced using Ortep 3v2



Crystal data for **101c**: formula  $C_{62}H_{68}Cl_{12}O_8$ ,  $M = 1366.65$ ,  $F(000) = 708$ , yellow needle, size  $0.020 \cdot 0.060 \cdot 0.220 \text{ mm}^3$ , triclinic, space group  $P -1$ ,  $Z = 1$ ,  $a = 6.1849(4) \text{ \AA}$ ,  $b = 15.7299(11) \text{ \AA}$ ,  $c = 16.9383(11) \text{ \AA}$ ,  $\alpha = 97.464(4)^\circ$ ,  $\beta = 94.271(4)^\circ$ ,  $\gamma = 96.956(4)^\circ$ ,  $V = 1615.07(19) \text{ \AA}^3$ ,  $D_{\text{calc.}} = 1.405 \text{ Mg} \cdot \text{m}^{-3}$ . The crystal was measured on a Bruker Kappa Apex2 diffractometer at 123K using graphite-monochromated Mo  $K_\alpha$ -radiation with  $\lambda = 0.71073 \text{ \AA}$ ,  $\Theta_{\text{max}} = 30.089^\circ$ . Minimal/maximal transmission 0.97/0.99,  $\mu = 0.567 \text{ mm}^{-1}$ . The Apex2 suite has been used for data collection and integration. From a total of 32270 reflections, 9430 were independent (merging  $r = 0.065$ ). From these, 4577 were considered as observed ( $I > 2.0\sigma(I)$ ) and were used to refine 370 parameters. The structure was solved by Other methods using the program Superflip. Least-squares refinement against  $F$  was carried out on all non-hydrogen atoms using the program CRYSTALS.  $R = 0.0526$  (observed data),  $wR = 0.0960$  (all data),  $\text{GOF} = 1.1104$ . Minimal/maximal residual electron density =  $-0.70/0.63 \text{ e \AA}^{-3}$ . Chebychev polynomial weights were used to complete the refinement. Plots were produced using Ortep 3v2



Crystal data for **103d**: formula  $C_{121}H_{108}Cl_2O_4$ ,  $M = 1697.09$ ,  $F(000) = 1800$ , colourless plate, size  $0.020 \cdot 0.170 \cdot 0.260 \text{ mm}^3$ , monoclinic, space group  $P 21/c$ ,  $Z = 2$ ,  $a = 19.4814(18) \text{ \AA}$ ,  $b = 18.4101(14) \text{ \AA}$ ,  $c = 18.5749(15) \text{ \AA}$ ,  $\alpha = 90^\circ$ ,  $\beta = 99.456(6)^\circ$ ,  $\gamma = 90^\circ$ ,  $V = 6571.4(10) \text{ \AA}^3$ ,  $D_{\text{calc.}} = 0.858 \text{ Mg} \cdot \text{m}^{-3}$ . The crystal was measured on a Bruker Kappa Apex2 diffractometer at 123K using graphite-monochromated Cu  $K_\alpha$ -radiation with  $\lambda = 1.54180 \text{ \AA}$ ,  $\Theta_{\text{max}} = 68.290^\circ$ . Minimal/maximal transmission 0.88/0.99,  $\mu = 0.750 \text{ mm}^{-1}$ . The Apex2 suite has been used for data collection and integration. From a total of 11798 reflections, 11798 were independent (merging  $r = 0.075$ ). From these, 5987 were considered as observed ( $I > 2.0\sigma(I)$ ) and were used to refine 586 parameters. The structure was solved by Other methods using the program Superflip. Least-squares refinement against  $F$  was carried out on all non-hydrogen atoms using the program CRYSTALS.  $R = 0.0912$  (observed data),  $wR = 0.2421$  (all data),  $\text{GOF} = 1.1016$ . Minimal/maximal residual electron density =  $-0.23/0.44 \text{ e \AA}^{-3}$ . Chebychev polynomial weights were used to complete the refinement. Plots were produced using Ortep 3v2

The structure contains large cavities occupied by disordered solvent molecules. As the data quality was not optimal, and as the solvent molecules appear heavily disordered, it was not possible to identify more than the DCM molecule in the centre of the structure. For this reason SQUEEZE (A.L.Spek, Acta Cryst. 2009, D65, 148-155.) was used in order to finish the refinement.



**3.1 REFERENCES**

- [1] Tellier, F.; Sauvêtre, R.; Normant, J.-F. *J. Organomet. Chem.* **1985**, *292*, 19.
- [2] Basler, J. M., University of Basel, 2011.
- [3] Llerena, D.; Buisine, O.; Aubert, C.; Malacria, M. *Tetrahedron* **1998**, *54*, 9373.
- [4] Wang, X.; Chakrapani, H.; Madine, J. W.; Keyerleber, M. A.; Widenhoefer, R. A. *J. Org. Chem.* **2002**, *67*, 2778.
- [5] Veliev, M. G.; Agaev, N. M.; Shatirova, M. I.; Chalabieva, A. Z.; Geidarova, G. D. *Russ. J. Appl. Chem.* **2010**, *83*, 1957.
- [6] Wu, L.-H.; Chu, C.-S.; Janarthanan, N.; Hsu, C.-S. *Journal of Polymer Research* **2000**, *7*, 125.
- [7] Qu, W.; Kung, M.-P.; Hou, C.; Oya, S.; Kung, H. F. *J. Med. Chem.* **2007**, *50*, 3380.
- [8] Elie, C.-R.; Noujeim, N.; Pardin, C.; Schmitzer, A. R. *Chem. Commun.* **2011**, *47*, 1788.
- [9] Ouchi, M.; Inoue, Y.; Liu, Y.; Nagamune, S.; Nakamura, S.; Wada, K.; Hakushi, T. *Bull. Chem. Soc. Jpn.* **1990**, *63*, 1260.
- [10] Xia, J.; Bacon, J. W.; Jasti, R. *Chem. Sci.* **2012**, *3*, 3018.
- [11] Jasti, R.; Bhattacharjee, J.; Neaton, J. B.; Bertozzi, C. R. *J. Am. Chem. Soc.* **2008**, *130*, 17646.
- [12] Omachi, H.; Matsuura, S.; Segawa, Y.; Itami, K. *Angew. Chem. Int. Ed.* **2010**, *49*, 10202.
- [13] Takaba, H.; Omachi, H.; Yamamoto, Y.; Bouffard, J.; Itami, K. *Angew. Chem. Int. Ed.* **2009**, *48*, 6112.
- [14] López, S.; Fernández-Trillo, F.; Midón, P.; Castedo, L.; Saá, C. *J. Org. Chem.* **2005**, *70*, 6346.
- [15] Komáromi, A.; Szabó, F.; Novák, Z. *Tetrahedron Lett.* **2010**, *51*, 5411.
- [16] Dektar, J. L.; Hacker, N. P. *J. Org. Chem.* **1990**, *55*, 639.
- [17] Vol. WO0024745 (A1) — 2000-05-04.
- [18] Chen, W.; Li, K.; Hu, Z.; Wang, L.; Lai, G.; Li, Z. *Organometallics* **2011**, *30*, 2026.

- [19] Shaporenko, A.; Elbing, M.; Błaszczuk, A.; von Hänisch, C.; Mayor, M.; Zharnikov, M. *The Journal of Physical Chemistry B* **2006**, *110*, 4307.
- [20] Ma, Y.; Song, C.; Jiang, W.; Wu, Q.; Wang, Y.; Liu, X.; Andrus, M. B. *Org. Lett.* **2003**, *5*, 3317.

# **Appendix**





## ABBREVIATIONS

Å	Ångström	ESI	Electron spray ionisation
Ac	Acyl	eV	Electron volt
Ar	Aromatic	FAB	Fast atom bombardement
AcOH	Acetic acid	FT	Fourier transformation
Alox	Aluminium oxide	GC	Gas chromatography
bp	Boiling point	GPC	Gel permeation chromatography
Bn	Benzyl	h	Hours
BuLi	Butyl lithium	HOMO	Highest occupied molecular orbital
calc.	Calculated	HRMS	High resolution mass spectrometry
CNT	Carbon nanotube	<i>i</i> -Pr	<i>iso</i> -Propyl
COD	Cyclooctadiene	<i>i</i> -PrOH	<i>iso</i> -Propanol
CPDMS	3-Cyanopropyltrimethylsilyl	IR	Infrared spectroscopy
CPP	Cycloparaphenylene	<i>J</i>	Coupling constant
CVD	Chemical vapor deposition	<i>k</i>	Rate constant
d	Days	kcal	
d	Doublet	kJ	Kilojoule
DBU	1,8-diazabicyclo[5.4.0]undec-7-ene	LUMO	Lowest unoccupied molecular orbital
DMF	Dimethylformamid	M	Molarity
DMSO	Dimethylsulfoxide	MALDI	Matrix-assisted laser desorption
dppf	1,1'-Bis-(diphenylphosphino)-ferrocene	Me	Methyl
EA	Elementary analysis	MeCN	Acetonitrile
EI	Electron impact	MeOH	Methanol
Eq.	Equivalents	M	Meta
Et	Ethyl	m	Multiplet (NMR)
Et <sub>2</sub> O	Diethyl ether	min	Minutes
EtOAc	Ethyl acetate	MO	Molecular orbital
EtOH	Ethanol	MOM	Methoxymethyl

mp	Melting point	TBAF	Tetra- <i>n</i> -butylammonium fluoride
MS	Mass spectrometry	TBME	<i>tert</i> -Butylmethyl ether
MsOH	Methane sulfonic acid	THF	Tetrahydrofuran
MWNT	Multi-walled nanotubes	TLC	Thin layer chromatography
MW	Microwave	TMS	Trimethylsilyl
m/z	Mass charge ratio	TMSA	Trimethylsilyl acetylene
NBS	<i>N</i> -Bromosuccinimide	TOF	Time of flight
NMR	Nuclear magnetic resonance	Ts	Toluene sulfone
p	Pentuplet	UV/VIS	Ultra violet — visible light
p	para	absorption	
ph	Phenyl	$\Theta$	Torsion angle
PP	polyphenylene	$\Phi_F$	Fluorescence quantum yield
ppm	Parts per million	$\lambda_{em}$	Emission wavelength
<i>p</i> -TsOH	<i>para</i> -Toluenesulfonic acid	$\lambda_{abs}$	Absorption wavelength
q	Quartet	$\tau_s$	Fluorescence life time
rt	Room temperature	$k_r$	radiative rate constant
s	Singlet (NMR)	$k_{nr}$	nonradiative rate constant
sat.	Saturated	$\delta$	Chemical shift
SWNT	Single-walled nanotubes		
t	Triplet		